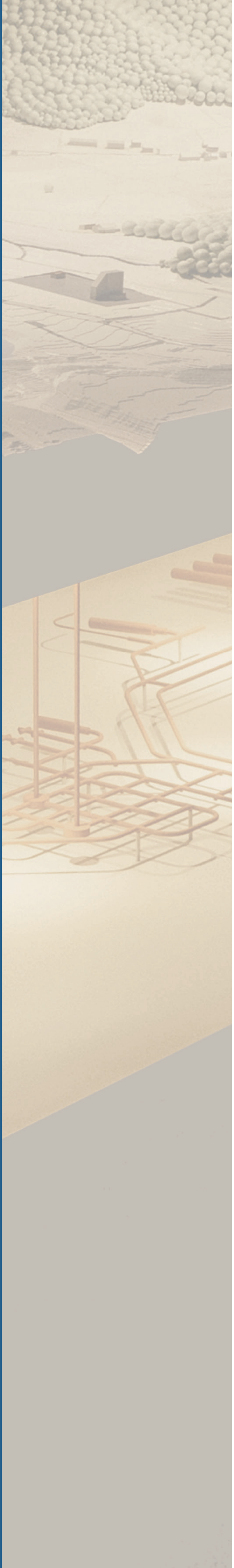

nagra

TECHNICAL REPORT 23-11

Degradation of Organic Materials in an L/ILW Repository

December 2023

Nagra | National Cooperative for the
Disposal of Radioactive Waste
Hardstrasse 73 | 5430 Wettingen | Switzerland
T. +41 56 437 11 11 | info@nagra.ch | nagra.ch

TECHNICAL REPORT 23-11

Degradation of Organic Materials in an L/ILW Repository

December 2023

T. Guillemot[1], E. Wieland[2],
L. Mosberger[3] & R. Warthmann[3]

[1] Nagra, Wettingen, Switzerland

[2] CWL Solutions GmbH, Kleindöttingen, Switzerland

[3] Zürich University of Applied Sciences (ZHAW), Life Sciences and Facility Management, Wädenswil, Switzerland

Nagra | National Cooperative for the
Disposal of Radioactive Waste
Hardstrasse 73 | 5430 Wettingen | Switzerland
T. +41 56 437 11 11 | info@nagra.ch | nagra.ch

ISSN 1015-2636

Abstract

In a deep geological repository for low- and intermediate-level waste, organic substances are predominantly present in the waste itself, and to a smaller extent (< 5%) in conditioning materials and tunnel support. The degradation of organics will take place by a combination of abiotic and biotic processes. The abiotic ones (i.e., radiolysis and hydrolysis) reduce the molecular size of complex polymers before microorganisms can degrade them into even smaller compounds, down to thermodynamically stable CO_2 and CH_4. The latter are predicted to be the second-most important gases generated in the near-field of an L/ILW repository after H_2. Quantitative assessments of CO_2 and CH_4 production rates during the degradation of organics are therefore required. Furthermore, the production of CO_2 induces the carbonation of the cement-based engineered barriers, reducing their safety performance in terms of radionuclide sorption and highly alkaline buffer capacity (which in turn contributes to limiting gas generation by corrosion and/or microbial activities). A comprehensive literature review was conducted to better estimate gas generation rates from the degradation of organics, with a focus on the various abiotic and biotic processes to which the main organic materials present in the Swiss inventory for low- and intermediate-level waste (ion-exchange resins, PVC, bitumen, plastics, cellulose and Plexiglas®) are exposed. In the near-field of a cement-based low- and intermediate-level waste repository, organic materials are assumed to degrade mainly by hydrolysis and microbial processes, although the latter might be inhibited due to the highly alkaline conditions as well as limited water and nutrient availability. The radiolytic degradation of organics can, however, not be completely disregarded and mainly takes place shortly after closure of the low- and intermediate-level waste repository, when oxygen is still available, and the dose release (mostly from γ-emitters) is still high. In the temperature range expected in the near-field of a cement-based low- and intermediate-level waste repository over the period under consideration of 100,000 years (i.e., < 50 °C), thermal degradation might only enhance radiolysis and hydrolysis by a factor of ~ 2. The simplified classification of organic low- and intermediate-level waste into easily and less degradable organics (i.e., O1 and O2, respectively) was kept for the general licence application, as no individual rates could be attested for any of the organics inventoried in the low- and intermediate-level waste. The only change made in this classification concerns the two types of plastic polyesters and polycarbonates. These are now grouped together with easily degradable organics because they are susceptible to hydrolysis, which was not reflected in the Stage 2 rates of the Swiss Sectoral Plan for deep geological repositories. Moreover, the lower bounds of the gas generation rates for the general licence application were not set to zero anymore, as it can be now qualitatively assumed that the degradation of the organic low- and intermediate-level waste will occur, at least partly, over the period under consideration of 100,000 years. The lower bounds were fixed, based on the lowest rates measured and available in the literature. From the gas generation rates, the degradation rates of the organics can be estimated with a simplified kinetic model, which can further be used to assign an expected lifetime of the organic waste. A small portion of the organic materials present in L/ILW (e.g., superplasticisers, Plexiglas®, polyester, polycarbonates, cellulose and LMW organics) are expected to completely degrade during the period under consideration of 100,000 years. For the vast majority (e.g., ion-exchange resins, polystyrene, PVC and bitumen), complete degradation is hardly expected to occur as their lifetimes were estimated to be close to or even beyond the period of 100,000 years.

Zusammenfassung

In einem geologischen Tiefenlager für schwach- und mittelaktive Abfälle werden organische Stoffe vorwiegend in der Abfallmatrix und nur zu einem kleinen Anteil (< 5%) in den Konditionierungsstoffen und im Tunnelausbau vorkommen. Der Abbau der organischen Stoffe erfolgt durch eine Kombination abiotischer und biotischer Prozesse. Abiotische Prozesse (Radiolyse und Hydrolyse) reduzieren die Molekülgrösse komplexer Polymere, bevor Mikroorganismen sie in noch kleinere Verbindungen bis hin zu thermodynamisch stabilem CO_2 und CH_4 abbauen können. Es wird erwartet, dass diese beiden Gase die zweitgrösste Gruppe an Gasen (nach Wasserstoff) bilden, die im Nahfeld eines Tiefenlagers für schwach- und mittelaktive Abfälle entstehen. Daher ist eine quantitative Bewertung der CO_2- und CH_4-Produktionsraten während des Abbaus organischer Stoffe erforderlich. Darüber hinaus führt die Produktion von CO_2 zur Karbonatisierung der zementbasierten technischen Barrieren, was deren Sicherheitswirksamkeit in Bezug auf die Sorption von Radionukliden und die hochalkalische Pufferkapazität (die wiederum zur Begrenzung der Gasbildung durch Korrosion und/oder mikrobielle Aktivitäten beiträgt) verringert. Um die aus dem Abbau organischer Stoffe entstehenden Gasbildungsraten besser abschätzen zu können, wurde eine umfassende Literaturrecherche durchgeführt. Der Schwerpunkt lag dabei auf verschiedenen abiotischen und biotischen Prozessen, denen die wichtigsten organischen Stoffe des Schweizer schwach- und mittelaktive Abfälle-Inventars (Ionenaustauscherharze, PVC, Bitumen, Kunststoffe, Zellulose und Plexiglas®) ausgesetzt sind. Es wird davon ausgegangen, dass organische Stoffe im Nahfeld eines zementbasierten Tiefenlagers für schwach- und mittelaktive Abfälle hauptsächlich durch Hydrolyse und mikrobielle Prozesse abgebaut werden. Letztere könnten durch stark alkalische Bedingungen sowie durch die begrenzte Verfügbarkeit von Wasser und Nährstoffen unterbunden werden. Der strahlenbedingte Abbau organischer Stoffe darf jedoch auch nicht völlig ausser Acht gelassen werden. Er kann vor allem kurz nach dem Verschluss des schwach- und mittelaktive Abfälle-Tiefenlagers dann stattfinden, wenn noch Sauerstoff zur Verfügung steht und die Strahlung (meist durch γ-Strahler) noch vergleichsweise hoch ist. In dem Temperaturbereich, der im Nahfeld eines zementbasierten schwach- und mittelaktiven Abfälle-Tiefenlagers über den Betrachtungszeitraum von 100'000 Jahren zu erwarten ist (d.h. < 50 °C), könnte der thermische Abbau die Radiolyse und Hydrolyse nur um einen Faktor von ~ 2 steigern. Folglich wurde die vereinfachte Einteilung der organischen schwach- und mittelaktive Abfälle in leicht abbaubare und schwer abbaubare Formen (d.h. O1 und O2) für das Rahmenbewilligungsgesuch beibehalten, da für keinen der in den schwach- und mittelaktiven Abfällen inventarisierten organischen Stoffe individuelle Werte nachgewiesen werden konnten. Die einzige Neueinteilung betrifft die zwei Kunststoffarten Polyester und Polykarbonate, die nun als O1 eingestuft werden, da sie im Vergleich zu anderen O2-Stoffen als stärker hydrolyseanfällig gelten. Dies war aus den während der Etappe 2 des Sachplanverfahrens geologische Tiefenlager gewonnenen Datensätzen nicht zu erkennen. Zudem wurde der untere Eckwert der O1- und O2-Gasbildungsraten für das Rahmenbewilligungsgesuch nicht mehr auf null gesetzt, da nun qualitativ begründet davon ausgegangen werden kann, dass der Abbau der organischen schwach- und mittelaktiven Abfälle zumindest teilweise während des Betrachtungszeitraums von 100'000 Jahren erfolgen wird. Die unteren Eckwerte wurden daher auf der Grundlage der niedrigsten gemessenen Werte festgelegt. Aus den für das Rahmenbewilligungsgesuch verwendeten Gasbildungsraten lassen sich die Abbauraten der organischen Stoffe anhand eines vereinfachten kinetischen Modells abschätzen. Mit diesem Modell lässt sich auch die erwartete Lebensdauer der organischen Abfälle bestimmen.

Table of Contents

List of Tables

List of Figures

List of Acronyms

ATW	Alpha-Toxic Waste
CEA	Commissariat à l'Energie Atomique
DIC	Dissolved Inorganic Carbon
DOC	Dissolved Organic Carbon
EDTA	Ethylene Diamine Tetraacetic Acid
EDZ	Excavation-Damaged Zone
GME	Gas Monitoring Experiment
HCs	HydroCarbons
HLW	High-Level Waste
HMW	High Molecular Weight
IERs	Ion-Exchange Resins
IRB	Iron-Reducing Bacteria
L/ILW	Low- and Intermediate-Level Waste
LMW	Low Molecular Weight
LS	LigninSulphonate
MIR waste	waste from Medicine, Industry and Research
NPP	Nuclear Power Plant
NTA	NitriloTriacetic Acid
OPA	Opalinus Clay
O1	Easily degradable organics
O2	Less degradable organics
PAE	PolyAryl Ether-based SPs
PCE	PolyCarboxylate Ether-based SPs
PC	PolyCarbonate
PE	PolyEthylene
PET	PolyEthyleneTerephthalate
PMMA	Poly(Methyl MethAcrylate)
PP	PolyPropylene
PS	PolyStyrene
PVC	PolyVinyl Chloride
RBG	Nagra’s general licence application (RahmenBewillingungsGesuch in German)
RH	Relative Humidity

SF	Spent fuel
SGT	Nagra’s Sectoral Plan for Deep Geological Repositories
SMF	Sulphonated Melamine Formaldehyde
SNF	Sulphonated Naphthalene Formaldehyde
SPs	SuperPlasticisers
SRB	Sulphate-Reducing Bacteria
TIC	Total Inorganic Carbon
TOC	Total Organic Carbon
VOCs	Volatile Organic Compounds
Zwilag	Zwischenlager Würenlingen (central interim storage facility)

1 Introduction

The potential impact of gas generation, accumulation and migration on the long-term performance of engineered and geological barriers in a deep geological repository for low- and intermediate-level waste (L/ILW) needs to be assessed to ensure that gas generation does not compromise post-closure safety (Diomidis et al. 2016). Significant quantities of gases can be generated after closure of an L/ILW repository as a result of various processes, most notably the anoxic corrosion of metals, producing mainly H_2 and the degradation of organic materials, assumed to generate both CH_4 and CO_2 (Diomidis et al. 2016, Poller et al. 2016).

Quantitative assessment of gas generation is important as the accumulation of gas might result in pressures that could irreversibly damage to the engineered and/or geological barriers. This may in turn influence groundwater movements and potentially the transport of radionuclides. Overall, the most important gases generated in a repository for L/ILW are: H_2, followed by CH_4 and CO_2 (Poller et al. 2016). The production of CO_2 is particularly important as its interaction with cement results in the carbonation of the cement-based engineered elements of the repository, reducing their capacity to sorb radionuclides and the pH of the porewater that in turn enhances metallic corrosion and the likelihood for microbial activity (Wieland & Kosakowski 2020).

Gas generation and transport in an L/ILW repository has been intensively studied over the last decades, both by Nagra and other international research organisations (Diomidis et al. 2016, Poller et al. 2016, Grogan et al. 1992, Nagra 2004, Small et al. 2008, Marshall et al. 2013, Norris et al. 2013, Moreno et al. 2001, Talandier 2005, Lanyon & Herbert 2021). Nagra's original assumptions regarding the CH_4/CO_2 generation rates from the degradation of organics were based on a few studies published in the 1980s (Molecke 1979, Wiborgh et al. 1986). These experimental studies were, however, not performed in conditions relevant to a cement-based L/ILW repository (i.e., near neutral and fully saturated conditions) (Nagra 2004) and were assessed as highly conservative (too pessimistic) (Hooker 2007). They were then used as the upper bound and worst-case scenario (Johnson & Schwyn 2007). The reference case rates could be reduced by a factor of ten, as gas generation rates were about one order of magnitude lower under partially saturated conditions and it was assumed that such conditions would prevail for a long time in the deep geological repository (Johnson & Schwyn 2007). More recently, the lower bound of the gas generation rates was set to zero (Diomidis et al. 2016) as it remained unclear whether any organic decomposition might occur under repository-relevant conditions (Warthmann et al. 2013).

The primary aims of this report are to provide a comprehensive review of the current state-of-the-art process understanding of the degradation of organic materials predominantly present in L/ILW for the documentation of Nagra's safety case. To achieve this objective, a thorough literature review was conducted to characterise the various processes that contribute to the degradation of organics, their relevance in the near-field of a cement-based L/ILW repository and to inventory all published degradation/gas generation rates based on experimental data.

This report serves as a scientific basis supporting further assessments of repository evolution, specifically the gas synthesis and L/ILW near-field evolution reports (Nagra 2024a, in prep., Kosakowski et al. 2023) and aims to address key research and development priorities for Nagra's safety case. Specifically, it provides new insights into the estimation of the gas generation rates from the abiotic and biotic degradation of organics, based on the latest scientific evidence available.

Following this introductory chapter, Chapter 2 describes the inventory of organic L/ILW and their conditioning, emplacement and the expected long-term chemical evolution of the near-field. Chapter 3 summarises the abiotic processes, including the radiolytic, alkaline and thermal types of degradations of the main organic materials present in the L/ILW inventory. Chapter 4 discusses the biotic degradation in the context of an L/ILW repository. In Chapter 5, the gas generation from the degradation of organics is defined. In parallel, the rates used in previous work are re-evaluated based on insights gained in both Chapters 3 and 4, plus recent experimental data. Chapter 6 finally concludes this report.

2 Inventory and disposal of L/ILW organics

2.1 Inventory of L/ILW organics

L/ILW (including alpha-toxic waste; ATW) arises from the operation and decommissioning of nuclear power plants (NPPs) and from medical, industrial and research applications (MIR waste). The inventory of all of Switzerland's radioactive waste that exists today and will be produced in the future has been compiled specifically for the general licence application in the database MIRAM-RBG ("Model Inventory of Radioactive Materials for the general licence application") and is documented in Nagra (2023b).

L/ILW is characterised by a high waste volume, comparatively low radiotoxicity/activity and a large heterogeneity in physicochemical properties. Material inventories are detailed in the MIRAM-RBG, which lists more than 200 materials. They are categorised into three main types: metals, inorganic and organic materials, and respectively represent ~ 71%, ~ 26% and ~ 3% of the total L/ILW mass within the waste matrix (Nagra 2023b). Organic substances form a substantial part of the waste (i.e., ~ 95%), whereas conditioning materials and tunnel support represent only a very small proportion, e.g., in the form of cement additives. It should also be noted that > 99% of organic substances are present in L/ILW, while only < 1% is in ATW. An overview of the distribution of organics in the L/ILW is given in Fig. 2-1. Ion-exchange resins (IERs), poly(vinylchloride) (PVC), bitumen, polystyrene/styrene, plastic, cellulose, poly(methyl metacrylate) (PMMA or commonly known under its trademark, Plexiglas®), polyethylene (PE), polyester, diethanol amine and polycarboxylates are the principle organic materials in term of mass (Nagra 2023b). They respectively contribute ~ 41%, ~ 23%, ~ 14%, ~ 4%, ~ 4%, ~ 3%, ~ 2%, ~ 1%, ~ 1%, ~ 1%, ~ 1% and ~ 1% to the total mass of organics inventoried (Fig. 2-1). They are also among the major organic substances inventoried in other European waste management programmes (Altmaier et al. 2021). In this report, the focus is on the degradation processes of these specific organics. A complete list of all the organic substances present in MIRAM-RBG, including their chemical formulae and abundance, is provided in Appendix A and in more detail in Nagra (2023b).

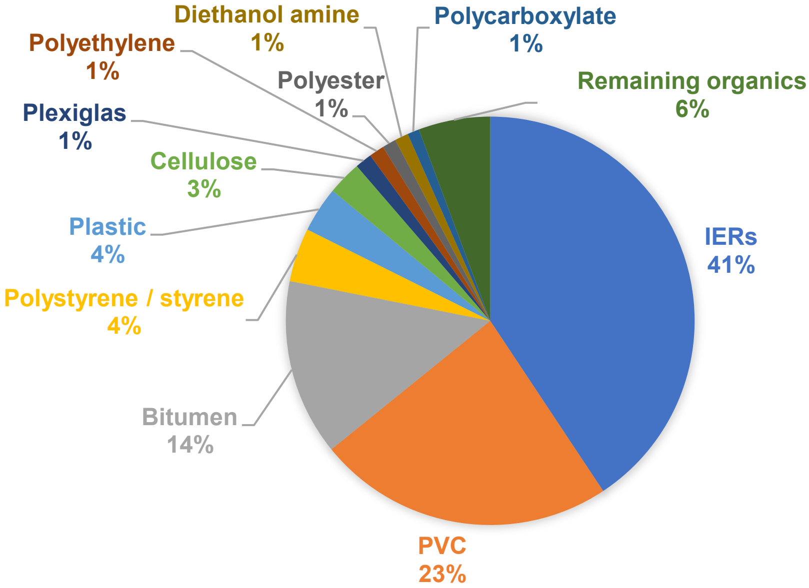

Fig. 2-1: Mass distribution of L/ILW organics based on the waste package type inventory From Nagra (2023b)

2.1.1 IERs, PS and styrene

IERs are macromolecular co-polymers based on styrene monomers cross-linked by divinylbenzene forming a polystyrene (PS) backbone (Fig. 2-2). This linear polymer, combining into various filaments, forms a three-dimensional, finely branched network with many cavities. The surface of the filaments, functionalised with sulphonic groups (e.g., $=R-SO_3^-$; $=R-CH_2-$) for cationic IERs or quaternary ammonium groups (e.g., $=R-N(CH_3)_3^+$) for anionic IERs (Fig. 2-2), selectively adsorbs anions or cations by ion exchange (Rizzo et al. 2018). In nuclear facilities, IERs are placed in filters and demineralisers and remove corrosive soluble ionic species and/or radionuclides from the reactor coolant and waste stream (Rizzato et al. 2017). More specifically, cationic IERs capture metallic radionuclides like $^{137}Cs^+$, $^{60}Co^{2+}$ and $^{90}Sr^{2+}$, while anionic IERs remove anionic radionuclides like $H^{14}CO_3^-$ or $^{36}Cl^-$ (Abrahamsen et al. 2015).

Two types of IERs can be used in NPPs: bead and powder forms. Bead IERs have a typical spherical shape with a 0.5 mm diameter and can be used either in the single chemical form (cationic or anionic) or in a mixed bed configuration, depending on the physicochemical conditions of the water coolant system and the specific needs (Rizzato et al. 2017, Rizzo et al. 2018). Powder IERs have a fine granulometry, providing a much higher surface area than the equivalent weight of bead IERs and resulting in a floc structure as soon as they agglomerate.

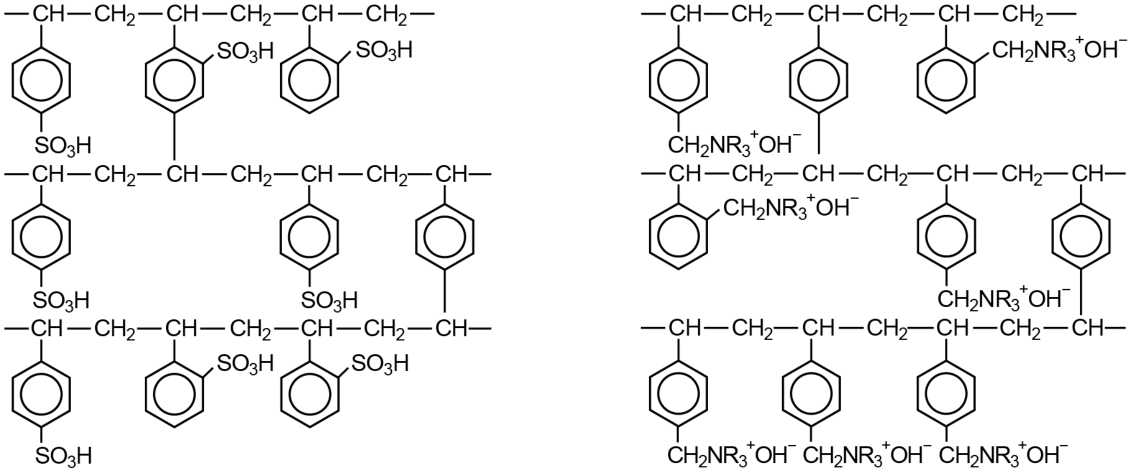

Fig. 2-2: Chemical structure of cationic (left) and anionic (right) IERs
From Rizzo et al. (2018)

PS consists of styrene monomers, which are aromatic hydrocarbons (HCs) composed solely of carbon and hydrogen. The polymerisation of PS is exothermic with a heat of -840 kJ/kg. The properties of PS vary from foam to films to glass-like materials depending on the manufacturing process (Maul et al. 2014).

Based on their chemical structures, both IERs, PS and styrene are assumed to be affected by similar degradation processes. They correspond to the largest group of organic materials in the Swiss L/ILW inventory with a total of ~ 39% total mass of L/ILW organics (Fig. 2-1) (Nagra 2023b).

2.1.2 PVC

PVC is a halogenated polymer produced from the polymerisation of the vinyl chloride monomer (CH_2CHCl) (Fig. 2-3). PVC can also be defined as an addition polymer as it contains no functional group in the main chain but only a repetition of the -CH_2CHCl- unit. The polymerisation reaction of the vinyl chloride monomers is strongly exothermic (-1,534 kJ/kg) (Fischer et al. 2014). As PVC consists of C atom chains with strong C-H bonds, a large chlorine atom and strong intermolecular forces between polymer chains (Fig. 2-2), the mobility of the chain is restricted. Consequently, in its pure form, PVC is a rigid, mainly amorphous material with little flexibility (Abrahamsen et al. 2015).

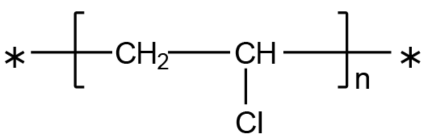

$$*-\left[CH_2-\underset{\displaystyle Cl}{\underset{|}{CH}}-\right]_n-*$$

Fig. 2-3: Chemical structure of PVC

PVC has various applications in the nuclear industry as well as in research. This rigid material is widely used for sewage pipes, electrical cables and window frames. In nuclear waste inventories, PVC is mostly used in its flexible form (Mijnendonckx et al. 2021) and can be found in glove boxes, cable insulations, soft tubing, filter casings, protective suits, etc. (Altmaier et al. 2021, Abrahamsen et al. 2015).

The flexibility of PVC is achieved through the addition of additives. Of these, plasticisers typically present the largest components, accounting for between 30% and 50% by volume. They are not covalently bonded to the polymer itself but rather sit between the layers. The presence of plasticisers between the otherwise rigid PVC layers serves to lubricate and protect the material according to their function. As an example, the plasticisers to make PVC flexible are often phthalate esters, e.g., bis(2-ethylhexyl)phthalate, di-isodecyl phthalate, di-isononyl phthalate. According to Smith (2013), bis(2-ethylhexyl)phthalate, di-isodecyl phthalate and di-isononyl phthalate account for over 80% of all PVC plasticiser applications. They have similar chemical structures, and the main difference lies in the nature and size of the aliphatic groups that are linked to the phenols groups via ester bonds. Besides plasticisers, PVC can contain a wide range of additives such as flame retardants or heat stabilisers (Tab. 2-1). These additives may leach out from the polymer in the course of degradation processes, influencing radionuclide mobility and microbial activities (Abrahamsen-Mills & Small 2021, Mijnendonckx et al. 2021). While diffusing out of the PVC, they can form a non-aqueous phase liquid (Baston & Dawson 2014), such as oils and solvents, with limited miscibility with water, thus forming a separate phase (NDA 2012). Stabilisers can also be added to PVC to prevent degradation by heat and light. Different types of stabilisers exist, and their proportion in the final product varies according to the technical requirements of the intended application (i.e., Tab. 2-1) (Smith et al. 2013).

Tab. 2-1: Common PVC additives

Adapted from Smith et al. (2013)

Additive function	Range of % by volume in PVC	Generic additives used
Plasticiers	30 – 50	Esters (phthalates, adipates, azelates, phosphates) Epoxies Trimellitates
Stabilisers	1 – 5	Lead compounds Cadmium compounds Organotins Barium/zinc compounds Calcium/zinc compounds
Fillers	10 – 20	Silicates Barium/calcium sulfate Calcium carbonate
Pigments	1 – 3	Metal oxides Organic dyes
Flame retardants	0 – 5	Chlorinated or brominated organics Antimony oxide

2.1.3 Bitumen

In the Swiss L/ILW inventory, bitumen is not a waste but a thermoplastic waste encapsulant mostly used to immobilise solid wastes such as IERs and water-soluble residues from reprocessing and effluent treatment (i.e., sludges and concentrated salt solutions), due to its good binding capacity, low solubility and permeability to water, and resistance to chemical and biological degradation (Valcke et al. 2009). Bitumen is obtained by partial distillation of crude petroleum and consists of high-molecular-weight (HMW) micelles dispersed or dissolved in oily low-molecular-weight (LMW) constituents. The micelles are assumed to be asphaltenes together with an absorbed layer of resins that act as a stabilising solvating layer (Valcke et al. 2009). Bitumen has a random polymer-like macromolecular structure composed of aliphatic compounds (paraffinics or alkanes), naphtenics (naphthalenes or cyloalkanes) and polycyclic aromatic HCs with functional groups containing nitrogen, sulphur and/or oxygen atoms (Fig. 2-4) (Abrahamsen et al. 2015). Bitumen also contains trace amounts of metals such as vanadium, nickel, iron, magnesium and calcium present in the form of inorganic salts, oxides or porphyrin structures (Read & Witheoak 2006). The precise composition of bitumen is extremely complex as it directly depends on the source of the crude oil from which it originates and on the modification induced during processing. Four broad chemical groups can still be identified in bitumen, namely asphaltenes (5 – 25 wt.%), saturates (5 – 20 wt.%), resins (10 – 25 wt.%) and aromatics (40 – 65 wt.%) (Mijnendonckx et al. 2021) (Fig. 2-4). In Switzerland, only distilled, soft bitumens from the straight reduction of crude oil are used in the nuclear industry (Mijnendonckx et al. 2021).

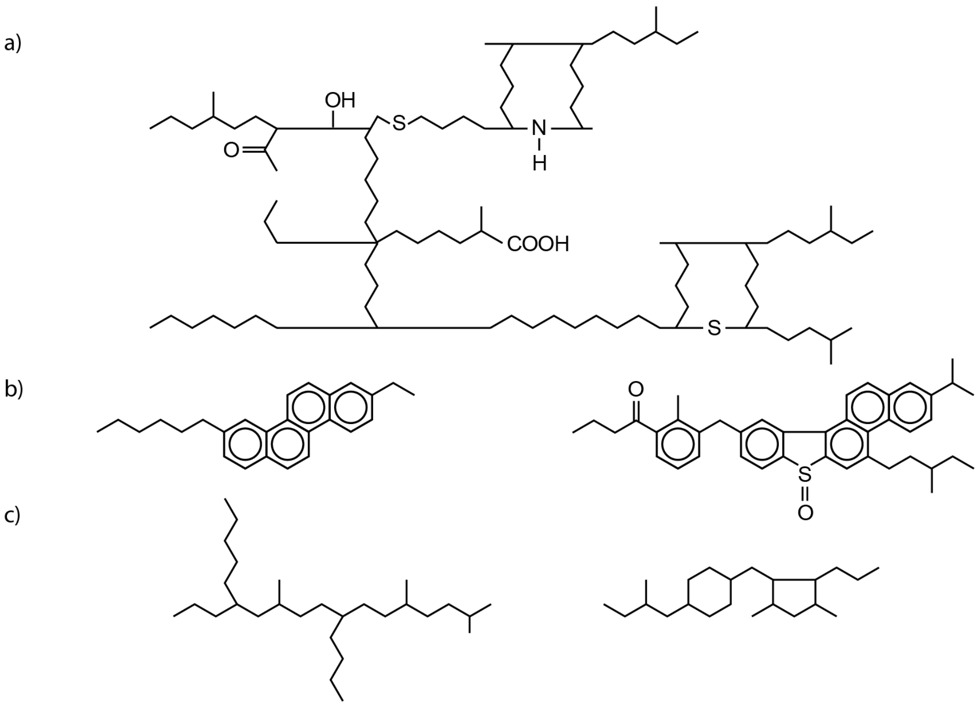

Fig. 2-4: Types of organic compounds found in bitumen

a) Asphaltene; b) aromatic; and c) saturated structures

From Read & Witheoak (2006)

2.1.4 Plastics

In the Swiss inventory of L/ILW organics, the term "plastic" corresponds to ~ 4% of the total mass distribution (Nagra 2023b). No additional information is available about the chemical nature of this material, leading to uncertainties related to its potential degradation. The generic term "plastics" commonly refers to PE, PVC, PS and others polymers such as polypropylene (PP), polycarbonate (PC) and polyester (Allen & Bevington 1989). As PVC, PS, PP, PE and polyester are listed as separate components in the Swiss waste inventory (Nagra 2023b), it can be assumed that the term "plastics" is a non-specific generic term referring to the polymers previously listed, as no precise distinction was required during the inventory. It can also refer to a non-specific composition containing various proportions of PVC, PS, PP, and/or PE. It was therefore decided to add in the "plastic" category PP, PE and polyester (including polyethyleneterephthalate or PET), which correspond to ~ 6% of the total L/ILW mass distribution (Nagra 2023b). As PVC is the only halogenated compound and is predominantly present in the Swiss waste inventory (Fig. 2-1), we decided not to include it in the group of "plastics" such as PS, which was already placed in the same category of IERs due to their chemical similarities (cf. Section 2.1.1).

PP, PE and polyester are all non-halogenated polymers and linear HCs. They are used similarly in nuclear facilities and can be found in laboratory (i.e., vials, sampling tubes, filters, containers, waste bags) and building equipment (i.e., wire film, piping systems, tapes) and also in clothing.

PE consists of nonpolar, HMW HC chains with the general chemical formula $(\text{-}CH_2CH_2\text{-})_n$, which is produced by the polymerisation of ethylene units (Fig. 2-5a). There are different types of PE. The high-density, low-density, and linear-low-density materials are the most common ones. High-density PE consists of weakly cross-linked polymer chains, whereas low-density PE is made of strongly cross-linked polymer chains. The material properties of PEs are determined by the molecular structure (e.g., crystallinity) and molar mass, which depend on the degree of cross-linking. For instance, the less the polymer chains are cross-linked and the lower the molar mass is, the higher the crystalline content of PE is.

Similar to PE, PP is a non-polar HMW HC polymer containing methyl as a functional side group $(\text{-}CHCH_2(CH_3)\text{-})_n$ produced by the polymerisation of propylene (Fig. 2-5b). Its properties are similar to those of PE, although the material is slightly harder and more heat-resistant. The condensation of PP is exothermic (2,514 kJ/kg) and can occur at normal pressure, while pressures of up to 2 MPa are common in industrial production to accelerate the process. PP is also partly crystalline, whereby the degree of crystallinity is determined by the orientation of the methyl group rather than the degree of crosslinking. The ratio of crystalline to amorphous regions is influenced by process parameters such as temperature as well as the addition of additives (i.e., nucleating agents) (Heggs 2014). The material properties of PP are determined by its molar mass as well as the crystallinity and the type and proportion of propylene used in polymerisation.

Polyester refers to a category of plastics with ester functional groups in each repeating unit of the HC backbone $(\text{-}R\text{-}COO\text{-})_n$. The best-known type of polyester is polyethyleneterephthalate (PET) (Fig. 2-5c;d). PC has a similar structure to PET, containing carbonate groups $(\text{-}R\text{-}CO_3\text{-})_n$ instead of carboxylic ester groups in the polymer chain. In both cases, R denotes aliphatic or aromatic HCs. The material properties are essentially determined by the degree of crystallinity (Kotova et al. 2021) and crosslinking of the polymer chains, the latter depending on the type of functional groups present in the monomer units.

It should be noted that commercial products of the previously mentioned plastics usually contain a mixture of additives, such as stabilisers, antioxidants and fillers, of which the chemical compositions are frequently unknown.

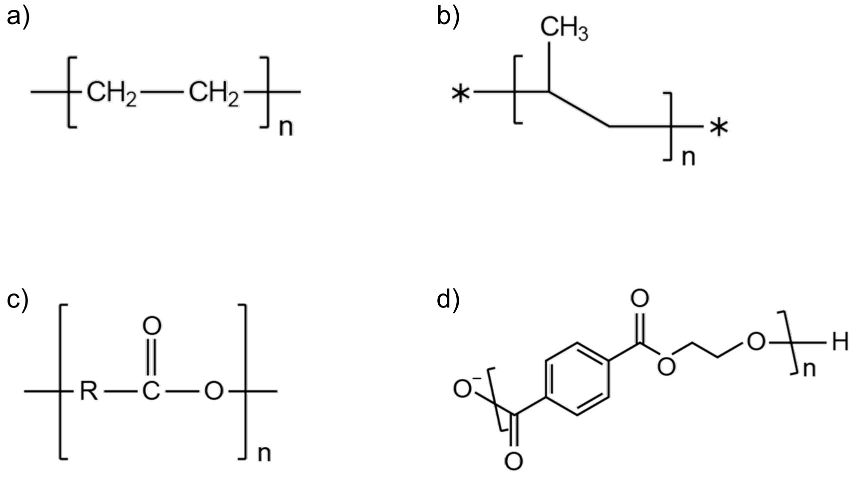

Fig. 2-5: Chemical structure of plastics

a) PE; b) PP; c) polyesters; d) PET

2.1.5 Cellulose, ISA and LMW organics

Cellulose is the most abundant easily degradable polymeric material (polysaccharide) present in the Swiss L/ILW inventory (Nagra 2023b) (Fig. 2-1). It is the main component of plant materials and can be found in almost pure form in cotton fibers (90%) and to a lesser extent in flax (80%), jute (60 – 70%) and wood (40 – 50%) (van Loon & Glaus 1998). The material is present in laboratory equipment (i.e., tissue for smear-testing potentially radioactive particles, paper, clothing, filters and cardboard materials) (Altmaier et al. 2021, Abrahamsen et al. 2015). Cellulose is a linear unbranched polysaccharide resulting from the polymerisation of glucopyranose units (up to 10,000) to form glucopyranose rings (Okamura 1991). The monomers are linked by a glycosidic bond. Each monomeric unit has three hydroxyl groups, forming intra- and intermolecular hydrogen bonds (Fig. 2-6), largely determining the macrostructure and physicochemical properties of the polymer. The number of glucopyranose units in cellulose accounts for its degree of polymerisation. Each cellulose molecule has both a non-reducing and reducing end (a latent aldehyde) (van Loon & Glaus 1998). Cellulose chains, having a diameter of ca. 35 Å and running through crystalline and amorphous regions, are ordered in strands as microfibrils by inter- and intra-molecular hydrogen bonds (Kennedy et al. 1985).

Isosaccharinic acid (ISA) is a C6 sugar acid and the main degradation product of cellulose (van Loon & Glaus 1998). It is of particular interest in the context of L/ILW disposal because it has strong complexing properties and can enhance radionuclide mobility (Cloet et al. 2014).

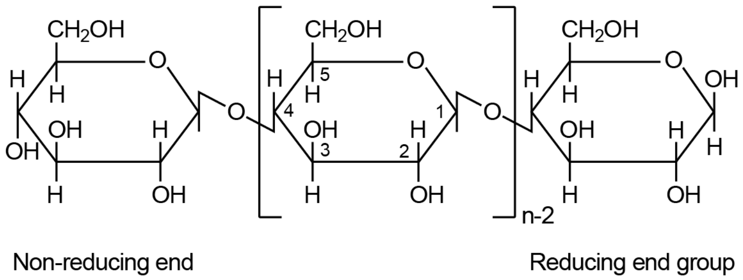

Fig. 2-6: Chemical structure of cellulose

From van Loon & Glaus (1998)

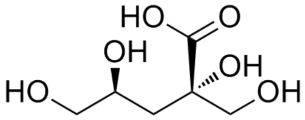

Fig. 2-7: Chemical structure of ISA

In the inventory of L/ILW organics, diethanol amine is present at only ~ 1% and considered easily degradable. It is an alkanolamine used as a surfactant and a corrosion inhibitor.

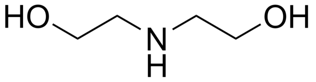

Fig. 2-8: Chemical structure of diethanol amine

Other LMW organics such as gluconic acid, ethylene diamine tetraacetic acid (EDTA), nitrilotriacetic acid (NTA) and cyanides present in MIRAM-RBG in negligeable amounts (< 0.1%; Nagra 2023b) may, however, negatively impact radionuclide retention due to the complexation of radionuclides with ligands which may increase their mobility (Cloet et al. 2014). Some of these are actually used in nuclear decontamination chemistry, especially because of their ability to bind radionuclides and remove them from contaminated surfaces (i.e., EDTA, NTA) (Keith-Roach 2008).

2.1.6 Plexiglas®

Plexiglas® is the trade name for a rigid, transparent thermoplastic poly(methyl methacrylate) (PMMA) produced by free-radical polymerisation of methyl-methacrylate. It is also known as acrylic or acrylic glass. PMMA is an ester of methacrylic acid ($CH_2=C[CH_3]CO_2H$), where the ester groups are attached to the aliphatic backbone (Fig. 2-9). Pure PMMA is rarely available and often modified to improve temperature resistance (i.e., by varying amounts of other co-monomers like butyl acrylate or additives like plasticisers), mechanical properties or cost-effectiveness (i.e., by using fillers). Negligible amounts of PMMA are included in the inventory of L/ILW organics (only ~ 1%) and are mostly found in laboratory equipment used in the nuclear industry. As an example, Plexiglas® is a lightweight or shatterproof alternative to glass that can be used as shielding against β-radiation and is part of dosimeter devices.

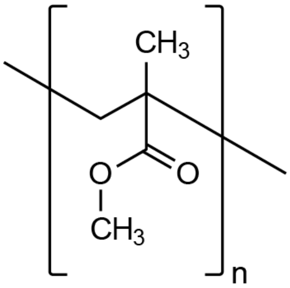

Fig. 2-9: Chemical structure of Plexiglas®

2.1.7 SPs

Superplasticisers (SPs) are the most commonly used cement admixture to improve the workability and mechanical properties of concrete and to reduce the amount of mixing water (Chernyshev et al. 2018). In Switzerland, most L/ILW is conditioned in a cement/mortar matrix and stored in concrete containers inside L/ILW emplacement caverns (cf. Sections 2.2 and 2.3 below), both containing SPs. Even if SPs are not the most abundant organic substances listed in the waste inventory (polycarboxylates correspond to only ~ 1% of the total mass inventory; Fig. 2-1) (Nagra 2023b), they are taken into account since they, and their degradation products, can potentially fuel microbial activity and act as complexing ligands, increasing the mobility of radionuclides (Chernyshev et al. 2018).

Several types of SPs are used in conditioning cement. The first generation of SPs was made from polymerised sulphonated naphthalene formaldehyde (SNF), sulphonated melamine formaldehyde (SMF) and modified ligninsulphonates (LS) (Fig. 2-10a-c). They are characterised by ionic sulphonate groups which enable SPs to be adsorbed on the positively charged surface of the cement minerals. The dispersion mechanism of cement particles is mainly attributed to electrostatic repulsion due to the negative charging of particle surfaces by the sorbed SPs molecules (Chernyshev et al. 2018). The modern generation of SPs is represented by polycarboxylate ether (PCE), consisting of a polymethacrylate backbone and polyethylene oxide side chains of varying length and density (Fig. 2-10d). In these types of SPs, the carboxylates groups are responsible for the adsorption of SPs onto the cement particles. The negative charge of the PCE, when adsorbed on the surface of the cement grains, induces an electrostatic repulsion, but the main mode of action of the PCE is a steric repulsion induced by the polyethylene oxide side chains protruding into the pore solution (Fig. 2-11) (Chernyshev et al. 2018). Due to this additional steric effect, PCEs are more effective than the former generation of SPs and are commonly used when high fluidity or a very low water/cement ratio is required. A new type of SPs, called polyaryl ether based SPs (PAE), was recently introduced and combines the structural features of SNF (e.g., aromatic rings) and PCE SPs (e.g., long side chains connected to the backbone) (Chernyshev et al. 2018). PAE is a phenol formaldehyde condensate whose backbone is an aryl condensate with aromatic rings and attached side chains of varying length and density, also containing organophosphate groups.

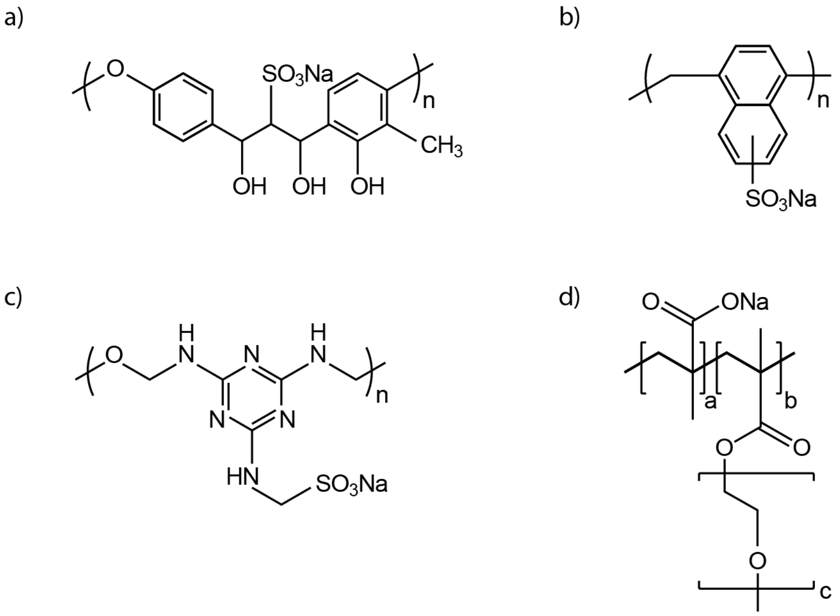

Fig. 2-10: Chemical structure of SPs

a) Monomeric units of lignosulphonate (LS); b) Sulphonated naphthalene-formaldehyde (SNF); c) Sulphonated melamine-formaldehyde (SMF); d) Polycarboxylate ether (PCE) based SPs

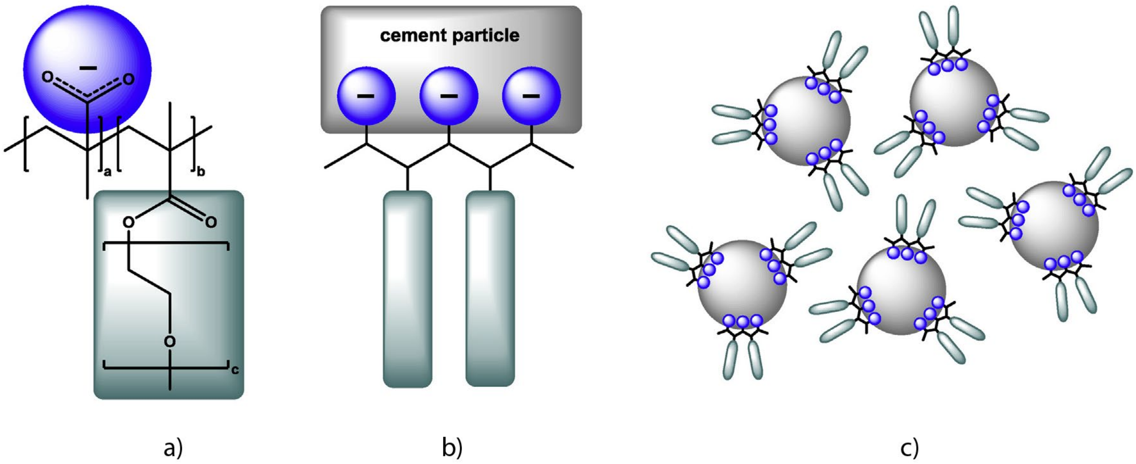

Fig. 2-11: Action of PCE SP

a) Composition of PCE SP (the carboxylate group is highlighted in dark blue and the side chain in light blue); b) Adsorption of the PCE SP on the cement particle; c) Dispersion of cement particles with the adsorbed PCE SP molecules due to steric and electrostatic action.

Figure from Chernyshev et al. (2018)

2.2 Conditioning of L/ILW organics

During waste conditioning, most of the contaminated organic materials are pressed, placed in standardised 200 L drums and embedded in a cement/mortar matrix. When the mixed waste also contains metals, sand is occasionally used to fill voidage. These drums are finally closed with a non-air-tight lid. Similar conditioning is foreseen for prognosed contaminated materials. With regard to decommissioning waste, different waste packages can be used and direct conditioning in final disposal containers is foreseen.

Since the 2000s, combustible waste with low activity has been incinerated in the Zwilag plasma plant. The incineration product, which is free of organic substances and corresponds to a borosilicate glass matrix, is then filled directly into specially prepared 200 L drums.

The conditioning of IERs differs from the other organic substances present in L/ILW. They can be solidified into three different types of matrices: cement, bitumen or styrene, according to their usage and the relevant conditioning facility. When IERs are conditioned in a mixture of cement, they are first ground (in case of bead IERs) before being placed into 200 L drums. When IERs are solidified in bitumen, they are initially dried with warm air (> 50 °C), and when IERs are conditioned in styrene, the free water is first removed from the IERs by suction. Note that conditioning in styrene corresponds to a polymerisation reaction at ambient temperature, similar to the cementation process (Wang & Wan 2015).

Within the current concept, waste packages of 200 L drums will be loaded into final disposal containers made of concrete with steel reinforcement in the encapsulation plant. After loading, these containers are backfilled with cement mortar and closed with a lid (Fig. 2-12). The interface between the lid of the drums and the container wall is designed to allow the gas to escape while slowing the inflow of water. After container closure, the concrete disposal containers will be transported to the L/ILW repository section (Nagra 2021b).

Fig. 2-12: Representation of a disposal container filled with 200 L steel drums containing L/ILW (waste packages) and backfilled with mortar

From Nagra (2022a)

2.3 Deep geological repository layout

A schematic layout of Nagra's current generic repository project is shown in Fig. 2-13. It is based on a combined repository with two disposal areas, one for spent fuel (SF) and high-level waste (HLW) grouped in an HLW repository section, and one for L/ILW and ATW placed in an L/ILW repository section (Nagra 2021b). After an extensive site selection programme, Nagra selected the Nördlich Lägern siting region for the combined repository, which will be constructed in Opalinus Clay (OPA) at a depth of around 900 m (Nagra 2024c, in prep.).

The combined repository will include the access tunnel, the operation and ventilation shafts, the operations and ventilation tunnels, the pilot facility, the test area, and the emplacement drifts for HLW and emplacement caverns for L/ILW (Fig. 2-13). The engineered barriers (i.e., waste matrix, disposal containers, caverns, structure backfilling and seals) of the L/ILW section are made of cementitious materials (Nagra 2021a). These provide high-pH conditions, limit corrosion as well as the degradation of organic substances, and associated gas generation. Moreover, the cementitious backfill is porous enough to provide sufficient gas storage capacity and will also be gas-permeable, transporting gas out from the disposal caverns, while limiting water flow. It should be noted that the cementitious materials used for the engineered barriers of the L/ILW repository section also provide strong retention of many radionuclides through sorption and limit their solubility (Nagra 2021a).

In the L/ILW repository section, the concrete disposal containers will be stacked in dead-end emplacement caverns, which are connected to the operations tunnel via a branch tunnel (Fig. 2-14). Each cavern is subdivided into several compartments. As soon as waste emplacement has been completed for one compartment of a cavern, the voids between the containers and the cavern lining will be backfilled with a specifically designed, grain-supported, highly porous mortar (Nagra 2021b).

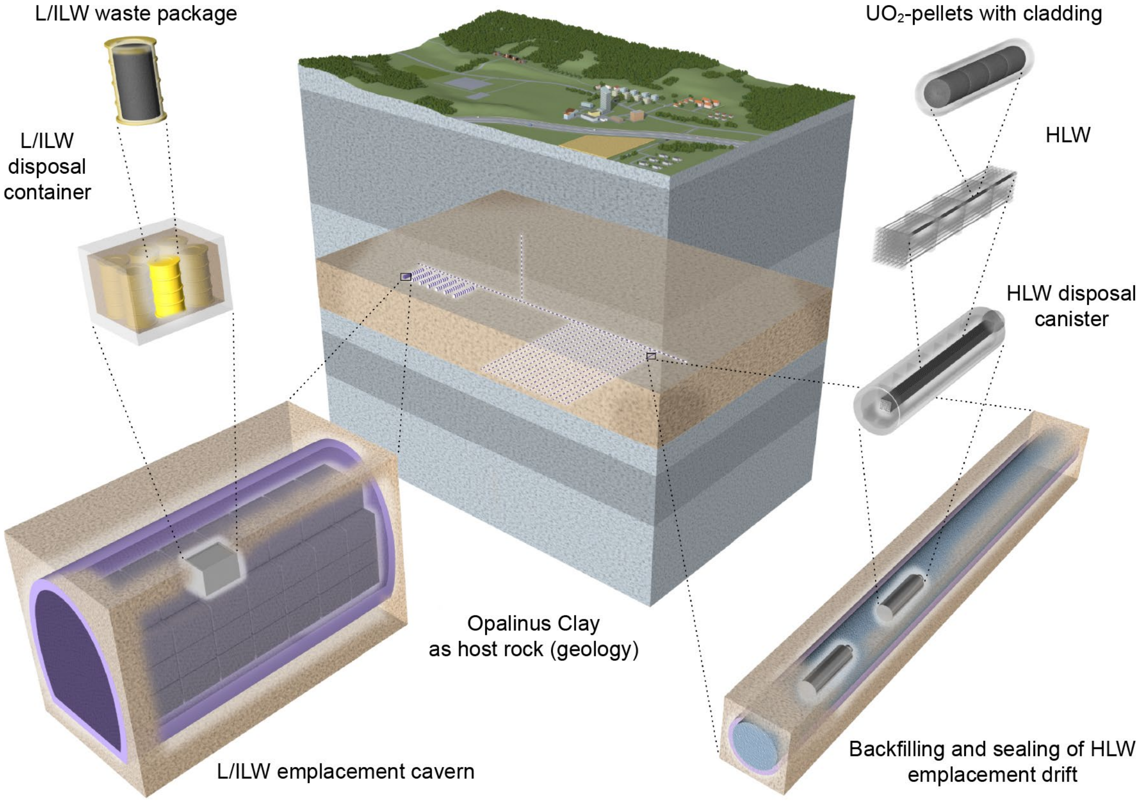

Fig. 2-13: Schematic view of Nagra's current concept for a combined repository and its main components after closure

The top part shows the overall architecture of the deep geological repository with the L/ILW repository section on the left and the HLW repository section on the right. The bottom left part shows the inner structure of an emplacement cavern for L/ILW with waste drums packed into concrete disposal containers that are themselves stacked on top of each other in the cavern. The bottom right part shows the inner structure of an emplacement drift for SF/HLW with SF assemblies loaded into disposal canisters that are themselves emplaced co-axially in the drift and surrounded by granular bentonite.

From Nagra (2021b)

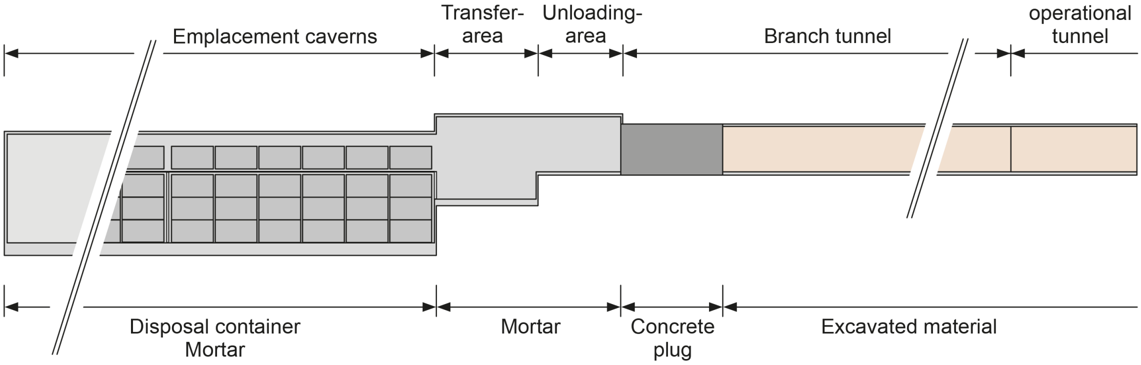

Fig. 2-14: Longitudinal section of an L/ILW emplacement cavern after closure

From Nagra (2016)

2.4 L/ILW repository near-field evolution

Based on phenomenology, the evolution of parameters and indicators that are relevant to assess the degradation processes of organic materials in an L/ILW repository are briefly summarised in this section. More details can be found in Nagra (2024b, in prep.) and Kosakowski et al. (2023).

2.4.1 Up to several hundreds of years after repository closure

Before their emplacement in the deep geological repository, L/ILW is stored in an interim storage facility (Zwilag or Zwibez). Internal degradation of organic materials will have already occurred during this time. The extent of degradation depends on the availability of water and O_2 as well as the type of waste emplaced in the drums (e.g., readily degradable organics will degrade faster) (Wieland et al. 2018, Wieland & Kosakowski 2020). The low water content within the waste matrix limits the possibility of chemical reactions during the interim storage of L/ILW. The period of interim storage is therefore expected to have little impact on the physical and chemical properties of L/ILW. It should also be noted that by the time they are emplaced in the L/ILW repository, both waste drums and disposal containers will have a negligeable heat output due to cement hydration. Hence, full integrity of the containers, waste packages and the concrete elements can be safely assumed.

Upon L/ILW emplacement, the availability of free water in the caverns will depend on the location of the materials and their initial saturation, the amount of water percolating through the host rock and the cavern lining, and the water update by capillary suction from the concrete elements and EDZ. Due to the slow inflow of porewater from the host rock, containment of the waste is ensured up to repository closure. Most of the cement pore solutions present in the emplacement caverns are assumed to be buffered at a pH of 12.5 or above (corresponding to cement-degradation stage II or lower; Fig. 2-14) due to the use of ordinary Portland cement for making the cementitious backfill material (Kosakowski et al. 2023). Moreover, anoxic conditions are expected to prevail within several hundreds of years after repository closure (Wersin et al. 2003) due to the consumption of O_2 by oxic corrosion and microbial activity. In parallel to the decrease of the O_2 concentration, other gases like H_2, CO_2 and CH_4 will start to arise in the L/ILW emplacement caverns as a result of anoxic corrosion of metals and degradation of organic materials. When gas is produced, it will mix with the remaining air and accumulate at the top of the cavern in the porous mortar. The temperature at 900 m below ground level is expected to reach temperature below 50 °C based on an ambient thermal gradient of 0.043 degree K/m and an average temperature at the ground surface of 10 °C (Nagra 2024b, in prep.). Heat in the L/ILW emplacement caverns can be produced by cement hydration in the backfill mortars. By the time of repository closure, the cement will be completely set (i.e., hydrated). The release of hydration heat from mortar used in plugs to close the repository and/or shortcrete used to stabilise underground structures would occur within a few months, leading to a relatively short-term temperature increase within and around the repository. Heat in the L/ILW emplacement caverns can also be generated by radioactive decay of the waste. As low heat emitting waste is stored in L/ILW repository, the temperature increase in the host rock is expected to be limited to around 5 – 10 °C (Leupin et al. 2016a). No thermal impact from the HLW repository section on the L/ILW one is foreseen (Nagra 2024b, in prep.).

2.4.2 In the long term

The expected evolution of the emplacement cavern in an L/ILW repository and over a period under consideration of 100,000 years is summarised in Fig. 2-15 (Nagra 2024b, in prep.). It should be noted, however, that due to the significant heterogeneity of the L/ILW inventory, all the various processes of resaturation, cement degradation, and gas generation by corrosion and degradation of organics, including evolving chemical conditions, are likely to vary in space and time (Wieland et al. 2018, Wieland & Kosakowski 2020).

The long-term chemical evolution of the L/ILW near-field is mainly controlled by the saturation of the repository, which determines the degradation of organic materials (and the associated degradation of cement), and the corrosion of metals, as all these reactions consume water (Wieland et al. 2018). Within the waste matrix, all water is expected to be consumed within a few hundred years, and the reactions in the waste packages are expected to come to a halt after 1,500 years if zeolites are present. In the absence of zeolites, the chemical evolution of the waste types is slower, extending to around 5,000 years (Wieland et al. 2018, Wieland & Kosakowski 2020). Within the caverns, partially saturated reducing conditions persist for several tens of thousands of years (Papafotiou & Senger 2016). The saturation distribution will depend on the combined effect of water percolation from the host rock, the accumulation of waste-generated gas, and gravity. In general, partially saturated conditions will persist longer in the upper part than in the lower part of the cavern (Nagra 2024b, in prep.). It should be however noted that the waste packages present at the top of the caverns will saturate faster than their surrounding backfill due to suction from the waste packages located below (Nagra 2024a, in prep.). Cement porewater present within the cement-based elements will be strongly alkaline (> pH 10) during the first 10,000 years, passivating the corrosion of metals embedded in a cement-matrix and inhibiting microbial activity (Nagra 2024b, in prep.). Carbonation at the surfaces of cement-based elements (e.g., tunnel support, infrastructural concrete elements, cement present in the backfill mortar) has already started at this point (Kosakowski et al. 2023). The cement will still be either in cement degradation stage II (i.e., portlandite buffer with a pH ~ 12.5 or above) or, for some cement formulations, where low pH cement has been applied, at the onset of degradation stage III (pH between 12.5 and 10) (Fig. 2-15). The rate-limiting factors for carbonation are the amount of CO_2 generated by the degradation of organics and its diffusion rate. Therefore, the gas-accessible surfaces of cement-based elements, which have a high porosity (infill and backfill mortar), are the first ones to be carbonated (Kosakowski et al. 2023). As the caverns will re-saturate from bottom to top, the containers in the lower rows could lose their mechanical integrity faster than those in the upper rows. Furthermore, gas overpressure, corrosion-induced fracking, tunnel convergence, corrosion of the rebars, the weight of the overlying containers, alkali-silica reaction, aggregate-cement interaction, carbonation or other mechanical damage could contribute to the loss of integrity of the waste packages within the disposal container. As a result, the waste from the waste packages can come into contact with the infill mortar of the disposal containers. If the waste includes large amounts of organics, the release of CO_2 from their degradation will lead to even stronger carbonation of the container infill mortar, which in turn will release some water available for further chemical reactions (i.e., corrosion, microbial activities). Note that carbonation is the only reaction in the near-field that releases water (Wieland & Kosakowski 2020).

The degradation of organic materials and the anoxic corrosion of metals will produce various gaseous products such as H_2, CO_2, CH_4, NH_3 and H_2S. CO_2 and H_2S are expected to react entirely with cement and/or water and are therefore not safety-relevant regarding gas pressure build-up. H_2, CH_4 and NH_3 are assumed not to react at the point of origin[1] and contribute to gas pressure build-up (Leupin et al. 2016b). Conceptual and mathematical models have been developed in SGT Stage-2 to evaluate gas generation in the L/ILW repository due to the degradation of organic materials and the corrosion of metals (Diomidis et al. 2016, Poller et al. 2016, Nagra 2024a, in prep.). The start time of the model coincides with the beginning of the post-closure phase, assuming that waste emplacement and closure of the repository occur simultaneously and that gas production from the waste itself is not delayed. All gas species produced are included under the term "gross gas production". For the period under consideration (100,000 years), H_2 originating mainly from the corrosion of metals is the dominant gas species. The second-most relevant gas species produced during this period are CO_2 and CH_4. They arise from the degradation of various organic substances (Fig. 2-16). This trend can be explained by the overall relatively small amounts of organics compared with metals in the repository (Nagra 2023b). L/ILW is subdivided into two different waste groups (AG1 and AG2) based on the potential amount of CO_2 or complexing agents that might be produced in the waste by the degradation of organic materials (Nagra 2023a). In L/ILW-AG2, CO_2 and CH_4 significantly contribute to gross gas production due to higher content of organic substances. Total gas production from L/ILW-AG2 is substantially lower than L/ILW-AG1, due to smaller content of metals present in these waste (Fig. 2-16).

---

[1] These gas species can react at other locations within the repository, such as in the access tunnel, where microbial interaction could take place.

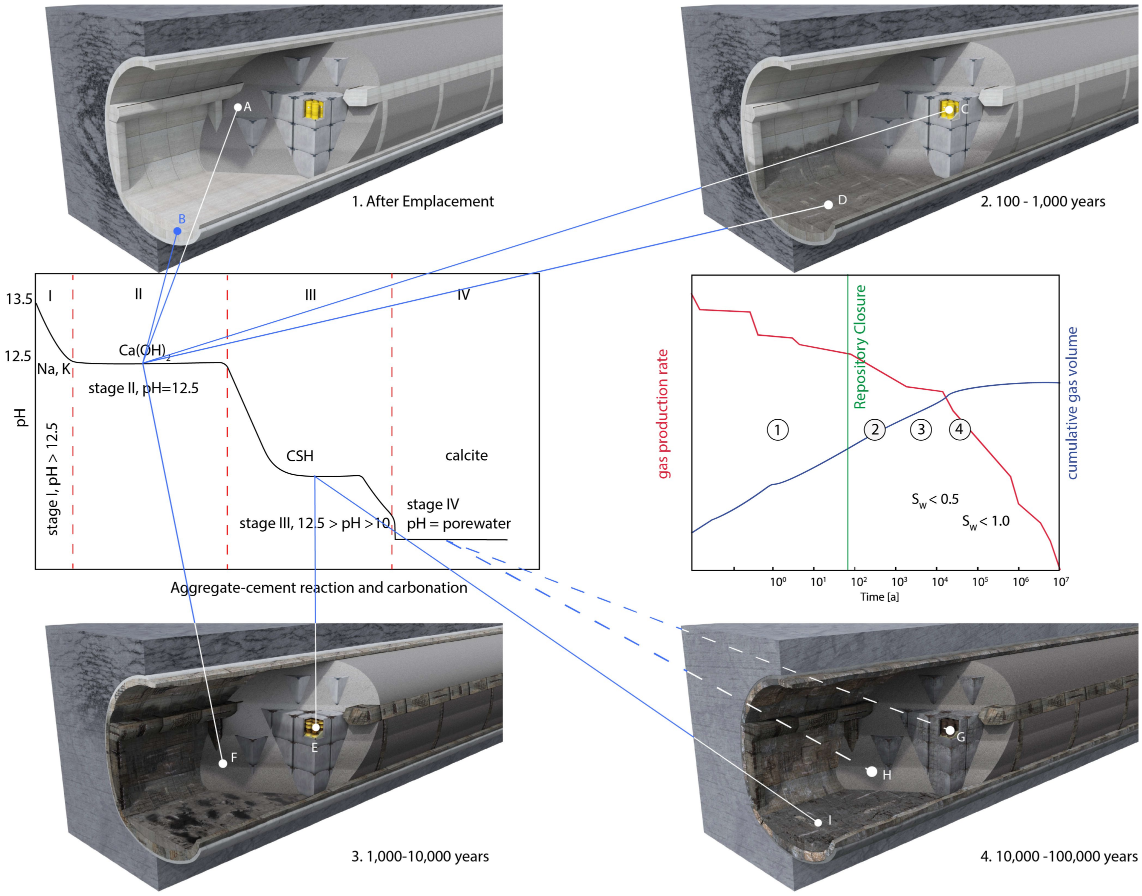

Fig. 2-15: Overview of the expected evolution of the L/ILW section of a combined repository

A: Most of the cementitious material used in the cavern cures rapidly and evolves to stage II within days to weeks. The backfill mortar is portlandite-buffered and contributes to a high-pH chemical near-field. Between the aggregates, the mortar provides interconnected gas storage space. B: The high pH of the in-situ concrete used for the sole and tunnel support is expected to remain stable for up to 1,000 years because of its low porosity and will degrade slowly. C: Metallic decommissioning waste will be embedded in a high-pH and low viscosity cement within the disposal containers. This infill mortar in the disposal container is designed such that the pH is buffered by portlandite. The high pH of the cement results in lower corrosion rates for up to about 1,000 years. D: In-situ concrete for the tunnel support will reach the end of the lifetime it has been designed for, i.e., structural support of the cavern. Towards the end of that period, portlandite will disappear, the pH will drop, and stage III will be reached. E: Most of the disposal containers in the lower rows will now reach stage III due to the porewater exchange and carbonation. F: Backfill mortar may remain in stage II for up to 1,000 years if calcareous aggregates are admixed and availability of CO_2 gas is limited. If siliceous aggregates are used, it will rapidly (< 1,000 years) reach stage III. G: Total degradation of the container infill mortar might now be reached depending on leaching rates and carbonation. H: Total degradation of the backfill mortar might now be reached by leaching of the cement depending on porewater exchange volumes. I: Due to the initially high portlandite content and low porosity, the in-situ concrete for the tunnel support might stay longer in stage III than the disposal containers and the backfill mortar. Based on Kosakowski et al. (2023) and Nagra (2024b, in prep.).

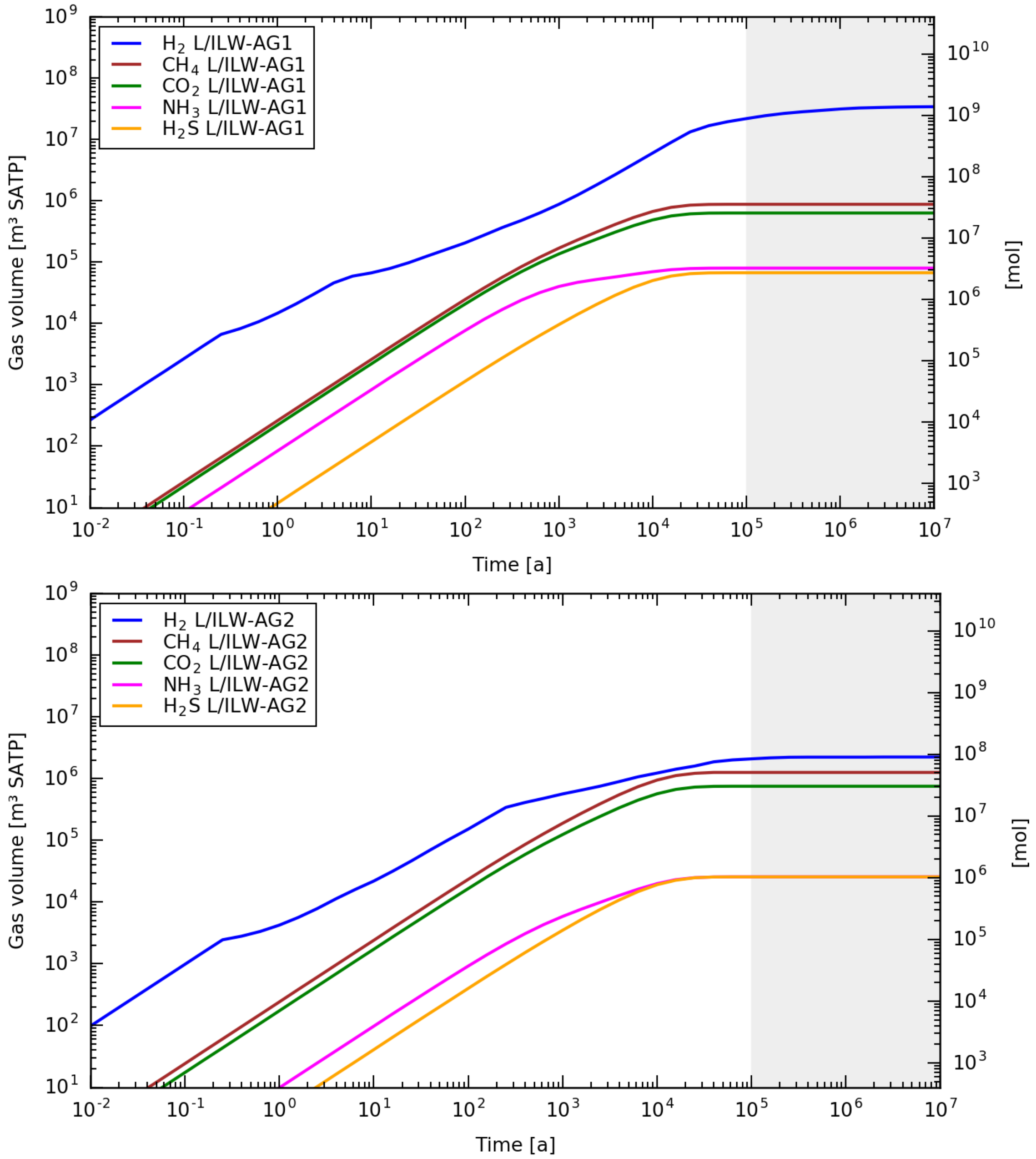

Fig. 2-16: Cumulative gross amounts of total gas produced in L/ILW

Above: L/ILW-AG1 and below: L/ILW-AGT2

From Poller et al. (2016)

In the L/ILW repository where both L/ILW and ATW are stored, the most important radionuclides contributing to the deposited dose within the waste matrices are, among others, ^{60}Co, ^{137}Cs (both γ-/ β-emitters), and ^{241}Am, ^{238,239,240}Pu (both α-emitters; only present in ATW). It should be noted that ATW makes up a minority of the waste in the Swiss waste inventory that contains only a low amount of organics (i.e., < 1% of the total mass of organics; Nagra 2023b). An estimation of the total absorbed dose of representative waste package type containing significant amounts of organic materials was calculated for the end of the period under consideration of 100,000 years. Based on the decay heat available in Nagra (2023b), the total decay energy was determined and assumed to be fully absorbed in the waste matrix, which is realistic for α and β radiation but rather conservative for γ radiation due to its significant penetration depth. The total energy decay was then integrated over 100,000 years and divided by the mass of the waste matrix to obtain the total absorbed dose for each waste package type. For a representative waste package containing IERs conditioned in a bitumen matrix with β- and γ-emitters as the main contributors, a total absorbed dose below 1 MGy was calculated for 100,000 years after repository closure. In ATW, α-emitters are dominant and generate a much larger decay heat. As a consequence, the total absorbed dose of organics present in such waste package types can reach an average of 100 MGy after the period under consideration of 100,000 years.

3 Abiotic degradation of organics

In the context of an L/ILW repository with a cementitious near-field, organics are subjected to three possible degradation pathways:

1. irradiation by radionuclide decay in the waste (radiolytic degradation)
2. hydrolysis in alkaline conditions (chemical degradation)
3. alteration at elevated temperatures (thermal degradation)

The presence of water (as dissolved phase or moisture) is an essential prerequisite for these types of degradation to take place. Radiolytic degradation results from the presence of the radiation field in the repository, while chemical (alkaline) degradation by hydrolysis may occur due to the high pH of the porewater of the cementitious near-field (van Loon & Hummel 1995). Since the temperature in a cement-based L/ILW repository is expected to be below 60 °C, thermal degradation is expected to be less significant. The three pathways of degradation will be discussed in this chapter and evaluated separately in each section, even though the processes may occur simultaneously and the relevant parameters (e.g., irradiation, hydrolysis and temperature) can influence each other. Indeed, in some experiments, the effects of irradiation, hydrolysis and temperature were found to influence each other. The results from these studies are discussed in those sections where the given parameter is expected to have the most important impact on the degradation of L/ILW organics.

3.1 Radiolytic degradation

3.1.1 Definition

Abiotic, radiolytic degradation of organics (further named radiolytic degradation) can be triggered by light, electrons (e.g., β-rays), X-rays, γ-rays, etc. In polymeric materials, high-energy radiation, such as γ-rays, gives rise to changes in their structure, thereby positively or negatively influencing the material properties (O'Donnell 1989). In addition to the nuclear context, which mainly focuses on aspects of degradation (van Loon & Hummel 1995, Filby et al. 2016, Altmaier et al. 2021), the effect of high-energy radiation on the properties of polymeric materials has been studied for industrial applications (Clough 2001, Rao 2009, Sunny et al. 2009). Numerous studies on radiation modifications of the properties of polymers (e.g., PVC, PE, PP etc.) can therefore be found in the literature.

The type of irradiation, i.e., α- (He nucleus, He^{2+}), β- (β^-: electron, β+: positron) and γ-radiation has an influence on radiolytic effects in polymers. The relevant parameter is the linear energy transfer, which accounts for the amount of energy that an ionising particle transfers to the material traversed per unit distance (Chapiro 1995). Because the relevant energy spectrum of the three types of radiation and their interaction are very different, β- and γ-radiation produce particles with a low linear energy transfer, while α-radiation leads to higher linear energy transfer (by a factor of ~ 1000). α-radiation has an energy spectrum ranging between ~ 2 and ~ 12 MeV with a typical range from 3 to 7 MeV depending on the size of the α-emitter. Due to the high energy and the strong interaction with matter, α-radiation is highly ionising, while the penetration depth is very shallow. The high linear energy transfer thus leads to severe damage to the polymeric materials, which, however, mostly affects the surface. β-radiation has a continuous energy spectrum with a radionuclide-specific, maximum kinetic energy. For example, tritium, an electron emitter, produces an energy spectrum of the β-radiation (electrons) with a maximum energy of 0.005 MeV, while ^{32}P produces an energy spectrum of β-radiation with a maximum energy of 0.605 MeV. The energies of β-electrons are thus much lower (typically < 1 MeV) than the energies of α-particles. In contrast, the penetration depth of β-radiation is greater than that of α-radiation. The energy of γ-rays from radioactive decay is greater than 0.1 MeV and goes up to approximately 8 MeV, depending on the radionuclide. Of the three types of radiation, γ-radiation has the greatest penetration depth and thus the most far-reaching effect in transferring energy to matter. In polymers subjected to low linear energy transfer radiation, i.e., β- and γ-radiation, the following chemical modifications have been observed: gas production, formation of unsaturated bonds, main-chain cleavage and/or crosslinking, depending on the chemical nature of the polymer (Chapiro 1995). O_2, if present during irradiation, induces oxidative degradation processes, which may lead to significant main-chain scission, even in polymers with a tendency towards cross-linking. For an assessment of the long-term behaviour of organics in an L/ILW repository, irradiation with γ– and α-rays is considered to have the most important effect on ageing or degradation of polymeric materials, respectively (e.g., Altmaier et al. 2021). In the Swiss L/ILW repository, the majority of the organic substances are contained in L/ILW, not ATW, and are therefore only exposed to both γ–/β-emitters (cf. Section 2.4.2). Due to the rather short half-life of the main γ–/β-emitters (i.e., 5.27 years for ^{60}Co and 30.19 years for ^{137}Cs), the main degradation induced by irradiation might occur over the first few hundred to thousand years, while less than 1% of the total mass of organics present in the ATW is expected to also be exposed to α-radiation in the long-term (i.e., $^{240}Pu_{t1/2}$ = 6,561 years) (cf. Section 2.4.2).

The adsorption of radiation depends only on the electron density of the compound or molecule, which is determined by its chemical composition and nature of the bonds. Mass density is a reasonable first approximation of the electron density (O'Donnell 1989). Many chemical bonds and groups are particularly sensitive to radiation, such as -COOH, -C-(F, Cl, Br, I), $-SO_2-$, -C=C, while aromatic groups (e.g., phenol) are less susceptible to radiolytic reactions (O'Donnell 1989). In general, polymers with aromatic groups in their molecular structure have a significantly higher radiation resistance than aliphatic polymers, regardless of the position of the aromatic groups in the chain. The aromatic rings provide a protective effect as they distribute the radiation energy across their de-localised bonding orbitals, thus dissipating the absorbed energy without cleavage of chemical bonds. Except for polymers with aromatic groups, almost all organic substances are sensitive to irradiation, their sensitivity depending strongly on the chemical composition but also on environmental factors such as the presence of O_2 (van Loon & Hummel 1995).

When radiation from a source of γ-rays, electron beams and X-rays interacts with a polymeric material, the radiation energy is absorbed by the material, and active species such as radicals are produced, thus initiating various chemical reactions (Bowmer 1979, Clough 2001, O'Donnell 1989). The radiation chemical yield is defined as the amount of radiolytic species that are formed in relation to the quantity of energy deposited by ionising energy (eV) and is expressed in terms of G-values (mol/J) (Altmaier et al. 2021, O'Donnell 1989).

Degradation of polymers is induced by the production of free radicals and hydrogen atoms due to the action of radiation:

Reaction 3-1: $R\text{-}H \rightarrow R\cdot + H\cdot$

The free radicals generated upon irradiation are often complex in nature (Dawson & Magalhaes 2012). These radicals are reactive and interact with the polymer matrix or the local environment to generate additional reactive radicals by propagation. When polymers are irradiated under inert conditions (e.g., vacuum, inert gas), the free radical reaction process are usually restricted to the polymer matrix. In the presence of air, however, the free radicals can also react with O_2, producing new, peroxy-based radicals. Thus, the dependence of degradation on dose rate may be stronger under irradiation in air (and water) than in inert atmosphere. The radicals produced in air and water are very reactive, leading to oxidative chain scission in polymers. In water, γ-radiation produces both radicals (e^-_{aq}, $H^\bullet$, $HO^\bullet$, $HO_2^\bullet$) and molecules (e.g., O_2, H_2, H_2O_2, CO, CO_2, CH_4) by radiolysis (Le Caër 2011, Mincher & Mezyk 2009, Spinks & Woods 1990). The radicals and molecules can act either as oxidants (e.g., $HO^{\bullet}$, $HO_2^{\bullet}$, H_2O_2, O_2) or reductants (e.g., e^-_{aq}, $H^{\bullet}$, H_2). Especially ·OH is a powerful oxidant that readily extracts H from C-H bonds. The presence of ferreous iron (Fe^{2+}) and hydrogen peroxide (generated from radiolysis of water) promotes the formation of ·OH. The number of radicals produced depends not only on the type of radiation (α, β, γ), but also on the dose. Radical abstraction reactions are generally exothermic and exergonic and are the thermodynamically favourable pathway to the formation of polymer backbone radicals (Allayarov et al. 2022). Radical reactions are terminated when two radicals, i.e., compounds with unpaired electrons, form an inactive product, which are either LMW-gaseous molecules or water-soluble compounds. After ionisation and excitation of the polymeric material, a variety of reactions can occur on the microscopic level (O'Donnell 1989, van Loon & Hummel 1995 and references therein):

a) Formation of chemical bonds between different molecules (crosslinking):

Crosslinking is one of the most important effects of radiation on polymers and results in an increase in molecular weight and especially in the formation of large three-dimensional molecular networks. This can already be achieved by a relatively small radiation dose (Bowmer 1979, Kerry Thomas 2007). It is the predominant reaction upon irradiation under inert conditions and when irradiating straight chain hydrocarbons (HCs). Little, if any, chain breaking takes place. Crosslinking is considerably enhanced by the presence of aromatic rings in the structure and the absence of tetra-substituted carbon atoms along the chain (Alexander & Charlesby 1954).

b) Irreversible cleavage of bonds resulting in fragmentation (scission):

Scission also has a major impact on polymers upon irradiation and leads to the degradation of the backbone chains into LMW molecules already at a relatively small radiation dose (Bowmer 1979, Kerry Thomas 2007). It predominates in a reactive environment such as air (O_2) and water, where oxidising free radicals are present. In the absence of O_2, scission can also be the primary degradation mechanism if polymers contain a large number of tetra-substituted carbon atoms along the chain. Many polymers are subject to both crosslinking and scission. However, whether a polymer predominately undergoes crosslinking or scission upon irradiation depends primarily on its chemical structure and the environmental conditions (Bowmer 1979). Scission could facilitate the biodegradation of some organic polymers by generating LMW molecules used as substrates (Negrin et al. 2018).

c) Formation or disappearance of unsaturated (C=C) bonds:

In addition to the processes of crosslinking and scission, the structure of the polymer can also change during irradiation, giving rise to variations in the manner by which the energy is transferred to the material. Properties of polymeric materials can also be affected such as the mechanical properties, thermal stability, chemical resistance, melt flow, brittleness, processability and surface properties.

d) Formation of degradation products:

It is generally observed that irradiation of polymers leads to the production of small radicals such as ·H, $\cdot CH_3$, ·CO, $\cdot CO_2$. These radicals can recombine with the polymer itself or with each other, the latter resulting in the formation of H_2, CO, CO_2, CH_4, C_2H_4 (e.g., Kudoh et al. 1996, Ferry et al. 2014, Altmaier et al. 2021, O'Donnell 1989). The formation of these gaseous species on the microscopic level is the result of atom or side-chain abstraction and occurs on the microscopic level at the end of the process, following ionisation and excitation of a polymer. The composition of the gas phase largely reflects the composition of the polymer, especially the chemical nature of the side groups in the repeating units. The main gas produced by the radiolytic degradation of most polymers under reducing conditions is H_2, while CO and CO_2 are mainly produced under oxidising conditions (Altmaier et al. 2021). The yields of CO and CO_2 formation can increase with the dose, itself influenced by the accumulation of oxidation products. However, CO and CO_2 can also be produced under anoxic conditions, as some polymers have C-O or O-O-O bonds in their structure (Altmaier et al. 2021). Irradiation of polymers (and organics in general) thus mainly leads to the formation of small gaseous molecules (i.e., H_2, CO, CH_4, C_2H_4, HCl), which contribute to gas formation. Generated gases can, in turn, react with the cementitious backfill material (CO_2, HCl) and accelerate steel corrosion (HCl). Dissolved LMW-oxidised species can also be produced by the radio-oxidation of the material and released when polymer waste comes into contact with water. These species can be complexing ligands and affect the retention of radionuclides in the near-field of the L/ILW repository (van Loon & Hummel 1995) or be used as substrates for microbial activities.

The dose rate (expressed, e.g., in terms of Gy/h) and the total absorbed dose (expressed, e.g., in terms of Gy) are the two parameters used to characterise radiation exposure in experimental investigations. The study of the effect of irradiation on organic substances often requires radiation sources with a high dose rate (range several tenths of kGy to MGy) to conduct the experiments within a reasonable period of time. The results of such high dose rate experiments are often extrapolated to repository conditions where the dose rate is about 1,000 – 10,000 times lower, a procedure that has often been criticised. According to O'Donnell (1989), it seems unlikely that such dose rates should occur due to the low spatial density of ionisations and excitations. The main effect of dose rate likely results from a rise in temperature and, in case of irradiation performed in air and water, from the control of degradation by O_2 diffusion (O'Donnell 1989, Dawson & Magalhaes 2012). In this case, exposure to high dose rates over short periods of time results in a high rate of O_2 consumption in the matrix of an irradiated polymer component, which is much higher than the rate of O_2 supply. Thus, oxidative degradation is limited to surface components. However, at low dose rates over long periods of time, the O_2 supply rate is sufficiently high to allow its continuous consumption. This allows oxidative degradation to occur uniformly throughout the component. For these reasons, a component may appear to be resistant to high radiation doses when tested at high dose rates but exhibit unacceptable degradation when exposed to much lower doses (Dawson & Magalhaes 2012).

The total absorbed dose thus appears to largely determine the amount of degradation products that will be formed regardless of whether this dose was absorbed in a short period of time at high dose rate or over a longer time at low dose rate. Since bonds must be broken, a minimum amount of energy (radiation intensity) is required. Correspondingly, a minimum dose rate is required to initiate the degradation process (van Loon & Hummel 1995). The formation of degradation products was observed to linearly increase in the range of low doses (typically < 3 – 5 MGy), while it reached a level of saturation at high doses. For example, the instantaneous yields $G_0(H_2)$ and $G_0(HCl)$ from PVC degradation were found to decrease as the dose was increased (Altmaier et al. 2021).

Furthermore, the amount of absorbed energy (total dose) affects temperature. An increase in the total dose leads to a temperature increase in irradiation experiments carried out in air or solution, since the chemical reactions induced by the irradiation of polymers only consume a small portion of the absorbed energy (O'Donnell 1989). Most of the energy is then converted into heat. For example, 0.1 Mgy of energy absorbed in water results in a temperature increase of at least 24 °C in a polymer (O'Donnell 1989). Note that the rates of chemical reactions increase with temperature as more molecules have energies in excess of the activation energy. This can promote radiolytic secondary reactions in polymers. The above considerations show that the total dose (i.e., absorbed energy) appears to be an important parameter determining the extent of radiolytic degradation of polymers, as it initiates inter- and intramolecular chemical reactions such as scission or cross-linking, etc.). The total dose also affects the environment of polymers, e.g., the number of radicals in air and water as well as temperature rise.

Several parameters were reported to influence the extent of the radiolytic degradation of organics (Altmaier et al. 2021): (i) the chemical composition of the material, including fillers and additives; (ii) the total dose over time; (iii) the chemical environment (e.g., air, alkaline conditions); (iv) the relative humidity; and (v) the temperature.

The following sections provide an overview on the current state of knowledge on the radiolytic degradation of the various polymeric materials to be disposed in an L/ILW repository, taking into account some of the parameters listed above that may influence the degradation of polymers by radiation. It should be noted that the focus of the discussion is on mechanisms and processes that may be relevant to an assessment of the long-term behaviour of polymers under L/ILW repository conditions. Radiation chemistry and radical reactions are not detailed as they have been reported elsewhere (Chapiro 1962, Dole 1973, Ivanov 1992). In addition, the following sections do not include a systematic compilation of radiolytic yields for gas production (G-values). They have been reported in Nagra (2023b).

3.1.2 IERs, PS and styrene

Over the past 50 years, radiolytic degradation of IERs has been extensively studied to determine the stability of resins for nuclear applications and the formation of degradation products upon irradiation at doses relevant to exposure in a cement-based L/ILW repository, as well as their influence on radionuclide mobilisation in the near-field (Altmaier et al. 2021, van Loon & Hummel 1995, Filby et al. 2016, Dawson 2013b). The IERs can be subject to additional degradation caused by the reactive species generated by water radiolysis. In the environment of a cementitious L/ILW repository, the combined effects of hydrolytic degradation by chemical action at high OH^- concentration and radiolytic degradation cannot be excluded.

Degradation mechanism and products

The degradation products result from the cleavage of the bonding between the surface functional groups and the PS backbone and from the formation of alkyl radicals (Altmaier et al. 2021, van Loon & Hummel 1995, van Loon & Hummel 1999a, van Loon & Hummel 1999b). In the case of the strongly acidic cation-exchange resins, sulphate (SO_4^{2-}) is the main degradation product upon irradiation (Swyler et al. 1983, van Loon & Hummel 1995, van Loon & Hummel 1999b, van Loon & Hummel 1999a). SO_4^{2-} is formed by splitting off the sulphonic acid groups from the backbone during irradiation and the subsequent oxidation of the SO_3 radical (van Loon & Hummel 1995):

Reaction 3-2: $\cdot SO_3^- + H_2O \rightarrow SO_4^{2-} + 2H^+ + e$

This reaction produces H^+, which is responsible for the drop in pH observed by van Loon & Hummel (1995) and van Loon & Hummel (1999a). The direct radiolytic scission of the SO_4^{2-} groups and subsequent hydrolysis of the radical products is not highly dependent on the pH environment and resin loading (Swyler et al. 1983).

In the case of strongly anionic IERs, the formation of trimethylamine was observed to be the major product formed during γ-radiolysis (Hall 1963, Ahmed et al. 1966, Swyler et al. 1983, van Loon & Hummel 1995, van Loon & Hummel 1999b). Similarly, as cationic IERs, the trimethylamine is split off from the PS backbone during irradiation:

Reaction 3-3: $R\text{-}CH_2\text{-}N(CH_3)_3^+OH^- \rightarrow R\text{-}CH_2\text{-}OH + N(CH_3)_3$

Trimethylamine was found to be further degraded to dimethylamine, which is then degraded to methylamine and ammonia (Hall 1963, van Loon & Hummel 1995, van Loon & Hummel 1999b).

Swyler et al. (1983) showed that γ-irradiation of IERs also releases gases. H_2 is the principal radiolytic gas produced, while CO, CO_2 and CH_4 are produced as minor gaseous species. $N(CH_3)_3$ was detected in the gas phase of degraded anionic-exchange resins. The atmospheric composition (i.e., irradiation in air or inert atmosphere) had no significant effect on gas composition. The release of H_2 from anionic-exchange resins was found to be significantly greater than from cationic-exchange resins. The study by Traboulsi et al. (2013) supports the earlier findings of Vinhas et al. (2003b).

O'Donnell et al. (1979) and Bowmer (1979) investigated the influence of O_2 on radiolytic changes in the molecular properties of PS by irradiation in air (dose rate: 4.7 kGy/h and 40 kGy/h, respectively; total absorbed dose: up to 0.9 and 2 MGy, respectively). On the molecular scale, crosslinking was found to be the dominant process, but increased scission was observed by reaction with O_2. Thus, an O_2 environment leads to enhanced scission at the expense of crosslinking, thus indicating further that crosslinking is the dominant process under anoxic conditions.

Influence of total absorbed dose and dose rate

The total absorbed dose is assumed to have a strong influence on the degradation process and the type of degradation products formed in contrast to the dose rate (van Loon & Hummel 1995). The aromatic benzene rings provide a good stability to ionising radiation. Cationic-exchange resins are expected to show strong radiation resistance up to maximal tolerated doses between 1 and 10 MGy, whereas radiation stability is lower in the case of the anionic-exchange resins with an identical PS backbone, already leading to degradation between absorbed doses of 0.1 and 1 MGy (Pillay 1986, van Loon & Hummel 1995, Traboulsi et al. 2012). Swyler et al. (1983) showed that the production of SO_4^{2-} increases linearly with a dose of up to ~ 4 MGy (or Mrad), while the production rate slowed down when the dose exceeds 4 MGy (Fig. 3-1). Swyler et al. (1983) also showed in their study that the gas pressure linearly increased with the dose (dose rate: 16 kGy/h; total absorbed dose: 2.4 – 16 MGy), mainly due to an increase in H_2 production.

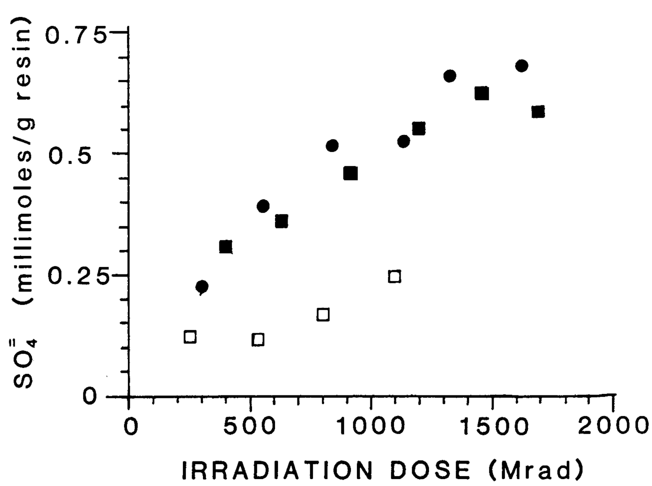

Fig. 3-1: Formation of SO_4^{2-} from a cationic IER (IRN-77) as a function of increasing dose

Range between 2 and 17 MGy. The different symbols refers to the IRN-77 loaded with different cations.

From Swyler et al. (1983)

Concerning anionic-exchange resins, the formation of degradation products is, as in the case of cationic-exchange resins, proportional to the increase in dose, but only up to a total dose of ~ 0.5 MGy. Afterwards, the production rate decreases with increasing dose (Fig. 3-2). The deamination of anionic-exchange resins can occur by direct action of radiation on the IERs or by attack of radiolysis products of water in contact or associated with the resin (Ahmed et al. 1966, van Loon & Hummel 1995). The relative importance of the two processes depends on the water content of the resin (Ahmed et al. 1966).

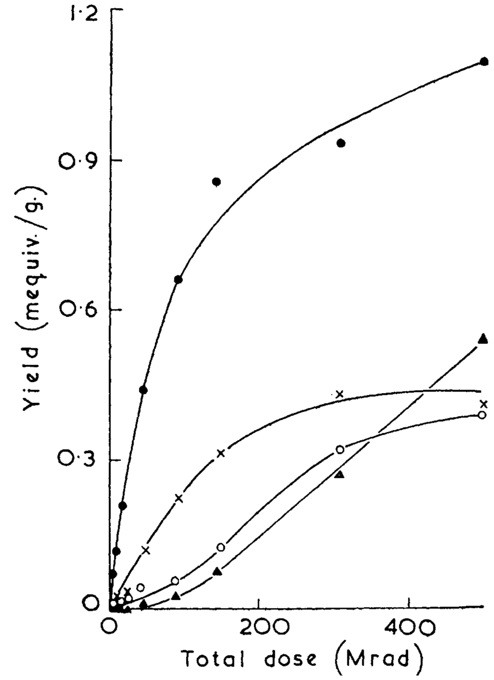

Fig. 3-2: Yield of basic degradation products

Filled symbol: trimethylamine, cross: dimethylamine, open symbol: methylamine, filled triangle: ammonia) as a function of total dose (range between 0.01 and 5 MGy) published by Hall (1963).

Influence of alkaline conditions

Van Loon & Hummel (1995) and van Loon & Hummel (1999a) performed irradiation experiments with two cationic-exchange resins in alkaline solutions (pH 12.7) (dose rate: 8.5 kGy/h; ^{60}Co source; total absorbed dose: 1.7 MGy). The IERs were converted into the Na form before they were used in the experiments. The formation of mainly SO_4^{2-} and dissolved organic carbon (DOC) was observed. A small portion of carbon (10 – 20%) was present in the chemical form of oxalate. The concentrations of Na^+, SO_4^{2-}, DOC, dissolved inorganic carbon (DIC), and oxalate were significantly higher in the irradiated systems than in the non-irradiated control solutions. The increase in the oxalate concentration could not be explained fully. The authors postulated that oxalate might have been formed by the reaction of two $\cdot COO_2$ radicals produced by the radio-oxidative degradation of the IERs. The rather low ratios of DOC/SO_4^{2-} observed in the study support the idea that the radiolytic degradation of the IERs is the result of the splitting-off of SO_4^{2-} groups from the organic backbone, while the organic backbone itself was not subject to major degradation due to its aromatic character. The DIC (CO_3^{2-}) measured in solution was expected to be formed by CO_2 generated from the organic matrix over irradiation.

Van Loon & Hummel (1995) and van Loon & Hummel (1999b) investigated the behaviour of strongly basic anionic-exchange resins (converted to the OH form) and mixed-bed IERs (i.e., IERs containing both sulphonic acid groups for cation exchange and quaternary ammonium groups for anion exchange), under the same experimental conditions during irradiation with a ^{60}Co source. During degradation of the anionic-exchange resins, mainly ammonia, amines and DOC were formed in accordance with the principal degradation mechanism. Up to 50% of the DOC could be identified as methyl-, dimethyl- and trimethylamine. Interestingly, the degradation of the mixed-bed IERs did not produce a mixture of the degradation products from the degradation of the cationic- and anionic-exchange resins as expected. Changes in pH and Na^+ concentration of the irradiated solutions indicated that both the surface functional groups $-SO_3$ and $-N(CH_3)_3$ were split off from the PS backbone. However, only a small amount of SO_4^{2-}, the main degradation product of cationic-exchange resins, was quantified. Furthermore, the amount of quaternary amines released during degradation was low. The authors concluded that other degradation products were formed during irradiation of the mixed-bed IERs and that the low concentrations of both SO_4^{2-} and amines were due to recombination of the radicals produced by both types of IERs, resulting in the formation of poorly characterised sulpho-amine products. Analytical evidence for such compounds could not be provided. Rébufa et al. (2015) confirmed this finding by observing that the mixed-bed IERs were globally more stable than their individual components in terms of H_2 and amine production.

Dawson (2013b) investigated the radiolytic degradation of a sulphonated styrene-divinylbenzene cationic-exchange resin in saturated and buffered alkaline solution ($Ca(OH)_2$, pH 12.4), (dose rates: 0.049 and 4 kGy/h; total absorbed dose: 0.15 and 10 MGy). Additional degradation experiments were carried out in glass vessels in air and under N_2 under the same irradiation conditions. The results show a drop in pH in the water in which the IERs were irradiated, while no change in pH occurred in the $Ca(OH)_2$ buffered alkaline solution. High TOC concentrations were measured in the non-irradiated samples and after irradiation of the Amberlite resin in alkaline solution (TOC ranging from 12 to 280 mg/L). It should, however, be noted that the TOC was found to be lowest in the systems irradiated with the highest absorbed dose (10 MGy). TOC was attributed to the presence of organic compounds with low carbon chain length (< C5). Only the cationic-exchange resin containing $Ca(OH)_2$ solution irradiated to 0.15 MGy at 49 Gy/h was analysed for the presence of individual organic compounds. Several HCs with the number of carbon atoms ranging from 5 (C5) to 22 (C22) were detected, e.g., tetrachlorethylene, dimethyl-dodecadienone, tetrachloro ethane, limonene, methyl-hexadecane. A few additional compounds could not be identified. H_2, CH_4, CO, CO_2, C_2H_6, C_2H_4 and ethyne were the gaseous products identified during irradiation of the IERs. No systematic trend in their concentrations was observed upon irradiation in air or N_2, respectively.

Influence of temperature

No studies have examined the influence of temperature on the radiolytic degradation of IERs. For PS, the temperature dependence of radiolytic effects was studied by Tabata et al. (1996) and Bowmer et al. (1981) under γ-irradiation (dose rate not stated; total adsorbed dose: up to 30 MGy) and under vacuum. Tabata and co-workers observed that the production of H_2 was not dependent on temperatures below ~ 35 °C. At higher temperatures, an influence of the crystallinity and structure of PS on the hydrogen yield ($G_0(H_2)$) values was observed. Crosslinking was the dominant degradation mechanism at lower temperatures, while chain scission was more efficient at ~ 75 °C and above. Bowmer et al. (1981) irradiated PS at 100 and 150 °C in air (dose rate: 25 kGy/h; total absorbed dose: 0.1 – 0.8 MGy) and observed that scission increased with temperature, while crosslinking was almost not affected by temperature. This finding suggests a strong dependence of the breakdown of aromatic polymers on temperature: crosslinking dominates at ambient temperature, while scission becomes significantly more important at elevated temperature.

Influence of humidity

Ichikawa & Hagiwara (1973) investigated the effects of the water content of the IERs and the species adsorbed by the cationic-exchange resins on their radiation stability. The degradation of wet IERs was assumed to result from either the action of H atoms (·H) produced by radiolysis of the IER matrix or from hydrated electrons formed during radiolysis of water. IERs with different water contents (range 1 – 305 mg H_2O/meq IERs) were loaded with different ions (H^+, Na^+, K^+, NH_4^+, Ca^{2+}, Mg^{2+}, Mn^{2+}, Cu^{2+}, Fe^{3+}, UO_2^{2+}) and exposed to γ-irradiation (dose rate: 1.3 kGy/h; total absorbed dose: 0.3 – 1.8 MGy). Experiments carried out on IERs with different water contents showed that only water molecules associated with the IER matrix (e.g., H_2O surrounding functional groups) contribute to the radiolytic degradation of the IERs, while the contribution of the reducing species formed by radiolysis of water is limited. The authors postulated that hydrated electrons probably cannot exist in such moist IERs because the number of water molecules in the IERs is too small for solvating electrons to be stabilised. Therefore, H atoms formed by radiolysis of water molecules in the IERs or of the IERs themselves lead to their degradation. The authors also observed that the IERs loaded with H^+, Na^+, K^+, NH_4^+, Ca^{2+}, Mg^{2+} and Mn^{2+} exhibited much lower radiation stability than the samples loaded with Cu^{2+}, Fe^{3+} and UO_2^{2+}. This result was attributed to the reduction of the latter cations during irradiation (electron scavenging), thus inhibiting the radiolytic damage of the IERs.

Swyler et al. (1983) concluded that the acidity and radiolytic attack can be reduced, but not eliminated, by drying the cationic-exchange resins. They further concluded that in water-saturated cationic-exchange resins, scission of the SO_4^{2-} functional groups is largely due to direct radiolysis. However, radicals generated by radiolysis of water, with the exception of the H atom, do not appear to play a dominant role in initiating radiolytic scission of the IERs. Nevertheless, degradation of IERs involving aqueous radiolysis products other than peroxide (H_2O_2) cannot be excluded. In saturated IERs, scission is considered to predominate over crosslinking as degradation mechanism, which was modelled in terms of first- and second-order kinetics.

Baidak & LaVerne (2010) observed an increased H_2 production with increasing water content of anionic-exchange resins. The IERs were prepared in different anion forms (NO_3^-, Cl^-, OH^-), which are the charge-compensating anions of the quaternary ammonium $R\text{-}N(CH_3)_3^+$ group, and then exposed to γ-irradiation (dose rate: 3.79 kGy/h; total absorbed dose: up to 0.5 MGy). The charge-balancing anions were found to be responsible for the difference in the water loading of the IERs in environments with different relative humidity. The authors also observed an influence of different electron scavengers (NO_3^-, N_2O, O_2) on H_2 production and concluded that solvated electrons play an important role in the formation of H_2 from the IERs. Solvated electrons are increasingly stabilised with increasing water content.

Leaching of IERs

Altmaier et al. (2021) summarises the results of studies conducted by the CEA (Commissariat à l'énergie atomique et aux énergies alternatives) on the leaching behaviour of cationic, anionic and mixed-bed IERs (Traboulsi et al. 2012). The total organic carbon (TOC) was determined in a leaching solution released from an anionic resin previously irradiated under "dry" and anoxic conditions to a total dose of 4 MGy. The release of water-soluble compounds was found to occur rapidly after contacting the irradiated IERs with pure water. The cumulative quantity of TOC changed little as a function of the leaching time. The water-soluble compounds identified were acetic acid, formic acid, trimethylamine, dimethylamine, methylamine and NH_4^+.

Influence of radiation type

Enomoto et al. (2008) investigated the effect of α-radiation (5 MeV ^{4}He atoms, dose up to 20 MGy) on the degradation of anionic-exchange resins and compared the results with those obtained with γ-irradiation at a lower dose (dose rate: 6 kGy/h; total absorbed dose: up to 0.05 MGy) at ambient temperature. The IERs were in the Cl^- and NO_3^- forms and had different water loadings. Regardless of the type of IERs, H_2 production increases with increasing water loading for both types of ionising radiation, as the effect of water radiolysis becomes more important. It should however be noted that H_2 production is higher for α-radiation. Despite these last two points, it can be generally assumed that IERs had a general high radiolytic stability for both types of radiation.

No information about radiolytic degradation kinetics is available for IERs, PS and styrene.

3.1.3 PVC

Radiolytic degradation of PVC and associated additives have been extensively studied, particularly for industrial (e.g., use in NPPs) and medical applications. The range of commercially available PVC formulations is very variable, especially due to the addition of various additives (plasticiser, stabilisers, fillers, pigments, flame retarders). The wide range of additives makes it difficult to predict the radiolytic effects in a range of commercial samples even if the tests are carried out under identical irradiation conditions (Smith et al. 2013). The following sections illustrate the most important aspects that have been addressed in irradiation studies with PVC and its additives.

Degradation mechanism and products

During irradiation of PVC (both in vacuum and exposed to air), a common observation is the formation of H_2, HCl, CH_4, CO and CO_2 (Miller et al. 1956, Decker 1976, Bacaloglu & Fisch 1995, Colombani et al. 2007, Altmaier et al. 2021). The formation of conjugated C=C double bonds (polyene structure) from single C-C bonds is responsible for HCl release (Fig. 3-3) (Miller et al. 1956). A similar mechanism leads to the detachment of H_2, i.e., replacing single C-C bonds by conjugated C=C double bonds.

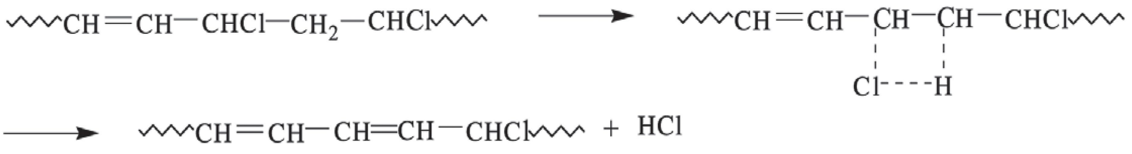

Fig. 3-3: Release of HCl and generation of unsaturated bonds in PVC

From Vinhas et al. (2003b)

The effect of irradiation on PVC was explained on the basis of free-radical, chain dehydrochlorination reaction, initiated by the exposure to radiation (Miller et al. 1956). The primary free-radical process involves scission of the C-Cl bond to produce the stable $-CH_2{\cdot}CH-$ polymer radical. Similarly, it has been postulated that the $-CH_2-{\cdot}C(Cl)-$ type radical is generated by the attack of alkyl radicals, resulting in the preferential abstraction of hydrogen atoms.

Salovey et al. (1969) studied the oxidative degradation of PVC by irradiating pure and additive-containing PVC with a beam of 1-MeV electrons at 15 °C in air or under vacuum (dose rate: 2.4 MGy/h; total absorbed dose: 0.08 MGy). In the absence of reactive additives, the concentration of polyene-free radicals was found to be stable, and an increase in the concentration of the conjugated double bonds was observed. Dehydrochlorination proceeds via a radiolytic radical chain mechanism.

Decker (1976) used non-stabilised commercial PVC, which was irradiated at 25 °C in an atmosphere with a known amount of pure O_2 (dose rates: 0.133 and 1.64 kGy/h; total absorbed dose: up to 2.47 MGy). The results show that polyene chains with long sequences are formed as a consequence of dehydrochlorination in an O_2-free environment. Radio-oxidative degradation reduces the formation of these long sequences due to oxidative attacks on the conjugated double bond system. In the presence of O_2, the radicals formed by γ-irradiation react very rapidly with the O_2 to form peroxy radicals. This leads to the formation of carbonyl and hydroxyl groups and the oxidation of the double bonds. Chain scission was assumed to be the dominant degradation process due to the high radiochemical yield for O_2 consumption.

Colombani et al. (2007) studied the irradiation of PVC at high doses (dose rate: 0.6 kGy/h; total absorbed doses: up to 4 MGy; room temperature) under anoxic (He atmosphere) and oxic (O_2 atmosphere) conditions. The authors observed different degradation mechanisms under anoxic and oxic conditions. Under anoxic conditions at high doses, radiolytic degradation of PVC was found to occur in three main reactions: i) formation of alkyl radicals; ii) formation of polyenic sequences (i.e., polyenes: unsaturated aliphatic HCs); and iii) crosslinking. The propagating and termination reactions induced by the radicals lead to the formation of polyenic sequences in PVC and crosslinking. Under oxic conditions at high doses, however, peroxyl radicals play an important role, and the degradation mechanisms can be described by two main reactions: i) formation of peroxyl radicals; and ii) scission. Peroxyl radicals are produced by the reaction between O_2 and alkyl radicals. The propagation reactions involve scission, which leads to a reduction in the average molecular weight of PVC and the release of aldehydes, HCl and/or carboxylic acids. It should be noted that the gas phase was not analysed in this study. The proposed mechanism of oxidative degradation supports the earlier analysis of reaction pathways by Bacaloglu & Fisch (1995) who indicate that the pathway for the oxidative degradation of PVC involves the formation of polyenes, reacting with O_2 to generate peroxides that decompose rapidly to highly reactive peroxy radicals. These further generate macro-radicals, which in turn initiate further degradation. Note that peroxide as well as $O_2^{\bullet}$ and $H^{\bullet}$ are also important radiolytic products formed during radiolysis of water. The study of Colombani et al. (2007) also indicates that scission is less important compared to crosslinking under anoxic conditions, while scission dominates under oxic conditions. Scission produces LMW-aliphatic HCs (e.g., carboxylic acids, aldehydes, alcohols). Under anoxic conditions, radiolytic degradation of PVC results in the formation of predominately gaseous species. In contrast, under oxic conditions, oxidised HCs are additionally produced and leached from the polymer structure once in contact with water.

Influence of total absorbed dose and dose rate

At low dose rates, the amount of gas produced was found to depend on the chemical composition of the material, in particular the presence of additives (plasticisers, stabilisers), and the total dose. Hegazy et al. (1981) observed in their study (dose rate: 10 kGy/h; total adsorbed dose: up to 0.85 MGy, room temperature) that the amounts of HCl and H_2 produced in vacuum and air were comparable and increased together with the total dose. Small total doses of up to 0.025 MGy at a dose rate of 10 kGy/h were found to induce no noticeable change in the macroscopic properties of the polymeric material, while radiolytic degradation could be attested by the formation of gaseous products (H_2, CO_2, CO, small alkanes) (Semenenko 1973).

The results reported by Vinhas et al. (2003b) indicate a proportional increase in the degradation index of PVC with increasing dose and an effect of plasticisers on radiation stability (Fig. 3-4). This effect is further discussed in the following subsection "Influence of additives".

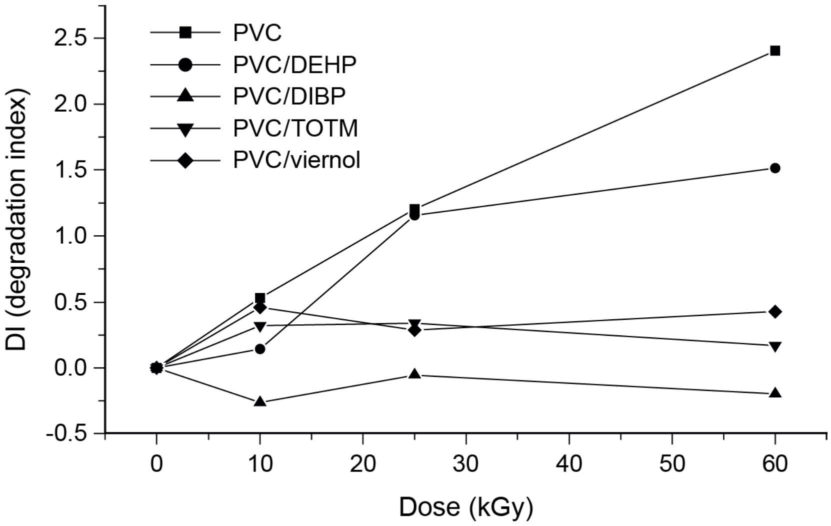

Fig. 3-4: Increase of the degradation index of pure and plasticised PVC with increasing dose

From Vinhas et al. (2003b)

Dawson (2013c) determined the amount and type of gas species released during irradiation of plasticised PVC under dry conditions in an inert atmosphere (N_2) and in air at room temperature and various dose exposures (dose rates: 4 Gy/h, 42 Gy/h and 4 kGy/h; total absorbed dose: 0.15 MGy and 10 MGy). The results show only a limited effect of the dose rate on the concentration of the gases. Increasing the dose rate by a factor of ~ 100 (from 42 Gy/h to 4000 Gy/h) to absorb a total dose of 0.15 MGy increased the concentration of the gases by a factor of ~ 10 at most. The largest difference was observed for H_2 (increase by a factor of ~ 10), while for the other gaseous species, the gas concentration generally increased by less than a factor of ~ 4. The difference in the concentration of the gaseous species in the samples exposed to N_2 or air was small (typically less than a factor of ~ 2). Thus, there is an effect of dose rate, but not in proportion to its increase. In contrast, the effect of the total dose is more pronounced. Increasing the total absorbed dose from 0.15 MGy to 10 MGy (factor of ~ 70) increased the total amount of gas released by a factor of ~ 20 in N_2 and ~ 35 in air. The increase is not proportional, but the effect of the total absorbed dose increase is clearly greater than that of the dose rate.

In contrast to the general conclusion from other studies, which indicate that the dose rate plays only a minor role in radiolytic degradation, Clough & Gillen (1981) stated: "Experimental observations made during the past three decades on radiation experiments performed under N_2 or vacuum have led to a general conclusion (often cited in review articles) that dose rate effects are not important under inert atmosphere. Clearly this conclusion is not valid for radiation experiments in the presence of O_2". The statement was based on degradation studies with aged PVC under irradiation in air (dose rate: 0.04 – 9.38 kGy/h; total absorbed dose: up to 0.5 MGy). The authors attributed the predominant cause of the observed dose rate effects to the peroxide breakdown mechanism. Peroxides are formed in reactions initiated by the radiation and found to be an important radiolytic oxidant in irradiated water. Other effects such as O_2 diffusion were also suspected to have a certain impact.

In summary, the dose influences the yields of gas formation, as $G_0(H_2)$ and $G_0(HCl)$ were found to increase together with the dose. It should be noted that the dose rate has only a limited influence on gas formation in inert atmosphere, but a pronounced effect in air. For the other gases and particularly those produced by the oxidative degradation of materials (CO, CO_2), the yields may also increase with the dose, which is a result of the accumulation of oxidation products (Altmaier et al. 2021). It can further be assumed that the amount of non-volatile degradation products also increases with dose. Furthermore, there is no direct evidence that the mechanism of degradation changes significantly with dose.

Influence of additives

Radiation stability was found to be enhanced by the incorporation of additives. For instance, PVC could be stabilised under irradiation by adding epoxy compounds, exhibiting a protective effect under γ-irradiation due to HCl capture in Lerke & Szymański (1983). Similarly, Szymański & Śmietańska (1979) observed a synergistic effect of plasticisers and stabilisers on the stability of PVC under irradiation when pure PVC, containing different amounts of additives, was exposed to γ-irradiation in air (dose rate: not stated, total absorbed dose: 0.03 MGy). Vinhas et al. (2003a), Vinhas et al. (2004a) and Vinhas et al. (2004b) investigated the degradation of a non-plasticised PVC (control sample) and four PVCs containing commercial plasticisers under γ-irradiation (dose rate. 5.87 kGy/h; total absorbed doses: 0.01, 0.025 and 0.06 MGy; environment: not stated, presumably in air). The commercial plasticisers were di(2-ethylhexyl)phthalate, di-isobutyl phthalate, tris(2-ethylhexyltrimellitate and Viernol® (a polymeric plasticiser). Radiolytic degradation was found to be significantly reduced in the presence of all plasticisers compared to the non-plasticised material. However, the plasticisers can diffuse out of PVC at elevated temperatures or due to the degradation of the polymer itself, which reduces its resistance towards radiation. Vinhas et al. (2003b) also noticed that di(2-ethylhexyl)phthalate had the least effect on radiation stability, while di-isobutyl phthalate had the greatest effect. More specifically, the scores from a principal component analysis of the pure PVC in comparison to plasticised PVC show that the PVC/di(2-ethylhexyl)phthalate samples were most strongly degraded by chain scission upon irradiation, especially at the two highest doses. The effect on the other formulations was significantly lower.

Additives were also found to influence the type of the released radiolytic compounds. Hegazy et al. (1981) showed that the presence of stabilisers (e.g., epoxy oil, Ca-Zn stearate) and plasticisers (dioctyl phthalate) particularly affect gas production and the oxidative degradation of PVC at doses below 0.2 MGy, whereas at doses above 0.2 MGy, these compounds decomposed. Chantreux et al. (2021) identified the volatile and non-volatile organic degradation products upon irradiation of a commercial PVC containing several additives (among these di-isononyl phthalate as plasticiser) in air (dose rate: 1 kGy/h; total absorbed dose: 0.5, 1, and 2 MGy; room temperature). They compared these degradation results with those of two specifically formulated PVCs and a PVC resin, which did not contain additives and was irradiated under the same conditions. They observed a large variety of organic products from the radiolytic oxidative degradation of the commercial and custom-made PVCs, while for the PVC resin, only three LMW carboxylic acids (C2 to C4) were identified in significant amounts. Larger molecules containing more than four carbon atoms (C4) were observed in the other PVCs, such as carboxylic acids, esters, ketones and alcohols. Phthalic acid was released from the irradiated commercial PVC containing di-isononyl phthalate as plasticiser, suggesting that radiolytic degradation of the plasticiser occurred. Generally, the phthalate plasticiser was found to be a major source of by-products such as phthalic derivatives, alcohols and monocarboxylic acids from C4 to C9 and dicarboxylic acids from C2 to C8. Thus, irradiation of plasticised PVC was found to produce an array of different organic compounds, such as alkanes, alcohols, ketones, carboxylic acids and the corresponding esters, often containing more than four carbon atoms.

Influence of alkaline conditions

In Dawson (2013c), PVC was exposed to γ-radiation in deionised water (pH ~ 7) and saturated $Ca(OH)_2$ solution (pH ~ 12.4) at room temperature and different dose exposures (dose rates: 4 Gy/h, 42 Gy/h and 4 kGy/h; total absorbed dose: 0.15 MGy and 10 MGy). The TOC was significantly higher for the irradiated samples than for the non-irradiated ones, both in deionised water and alkaline solution. For the irradiated samples, the TOC was found to be higher in deionised water than in alkaline solution by a factor of around 2, showing a rather limited influence of the pH on radiolytic degradation. Whilst an increase in the total dose led to higher TOC, the higher values were observed for lower dose rates, indicating a dose-rate effect. A variety of dissolved organic compounds were identified, including HCs, alcohols, aldehydes, ketones, and carboxylic acids. In alkaline solution, the identified volatile organic compounds (VOCs) were aliphatic and aromatic HCs, such as 1-butanol, 2-butanone, propanol (methoxy-methylethoxy), ethyl acetate, isobenzofuranone, phthalic anhydride, benzoic acid, benzene, octadecanoic acid (oxo methyl ester), phenol (bis dimethylethyl), furancarboxaldehyde (hydroxymethyl), nonane, and chlorinated HCs (dichloromethane, tetrachloroethylene). Some of the compounds were attributed to the presence of plasticisers. A few compounds could not be identified, but since pure PVC contains chlorine, these were assumed to include certain chlorinated species. The diversity of organic compounds was greater in deionised waster than in alkaline solution.

In a later study, Baston et al. (2017) studied the leaching from plasticised PVCs with di-2-ethylhexyl phthalate, di-isononyl phthalate and di-isodecyl phthalate. The PVC and plasticisers were irradiated at different total doses (0.25; 0.5; 0.75 and 1 MGy) in the presence of a cement-type solution (saturated $Ca(OH)_2$ solution) at ambient temperature. Irradiation was also performed at high temperature (80 °C) on PVC samples at a dose of 0.75 MGy. The water-soluble organic compounds identified were phthalic acid, 2-ethylhexanoic acid, 2-ethyl-1-hexanol and several phenolic compounds (phenol, 2-isopropylphenol, 3-isopropylphenol, 4-isopropylphenol and 4,4-(1-methyl-ethylidene)-bisphenol).

In a recent study carried out by CEA/Orano on an irradiated plasticised PVC in air (dose rate (3 – 4 kGy/h; total dose: 0.1 to 4 MGy) summarised in Altmaier et al. (2021), water-soluble degradation products have been leached from plasticised PVC irradiated with γ-radiation up to a dose of 10 MGy by a cement-type solution (pH 13.2) at 60 °C. The organic compounds identified were acetic, formic, glutaric, succinic, adipic, oxalic, malonic, phthalic and benzoic acids. Phthalic and benzoic acids are related to leaching of the plasticiser and its hydrolytic degradation product.

Influence of temperature

Rabie et al. (1985) report the influence of temperature (25 °C to 180 °C) on radiolytic degradation of commercial PVC in air (total adsorbed dose: 0.005 MGy and 0.15 MGy). While the results show that increasing the dose leads to significant changes in the polymer structure (interpreted in terms of peroxide-mediated oxidative degradation), heat treatment of the irradiated PVC samples did not have any further impact on the structure.

In their experiment with plasticised PVC irradiated in air (dose rate: 10 kGy/h; total absorbed dose: 2 – 26 MGy; room temperature), Colombani et al. (2009) measured that the leach rate of the organic products increased with temperature, while it decreased after irradiation at a high dose due to modification of the PVC composition and internal crosslinking and grafting reactions.

Labed et al. (2013) investigated the separate and combined effects of temperature and relative humidity on the HCl production yields during the radiolytic degradation of PVC (dose rate: 0.4 kGy/h and 4 kGy/h; total absorbed dose: 0.1 to 4 MGy) at three temperatures (room temperature, i.e., 25 ± 5 °C and 30 ± 5 °C, and 70 °C) and different relative humidity (< 10%, 70 – 75%, 100%). The authors studied two types of PVC, a pure PVC and a commercial, plasticised one, consisting of 27% pure PVC and 73% organic and inorganic additives, which are, in turn, mainly composed of di-isononyl phthalate, di-n-butyl phthalate, and 2-ethylhexyl diphenyl phosphate. The results show that, for both PVCs, the release of HCl slightly increases (factor of 1.2 to 1.3) for a temperature increase of 45 °C. At room temperature, an increase in HCl release was observed in the case of pure PVC at high dose rate, whereas no significant effect was observed at a low dose rate for the same material. HCl release, however, is significantly reduced (50%) at a low dose rate and at 70 °C. For plasticised PVC, a temperature-dependent increase (factor of 1.7) was observed only at low relative humidity.

Boughattas et al. (2016) studied the influence of temperature on the radiolytic yields of HCl, H_2 and benzene formation during irradiation of additive-free (pure) PVC and commercial (plasticised) PVC in an inert atmosphere (He) and in air at different temperatures (80 °C, 100 °C, 120 °C and 150 °C). For both pre-irradiated PVCs, the largest weight loss was attributed to the release of HCl as well as a small amount of CO_2 and benzene. The results further show that the temperature has a relatively small effect on the production of H_2 from pure and plasticised PVC. On the other hand, the radiolytic yield of HCl (G_{HCl}) for additive-free PVC was found to increase with temperature. The generation of HCl in air was systematically higher than that determined under inert conditions, indicating the influence of O_2. Thermo-desorption of additive-free PVC released a large number of LMW organics with one to six carbon atoms (C1 – C6). Acetaldehyde, formic acid, propanal, acetic acid, benzene and succinic anhydride were the most abundant products identified. For plasticised PVC, additional compounds generated by the irradiation of the plasticisers were observed, such as propene, 2-pentanone, 2-hexanone, propanoic acid, pentanoic acid, butanoic acid and hexanoic acid. These originate from the radio-oxidation of alkyl groups of phthalates (main additive). Thus, irradiation of PVC was found to have an impact on the thermal stability of PVC.

The study of Castañeda-Facio et al. (2014) with irradiated plasticised PVC (dose rates: 0.24 Gy/h and 2.8 Gy/h; total absorbed dose: 0.075 MGy) shows that the dose rate has no influence on the maximum loss of HCl during heating (thermal degradation).

Influence of relative humidity

Labed et al. (2013) also showed that the HCl increase seemed to be independent of the relative humidity in the case of plasticised PVC at 25-30 °C and 70 °C and for low and high dose rates.

In the study of CEA/ORANO, the difference of the radiolytic yields of HCl ($G_0(HCl)$ and H_2 ($G_0(H_2)$)) under low relative humidity (~ 10%) and high relative humidity (74%) was found to be less than 10% (Altmaier et al. 2021). This finding suggests that the availability of water (humidity) is not a decisive parameter in the radiolytic degradation of PVC, confirming the trend previously observed by Labed et al. (2013).

Influence of radiation type

Most studies have employed γ-radiation, while less work was published on the effect of α-radiation on PVC. Reed & Molecke (1994) investigated the degradation of PVC under α-irradiation (^{241}Am source, dose rate: 2 kGy/h; total absorbed dose: 0.11 – 0.12 MGy) in air and under inert atmosphere (N_2). Water, as water vapour, was added to establish a relative humidity of ~ 70%. The study shows that α-radiation involves degradation processes that produce an array of different products (α-irradiation is a surface phenomenon due to the low penetration depth of α-radiation). H_2 and CO_2 were the predominant gaseous products. The yields were slightly higher in air than under N_2. Gas production increased linearly with the absorbed dose. A wide diversity of LMW organics were detected, such as alkanes, alkenes, ketones, aldehydes, and benzene derivates. Acetone was found to be the most abundant species.

No information about radiolytic degradation kinetics is available for PVC.

3.1.4 Bitumen

There are many types of bitumen, which greatly vary in chemical composition according to their origin and treatment, making it difficult to compare the radiolytic behaviour of the different materials used. When used as waste encapsulant, bitumen is considered as radiolytically stable at total absorbed doses < 10 MGy (Eschrich 1980).

Degradation mechanism and products

As with other polymers, irradiation of bitumen leads to physical and mechanical changes (e.g., increase in volume, hardening) and produces gases and water-soluble organic degradation products. Under anoxic conditions and in absence of water, H_2 is the main radiolysis gas produced by de-hydrogenation of cycloalkanes and related aromatisation of bitumen (increase of the C/H ratio; formation of C=C bonds) (Valcke et al. 2017, Eschrich 1980). Other gases have been found in smaller amounts under these conditions, such as such as NO, CO, and C1-C3 HCs (e.g., CH_4, C_2H_6, C_2H_4, ethine, etc.), which are produced as a result of the cleavage of covalent bonds in organic molecules and the subsequent reaction of small radicals (Valcke et al. 2017). When bitumen is irradiated in the presence of O_2, the fraction of CO_2 in the gas mixture increases (Valcke et al. 2017). Small and larger radicals can also react with each other, leading to the formation of smaller or larger water-soluble organic compounds such as carboxylic acids, linear alcohols, glycols, linear carbonyls, aromatic compounds like (alkyl substituted) naphthalene, substituted phenols or anilines, and S- and N-containing compounds (Valcke et al. 2017). Radicals produced by the radiolysis of water also react with bituminous compounds.

Kagawa et al. (2000) irradiated bitumen in deionised water (dose rate: 10.65 kGy/h; total absorbed doses: 1 and 10 MGy) in air at room temperature. A comparison of the TOC determined in irradiated and non-irradiated samples is not possible because different exposure times were used. The main water-soluble degradation products identified after irradiation were oxalate and HMW organic carboxylic acids (not specified) at lower concentrations.

Rotif et al. (2006) and Valcke et al. (2009) studied the ageing of Eurobitumen by γ-irradiation (dose rate: ~ 0.02 – ~ 0.14 Gy/h; total absorbed dose: ~ 0.14 – ~ 0.75 MGy) in air and inert atmosphere (N_2). The authors found that radiolytic degradation involves de-hydrogenation of cycloalkanes and aromatisation leading to the formation of C=C bonds along with the release of H_2 and the formation of inter- and intramolecular covalent bonds (e.g., crosslinking). The effect of radiolysis was found to be highly dependent on the access of O_2 into the matrix of (hard) bitumen. It was also found that oxidative degradation leads to the formation of O_2-containing groups, such as hydroxy (OH), carbonyl (C=O), carboxylic (COOR), or sulphoxide (S=O) groups, with C=C and C=O functionalities increasing in linear proportion. Despite these changes, Rotif et al. (2006) and Valcke et al. (2009) considered that the effect of γ-radiation on Eurobitumen was small, even at the highest doses. Valcke et al. (2009) found that in the case of distilled (soft) bitumen, the role of O_2 in the degradation process may be less important than for hard bitumen as the material is less accessible to O_2. Irradiation of bitumen in the absence of O_2 resulted only in a slight increase in C=C bonds, while O_2-containing groups (e.g., C=O) were hardly observed, suggesting that bitumen might have a higher stability upon irradiation under anoxic conditions.

The radiolytic degradation of bitumen can hence be summarised as:

- the production and release of light gases (H_2 >>> CH_4, CO, CO_2 > C_2H_6, C_2H_4, ethine)
- the increase in the fraction of C=C bonds at the expense of C-C bonds, especially in anoxic conditions, leading to the formation of polyene structures in linear HCs, aromatisation of cycloalkanes and crosslinking;
- and the incorporation of O_2 in the bitumen, e.g., by the formation of C=O bonds, coinciding with an increase of the asphaltene content (Valcke et al. 2001), knowing that oxidative degradation occurs mainly at the surface and subsurface parts of the waste, in those parts of bitumen accessible to O_2

Influence of total absorbed dose and dose rate

Kagawa et al. (2000) observed an increase in TOC and especially oxalate by increasing the total absorbed dose in line with van Loon & Kopajtic (1991). Valcke et al. (2017) also highlighted that the amount of gas produced is proportional to the total absorbed dose, while the influence of the dose rate appears to be insignificant.

Influence of alkaline conditions

Van Loon & Kopajtic (1991) investigated the influence of the radiolytic degradation products of bitumen on the speciation of radionuclides under strongly alkaline and anoxic conditions. Two types of bitumen were irradiated in a solution at pH 12.5 in air at ambient temperature (dose rate: 11 kGy/h; total absorbed dose: 5 MGy). TOC and TIC (total inorganic carbon) were significantly higher after irradiation than in the non-irradiated solutions, indicating the formation of carbon compounds. The pH of the solutions after irradiation was generally lower, indicating the production of acids. Most of the products identified were LMW carboxylic acids like oxalic acid, acetylacetic acid and phthalic acid, but also long-chain mono- and dicarboxylic acids with up to 18 carbon atoms, such as caprylic, myristic, palmitic, and stearic acids and dibutylester of phthalic acid (van Loon & Kopajtic 1991, Valcke et al. 2001). The concentration of these larger carboxylic acids was, however, very low. They were assumed to be leached from the bitumen rather than being formed by irradiation. For example, dibutylester phathalate is a common plasticiser that is also found in PVC and plastics. The main radiolytic degradation products of bitumen identified by van Loon & Kopajtic (1991) and Valcke et al. (2001) were oxalate and CO_3^{2-}. The formation of oxalate was thought to be due to the reaction of two $\cdot COO^-$ radicals formed by decarboxylation of the carboxylic acids. Its concentration increased with increasing dose and reached a saturation level at a total absorbed dose of above ~ 6 MGy. The water-soluble degradation products were found to have no influence on radionuclide speciation under conditions relevant for a cement-based L/ILW repository (van Loon & Kopajtic 1991, Greenfield et al. 1996).

Influence of radiation type

Eschrich (1980) states that the type of irradiation (α, β, γ) has no significant influence on gas formation, while Valcke et al. (2001) attest that the amount, but not the nature of the gaseous degradation products, depends on the type of radiation.

No information about the influence of temperature and radiolytic degradation kinetics is available for bitumen.

3.1.5 Plastics

Plastics include a variety of synthetic or semi-synthetic polymeric materials. In the Swiss L/ILW inventory, it is assumed that the term "plastics" mainly refers to PE, PP, polyesters and polycarbonates (cf. Section 2.1.4).

3.1.5.1 PE and PP

The behaviour of PE under γ-irradiation and resulting changes in material properties have been extensively investigated in the context of industrial and medical applications. These studies have been carried out to investigate improvements of the polymer properties by γ-irradiation with lower doses. In the following section, the discussion is limited to the aspects considered as relevant in the context of an L/ILW repository.

Degradation mechanism and products

In general, radiolytic degradation of PE and PP occurs by three distinct and simultaneously competing processes: oxidative chain scission in amorphous regions, crosslinking (inter- and intramolecular) in crystalline regions and crystal destruction and/or crystallisation. The latter process produces an apparent increase of crystallinity and density due to the formation of polar groups, increasing the intermolecular attraction forces which result in higher density.

Upon irradiation, the polymers generate free radicals in considerable amounts, which combine competitively with each other or with molecular oxygen and are uniformly distributed in the polymer. Sohma (1983) showed that free radicals in PE and PP migrate by γ-irradiation from their point of origin into amorphous regions, where they decay by recombination or are stabilised. The unpaired electrons migrate in the polymer matrix in a way similar to that of an elastic collision of molecules in the gas phase until they are stabilised. Thus, the presence of radicals plays an important role in any degradation. The local concentration of radical intermediates leads to radiolytic degradation through competition between crosslinking and scission. The decay of radicals is not directly influenced by primary excitation (ionisation by γ-radiation), but by both the chemical species of radicals and the molecular structure of the polymer in which the radicals are entrapped (Sohma 1983). Recent studies have further shown that energy and radicals can be trapped at defects created by oxidative degradation or at C-C bonds (Ferry et al. 2016 and references therein). This process leads to a reduction in the instantaneous H_2 emission rates.

The molecular structure of PE and PP was found to depend on a variety of factors, such as molecular weight and density, processing conditions, extent and distribution of crystallinity and environmental conditions. The differences in the reactivity of the crystalline and amorphous parts in PE and PP are an important aspect of their radiolytic degradation (Johnson et al. 1973, Arakawa et al. 1982, Torikai et al. 1986, Torikai 1994, Geetha et al. 1989). The role of the amorphous fraction in the radiolytic degradation of PE was demonstrated by Johnson et al. (1973). The authors especially studied the decay of the alkyl radical $-CH_2{\cdot}CHCH_2-$ in γ-irradiated PE. Decay was interpreted in terms of a fast and slow first-order decay process. The constant of the latter process was found to increase with increasing amorphous fraction. Furthermore, H_2, which was only soluble in the amorphous fraction, had a marked catalytic effect on both decay processes. Torikai et al. (1986), Torikai (1994) and Geetha et al. (1989) irradiated linear low-density PE and high-density PE in vacuum and in air at room temperature (dose rate: 4.4 kGy/h; total absorbed dose: 0 – 1 MGy). When irradiated in vacuum, crosslinking was more advanced in linear low-density PE than in high-density PE, as crosslinking is expected to occur predominantly in the amorphous region. Furthermore, linear low density PE has only short side branches and can crosslink more readily. For both materials irradiated under vacuum, crosslinking strongly increased in the low dose range of 0 – 0.01 MGy and then linearly between 0.01 and 1 MGy. However, when irradiated in air, more crosslinking was observed in high-density PE than in linear low-density PE, which was explained by the different reactivity of the materials. In linear low-density PE, oxidative degradation (chain scission) predominates over intermolecular crosslinking due to the presence of more amorphous regions compared to high-density PE. In high-density PE, on the other hand, there are fewer amorphous regions, which reduces oxidative degradation and increases crosslinking. The products of oxidative degradation were not identified, while increased formation of carbonyl function (C=O) groups of polymer residues was observed. Under oxic conditions, chain scission occurs predominantly in PE, while anoxic conditions promote crosslinking. Similarly to PE, the importance of the amorphous fraction on the radiation stability of PP was shown by Kagiya et al. (1985). Demertzis et al. (1999) irradiated PE and PP with low doses in air (dose rate: 2.1 kGy/h; total absorbed dose: 0.044 MGy). PP was found to have slightly lower radiation resistance compared to PE. The branched structure in PP allowed the formation of more persistent radicals, which reacted with O_2 to produce peroxides and peroxide radicals for oxidative degradation of the polymer.

The influence of the environment and especially the presence of O_2 on the degradation of ethylene propylene diene terpolymer was shown by Hacıoğlu et al. (2013). The samples were irradiated with low and high doses in ambient atmosphere and in an aqueous environment (dose rates: 0.063 and 0.993 kGy/h; total absorbed dose: up to 2.2 MGy). The results show that oxidative degradation is the underlying deterioration process as an increase in hydroxyl, carbonyl, ether, epoxide and double bond formation was observed. The dose rate was found to have an influence on oxidative degradation and thus on material properties. Oxidation was limited at a high dose rate as O_2 consumption by oxidative degradation was much higher than its supply. The same interdependence, i.e., rate of O_2 diffusion in air and aqueous environment versus its rate of consumption in oxidative degradation, could explain the lower degree of degradation in water compared to air. It should be noted that O_2 supply by diffusion is more restricted in water than in air. The influence of O_2 was also demonstrated by Seguchi et al. (1981a) and Seguchi et al. (1981b), which showed the relationship between O_2 diffusion into samples, its solubility in the sample and consumption during irradiation, and observed that radiolytic oxidative degradation of PE was dependent on the dose rate. However, the effect was not observed when the PE contained antioxidants, which suppressed the oxidative degradation mechanism. This result again demonstrates that O_2 supply influences oxidative degradation of PE at different dose rates. Seguchi et al. (1981a) and Seguchi et al. (1981b) also showed that the degradation of PE is independent of the dose rate if O_2 is not involved in the degradation process. Arakawa et al. (1982) additionally highlighted that O_2 consumption and yield of oxidation products were independent on the O_2 pressure, if O_2 was in excess during irradiation.

The degradation processes lead, as in other polymers, to the formation of gaseous species such as H_2, CO_2, CO, CH_4 (Altmaier et al. 2021). The radiolytic yields of the different species depends on the material properties and the environmental conditions during irradiation (e.g., oxic or anoxic). In the study of Ferry et al. (2016), a high-density PE was irradiated in a two-step procedure in air (dose rate: 0.36 kGy/h; total absorbed dose: 10 MGy) and H_2, CO, and CO_2 were identified as the main gas products, indicating H abstraction during crosslinking (H_2) and oxidative chain scission (CO_2). In Chang & LaVerne (2000a) and Chang & LaVerne (2000b), the radiolytic yield of H_2 ($G_0(H_2)$) of PE and PP is at least an order of magnitude higher than those of PS and PMMA, indicating a higher reactivity of aliphatic HC chains. Indeed, aliphatic HCs are largely subject to abstraction reactions, and the yield of H_2 is usually high. Thus, the relatively high H_2 yields by PE and PP suggest that H atom abstraction reactions are of great importance in these materials. Finally, Miller et al. (1956) reported that during γ-irradiation of PE, 40% of the H_2 was produced by H abstraction and the formation of C=C bonds, while 60% was due to crosslinking. Volatile HCs (not specified) resulted from C-C scissions near the chain-ends and also at the short branches in PE.

Little information on the nature of the water-soluble degradation products is available in the literature (Demertzis et al. 1999, Chytiri et al. 2005, Filby et al. 2016, Dawson & Magalhaes 2012). Otherwise, similar effects of irradiation were observed for both materials. Chytiri et al. (2005) irradiated PE in air at room temperature (dose rate: 1.4 kGy/h; total absorbed dose: 0.005 – 0.06 MGy) and identified a large number of radiolysis products by gas chromatography-mass spectrometry, such as alkanes, alkenes, aldehydes, ketones, alcohols, carboxylic acids and esters with carbon atoms from C7 to C13 (a total of 54 organic compounds). Similar water-soluble degradation products were also reported in Filby et al. (2016) and references therein. In general, these compounds seem to degrade with increasing dose to LMW species and gas.

Influence of total absorbed dose and dose rate

In addition to the study of Hacıoğlu et al. (2013) previously described, Clough & Gillen (1981) reported dose rate-dependent degradation for PE. As with PVC, this process was attributed to a peroxide breakdown mechanism. Peroxides are formed in reactions initiated by radiation in air and have been found to be an important radiolytic oxidant in irradiated water.

Influence of radiation type

It is assumed that α- and γ-irradiation cause qualitatively similar degradation effects in polymers such as PE and PP (Filby et al. 2016 and references therein).

Influence of alkaline conditions

In the case of PE, the radiolytic degradation under alkaline (aqueous) conditions was investigated by Dawson (2013a). In this study, a commercial, low-density PE containing a mixture of additives was irradiated in both deionised water (pH ~ 6.44) and alkaline solution with an excess of solid $Ca(OH)_2$ to maintain a pH of 12.5 at room temperature (dose rates: 0.045 and 4 kGy/h; total absorbed dose: 0.15 MGy to 10 MGy). While the pH did not change under alkaline conditions due to the large buffering capacity of the $Ca(OH)_2$ saturated solution, it was lower by ~ 1.5 pH units in deionised water (pH range 6.49 to 4.71). Compared to the beginning of the experiment, the TOC varied by a maximum factor of 3 at the end of the experiment, irrespective of the dose rate and total dose applied to the systems. It was, however, comparable in deionised water and alkaline solutions after irradiation, as well as in the non-irradiated samples. This therefore indicates that the TOC content was largely unaffected by irradiation in both environments. In the gas phase, H_2 was the main gaseous species determined from direct irradiation of low-density PE under vacuum and in air, while the amounts of CO_2, CO, CH_4, C_2H_6 and C_3H_8 were much lower. In alkaline solution, oxalate was the only dissolved LMW organic compound identified. Other LMW carboxylic acids, such as acetate, glycolate, lactate, etc., were not detected. Long-chain alkanes and benzenedicarboxylic acid were also measured (the latter compound was also detected in deionised water). The main degradation products of irradiated low-density PE were VOCs, such as alkanes, alcohols, and ketones with a number of carbon atoms between C4 and C10. The most abundant ones were butane, pentane and 3-methyl butane.

Influence of temperature

Matsui et al. (2002) investigated the radiolytic degradation of PE at 40, 60 and 80 °C in a water bath at low doses (dose rates: 0.00645, 0.018, and 0.05 kGy/h; total absorbed dose: 0.067 to 0.136 MGy). Degradation occurred through the absorption of O_2 dissolved in the water by PE and led to the formation of carbonyl compounds. As degradation increased, the amount of carbonyl groups in the polymer disappeared, as they were converted into water-soluble degradation products. Interestingly, the degree of degradation decreased with increasing temperature, which was explained by the formation of antioxidants formed by γ-irradiation in water that may suppress degradation with increasing temperature.

Altmaier et al. (2021) report a study on the effect of temperature on the production of gas during γ-irradiation of PE. A series of irradiation experiments were carried out under inert atmosphere (He) and in air at ambient temperature and at 120 °C. An increase in H_2 production was observed at 120 °C regardless of the environment. However, this increase was found to be significantly higher in the presence of O_2, indicating a stronger temperature-dependence of the oxidative degradation.

No information about radiolytic degradation kinetics is available for PE and PP.

3.1.5.2 Polyester and PC

Degradation mechanism and products

In general, the ester $(\text{-R-COO-})_n$ and carbonate $(\text{-R-CO}_3\text{-})_n$ groups in polyesters (e.g., PET) and PC, respectively, exhibit moderate resistance to γ-irradiation. The electron affinity of the ester and carbonate groups is considered to be an important elementary step in the radiolytic degradation of PET and PC (Torikai et al. 1984, Torikai & Fueki 1985). The formation of alkoxy and C-centred radicals from the degradation of unsaturated vinyl ester polyester resins was found to primarily consist of intermediate radiolytic products (González-López et al. 2022). The alkoxyl radicals are very reactive and decay through the abstraction of H-atoms from neighbouring chains to form C-centred radicals. The presence of O_2 enhances the decay of the C-centred radicals, which produce peroxide radicals and cause a very rapid scission at the glycosidic bonds connecting the monomers. This process was found to be facilitated in water compared to other solvents.

The studies of Aliev et al. (2006), Mariani et al. (2007) and Malavasi et al. (2016) especially highlighted the protective effect of aromatic rings against radiolytic degradation of polyesters.

Aliev et al. (2006) investigated the degradation of the aromatic polyesters poly(1,4-butylene terephthalate), PET and poly(ethylene 2,6- naphthalene-dicarboxylate) by γ-irradiation (dose rate: 6 kGy/h; total absorbed dose: 0.5 – 4 MGy) under vacuum. The results show that different yields and compositions of the formed gaseous mixtures were observed for the three polyesters, which was explained by the presence of different aromatic and aliphatic groups. Crosslinking reactions and chain scission occur simultaneously. However, the absence of a gel fraction indicated absence of crosslinking, suggesting that chain scission is the main degradation process. The cleavage of ester bonds, indicated by the formation of carbon oxides (CO, CO_2), leads to the observed reduction of the molecular weight in poly(1,4-butylene terephthalate) and PET due to chain scission. The contribution of the cleavage of aliphatic chains to polymer degradation was considerably lower. The molecular weight of poly(ethylene 2,6-naphthalene-dicarboxylate) was almost constant due to the high protective effect of naphthalene against radiolytic degradation by chain scission.

Similar results were reported by Mariani et al. (2007), who also investigated irradiation of PET and poly(ethylene 2,6-naphthalene-dicarboxylate) in air. They also demonstrated that oxidative degradation occurred only if O_2 was easily available, while intermolecular reactions (crosslinking) dominated as soon as O_2 was depleted.

The protective effect of naphthalene and its derivates was further studied by Malavasi et al. (2016). Three naphthalene-based polyesters, which carried different numbers of aromatic rings, were irradiated in air at different absorbed doses (dose rate: 2.5 kGy/h; total absorbed dose: 0.1 – 1 MGy) and characterised using several techniques. As expected, aromatic polymers proved to be very stable towards irradiation: the higher the number of aromatic rings, the higher the radiation resistance. However, the introduction of heteroatoms, which decreased the ability of the polymers to crystallise, and the presence of ether and thio-ether linkages along the backbone, reduced their radiation resistance. Thus, the stability of the polymers towards ionising radiation was found to correlate with the number of aromatic rings as well as with the crystallinity and chemical structure (e.g., O- and S-linkages) of the polymers.

Influence of total absorbed dose and dose rate

According to Mariani et al. (2010), the relative importance of crosslinking and scission depends on the total absorbed dose. The authors irradiated poly(ethylene isophthalate) in air (dose rate: 1 kGy/h; total absorbed dose: 0 – 1 MGy). A decrease in the molecular weight was observed at the highest doses (i.e., > 0.2 MGy), indicating an oxidative degradation supposed to occur in the amorphous regions of the polymer. A constant molecular weight was found in the dose range between 0.1 and 0.2 MGy, while the molecular weight also decreased to a minimum at very low doses (< 0.1 MGy). The authors explained this behaviour by the antagonistic effects of chain scission, crosslinking and oxidative degradation on the molecular weight of polymers. It was further considered that peroxide radicals formed due to irradiation in air and upon diffusion of O_2 into the amorphous regions of the polymer. Under irradiation in air (and water), the ratio between crosslinking and oxidative chains scission depends on the dose rate due to the diffusion-limited supply of O_2. Oxidative degradation occurring in the amorphous regions of the polymers leads to the observed decrease of the molecular weight at the lowest doses as O_2 supply is not limited. At the intermediate doses, the predominant mechanism is crosslinking, while oxidative chain scission and crosslinking counterbalance loss and gain in molecular weight. At the highest doses, chain scission again dominates by rupture of ester groups that are particularly sensitive to radiation.

Chain scission was also observed in the case of PC as the dominant mechanism at very high doses of 3.28 and 4.341 MGy, significantly changing the thermal, mechanical and molecular properties of the materials (Hacıoğlu et al. 2013).

The study of Acierno et al. (1980) further revealed that when PC is γ-irradiated (dose rate: 8 kGy/h; total absorbed dose: up to 0.2 MGy), crosslinking effects predominate at small doses (< 0.05 MGy), while scission of the main chain is more effective above 0.05 MGy.

The predominance of chain scission at higher doses was confirmed by Araújo et al. (1998) only in the presence of water (i.e., O_2). In the absence of water, PC was found to be essentially insensitive to irradiation.

There are no irradiation studies carried out with polyester and PC under alkaline conditions, nor have the influence of the type of radiation and temperatures been the subject of detailed irradiation studies. No information is available on radiolytic degradation kinetics, either.

3.1.6 Cellulose, ISA and LMW organics

3.1.6.1 Cellulose

Degradation mechanism and products

Cellulose is expected to be susceptible to radiolytic degradation due to the presence of oxygen in its structure, either as an oxygen atom connecting the ring-shaped basic structure of the monomers and or as hydroxyl groups. γ-irradiation especially leads to the reduction of the degree of polymerisation due to the formation of disordered defect areas (Ershov & Klimentov 1984, Ershov 1998, Ponomarev & Ershov 2018). It can generally be assumed that chain scission is the predominant radiolytic degradation mechanism of cellulose, reducing its molecular weight, crystallinity and viscosity, and increasing its solubility (Humphreys et al. 2010b). The fragmentation of cellulose was found to be particularly effective during irradiation under oxic conditions (CORI 2021).

γ-irradiation initially leads to the formation of free electrons by ionisation, which subsequently generates free radicals in the polymer, such as H[•] and carbohydrate, as a result of C-H bond breaking (Ershov & Klimentov 1984, Ershov 1998). As observed by Sultanov & Turaev (1996), the radicals initiate the subsequent cleavage of the glucopyranose ring, generating CO_2 (or CO) and polymeric compounds with terminal carbonyl and carboxyl groups. The subsequent hydrolysis of these LMW polysaccharides leads to the formation of water-soluble deoxy- and deoxyketo-saccharides, complex and simple organic acids and sugars, among others (Ershov & Klimentov 1984, Ershov 1998). The reduction of the degree of polymerisation upon irradiation increases the susceptibility of cellulose to subsequent alkaline degradation.

In addition to chain scission, there is evidence that radiolytic chemical crosslinking also occurs on cellulose and has an influence on the physicochemical properties of air-dry irradiated cotton cellulose (Kovalev & Bugaenko 2003).

The water-soluble degradation products of cellulose identified by Bluďovský et al. (1984) in a study with cotton cellulose irradiated in O_2-rich and inert (N_2) environments (dose rate: > 2.88 kGy/h; total absorbed dose: up to 0.13 MGy), were sugars (arabinose, glucose, xylose), desoxysaccharides, carboxylic acids (formic, gluconic, glucuronic and oxalic acids), aldehydes (acetaldehyde, formaldehyde, malonaldehyde) and ketones (acetone). No significant differences in the nature of the degradation products were found in O_2-rich or inert environments, respectively, although the presence of O_2 increased the overall yield of the degradation products.

According to the recent study by Altmaier et al. (2021), the presence or absence of water was found to have only a limited effect on the extent of cellulose degradation under irradiation (irradiation of dry or dispersed cellulose).

Influence of total absorbed dose and dose rate

Published work indicates that the degree of cellulose degradation depends on the total absorbed dose, while no information on the influence of the dose rate is available. Bond scission was found to increase with increasing radiation dose up to very high doses (Ershov & Klimentov 1984). The accumulation of the gaseous by-products and the formation of carbonyl and carboxyl groups in cellulose was also found to increase linearly with the absorbed dose up to doses of ~ 0.3 MGy. Above this value, a square root dependence of the accumulation of the degradation products with dose was found (Tissot et al. 2013).

Complete degradation and dissolution of cellulosic materials can occur at radiation doses of 0.5 MGy and above in aqueous environments (Filby et al. 2016). In alkaline solutions, Baston et al. (2002) found that about 10% of the cellulose was completely degraded at a total absorbed dose of ~ 0.23 MGy. Tissot et al. (2013) estimated that, according to published results, a total absorbed dose of 23.52 MGy would be required to completely decompose the cellulose polymer into monomer units. Exposed to a dose of 1.68 MGy, the degree of polymerisation can be reduced to 14 units. These results suggest that substantial cellulose degradation already occurs at low irradiation doses.

Within the framework of CORI (2021), cellulose was irradiated under oxic and anoxic conditions (dose rates: 0.3 and 0.6 kGy/h; total absorbed dose: up to ~ 1.4 MGy). The focus was on determining the release of light gases, degree of polymerisation and molar mass distribution. The radiolytic yields of H_2, CO and CO_2 (G-values) increased with increasing total absorbed dose, while no significant effect of the dose rate on G-values was observed, neither under oxic nor anoxic conditions. The release of CO and CO_2 was, however, significantly enhanced under oxic atmosphere. With increasing dose, a clear shift in the molar mass distribution towards smaller-size molecules was observed, indicating fragmentation of cellulose. The degree of polymerisation decreased by a factor of ~ 25 in material irradiated at the highest dose (~ 1.4 MGy) compared to non-irradiated material. Furthermore, the degree of crystallinity decreased upon irradiation of cellulose at the highest dose. Under oxic conditions, lower crystallinity was already observed at a dose of ~ 0.8 MGy, indicating that the presence of O_2 promotes amorphisation. In agreement with Kovalev & Bugaenko (2003), the authors concluded that both crosslinking and scission occur at low doses, while chain scission is the dominant mechanism at high doses.

Influence of alkaline conditions

Synergistic effects of radiation and hydrolysis of cellulose in alkaline solutions were reported by Takács et al. (2000), Földváry et al. (2003) and Baston et al. (2002). Takacs and co-workers irradiated cotton cellulose in air and under inert N_2 (dose rate: 10 kGy/h; dose: 0.1 – 1.5 MGy). The materials were then subjected to alkali treatment in 12 – 16% NaOH. As expected, irradiation was found to reduce the degree of polymerisation and increase the content of carbonyl groups in the material. No change was observed up to a total absorbed dose of 0.001 MGy, but irradiation further transformed the crystalline structure so that cellulose reacted more strongly during alkali treatment. Degradation was marginally greater under irradiation in air as compared to irradiation under inert atmosphere, although the difference was found to be small. Földváry et al. (2003) carried out a subsequent study on the alkali treatment of irradiated and non-irradiated cotton cellulose under the experimental conditions previously used by Takács et al. (2000) (dose rate: 10 kGy/h; dose: 0.5 – 1.5 MGy, alkaline treatment with 6 M NaOH). As expected, the irradiation led to cleavage of the cellulose chains and to weight loss. However, some weight loss was also observed during alkali treatment of non-irradiated materials. When treated with alkaline solution, small fragments containing aldehyde and keto groups were dissolved from the irradiated samples. Their concentration was found to increase with both the duration of irradiation and alkali treatment after irradiation.

Within the framework of the EU "MIND" project, the combined effects of irradiation and biodegradation of cellulose under alkaline conditions was examined. Irradiation of cellulose under hyperalkaline conditions (pH 12.7) was found to enhance the rate of the abiotic hydrolysis of cellulose by alkali. Irradiation also led to an increase in the concentration of dissolved organic carbon, including ISA, and made the cellulose more bioavailable for microbial degradation at a starting pH value of 12.5 (Lloyd & Cherkouk 2021).

Baston et al. (2002) observed considerable amounts of dissolved organic species and complexing agents when cellulose was irradiated in alkaline solution (0.23 MGy). However, the nature of these products was not identified.

The experiments confirmed the expected synergy between radiation and alkaline degradation, as the concentration of organic compounds in solution formed by alkaline degradation alone was much lower (~ 10 ppm compared to 600 ppm for irradiation).

Influence of temperature

Ponomarev & Ershov (2018) published a comprehensive summary of the radiolytic degradation mechanism of cellulose for the temperature range 27 – 277 °C. The radiolytic degradation mechanism of cellulose can vary with temperature, being accelerated at elevated temperatures. Ponomarev & Ershov (2018) found that cleavage of the glycosidic bond and the preferential elimination of CO_2 is the dominant degradation mechanism at moderate temperatures (17 – 97 °C) and low dose rates (non-chain depolymerisation). Above a temperature of 97 °C, chain depolymerisation starts. In general, irradiation leads to the formation of defects in the cellulose fibres, such as weakened bonds, reactive groups and radicals that activate scission of the polymeric chain. This increases the reactivity of the irradiated cellulose and promotes the degradation process at elevated temperatures (Tissot et al. 2013, Ponomarev & Ershov 2018). Thus, it can be assumed that the yield of radiolytically produced scission fragments from irradiated cellulose increases with increasing temperature. This increase, however, is small within the temperature range relevant for an L/ILW repository (20 – 60 °C). In this temperature range, the study of Ponomarev & Ershov (2018) indicates that cellulose cleavage increases by a maximum factor of ~ 1.5.

No information on the influence of the radiation type and radiolytic degradation kinetics is available for cellulose.

3.1.6.2 ISA and LMW organics

Degradation mechanism and products

Several studies have reported on the radiolytic degradation of LMW organics, such as aliphatic carboxylic acids, their salts, anhydrides and esters (Johnsen 1959, Ayscough et al. 1971, Ayscough & Oversby 1971, Ayscough & Oversby 1972, Jones 1971a, Jones 1971b, Jones 1972). Less information is available on the radiolytic degradation of ISA, the main product identified upon the chemical degradation of cellulose under alkaline conditions (CORI 2021, Humphreys et al. 2010b).

Johnsen (1959) studied the decomposition of aliphatic carboxylic acids by γ-irradiation with special reference to decarboxylation (dose rate and total absorbed dose not given). They concluded that direct decomposition to CO_2 and CH_4 during irradiation is only of minor importance, as most of the radiolytic degradation occurs via alkyl- and carboxyl-free radical intermediates. This finding was later further substantiated by Ayscough & Oversby (1971) who investigated the radiolysis of acetic acid at cryogenic temperatures (dose rate: 0.36 kGy/h; total absorbed dose: up to 0.72 kGy). The products of the radiolysis included H_2, CO_2, CH_4, and H_2O along with smaller amounts of CO, CH_3COCH_3, N_2, C_2H_6, CH_3CHO and $(CH_3CO)_2$. In the gas phase, the main products were CO_2 and CH_4. In solution, succinic acid was predominant. Degradation occurred via a sequence of propagation reactions involving various transient radical species, such as $CH_3{\cdot}COOH^-$, $CH_3{\cdot}COOH^+$, $\cdot CH_3$, $CH_3CO\cdot$, and $\cdot CH_2COOH$. In a later study, Ayscough et al. (1971) examined the radiolytic degradation of other longer-chain monocarboxylic acids with carbon atoms ranging from 3 to 18. The proposed degradation mechanism was similar to that previously reported for acetic acid. In the case of esters, Ayscough & Oversby (1972) found that they behave in a much more complex manner than carboxylic acids under irradiation. The authors proposed that decomposition of the ester group involves a sequence of radical reactions, which in turn involve a liberation of electrons by ionization. These are captured by the ester group, leading to the dissociation of the radical-anion and further formation of alkyl radicals.

Jones (1971a), Jones (1971b) and Jones (1972) investigated the influence of molecular structures and phases on the radiolytic fragmentation of long-chain aliphatic carboxylic acids, in particular the radiolytic yield of CO_2 (dose rate: ~ 0.3 kGy/h; total absorbed dose: up to 0.02 MGy). The materials were irradiated as solids or dissolved in solution at different temperatures. In solution, the radiolytic yield of CO_2 was found to decrease with increasing chain length (number of carbon atoms) of the carboxylic acids. For carboxylic acids with more than two carbon atoms, the CO_2 yields decreased continuously, but not proportionally to the increase in the chain length. The effect was independent of temperature and less pronounced when the materials were irradiated as solids. The author interpreted these results in terms of the different effectiveness of electrons in different parts of the RCOOH molecule to convert it to the unstable state leading to subsequent decomposition. Accordingly, the interaction with electrons of atoms farther away from the carboxyl group is less effective in propagating the degradation process. An empirical approach was developed showing that the radiolytic yield of CO_2 is inversely related to the total number of electrons in the monocarboxylic acids.

Based on these studies on LMW organics and the latest results obtained from CORI (2021), it is expected that radiolytic fragmentation of ISA to smaller molecules and the associated formation of gaseous species occurs during irradiation (Humphreys et al. 2010b, Baston et al. 2002).

Influence of total absorbed dose and dose rate

Kani et al. (2008) and Kani et al. (2009) observed no influence of the dose rate (range 0.01 to 1 kGy/h) on the radiolytic degradation of acetic acid. There is no specific experimental work reporting the effect of a dose increase on the degradation of LMW organics, although it can be assumed that an increase in the total absorbed dose results in increasing fragmentation to smaller molecules and gaseous species.

Influence of alkaline conditions

Kani et al. (2008) and Kani et al. (2009) studied the decomposition of ^{14}C-bearing organic carbon compounds (acetic acid, ethanol, formaldehyde) under γ-irradiation at room temperature under conditions relevant to a cement-based L/ILW repository (pH 10 and 12.5) (dose rates: 0.01 to 1 kGy/h; total absorbed dose: ~ 1.5 – 1.9 kGy). The decomposition of the organics was explained by a reaction with OH radicals (and/or O^- radicals). Acetic acid, ethanol, and formaldehyde thus reacted with OH radicals to produce carbonic acid (H_2CO_3). Interestingly, a dose rate of only 0.01 kGy/h (at a low total absorbed dose of ~ 2 kGy) was found to produce enough oxidants to decompose ~ 90% of the acetic acid initially present (10^{-6} mol/L) into H_2CO_3. The authors also estimated the decomposition efficiency of the different compounds on the basis of the consumption of OH radicals. The results show a significantly higher decomposition efficiency for formaldehyde compared to acetic acid and ethanol, which is related to the cleavage of C-C bonds. Indeed, the cleavage of a C-C bond is required in the case of acetic acid and ethanol, which both have two carbon atoms, while formaldehyde has only one carbon atom and does not require the cleavage of a C-C bond.

Toste et al. (1994) investigated the effect of radiolysis on the stability of citrate ($C_6H_8O_7$) (initial concentration 43.5 mM) in a simulant mixed waste under alkaline conditions (pH 13.5) and at elevated temperature (90 – 95 °C) caused by heat-producing radioactive decay (dose rate: 0.75 kGy/h; total absorbed dose: range 0.0075 – 0.0375 MGy). Even at the low doses applied, the authors observed rapid decomposition of citrate over time. The only product identified in significant concentrations was propanedioic (malonic) acid ($C_3H_4O_4$), while most of the decreasing TOC could not be characterised. It is possible that CO_3^{2-} was an important product of radiolytic degradation of TOC, which would precipitate as carbonate under the given chemical conditions (high pH, high initial concentration). About half of the waste's TOC disappeared after 100 hours of irradiation. In contrast, control tests on the chemical degradation of citrate in the simulant showed that the degradation process was much slower but resulted in more diverse products (ethanedioic, propanedioic, and butanoic acids) as well as traces of other mono- and dicarboxylic acids.

In a later study, Toste (1999) investigated the degradation of nitrilotriacetic acid (NTA) under the same experimental and environmental conditions as in their previous study (Torikai 1994). Complete NTA degradation was observed, leading to the formation of chelator fragments such as N-hydroxylmethyl-N-methyliminoacetic acid and carboxylic acids, i.e., ethanedioic and hexanoic acids. Again, the TOC decreased drastically with increasing irradiation but remained almost constant in the control tests without irradiation, even at elevated temperatures. No information about the radiolytic degradation of EDTA (ethylenediaminetetraacetic acid), the other important aminopolycarboxylic acid, could be found in the literature, though it was assumed that EDTA is also susceptible to radiation and degrades similarly to NTA.

No information on the influence of the type of radiation, temperature, and radiolytic degradation kinetics is available for ISA and LMW organics.

3.1.7 Plexiglas®

Plexiglas® is the trade name for a rigid, transparent thermoplastic called PMMA produced by free-radical polymerisation of methyl methacrylate. Several studies have reported on the radiation stability of PMMA (Alexander & Charlesby 1954, Hiraoka 1977, Kumar et al. 1986, Hill et al. 1990, Hill et al. 1992, Chang & LaVerne 2001), but unfortunately not under conditions relevant to an L/ILW repository. However, some information about degradation mechanisms and products can still be extracted.

Degradation mechanism and products

As for the other polymers, similar radiolytic degradation processes are expected to prevail, i.e., breakdown of the main chain, and decomposition of the side chain, i.e., crosslinking and scission (Alexander & Charlesby 1954, Kumar et al. 1986). Radiation resistance of PMMA is considered to be limited due to the presence of the tetra-substituted carbon atom, and main-chain scission is the primary degradation process. Alexander & Charlesby (1954) in particular, suggested that degradation occurs by random rupture of the main-chain C-C bonds through rearrangement of the excited polymer, and that for each main-chain rupture, approximately one ester side chain is also simultaneously split off from the main chain. Similarly, Hiraoka (1977) considered a main-chain scission induced by side group elimination (acid, ester) as the common feature of the radiolytic degradation of all poly(methacrylates).

Kumar et al. (1986) studied the degradation of polycyclohexyl methacrylate under γ-irradiation (dose rate: 2.64 kGy/h; dose: up to 0.86 MGy) in air. The types of starting materials were prepared by irradiation: one with very low branching (initial stage of polymerisation process), and one with a high degree of branching (accelerated stage of irradiation process). The results show H_2, CO, and CO_2 release during irradiation, indicating radiolytic degradation. Only small amounts of CH_4 were released, indicating that the methyl group attached to the polymeric backbone is quite stable towards radiation and bond-breaking occurs mainly in the ester group. The mechanism of degradation of the ester group was found to be independent of the chemical nature of this group (aromatic, alicyclic, methyl) attached to the oxygen. The most important degradation mechanism was therefore assumed to be scission (cleavage of the ester group), although the occurrence of crosslinking was also suspected.

Hill et al. (1990) studied the degradation mechanism of poly(methacrylic acid) (PMAA) and poly(acrylic acid) (PAA) under γ-irradiation (dose rate: 4 kGy/h; total absorbed dose: 0 – 0.55 MGy) at ambient temperature in air. The results show no detectable crosslinking of PMAA and no detectable scission of PAA. Hill et al. (1992) carried out similar experiments in air and in liquid nitrogen (-196 °C) with the same compounds. The main volatile products quantified were CO_2 and CO with smaller amounts of H_2 and CH_4 for both materials. For both polycarboxylic acids, scission of the COOH groups occurred as observed for LMW-aliphatic carboxylic acids. It was shown that the scission of carboxylic groups occurs via both cationic and anionic radicals produced during the irradiation of the COOH groups. In the case of PMAA, the radicals observed at room temperature led to chain propagation, indicating a predominance of chain scission. In contrast, for PAA, the radicals were found to be generated by hydrogen abstraction from the polymer chain, which subsequently led to crosslinking reactions. Thus, scission was found to be the dominant mechanism in PMAA, while crosslinking was also important in PAA, confirming the results from the earlier study of Hill et al. (1990).

Chang & LaVerne (2001) confirmed the production of CO, CO_2, H_2 and CH_4 from γ-irradiation of PMMA. The formation of H_2 and CH_4 was attributed to reactions between appropriate radical precursors and $-CH_2-$ units from the main chain, while the decomposition of the ester group radical ($\cdot COOCH_3$) led to the formation of CO and CO_2. Production of the gases increased with increasing dose.

No information on the influence of the type of radiation, alkaline conditions, temperature, and radiolytic degradation kinetics is available for Plexiglas®.

3.1.8 SPs

Degradation mechanism and products

Experimental studies on the stability of SPs exposed to γ-irradiation are scarce (Filby et al. 2016, Baston et al. 2019, CORI 2021). Filby et al. (2016) reports the result of a study performed with irradiated cementitious and aqueous samples containing a PCE-type SP (ADVA CAST 550) (dose rate: 1 and 4 kGy/h; total absorbed dose: 2 and 9 MGy). The cementitious samples were mixtures consisting of either pulverised fly ash and ordinary Portland cement or blast furnace slag/ordinary Portland cement. Both grouts contained 0.8% (w/v) SP. The aqueous samples were alkaline solutions with $Ca(OH)_2$ saturated at pH ~ 12.5, containing SP at 1 and 10% (w/v), respectively. The TOC and individual compounds of the aqueous solutions and the solutions squeezed from the cementitious materials were determined. The results can be summarised as follows:

- The TOC of the samples decreased after irradiation, with a greater effect at higher dose;
- The TOC also depended on the grout formulation: the blast furnace slag/OPA pore solution had a higher TOC than the pulverised fly ash/OPA pore solution.
- The presence of LMW products indicated chain scission.
- Alcohols, ketones, carboxylic acids and HCs were identified as degradation products in the pore solution squeezed from the grouts, while the degradation products in the irradiated aqueous solutions varied.
- LMW organic anions identified by ion chromatography were only observed in the aqueous sample containing 10% SP.

Baston et al. (2019) investigated the radiolytic degradation of PCE SPs. The materials were a model SP that did not contain additives and a commercial product with a full range of usual additives. The samples were irradiated (dose rates: 0.015 and 0.1 kGy/h; total absorbed dose: 0.01 to 0.2 MGy) in $Ca(OH)_2$ saturated solution (pH ~ 12.4) at ambient and elevated (80 °C) temperatures. On the sample irradiated up to a total absorbed dose of 0.2 MGy, only a partial degradation of the PCE SPs was measured. A decrease in TOC was observed at doses of 0.05 MGy and above compared to the control sample. This reduction suggests that either the LMW compounds formed were volatile and escaped from solution (e.g., CH_4, ethane, ethene) or that the TOC was converted into CO_2 and precipitated as $CaCO_3$. The TOC content in the solutions from the samples exposed to 0.1 and 0.2 MGy was also determined following 10 kDa MWCO filtration. For the controls, only 15 – 25% of the TOC of the initial solution passed through the filter, indicating the presence of LMW and HMW fractions in the non-irradiated samples. The TOC was slightly higher for the 0.1 MGy irradiated samples (~ 30%). However, after irradiation to 0.2 MGy, all the organic carbon passed through the filter and appeared in the LMW fraction, indicating that irradiation effectively degraded PCE and produced increased proportions of the LMW fraction. However, the TOC was lower after filtration compared to the TOC of the initial solution before filtration, possibly because the products of further analysis were gaseous compounds and escaped during filtration (e.g., ethane, ethene, etc.) or CO_2 that would precipitate as $CaCO_3$. This finding shows that continuous irradiation produces smaller molecules from larger ones over time and leads to a gradual increase in the number of organic compounds with an LMW or even gaseous species. Gel-permeation chromatography analysis clearly demonstrated the shift to lower molecular weights of the compounds with increasing dose. Identification of the water-soluble degradation products showed the presence of polyethylene glycol compounds like hexagol and 3,6,9,12-tetraoxatetradecan-1-ol. Additional compounds were recorded but could not be identified.

Radiolytic degradation of LS, SMF and PCE-based SPs is a focus of the ongoing EURAD (European Joint Programme for Radioactive Waste Management and Disposal) project "CORI" (CORI 2021). PCE was irradiated (total absorbed dose: 0.003 – 0.023 MGy) in air using a suspension with different contents. Production of the gaseous species H_2, CO_2, SO_2 and CH_4 was found to increase with increasing dose. Interestingly, a decreasing radiolytic yield of H_2 and CO_2 production with increasing PCE content was observed, which is currently not fully understood. PCE suspended in water (pH ~ 5) and in a cement-type porewater (pH 13.7) was also irradiated with α-radiation (total absorbed dose: 0.004 – 0.016 MGy) in a synthetic air atmosphere. The release of H_2 was higher at pH 13.7 than under near-neutral conditions, while gaseous CO_2 releases could not be quantified in the cement-type porewater due to solvation as carbonate under alkaline conditions.

The stability of the currently most important commercial SPs, i.e., SMF, SNF and PCE, is tentatively assessed based on their polymer structure due to a general lack of experimental studies on the radiation resistance of SPs. Although their sensitivity to radiation may vary, it can be assumed that they are all susceptible to radiolytic degradation due to their structural features, which suggest only limited stability against irradiation. Due to the polycyclic aromatic nature of the backbone, SNF is expected to be the most stable polymer upon irradiation. Its radiation resistance may be comparable to that of IERs. On the contrary, the heterocyclic structure of SMF and the presence of ester and ether linkages in the aliphatic backbone of PCE make these SPs less resistant to radiation.

No information is available on the influence of total absorbed dose and dose rate, type of radiation, alkaline conditions, temperature and radiolytic degradation kinetics for SPs.

3.2 Chemical (alkaline) degradation

3.2.1 Definition

The presence of water, either as free water or as moisture, is crucial for the chemical degradation of organics (Wieland et al. 2018, Wieland & Kosakowski 2020). In general, it has been observed that a minimum humidity of 60% is necessary to create a continuous water film on the reactive materials, which is required to allow chemical reactions to occur (Wieland & Kosakowski 2020). Below this threshold, chemical reactions are strongly inhibited or not possible.

In the near-field of an L/ILW repository, hydrolysis[2] is the only chemical process that can enable the degradation of organic polymers.

Hydrolysis

The interaction of water (e.g., intruding formation water) with the cementitious near-field of an L/ILW repository generates alkaline conditions. Under the alkaline conditions of a cementitious near-field, the hydroxyl concentration of the porewater is high, i.e., $[OH^-] > 10^{-4}$ M in all stages of cement degradation, decreasing the porewater pH from ~ 13 to ~ 10 (cf. Section 2.4). OH^- is a nucleophile, which in principle favours the hydrolysis of organic compounds. During hydrolysis, either chemical bonds are broken by the addition of H_2O or OH^- to form new products, or a functional group is exchanged with OH by nucleophilic substitution (e.g., Speight 2018). Alkaline degradation is thus indicated by nucleophilic attack of the OH^- ion on the polymer chain or by deprotonation (van Loon & Hummel 1995).

---

[2] In this report, hydrolysis specifically refers to an abiotic process, even though hydrolysis could also occurs enzymatically by microorganisms.

Reaction 3-4: $RX + OH \rightarrow ROH + HX$

By adding H_2O, the new bonds could be connected to the H or the OH component of the water molecule. It should be noted that hydration is the process variant in which water reacts with a compound without causing its decomposition.

Hydrolysis is the first and often limiting step to transform long chain polymeric matter into soluble and smaller molecules accessible to biotic degradation. Reaction 3-5 accounts for the hydrolytic degradation of cellulose where the polymeric molecule $[C_6H_{10}O_5]_x$ is hydrolysed to form monomeric glucose units:

Reaction 3-5: $[C_6H_{10}O_5]_x + x\ H_2O \rightarrow x\ C_6H_{12}O_6$

Hydrolysis is either purely abiotic or mediated by microorganisms.

The presence of reactive carbon atoms in an organic compound that is susceptible to nucleophilic attack is the most important factor determining whether hydrolysis occurs. The reactivity of a carbon atom is largely determined by the functional groups attached to the atom. Electronegative functional groups (e.g., carbonyl) or heteroatoms (N, O, S) attached to the carbon atom can withdraw electron density, resulting in an electron-deficient (partly positively charged) carbon atom that is susceptible to nucleophilic attack and therefore easily hydrolysed. In contrast, alkenes do not react with water because the O-H bond in the water molecule is too strong to allow the hydrogen to act as an electrophile. Water cannot protonate a double bond, and therefore C=C double bonds cannot be subject to hydrolysis reactions unless a strongly acidic catalyst is present.

Reactivity of the polymers

In general, two categories of polymers can be distinguished with respect to their chemical reactivity under alkaline conditions: i) addition polymers and ii) condensation polymers (van Loon & Hummel 1995, Lodge & Hiemenz 2020).

The main characteristics of addition polymers are:

- all-carbon-chain backbone with no functional groups in the main chain (homo-chain polymers), but pendant non-reactive substituent groups;
- a repetition of units having the same composition;
- no loss of atoms during polymerisation;
- insensitive to alkali attack.

PE, PP, PS, PVC, PMMA (Plexiglas®), rubbers, PCE-based SPs are examples of addition polymers.

Condensation polymers have the following characteristics:

- a carbon-chain backbone with regularly recurring functional groups in the main chain (hetero-chain polymers);
- a repetition of units arising from the reaction of two different functional groups on different monomers;
- an elimination of small molecules during condensation (e.g., water);
- they are sensitive to alkali attack.

Condensation polymers include cellulose, polyester (e.g., PET), PC, SMF and SNF-based SPs.

3.2.2 IERs, PS and styrene

Degradation mechanism and products

The chemical structure of IERs provides virtually no opportunity for alkaline attack. The main backbone of IERs consists of divinylbenzene cross-linked PS chains, which do not contain reactive carbon centres with a partial positive charge and are therefore not susceptible to nucleophilic attack by the OH^- ions. However, the reactive-side, sulphonic acid groups (for strongly cationic IERs) and quaternary ammonium groups could possibly be split off.

Few studies have considered the chemical degradation of IERs under conditions representative of a cement-based L/ILW repository. Van Loon & Hummel (1995), van Loon & Hummel (1999a) and van Loon & Hummel (1999b) conducted degradation experiments with IERs in alkaline solutions in addition to the irradiation experiments. In the degradation experiments with cationic-exchange resins under alkaline conditions (pH ~ 12.8), a lower DOC was observed compared to irradiated samples and no SO_4^{2-} was detected. This anion is an indicator for the scission of sulphonic acid groups, and the absence of SO_4^{2-} therefore indicates that sulphonic acid groups are resistant to alkaline hydrolysis. Degradation of anionic-exchange resins in alkaline solution (pH ~ 12.5) also resulted in lower DOC, and no amines were detected. This result suggests that even the quaternary ammonium functional groups of strongly basic IERs are not susceptible to alkali attack. The results from the tests with mixed-bed resins are in general agreement with those from the tests with strongly acidic and basic IERs, (showing a much lower DOC in solution with very low concentrations of sulphate, ammonia, and amines). The very low DOC observed for both the cationic, anionic and mixed-bed IERs supports the assumption that the PS backbone as well as the superficial functional groups are chemically stable under highly alkaline conditions. The chemical resistance of anion exchange membranes with a styrene-divinylbenzene copolymer-based backbone under alkaline conditions was confirmed by Mohanty et al. (2016), where various polymer structures, including poly(arylene ether)s, poly(biphenyl alkylene)s and PS-based polymers were investigated for their stability in alkaline solutions. Polymers with aryl-ether bonds in the repeating unit, i.e., R-O-R' where R and R' represent the aryl or alky groups, showed little chemical stability, while polymers without aryl ether bonds, such as PS copolymers, remained stable.

Influence of temperature

The influence on temperature on chemical degradation has not been investigated.

No information about chemical degradation kinetics for IERs, PS and styrene is available.

3.2.3 PVC

Degradation mechanism and products

No literature reviews of the purely chemical degradation of PVC under highly alkaline conditions representative of an L/ILW repository have been performed. Activation of the C-Cl bond by the presence of $Ca(OH)_2$ followed by dehydrochlorination is considered to be the relevant process that could lead to PVC degradation, but this process was only observed at temperatures above ~ 80 °C (Baston & Dawson 2014). In view of the structural properties of PVC, i.e., the presence of conjugated double bonds with Cl as functional groups, there is no evidence of a possible reaction with OH^- and thus of a hydrolysis-induced degradation process under alkaline conditions (Doi et al. 2020). PVC is considered a typical non-(bio)degradable plastic resistant to chemicals and ageing at ambient temperature (Shah et al. 2008). Nevertheless, the activation of C-Cl bonds in the polymer backbone seems more feasible compared to C-C and C-H bond activation in PE and PP, respectively.

Doi et al. (2020) investigated the durability of cation-exchange membranes with a PVC backbone in highly alkaline solutions (immersion in NaOH concentration of 0.01, 0.1, 1, and 6 M at a temperature of 40 °C for 3 h, one day, and one week). In solutions with NaOH concentrations below 1 M, no change was observed. However, under more extreme conditions, i.e., 6 M NaOH solution, changes in colour, chemical structure and membrane properties were observed. These changes were due to the formation of polyenes in the polymer structures, while dechlorination did not occur. This suggests chemical stability of PVC in alkaline solutions with NaOH concentrations $\leq$ 1 M.

In contrast to pure PVC, there is clear evidence of chemical degradation of plasticisers under the aqueous alkaline conditions representative of a cement-based L/ILW repository (NDA 2012, Baston & Dawson 2014). Phthalate esters and phthalic acid esters are among the most commonly added plasticisers to PVC. They are degraded by alkaline hydrolysis of the ester linkages leading to the formation of various phthalic acids or phthalate and phenols (Baston & Dawson 2014).

Influence of temperature

Baston & Dawson (2014) investigated the stability of plasticised PVC by ageing in deionised water and in $Ca(OH)_2$ saturated solution (pH ~ 12.4) at 80 °C over a period up to 120 days. The temperature was chosen so that maximum ageing occurred during the experimental period, while also being the threshold at which thermal degradation of PVC starts. The authors pointed out that this threshold may vary depending on the formulation. The PVC was found to degrade readily in $Ca(OH)_2$ solution but was more stable in deionised water. The weight loss was ~ 30% after 120 days of ageing at 80 °C in the alkaline solution. The release of chloride and the colour change of the material indicated dechlorination and polyene formation. The TOC was increased by a factor of ~ 6 compared to ageing in deionised water. Phenol compounds were detected in significant quantities in both solutions, suggesting that leaching of plasticisers is a relevant process in this study. The authors concluded that plasticisers migrated from the PVC matrix into the solution, where they underwent hydrolysis reactions in contact with water. Consistent with the higher TOC, hydrolysis was more advanced in the $Ca(OH)_2$ solution. The study shows that plasticised PVC probably already releases HCl by dechlorination at 80 °C due to thermal degradation. At this temperature, plasticisers were also leached from the polymer matrix. It is conceivable that thermal degradation rather than chemical (alkaline) degradation was the predominant process, as the temperature chosen was close to the threshold at which thermal degradation of PVC begins, although the authors attributed the degradation of PVC to a purely chemical process. It should be noted that, at present, it is not certain whether the experimental results are representative of ambient temperature or not.

There are no information about chemical degradation kinetics for PVC.

3.2.4 Bitumen

Degradation mechanism and products

The chemical degradation of bitumen occurs through ingress of highly alkaline porewater from the cementitious near-field into the bitumised waste forms. In general, bitumens are considered to be very resistant to many chemicals at ambient temperature (Valcke et al. 2017). The chemical degradation of bitumen initially involves an ageing process that leads to changes in the physical and rheological properties, which are reflected in a change in hardness, brittleness, and plasticity (Valcke et al. 2009, Eschrich 1980). The extent and rate of this ageing process depend on various factors such as the chemical composition and structure of bitumen, exposure to O_2, temperature, time, etc. (Valcke et al. 2017). At the molecular level, the reorientation of bitumen molecules and slow recrystallisation of waxes also contribute to the ageing process. Details on bitumen ageing have been described elsewhere (Valcke et al. 2009, Valcke et al. 2022). This ageing process requires a continuous supply of O_2, which may arise during interim storage, L/ILW emplacement in the repository and at the early post-closure stage. Oxidation leads to an increase in the number of carbonyl groups (C=O) and unsaturated bonds (C=C) in bitumen, an increase of the asphaltene content, and a decrease in saturates and aromatics, while the amount of resins remains constant. As a result of ageing, some volatiles (non-specified) are also expected to escape from bitumen prior to disposal, while light gases (H_2, CH_4, etc.) may become embedded in the matrix as a result of radiolytic degradation processes (Valcke et al. 2009, Valcke et al. 2017, Valcke et al. 2022).

In general, chemical degradation of bitumen and bituminised waste in alkaline conditions leads to the formation and leaching of a variety of water-soluble organic molecules due to their various chemical compositions (Kagawa et al. 2000, Walczak et al. 2001, Valcke et al. 2001, Valcke et al. 2009, Valcke et al. 2022). Kagawa et al. (2000) investigated bitumen degradation in contact with different solutions (deionised water, $Ca(OH)_2$ saturated at pH ~ 12.5, 0.1 M $NaNO_3$, and 10 M NaOH solutions) at 90 °C for up to three years under oxic, anoxic and reducing conditions. The TOC increased during degradation under oxic conditions, while it remained constant under anoxic conditions. This indicates oxidative degradation and almost negligible anoxic degradation. LMW carboxylic acids, such as formic, acetic and oxalic acids, and HMW carboxylic acids (not specified) were identified as important degradation products. In line with the TOC measurements, their concentration was much higher under oxic conditions than anoxic conditions. The presence of LMW carboxylic acid was also confirmed by Valcke et al. (2001).

Walczak et al. (2001) identified the water-soluble organic compounds in the leachates of bitumen. Leaching was carried out under probably oxic conditions with different solutions (e.g., deionised water, cement-type alkaline solution at pH 13.5), and under different conditions (e.g., ionic strength, different solid-to-liquid ratios). The TOC was found to be significantly higher in the alkaline leachate than in deionised water, indicating chemical degradation in addition to solubilisation of compounds. Alcohols, carbonyl compounds (e.g., aldehydes, ketones), glycols, aromatic compounds (e.g., naphthalene), nitrogen compounds (e.g., 4-methyl-1,3-benzenediamine) and small carboxylic acids with a maximum of four C atoms were identified as degradation products.

The influence of temperature was not specifically addressed in these studies and no information about chemical degradation kinetics is available for bitumen.

3.2.5 Plastics

PE and PP are addition polymers and therefore resistant to alkali attack. In contrast, polyesters (e.g., PET) and PC belong to the condensation polymers whose functional groups in the main chain make them susceptible to chemical (alkaline) degradation.

3.2.5.1 PE and PP

PE and PP are considered chemically inert when exposed to highly alkaline solutions. In an L/ILW repository environment, the degradation of PE and PP must therefore involve oxidants such as ·OH, or peroxy radicals or hydrogen peroxide, which are produced during radiolytic oxidative degradation or by the radiolysis of water. It should be noted that abiotic oxidation is also the first and rate-determining step of biodegradation (Hakkarainen & Albertsson 2004). Note, however, that additives leached from PE and PP can be susceptible to chemical degradation.

The influence of temperature was not specifically addressed in these studies and no information about chemical degradation kinetics is available.

3.2.5.2 Polyester and PCs

Degradation mechanism and products

Polyesters and PCs can contain different types of ester and carbonate groups with different hydrolytic reactivity of the carbonyl group (C=O) in the main chain (Bellenger et al. 1995, Bélan et al. 1997). Alkaline hydrolysis by the nucleophilic attack of OH^- on the ester group ($pH > 7$) leads to chain scission. It should be noted that esters also undergo hydrolysis reaction under acidic and neutral conditions ($pH \leq 7$), which is induced by protonation of the carbonyl with H_2O as nucleophile. A comprehensive review of the hydrolytic degradation of polyesters was published by Larranaga (2019). The dominant mechanism under alkaline conditions is the so-called acyl oxygen cleavage, in which the C-O bond between the central carbonyl (C=O) and the acyl group (OR') is broken (Fig. 3-5):

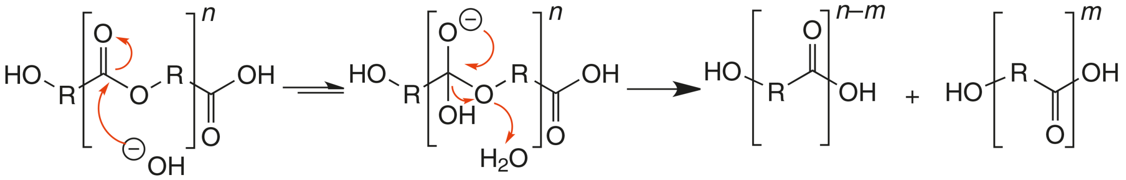

Fig. 3-5: Base-catalysed hydrolysis of polyesters

From Murthy et al. (2012)

The reactivity of the carbonyl C=O is influenced by the electron-withdrawing effect of the attached alkyl group (R) (Kint & Muñoz-Guerra 1999, Rydz et al. 2015). Ester hydrolysis in alkaline solution is an irreversible reaction. Attempts have been made to determine hydrolysis rates and to predict the lifetime of the materials (Zaikov & Livshits 1984, Launay et al. 1994, Bellenger et al. 1995, Bélan et al. 1997). However, the extent and rate of degradation are still a matter of controversial debate as the hydrolysis process of polymeric materials is also dependent on physico-chemical parameters (e.g., alkali concentration, temperature, and duration of alkaline hydrolysis treatment) and structural properties (e.g., hydrophilicity of the polymer matrix, diffusion into the matrix, osmotic cracking, morphological heterogeneity like amorphous and crystalline regions, non-random scission, etc.) (Bellenger et al. 1995, Murthy et al. 2012). Therefore, it is hardly possible to develop a realistic quantitative model of the chemical (alkaline) degradation of polyesters and PCs based only on a relationship between the structure of the polymer and the hydrolysis rate from laboratory experiments.

Studies on the durability of PET fibres for use in cement-based materials confirm that PET degrades under alkaline conditions, leading to rapid loss of fibre strength in concrete matrix (Da Silva et al. 2005, Rostami et al. 2020, Onuaguluchi & Banthia 2017). In another study, Onuaguluchi & Banthia (2017) carried out tests with polymeric scrap tire fibres mainly made of polyester (PET). These fibres were immersed in a cement-type porewater (pH 13) for three months. After exposure to the alkaline medium, the PET fibres showed a strong degradation at their surface.

The stability of PC is comparable to that of polyester under alkaline conditions. In the alkaline hydrolysis of PC, cleavage of the polymer occurs at the carbonate group $(\text{-R-CO}_3\text{-})_n$ instead of the ester group: $(\text{-R-COO-})_n$. Although the carbonate group is more susceptible to alkaline hydrolysis than the ester group, it has been found that the rate of degradation of an aliphatic PC is slower than that of polyester (Davis & Golden 1969). One possible reason for this behaviour could be the different electronegativity of the carbon and the three oxygen atoms in the two polymers.

However, the difference in reactivity is irrelevant in view of the period under consideration for an L/ILW repository (i.e., 100,000 years).

The water-soluble products formed by ester hydrolysis largely correspond to the monomer units used to build the polyesters. PET, for example, is formed by the polymerisation of ethylene glycol ($OHCH_2CH_2OH$) and terephthalic acid ($C_6H_4(COOH)_2$ or dimethyl terephthalate), producing alternating ethylene glycolate and terephthalate subunits linked by ester bonds. During alkaline treatment of PET, these monomers were observed in solution (Brueckner et al. 2008). An increase in NaOH concentration led to an almost proportional increase in the amount of degradation products.

Influence of temperature

Dave et al. (1987) showed that increasing temperature led to increasing degradation of polyester fabrics in NaOH solutions, thus indicating an influence of temperature on the hydrolysis of polyester fabrics. However, the dependence on temperature is relatively small and results in a weight loss by a factor of ~ 2 in the temperature range 40 – 60 °C. A gradual increase in weight loss was observed up to nearly 70 °C, followed by a steep increase in weight loss with a further increase in temperature. The observed nonlinear dependence of degradation on temperature was attributed to different molecular mechanisms that may be involved over the temperature range.

No information about chemical degradation kinetics is available for polyesters and PCs.

3.2.6 Cellulose, ISA and LMW organics

3.2.6.1 Cellulose

Degradation mechanism and products

Cellulose is unstable under alkaline conditions and is chemically degraded in this environment, producing water-soluble LMW degradation products like ISA, which forms strong complexes with safety-relevant actinides. Hence, cellulose degradation mechanisms and their impact on radionuclide retention in the near-field and host rock have been extensively studied over the last decades in the context of the safe disposal of radioactive waste (Baston et al. 1992, Baston et al. 1994, Greenfield et al. 1994, Bourbon & Toulhoat 1996, van Loon & Glaus 1997, van Loon & Glaus 1998, Glaus et al. 1999b, Askarieh et al. 2000, Vercammen et al. 2001, Pavasars et al. 2003, Allard & Ekberg 2006, Gaona et al. 2008, Glaus & van Loon 2008, Humphreys et al. 2010b, Baston et al. 2012, Evans et al. 2012, Diesen et al. 2017, González-Siso et al. 2018, Kobayashi et al. 2017, Kobayashi et al. 2019, Tasi et al. 2018b, Tasi et al. 2018a, García et al. 2020, Missana et al. 2022).

The complexation behaviour of cellulose under anoxic alkaline conditions has been described in terms of three main reactions (Fig. 3-6) (van Loon & Glaus 1997, van Loon et al. 1999, van Loon & Glaus 1998, Knill & Kennedy 2003, Glaus & van Loon 2004b):

(i) An initial rapid degradation of cellulose takes place by cleavage of the 1,4-glycosidic bond between the glucose units (called the "peeling-off reaction") and leads to the formation of soluble degradation products such as ISA. This process is initiated by a nucleophile addition of OH^- to reducing end groups (latent aldehydes).

(ii) A second, slower step of cellulose degradation is mid-chain scission triggered by stochastic deprotonation of glucose subunits of the cellulose chain (alkaline hydrolysis). This process occurs at a random location along the cellulose chain and generates new reducing end groups that can further participate in the peeling off reaction. Mid-chain scission is thought to be slow, which can make it relevant in the long term (> 1,000 years) (van Loon & Glaus 1998, Askarieh et al. 2000, Glaus et al. 2008b, Glaus & van Loon 2008, Glaus & van Loon 2004b).

(iii) Complete stopping of cellulose degradation occurs by either a chemical or physical process. Chemical stopping involves the conversion of a reducing end group into a stable metasaccharinate acid end group, thereby stopping the peeling-off process. This happens as soon as a reducing end reaches the crystalline region of the cellulose fibre, where it is no longer accessible to the attack of OH^- ions. Since the amorphous regions are no longer accessible, mid-chain scission comes to an end. This process of physical stopping gradually slows down during transition from the amorphous to the crystalline region of the cellulose fibre. However, it is not clear whether cellulose chains that have undergone the stopping reaction remain resistant to further alkaline degradation over the period under consideration of 100,000 years (Askarieh et al. 2000). According to the mechanism described above, the degree of degradation of cellulose and the resulting production of ISA and other products is high in the initial phase and corresponds to the degradation of less than 25% of the insoluble cellulose (Glaus 2004a). The second phase, where mid-chain scission dominates, results in slower degradation of cellulose (van Loon & Glaus 1998, Glaus et al. 2008b, Glaus & van Loon 2008, Glaus & van Loon 2004b).

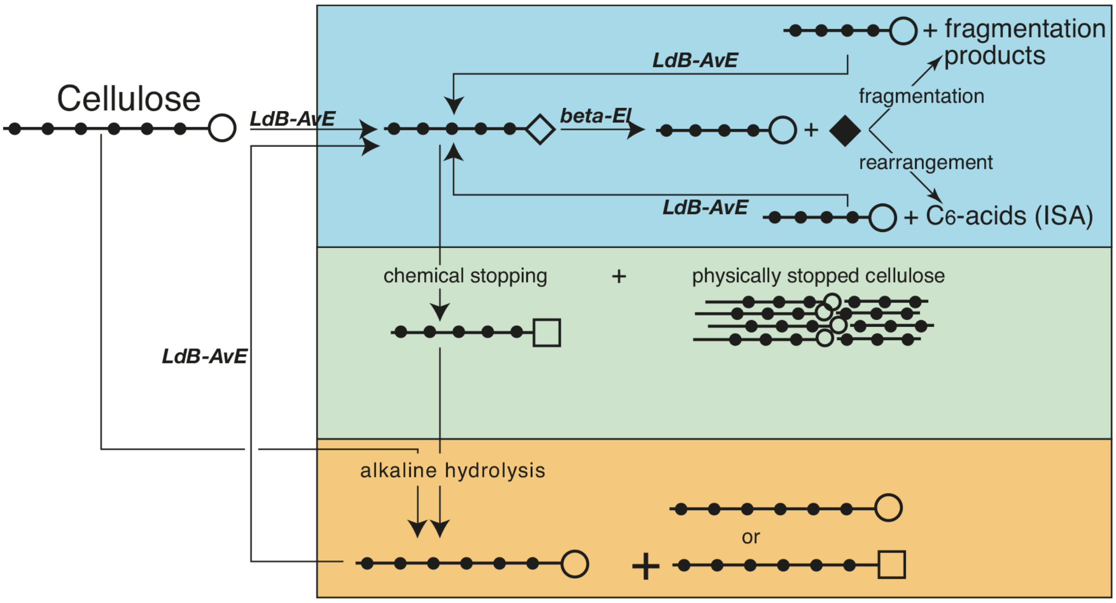

Fig. 3-6: Schematic representation of the processes involved in the alkaline degradation of cellulose

From Glaus & van Loon (2004b)

The filled black circle represents a glucose monomeric unit; the black open circle, a reducing end-group (aldehyde functional group); the open black square, a chemically stopped end-group (metasaccharinic acid or others); the open black rhomb, an activated end-group (enolate functional group); the filled back rhomb, an intermediate product (4-deoxy-2,3-hexodiulose). LdB-AvE corresponds to the reaction Lobry de Bruyn-Alberta van Ekenstein transformation and beta-EI to β-elimination.

Two isomers of ISA, i.e., α-ISA (3-deoxy-2-C-(hydroxymethyl)-erythro-pentanoic acid) and β-ISA (3-deoxy-2-C (hydroxymethyl)-threopentonic acid) are produced during cellulose degradation. In the study of Glaus et al. (1999a) with four different types of cellulosic materials (pure cellulose, tela tissues, cotton, recycling paper) immersed in cement-type pore solution (pH 13) in an inert atmosphere and at room temperature (25 °C), these two ISA isomers accounted for ~ 80% of the DOC. Other compounds like formic, acetic, lactic, glycolic, glyceric, and threoic acids were also present but contributed to less than 10% of the DOC. They were likely formed by a fragmentation reaction of the intermediate products. The amounts of α- and β-ISA and LMW organic compounds (and unidentified compounds) were found to differ depending on the cellulosic material degraded. In agreement with the study by Glaus et al. (1999b), Pavasars et al. (2003) identified ISA as the main degradation product of cellulosic materials (pure cellulose powder, softwood sawdust) in a cement-type pore solution in inert atmosphere at ambient temperature (19 – 23 °C). After three years of degradation, ISA accounted for 70 – 85% of the products quantified by capillary zone electrophoresis. In degradation experiments with cellulosic materials carried out under the UK waste management programme and reported by Filby et al. (2016), the following main degradation products were detected and identified: i) ISA, which was the main degradation product; ii) significant amounts of X-ISA, which is structurally similar to ISA and results from the degradation of hemicellulose; iii) acetic, lactic, and glycolic acids; and (iv) LMW organic acids and alcohols in low concentrations. In general, it was observed that the nature of degradation products and their concentrations depends on the type of cellulosic material and temperature.

Although the anoxic conditions are expected to mainly prevail during the period under consideration of 100,000 years, the waste will be exposed to oxic conditions during interim storage, waste emplacement and at the early post-closure stage of the L/ILW repository. The oxidation of cellulose by atmospheric O_2 under alkaline conditions is a well-known process (Knill & Kennedy 2003 and references therein) and leads to the formation of carbonyl-containing oxidised cellulose (oxycellulose), containing mostly ketone groups and partially also aldehyde and carboxyl groups. Oxidised cellulose containing carbonyl groups at positions other than the end groups, i.e., at C2, C3, C6 positions, or combinations thereof, is very labile and susceptible to alkaline degradation. The reaction is non-specific and can be accompanied by chain scission, but not systematically (Knill & Kennedy 2003 and references therein). The alkaline degradation of cellulose and oxycellulose is based on similar mechanisms and therefore, the degradation products found in the oxic degradation of cellulose under alkaline conditions are mostly identical to those found during anoxic degradation, especially in the case of ISA.

Degradation kinetics

The alkaline degradation of cellulose was modelled using two reactions: peeling-off (endwise chain depolymerisation by clipping of monomeric glucose units) and alkaline hydrolysis (mid-chain scission due to cleavage of glycosidic bonds), considering also related termination reactions (chemical and physical stopping) (van Loon & Glaus 1998). The peeling-off reaction was modelled in terms of a pseudo-first-order kinetics, which depends on the number of reducing end groups. The rate constants determined experimentally by (van Loon & Glaus 1998, van Loon & Glaus 1997) for this reaction at 25 °C agreed with literature data in the temperature range from 65 to 132 °C. The kinetic constants for alkaline hydrolysis, which produces new end groups, was derived from the extrapolation of the literature data determined at high temperature to ambient temperature. Termination reactions (physical and chemical stopping) were also modelled by pseudo-first-order kinetics. Further assumptions were made regarding the degrading cellulosic materials (mainly present as tissues and paper) and their degree of polymerisation, the amount of reducing end groups and the pH (worst case: constant pH of 13.3). Based on these assumptions, van Loon & Glaus (1998) and van Loon et al. (1999) predicted cellulose degradation over time in conditions relevant for an L/ILW repository, using the derived kinetic constants (Fig. 3-7). The uncertainty in the extrapolated kinetic constants of the alkaline hydrolysis (mid-chain scission) was assumed to be large and has a significant effect, as shown by the broad uncertainty band in Fig. 3-7. The model predicts that the degradation of cellulose occurs through the peeling-off reaction and stops after a few years. The mid-chain scission reaction over the time period up to ~ 10,000 years is so slow that no significant impact on cellulose degradation appears. The effect of this very slow process on cellulose degradation only becomes effective after ~ 10,000 years and leads to complete degradation of cellulose within ~ 100,000 years. In the long term, alkaline cleavage of the glycosidic linkage (alkaline hydrolysis) is therefore the rate-limiting step in cellulose degradation. This prediction suggests that a significant portion of the cellulose disposed of in a cement-based L/ILW repository will not be chemically degraded over the period under consideration of 100,000 years.

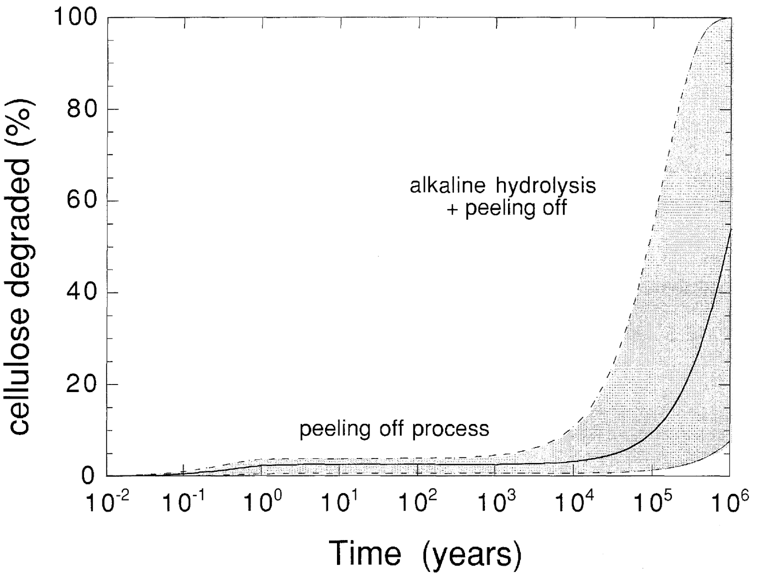

Fig. 3-7: Long-term degradation of cellulose at 25 °C and 0.3 M OH^- under conditions relevant to a cement-based L/ILW repository

From van Loon & Glaus (1998)

Pavasars et al. (2003) used the model proposed by van Loon & Glaus (1998) to fit their experimental data and make long-term predictions of cellulose degradation under the conditions relevant to a cement-based L/ILW repository. The authors used a significantly different kinetic constant for alkaline hydrolysis, which was five orders of magnitude higher than those used by van Loon & Glaus (1998). Alkaline hydrolysis, i.e., breaking of the glycosidic bonds, was therefore the dominant and rate-determining step throughout most of the cellulose degradation period. Using their kinetic constants, Pavasars et al. (2003) predicted complete degradation of cellulose within 150 to 500 years.

Influence of temperature

The controversial findings by van Loon & Glaus (1998) and Pavasars et al. (2003) were further addressed by Glaus & van Loon (2004b). Glaus and co-workers studied cellulose degradation (pure cellulose, cotton cellulose) under alkaline conditions (cement-type porewater at pH 13.3) at temperatures of 60 and 90 °C over a period of one to two years (Glaus & van Loon 2004b). The aim was to determine the reaction rate constant for the alkaline hydrolysis of cellulose (mid-chain scission) as a function of temperature. TOC of the solutions was determined, and the remaining cellulose solids were analysed for dry weight and degree of polymerisation. Glaus & van Loon (2004b) observed three distinct phases in their degradation experiments: (i) an initial fast reaction lasting a few days; (ii) a slow further reaction over ~ 100 days; and (iii) a complete stop of the degradation levelling-off at ~ 60% of cellulose degraded. Interestingly, the degree of cellulose degradation over time was found to be almost identical at 60 and 90 °C and showed no dependence on the type of cellulosic material. The authors concluded that degradation behaviour of the cellulosic materials cannot be explained in terms of the combination of fast endwise clipping of monomeric glucose units (peeling-off) and slow breaking of the glycosidic bonds (alkaline hydrolysis, mid-chain scission). They even speculated that alkaline hydrolysis was not observed in the experiments at elevated temperatures and that hitherto unknown reactions determined the degradation process. With regard to the discrepancy between the predictions by van Loon & Glaus (1998) and Pavasars et al. (2003), Glaus & van Loon (2004b) stated that, "With respect to long-term predictions for cellulose degradation at room temperature it can be concluded that the kinetic parameters for alkaline hydrolysis as proposed in the work of Pavasars (Linköping Studies in Arts and Science, 196, Linköping University, Sweden, 1999) (and published by Pavasars et al. 2003, author's note) are too large and that complete cellulose degradation at these temperatures occurs only within time scales larger than hundreds of years. However, it is not possible from the experimental evidence to corroborate the validity of a linear extrapolation ("Arrhenius equation") of the reaction rates measured at temperatures between ~ 140 and 190 °C to room temperature, from which it was previously concluded that complete cellulose degradation would take time spans of the order of millions of years." Thus, the validity of the extrapolations used by van Loon & Glaus (1998) to derive the kinetic constants for alkaline hydrolysis could not be supported by Glaus & van Loon (2004b) (Fig. 3-8). The current situation suggests that the prediction of chemical degradation of cellulose in a cement-based L/ILW repository made by Pavasars et al. (2003) seems to be too pessimistic (too fast), while the one presented by van Loon & Glaus (1998) seems to be too optimistic (too slow).

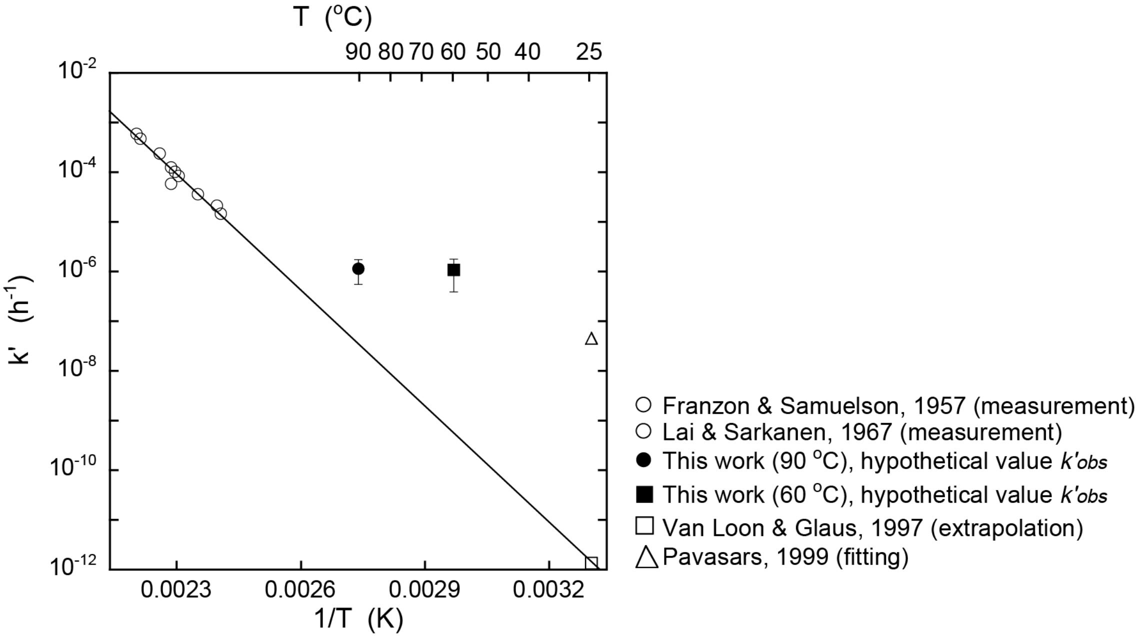

Fig. 3-8: Reaction rate constant of alkaline hydrolysis

Arrhenius plot published in Glaus & van Loon (2004b)

Long-term degradation of cellulose

Glaus et al. (2008a) and Glaus & van Loon (2008) conducted a study on the long-term degradation of cellulosic materials over a period of 12 years under alkaline, anoxic conditions at ~ 25 °C. The samples were prepared and analysed as previously described by Glaus & van Loon (2004b). A fast reaction phase (2 – 3 years) was identified, dominated by chain depolymerisation of cellulose, i.e., sequential cleavage of terminal monomeric glucose units producing α- and β-ISA by a peeling-off reaction. Thereafter, a very slow reaction phase was observed during which α- and β-ISA were also produced but could not be modelled in terms of the classical mid-chain scission reaction (alkaline hydrolysis). Modelling of the experimental data showed that most of the data could not be adequately described either by the reaction rate constants determined by van Loon & Glaus (1998) and van Loon et al. (1999) or by those determined by Pavasars et al. (2003). The authors considered two processes that could explain the slower second phase of cellulose degradation: (i) mid-chain scission of the polysaccharide chain combined with subsequent peeling-off of reconstituted reducing end groups, or (ii) a strongly decelerated reaction of the reducing end groups, which temporarily become accessible to nucleophilic attack by OH^- in a dynamic equilibrium between crystalline and amorphous regions of cellulose (called a decelerated peeling-off reaction) (Glaus & van Loon 2008). Process (i) is known from the literature, while no quantitative information is available for process (ii). It should be noted that the peeling off of reconstituted reducing end groups in process (i) differs from that in the fast process (primary peeling off), which already stops during the second slow phase of cellulose degradation. The authors concluded that, based on the experimental data, it is not possible to distinguish between the two processes postulated to explain the slow phase of cellulose degradation, and that the experimental observations cannot be explained by mid-chain scission. They postulated that a previously unknown process, such as decelerated peeling off, could be responsible for the cellulose degradation in the second, slower reaction phase. With regard to the prediction of cellulose degradation in an L/ILW repository, the authors concluded that the previous kinetic models (based on peeling-off and mid-chain scission reactions) cannot adequately describe the long-term behaviour of cellulose degradation under alkaline conditions. A currently unknown mechanism by which crystalline or inaccessible reducing end groups of the cellulose chain become temporarily accessible to alkaline attack appears to be responsible for the long-term degradation of cellulose in a cement-based L/ILW repository (Glaus & van Loon 2008).

3.2.6.2 ISA and LWM organics

Degradation mechanism and products

LMW organics, such as alcohols, aldehydes, ketones and carboxylic acids are expected to be chemically stable under alkaline conditions at ambient temperature. Only deprotonation of weakly acid groups may occur. Esters might, however, be degraded by alkaline hydrolysis, according to the following reaction:

Reaction 3-6: $\text{R-OCOR'} + OH^- \rightarrow \text{R-COO}^- + \text{R'OH}$

Note that other potential hydrolysing functional groups, such as amides, are much more resistant to alkaline hydrolysis than esters. Strongly radionuclide complexing agents like NTA and EDTA (both aminopolycarboxylic acids), are expected to be chemically stable under alkaline conditions.

The possibility of ISA degradation in strongly alkaline conditions was investigated by van Loon & Glaus (1998), Glaus et al. (2008a) and Glaus & van Loon (2008). Van Loon & Glaus (1998) investigated the chemical stability of α-ISA under anoxic conditions in a cement-type pore porewater (pH 13.3) at room temperature (~ 25 °C). α-ISA was found to be chemically stable over the three-year time period of the experiments. This may also apply to β-ISA.

Influence of temperature

Glaus et al. (2008a) and Glaus & van Loon (2008) extended the previous study of van Loon & Glaus (1998) on the chemical stability of α-ISA under alkaline conditions. Solutions of the lactone form of α-ISA were prepared in cement-type porewater (pH 13) and with various amounts of $Ca(OH)_2$ and stored either in an inert atmosphere (glove box, protective gas) or under laboratory air at different temperatures (25 ± 2 °C and 90 ± 2 °C). α-ISA was found to be stable in solution in the absence of $Ca(OH)_2$ as previously reported by van Loon & Glaus (1998). However, degradation of α-ISA was observed in oxic conditions and in the presence of $Ca(OH)_2$. The reaction also proceeded faster at 90 °C than at room temperature. The authors concluded that the degradation of α-ISA only occurs by oxidation. Stoichiometric amounts of the oxidising agent (O_2, or unknown impurities in $Ca(OH)_2$) are required to degrade α-ISA to short-chain carboxylic acids such as glycolate, lactate and acetate. Under anoxic conditions and in the presence of $Ca(OH)_2$, it was assumed that α-ISA sorbs onto $Ca(OH)_2$ and reacts with an unknown impurity in $Ca(OH)_2$, which acts as an oxidising agent and produces LMW carboxylic acids. However, the authors cautiously concluded that "the observed chemical transformation of α-ISA cannot be used as a justification to postulate α-ISA concentrations being decreased to insignificant amounts under chemically-reducing repository conditions" (Glaus et al. 2008b). This implies that the authors suggested considering α-ISA to be chemically stable over the period under consideration of 100,000 years.

Tits & Kunz (2020) investigated the chemical stability of formic and acetic acid in a cement-type porewater (pH 12.5) in the presence of H_2 and Fe(0) powders. These conditions were assumed to be similar to those in the near-field of an L/ILW repository, where Fe(0) is present as metallic waste and corrodes under alkaline, anoxic conditions, giving rise to an enhanced partial pressure of H_2. Thermodynamic modelling shows that under these conditions and in the case of full thermodynamic equilibrium in the C-H-O system, CO_2 (i.e., CO_3^{2-} at pH > 10) and CH_4 should be the dominant carbon species produced (Wieland 2015). The degradation experiments with formate and acetate were carried out in airtight pressurised reactors at elevated temperatures ($50\ °C \leq T \leq 200\ °C$) and pressures ($2\ bar \leq P \leq 16\ bar$). Abiotic degradation of the two LMW organic compounds was assumed to occur via redox processes leading to the formation of CO_2 and CH_4. At moderate temperatures and pressures, most of these redox reactions are extremely slow, although some reactions can be accelerated by the presence of catalytic surfaces such as iron oxides on steel surfaces. For this reason, elevated temperatures were chosen as it was suspected that the degradation reactions, if they occurred at all, would be very slow. The results show that the degradation of formate and acetate at room temperature is indeed too slow to observe any changes in the aqueous concentrations of formate and acetate within a reasonable period of time. However, formate was found to decompose in the presence of $Ca(OH)_2$ and iron corrosion products at temperatures up to 200 °C. The decomposition rates of formate were similar to those given in the literature for formate degradation under hydrothermal conditions. The decomposition of formate could be interpreted in terms of a decarboxylation process given by:

Reaction 3-7: $COO^- + H_2O \Leftrightarrow CO_2 + H_2(g)$

Formate decomposes into CO_2, which is present in alkaline solution at pH 12.5 as CO_3^{2-}, and gaseous H_2. Thermodynamic calculations show that formate is unstable under anoxic conditions, even under moderately reducing conditions induced by the presence of Fe powder, and decomposes into CO_2 and H_2 by the decarboxylation reaction (Tits & Kunz 2020). In the presence of metallic Fe, however, more strongly reducing conditions are created, resulting in the stabilisation of formate.

Acetate was chemically stable over reaction times up to 8 months, even under conditions of elevated temperatures that promoted formate decomposition (Tits & Kunz 2020). The results show that both formate and acetate seem to be chemically stable under alkaline conditions at ambient temperature in the presence of Fe(0) and at elevated partial pressure of H_2. Thus, if degradation of these LMW organics occurs over the period under consideration for an L/ILW repository, the process will be extremely slow.

No information about chemical degradation kinetics is available for ISA and LMW organics.

3.2.7 Plexiglas®

Degradation mechanism and products

Also belonging to the category "addition polymers", chemical resistance to alkali attack is also expected in the case of Plexiglas®, which has a pure carbon backbone and no vulnerable sites for alkaline hydrolysis. No specific information is available on the degradation of PMMA and other polymers based on poly(acrylic acid) (PAA) under alkaline conditions. Indirect evidence of the degradability is provided by recent studies in which a degradable version of PAA was synthesised and characterised. To make the PAA degradable, a carbonate linkage was introduced into the single carbon polymer backbone, resulting in a structural mimic of PAA, namely poly(glyceric adic carbonate) (Zhang et al. 2015) which contains a carbonate group $(\text{-R-CO}_3\text{-})_n$ susceptible to alkaline hydrolysis.

The influence of temperature on the chemical degradation has not been investigated and no information on the chemical degradation kinetics is available.

3.2.8 SPs

Degradation mechanism and products

The three main types of SPs currently in use have different structural features. The SMF condensate has a chemical substitution of the backbone (N atom), while SNF and PCE have a pure carbon backbone. Therefore, in the case of SMF, limited resistance to alkali attack is expected, while SNF and PCE are expected to be resistant to hydrolysis under alkaline conditions.

Yilmaz et al. (1993) investigated the degradation of SMF and SNF condensates in 1 M KOH solution (pH 14) for up to 20 days in the absence of air. The concentration of SMF decreased significantly with time, and the formation of a white precipitate was observed. The analysis showed that more than 65% of the original SMF had precipitated. Characterisation of the SMF precipitate further showed that its chemical and physical properties were significantly different from those of the original SMF. However, no chemical characterisation of the precipitate was provided, so it was not possible to propose a conclusive degradation pathway. In contrast, the concentration of SNF decreased only slightly (10% of the initial concentration) within the first day and remained constant thereafter. In the case of SNF, no precipitate was observed. The results support the idea that SMF is susceptible to alkaline hydrolysis, while SNF is likely to be persistent under alkaline conditions.

Chernyshev et al. (2018) investigated the degradation and complexation properties of an SPs-based PAE in alkaline solution (NaOH solution, pH 12) under inert atmosphere (Ar) at 22 °C for up to 86 days. The results showed a gradual pH decrease over time, which was attributed to a degradation process. ^{31}P nuclear magnetic resonance spectroscopy measurements showed that organophosphate groups were cleaved from the backbone and reacted with OH^-, thus continuously lowering the pH. However, no evidence of carbon backbone fragmentation was provided in this study, confirming that pure carbon backbones of SPs are likely resistant to alkaline hydrolysis. It can be assumed that PCE and PAE have similar resistance to alkaline hydrolysis due to their chemical structure.

Glaus & van Loon (2004a) studied the influence of concrete admixtures (SMF-, SNF- and PCE-based SPs from different manufacturers) on the uptake of radionuclides by hardened cement paste (pH 13.3 of porewater). The degradation process of SPs was not specifically investigated. However, it was indirectly demonstrated that they were chemically stable during the experimental period (up to 14 months), as no changes in the concentration were observed. Similarly, the leaching tests of PCE-based SPs of Andersson et al. (2008) also provide indirect evidence for their chemical stability, as the high molecular weight fractions of PCE were found to not be leachable. In contrast, Fujita et al. (2008) show the presence of LMW organics in the porewater extracted from hardened cement paste, but these could not be attributed to the degradation of SPs (PCE in both studies).

The influence of temperature on the chemical degradation has not been investigated and no information about the chemical degradation kinetics is available.

3.3 Thermal degradation

3.3.1 Definition

The thermal stability of a polymer chain depends on how easily the thermal cleavage of the main chain occurs. At moderately enhanced temperature, thermal degradation leads to changes in the chemical properties. At strongly enhanced temperature (pyrolysis), damaging chemical changes can occur, resulting in depolymerisation. This onset of thermal degradation is the limit at which polymers can be used. Studies on the rates of polymer degradation have been limited to temperatures in the range from ~ 200 °C to ~ 600 °C. In this temperature range, the rate of degradation tends to double for every 10 °C rise in temperature. The nature of the volatile degradation products largely depends on the temperature employed (Madorsky 1964). Most experimental studies on thermal degradation of polymers have been conducted up to temperatures of ~ 400 – 500 °C and under vacuum, as the presence of a gas increases the probability of secondary chemical reactions and could therefore mask the pure thermal effects of polymer degradation. For the evaluation of the thermal degradation of polymers under L/ILW repository conditions, the experiments performed at such high temperatures and under vacuum are therefore of limited use. In an L/ILW repository, the temperature at 900 m below ground level is expected to be < 50 °C after closure (Papafotiou & Senger 2016). "Pure" thermal degradation processes like pyrolysis that can only occur above this threshold are not relevant. At this temperature, thermal degradation always occurs in combination with radiolytic or chemical (hydrolytic) degradation. This is the reason why the influence of temperature on radiolytic and hydrolytic degradation of organic waste was specifically discussed in Sections 3.1 and 3.2. In the temperature range between 25 and 60 °C, a stronger radiolytic and hydrolytic degradation of organics by less than a factor of ~ 2 was indeed observed with increasing temperature.

The temperature range of "pure" thermal degradation is related to the thermal properties of polymers. In this context, two temperatures are important as they influence the thermal properties of the polymers (Lodge & Hiemenz 2020): i) the lower glass transition temperature (T_g), corresponding to the transition from a hard, rigid glass-type to the final expected material; ii) the higher melting temperature (T_m), corresponding to the transition of the regular material into a liquid. Between these temperatures, the material is converted from 100% crystalline to 100% amorphous. For example, PVC has a T_g = 90 °C and a T_m = 270 °C, PS has a T_g = 100 °C and T_m = 240 °C and PE has a T_g = -120 °C and T_m = 135 °C.

"Pure" thermal degradation involves several mechanisms that run either concurrently or consecutively:

i) chain mechanisms involving crosslinking and/or scission;

ii) depolymerisation in which the monomer units are sequentially cleaved one by one from the polymer (e.g., PMMA);

iii) side group elimination in which functional groups attached to the backbone are cleaved (e.g., PVC);

iv) random chain scission in which scission starts randomly on the backbone;

v) and thermal oxidation in which peroxide radicals are formed and involved in the degradation process.

Similarly to radiolytic degradation, the formation of free radicals occurs at the onset of thermal degradation and is generated by the activation of electrons at elevated temperatures (Plota & Masek 2020). Thermal degradation of most polymers also involves a radical chain mechanism with initiation, H-abstraction, β-scission, and ends with radical recombination reactions. As in radiolytic degradation, the chain mechanism involves crosslinking and/or scission. The reactions end when radicals react with each other, forming gaseous or water-soluble products. At temperatures above ~ 600 °C, fragmentation of the polymer by scission was found to be the main degradation process (Madorsky 1964). Fragmentation is also stronger when thermal degradation is carried out in the presence of a gas rather than under vacuum.

Reaction rates can be determined by various methods in the studies of thermal degradation of organics, such as by weight loss or molecular weight distributions, pressure changes caused by gaseous degradation products, which are based on the viscosity of the residues, and by identification and quantification of end-groups. Reactions can very rarely be described in terms of zero-order kinetics where only one mechanism is involved. In most cases, the degradation reaction involves two or more mechanisms that run either concurrently or consecutively.

3.3.2 IERs, PS and styrene

Thermal degradation of cationic-exchange resins in an aqueous medium at 250 °C resulted in a cleavage of sulphonate groups (Fernandez-Prini & Schulman 1984). No further degradation of the PS backbone was observed at the given temperature. According to Nassoy et al. (1989) and Scanlan et al. (1989), thermal degradation of cationic-exchange resins in aqueous media leads to the formation of acid which could attack the polymer backbone. At ~ 300 °C, thermal degradation of cationic-exchange resins was found to occur by random rupture of the polymer backbone due to the cleavage of sulphonic acid groups and intramolecular hydrogen transfer (Nassoy et al. 1989, Scanlan et al. 1989). The major degradation products formed were dimeric, trimeric and tetrameric styrene molecules, indicating scission as an important degradation process. The formation of unsaturated organic compounds (polyenes) by crosslinking was not considered as an important degradation process at ~ 300 °C, while it has been observed above 300 °C.

In the case of anionic-exchange resins, thermal degradation at 250 °C resulted in a loss of exchange capacity due to cleavage of the quaternary ammonium functional groups (Fernandez-Prini & Schulman 1984). This process was already reported by Tulupov & Polyanskii (1973) at temperatures ≥ 100 °C. Signs of oxidation of the polymer backbone were also observed due to the presence of CO_2 (Fernandez-Prini & Schulman 1984).

According to McNeill (1997) and Faravelli et al. (2001), the thermal degradation of PS does not occur to any significant extent below ~ 300 °C, as indicated by the absence of volatile degradation products. However, monomers can be released below this temperature by unzipping reactions, due to the presence of weak linkages. At temperatures above 300 °C, volatile products are formed at a maximum rate between 400 and 420 °C. Above this range, rapid degradation occurs, and at temperatures above ~ 450 °C, the polymer is completely decomposed (Fig. 3-9). The products formed are monomers, small amounts of toluene, α-methylstyrene and other fragments (McNeill 1997, Peterson et al. 2001). The degradation mechanism is based on chain-end and random scissions of the polymers. It especially includes: i) a radical-induced depropagation forming monomers like styrene; ii) an intramolecular radical transfer leading to the formation of dimers and other short chain fragments; and iii) an intermolecular radical transfer generating chain scission (McNeill 1997). Thermo-oxidative degradation in air differs from purely thermal degradation under an inert atmosphere by the contribution of the oxidative chain mechanism, which produces reactive peroxy and hydroperoxyl structures in the chain (Peterson et al. 2001). As a result, the temperature at which complete degradation starts is shifted by ~ 100 °C (i.e., from ~ 400 °C to ~ 300 °C).

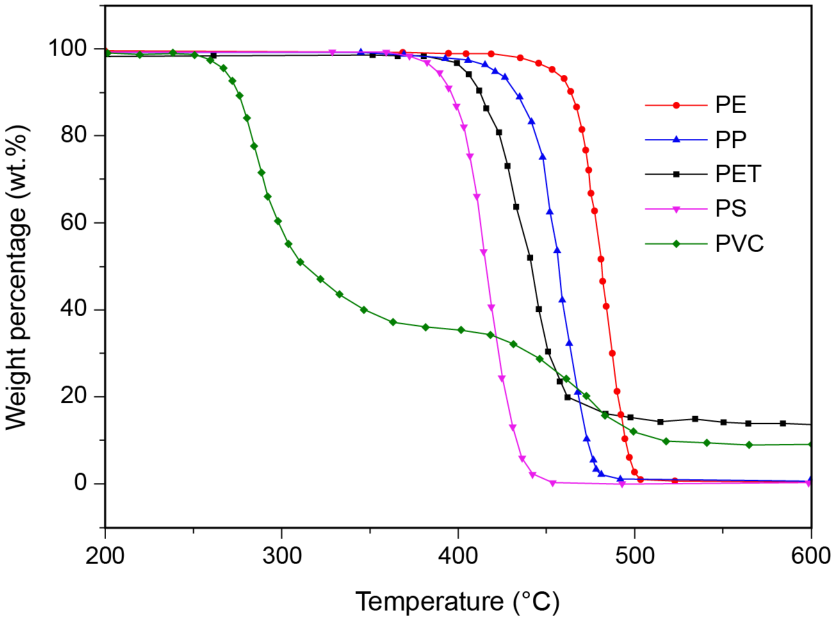

Fig. 3-9: Degradation (weight loss) of PE, PP, PET, PS and PVC as a function of temperature

From Yu et al. (2016)

Under conditions relevant to an L/ILW repository (T < 60 °C), Rizzato et al. (2017) observed slightly higher ^{14}C releases at 50 °C in a closed system and in the presence of small amounts of water (ca. 12%), defined as a slow thermal degradation of IERs.

3.3.3 PVC

Although many studies on the thermal degradation of PVC are available (Yu et al. 2016, Abbas-Abadi 2021), only a few aspects are expected to be relevant in the context of an L/ILW repository.

PVC degrades in several time-dependent steps (Braun 1971, Nagy et al. 1980b, Bacaloglu & Fisch 1994a, Yu et al. 2016). Up to about 250 °C, HCl is the only volatile degradation product, indicating dehydrochlorination and the formation of polyenes (conjugated bonds). In the presence of O_2, oxidation reactions can occur in addition to dehydrochlorination, potentially initiating chain scission (Nagy et al. 1980a). In the temperature range of 250 – 350 °C, the polyenes decompose to LMW organic compounds, such as benzene. Polymer breakdown occurs above 350 °C, where the polymeric residue decomposes mainly into LMW aromatic compounds, e.g., toluene, benzene, and others. It should be noted that the onset temperature of PVC decomposition is much lower than those of other plastics (Fig. 3-9) (Yu et al. 2016).

Various models have been developed to explain the mechanism of PVC degradation, including the determination of the kinetics of degradation processes (Šimon & Valko 1990, Bacaloglu & Fisch 1994a, Bacaloglu & Fisch 1994b, Fisch & Bacaloglu 1995, Starnes 2002, Yu et al. 2016) and references therein). The degradation of PVC is believed to be an autocatalytic process, where HCl acts as a catalyst for the decomposition of the PVC backbone. PVC additives such as stabilisers can have an impact on the thermal degradation by either accelerating or hindering dehydrochlorination (Castañeda-Facio et al. 2014). Irradiation of PVC also impacts thermal degradation. Pre-treatment of additive-free PVC by γ-irradiation (total absorbed dose: 1 MGy) under an inert atmosphere resulted in a reduction of the onset of thermal degradation from 240 °C for non-irradiated PVC to 110 °C for irradiated PVC (Boughattas et al. 2016). The effect of γ-irradiation in air on plasticised PVC was less significant, and the initial degradation temperature shifted from 183 °C for non-irradiated PVC to 100 °C for irradiated PVC. This behaviour was attributed to the formation of oxidising end groups and polyenes by irradiation.

Overall, radiolytic and thermal degradation of PVC show great similarity in terms of the radical-induced processes involved and the products formed.

3.3.4 Bitumen

Bitumen is a mixture of polymeric materials, and therefore its susceptibility to thermal degradation is expected to be variable. Bitumen samples were exposed to air at 130 °C and aged for up to 64 h. Oxidation of bitumen accounts for the chemical ageing upon heating, which leads to an increased number of carbonyl (C=O) and polyene (C=C) groups in the matrix and increases the asphaltene content. Heating proved to be more efficient in oxidising bitumen than irradiation. Both processes led to the formation of C=O and C=C bonds, although the ratio in the two treatments was different. This indicates that largely the same mechanisms are responsible for bitumen ageing during thermo-oxidative treatment and irradiation in air (cf. Section 3.1.4). For both ageing treatments, the availability of O_2 is a limiting factor, which relates to its diffusion into bitumen. The limitation of O_2 supply was previously found as the limiting factor under γ-irradiation at high dose rates. In the absence of air during γ-irradiation, bitumen ageing led to the formation of C=C bonds, while almost no increases in C=O bonds were observed (cf. Section 3.1.4). Based on the idea that the chemical reactions in bitumen are similar during γ-irradiation and thermal treatment, this process might therefore also apply to thermal ageing. As previously stated by Lőrinc (1966), chemical decomposition of bitumen does not occur in the given temperature range (100 – 130 °C), although the polymeric components of bitumen are subject to chemical conversions.

3.3.5 Plastics

PE and PP

Thermal degradation of PE and PP at temperature above 400 °C is kinetically described by a process consisting of a large number of independent first- order reactions producing large amounts of HCs with 1 to 70 C atoms, including gaseous and aliphatic species (Ranzi et al. 1997). In contrast to PS, unzipping of monomer units does not seem to be an important process (Peterson et al. 2001). The formation of larger degradation products is attributed to a favourable H abstraction at certain C atoms of the backbone, which leads to chain scission. This mechanism begins at weak bonds along the polymer chain once thermally induced scission has occurred (Peterson et al. 2001).

The primary degradation pathway for PE involves random scission of the polymer chain, followed by radical transfer processes and potential branching (i.e., crosslinking). Above the polymer breakdown temperature of ~ 450 °C, PE degradation occurs in a single mass loss step (Fig. 3-9). PE is completely degraded at ~ 500 °C. Thermal degradation of PE in the presence of O_2 shifts the onset of mass loss from ~ 450 °C to ~ 230 °C (Hoff et al. 1982, Peterson et al. 2001).

Thermal degradation of PP is also due to random scission with the involvement of radical transfer processes. However, no chain branching (i.e., crosslinking) was observed. Thermal degradation of PP in the presence of O_2 decreases in temperature by ~ 200 °C (from ~ 400 °C to ~ 200 °C) where complete degradation begins in a single mass loss step (Peterson et al. 2001). Thermo-oxidation in the temperature range above 200 °C has been found to produce a large number of oxygenated carbon compounds, among which fatty acids, formaldehyde and acetaldehyde are the most common (Hoff et al. 1982).

Polyester and PC

Above 380 °C, the initial decomposition stage of PET is due to the scission of the ester bonds on the main chain. It is an ionic process (intramolecular exchange) followed by a transfer reaction of an H atom in β-position and occurs via six-membered or four-membered cyclic transition states (cyclisation) (Montaudo et al. 1993). In contrast to the thermal degradation of other polymers, radical-induced reactions are less likely than ionic processes because the energies required for radical reactions on the main chain were found to be higher than those of concerted chemical reactions (Huang et al. 2022). Thermal degradation leads to the formation of ethenyl-terminated and carboxyl-terminated groups (Buxbaum 1968, Montaudo et al. 1993, Gałko & Sajdak 2022, Huang et al. 2022). The decomposition of transitions states and secondary reactions lead to a variety of degradation products like terephthalic acid, vinyl terephthalate and divinyl terephthalate, indicating the cleavage of condensation dimers. The polymer breakdown temperature is ~ 380 °C for both PET and PC (Feng et al. 2014). Above this value, degradation occurs as single mass loss step (Fig. 3-9). Thermo-oxidative degradation in air lowers the breakdown temperature by ~ 80 °C (Jabarin & Lofgren 1984).

In the case of PC, the carbonate group was found to be the part of the polymer molecule most sensitive to thermal degradation in the temperature range below polymer breakdown (300 – 389 °C) (Davis & Golden 1968). Thermolytic cleavage occurs through so-called β-H-elimination (reaction of the H-atom in the β-position) with the formation of a cyclic transition structure (van Speybroeck et al. 2001). Several degradation products have been observed such as CO_2, olefins and other LMW organic compounds, and the process occurs by chain scission (Davis & Golden 1968, van Speybroeck et al. 2001, Feng et al. 2014).

3.3.6 Cellulose and LMW organics

Cellulose

The thermal degradation of cellulose takes place in temperatures ranging between ~ 150 and 500 °C (mainly between 300 and 390 °C) and involves a number of temperature-dependent processes (Jusner et al. 2021, Collard & Blin 2014). Between ~ 150 and 240 °C, random cleavage of the cellulose chain and release of water occurs, leading to conformational changes in the cellulosic glycopyranose unit and generating anhydrocellulose. Partial depolymerisation also occurs at this stage. Water plays an important role in the thermal degradation of cellulose due to its auto-accelerating influence (Scheirs et al. 2001). Thermal degradation in this temperature range and under inert atmosphere (N_2) rarely leads to the formation of gaseous and organic carbon compounds (Collard & Blin 2014), while in other studies conducted in alkaline media, the formation of a variety of LMW hydroxy monocarboxylic acids and dicarboxylic acids was observed, such as formic, glycolic, lactic and oxalic acids (Niemelä & Sjöström 1986). Dehydration reactions lead to new intramolecular (within a glucopyranose unit) or intermolecular (between two chains) bonding, the latest resulting in cross-linked structures. Note, however, that crosslinking can only result from the interaction of carboxyl groups with hydroxyl groups of neighbouring chains in formal esterification reactions. In the temperature range between ~ 200 and 280 °C, breakage of the glycosidic bonds between the monomer units (chain scission) occurs in non-crystalline cellulose regions, resulting in a levoglucosan chain end and a non-reducing chain end, which are prone to easy dehydration (H_2O release). According to Niemelä (1990), thermal degradation under inert atmosphere forms degradation products similar to those in the lower temperature range. Between 270 and 300 °C, cellulose loses its crystallinity. The maximum water release of cellulose under inert conditions was observed in the temperature range between ~ 300 and 350 °C as a result of depolymerisation and leads to complete degradation of the polymer. During this step, most of the degradation products are condensable organic compounds, such as phenolic HCs, and (oligo)saccharides (Collard & Blin 2014). It should be noted that the amorphous part is thermally less stable than the crystalline part, which can shift the onset temperature of depolymerisation downwards by 20 – 40 °C. Moreover, hemicellulose is less stable under thermal conditions than pure cellulose (Yang et al. 2007). Thermo-oxidative degradation of cellulose leads to the formation of a large number of oxygenated carbon compounds, more especially carbonyl and carboxyl groups along the cellulose chain. These groups are susceptible to OH^- attack under alkaline conditions.

LMW organics

The thermal stability of LMW organics has been studied extensively in the context of hydrothermal geological environments and industrial applications, i.e., temperatures ranging between ~ 200 and ~ 450 °C and pressures up to 40 MPa (Tits & Kunz 2020 and references therein). Under high-temperature conditions, LMW organics can be transformed by various reactions, the most important being decarboxylation (CO_2 release) and dehydration (H_2O release) (Tits & Kunz 2020). For example, formic acid has been observed to undergo decarboxylation at temperatures up to 200 °C.

The hydrothermal treatment of several aromatic compounds (benzoic, terephthalic, o-phthalic, isophthalic, 2,6-naphthalene dicarboxylic acids, biphenyl, trimellite anhydride) was performed in the temperature range between 250 and 410 °C for a period of one hour (Dunn et al. 2003). The results show that decarboxylation is also an important process at elevated temperatures.

3.3.7 Plexiglas®

PMMA appears to be stable up to ~ 160 °C. In an inert atmosphere (e.g., vacuum, Ar, N_2), complete degradation occurs between ~ 165 and 400 °C in four overlapping substeps (Ferriol et al. 2003). The first stage of degradation occurs in the temperature range between 165 and 350 °C and corresponds to the cleavage of the vinylidene end groups (-CH=CH-) from the vinylidene-terminated chains and scission of the abnormal linkages (head-to-head linkage within the chain). Thermal initiation of degradation at vinylidene end groups and abnormal linkages leads to the formation of polymer radicals that react further. The second stage in the degradation occurs after cleavage of the reactive end groups in the temperature range between ~ 270 and 400 °C. It corresponds to cleavage at unsaturated ends and random chain scission. These processes are initiated by H-abstraction from the polymer chain (Kashiwagi et al. 1989, Ferriol et al. 2003). The degradation products formed are gaseous species (e.g,, CO, CO_2 and CH_4) and monomeric units. Thermo-oxidative degradation in the presence of O_2 improves PMMA stability (instead of decreasing it as in other polymers) due to the formation of a peroxy radical by the reaction of the end group radicals with O_2 (Song et al. 1992, Peterson et al. 1999). This radical is thermally more stable than the radicals formed in the absence of O_2, and thus inhibits unzipping of the polymer chain. Since this process is suppressed, degradation occurs only through random scission, producing only small amounts of volatile LMW degradation products. As a result, the mass loss shifts to higher temperature under air than under an inert atmosphere. It was, however, suggested that random chain scission could already occur at lower temperatures (50 – 125 °C) (Martin et al. 1987). Thermo-oxidative degradation of PMMA produces, apart from the monomer, carbonic acid methyl esters and acetaldehyde formed by chain scission.

3.3.8 SPs

No specific information was found on the thermal degradation of the LS, SMF, SNF, PCE and PAE-based SPs. The thermal stability of the monomeric building blocks of the condensates, i.e., melamine in the case of SMF and naphthalene in the case of SNF, has been reported elsewhere (García et al. 2018).

3.4 Overview

Radiolytic degradation

In the Swiss waste inventory, more than 99% of the total mass of organics present are stored in L/ILW and the rest in ATW (Nagra 2023b) (cf. Section 2.4.2). Organic materials are therefore mainly exposed to γ-/β-radiations and subject to external irradiation. The initial dose rate rapidly decreases due to the short half-life of ^{60}Co and ^{137}Cs, the main γ-emitters inventoried in L/ILW. After the period under consideration of 100,000 years, the total absorbed dose will, on average, fall below 1 MGy. In ATW, the total absorbed dose can reach values several orders of magnitude higher (i.e., 100 MGy on average) after 100,000 years due to the larger decay heat of the α-emitters. However, only a limited amount of organic material was inventoried in ATW (i.e.,< 1%) and exposed to such doses.

Radiolytic degradation of organics is hence expected to happen initially during interim storage, waste emplacement and in the early post-closure stage of the L/ILW repository. During this period, oxidative degradation will occur under irradiation due to the presence of O_2 in the waste matrix and in the caverns (gas exchange between the atmosphere and the interior of the waste packages is likely since they are not hermetically sealed). However, it should be noted that oxidative degradation is severely limited by O_2 supply through the slow diffusion into the waste matrix, which may significantly reduce the extent of radiolytic degradation of the organics. Anoxic-reducing conditions are expected to develop rapidly after closure of the repository (cf. Section 2.4) due to O_2 consumption by several processes such as corrosion of metals and microbial activity. This implies that oxidative degradation is likely to occur only over a very short period relative to the longevity of the L/ILW repository.

Complete resaturation of the L/ILW caverns is expected to take more than 100,000 years and will start by resaturating the bottom (cf. Section 2.4). The absence of free water in most parts of the L/ILW repository limits the degree to which organic materials can be degraded by radiolytic oxidative degradation, as no oxidants (radicals, peroxide) will be produced due to radiolysis of water under γ-irradiation. As a minimum humidity of 60% is necessary to create a continuous water film on the reactive materials and allow chemical reactions to occur (Wieland & Kosakowski 2020), a minimum of 60% RH might be required to start radiolytic degradation. Under fully saturated conditions, radiolytic degradation is assumed to be more significant. But as the resaturation of the L/ILW caverns is expected to be low, the dose rate will be already low at the time water is not limiting.

The resistance of the different types of polymers to radiation is largely determined by their chemical structure, in particular by their molar mass (i.e., different degrees of condensation or values of n, respectively), aromaticity (i.e., cyclic molecular structure of the backbone), but also by the presence of bonding pattern of carbon atoms in the polymer matrix (e.g., aliphatic carbon chains, quaternary carbon atoms, etc.), heteroaromatics (i.e., atoms other than carbon in the cyclic structure), and polymer condensation with heteroatoms in the main chain (e.g., formation of glycosidic linkages in cellulose and presence of ester and ether bonds in the aliphatic chains). In general, polymers with aromatic groups in their molecular structure (e.g., PS) have a significantly higher radiation resistance than aliphatic polymers, regardless of the position of the aromatic groups in the chain (e.g., PVC, PE and PP) (Tab. 3-1).

Crosslinking and scission are the main radiolytic degradation mechanisms. The former mechanism leads to the formation of large three-dimensional molecular networks and increases the degree of polymerisation and probably also its chemical stability over the period under consideration for an L/ILW repository (i.e., 100,000 years). In contrast, scission leads to depolymerisation and fragmentation, increasing the probability that the polymer will be fully degraded within 100,000 years of storage. Whether a polymer predominately undergoes crosslinking or scission upon irradiation depends primarily on its chemical structure and the environmental conditions. Crosslinking is expected to be the predominant reaction upon irradiation under inert conditions, expected in the unsaturated near-field of an L/ILW repository. In general, scission is the primary degradation mechanism when polymers contain a large number of quaternary carbon atoms along the chain (e.g., PMMA or Plexiglas®). If this structural feature is absent, crosslinking predominates (e.g., PE, PS and PVC). Crosslinking appears to be significantly enhanced by the presence of aromatic rings in the structure. It should, however, be noted that both processes can also occur simultaneously (Tab. 3-1).

Polymers that are predominantly degraded by the crosslinking mechanism are unlikely to fully degrade during the period under consideration. This is true for most polymeric materials that will be disposed of in the L/ILW repository, such as PVC, PS and the backbone of IERs and bitumen. The aliphatic backbone of PE and PP is expected to be less stable under radiation, but crosslinking is still expected to be the dominant mechanism under anoxic conditions. The presence of ester and carbonate groups in polyesters and PC exhibit moderate resistance to irradiation, noting that if aromatics are present in the polymer backbone, the radiation stability is improved. The main radiolytic degradation process for polyesters and PC is chain scission. Cellulose is also susceptible to radiation with chain scission as the predominant mechanism. This may also apply to the main degradation product of cellulose, ISA, although no experimental data could currently prove this statement. The predominant radiolytic degradation mechanism for LMW organics is fragmentation. PMMA is susceptible to irradiation due to the presence of tetra-substituted carbon atoms. Moreover, ester groups are prone to cleavage from the aliphatic backbone. Chain scission seems to be the predominant radiolytic degradation process. Among the considered SPs, SNF is expected to be the polymer most resistant to irradiation due to the polycyclic aromatic nature of the backbone. Crosslinking is expected to be the dominant radiolytic degradation mechanism for SNF and PCE, while scission is considered to predominate in the case of SMF. The additives contained in some of the main organic materials previously mentioned (i.e., plasticisers) are likely to degrade completely over time.

Radiolytic degradation produces a large number of different molecules (Tab. 3-1). There is evidence that the dose rate has no or at least only limited influence on the type of degradation products formed. For most polymers, the degradation products are generally very similar and consist of mixtures of HCs, alcohols, aldehydes, ketones, and carboxylic acids with a number of carbon atoms between ~ C5 and ~ C20. They are mainly gaseous species, such as H_2, CH_4, CO, CO_2, and small alkanes, alkenes and alkyne formed by the recombination of small radicals. The recombination of small and large radicals leads to the formation of larger, water-soluble organic molecules. The nature and amount of the degradation products strongly depend on the type of polymer (structure, chemical composition) and the local irradiation environment. Therefore, it is currently impossible to provide a list of all the compounds that could be formed over time when polymers are irradiated. The degradation products are subject to further degradation by irradiation, as continuous irradiation appears to promote the gradual decay of larger molecules into smaller ones over longer irradiation periods, reacting with the cementitious near-field materials for inorganic compounds or used as carbon sources for microbial activities for organic compounds.

The degree of radiolytic degradation is uncertain as it depends both on the material properties, (e.g., type of polymer) and environmental conditions like the total absorbed dose, presence of O_2 and water, temperature, etc. There are currently no systematic kinetic models and rates available that allow quantitative predictions of the degradation of polymeric materials as a function of the total absorbed dose over the period under consideration. Furthermore, kinetic models for the degradation of polymeric materials under the conditions relevant for an L/ILW repository are lacking and no rates could be found in the currently available literature (Tab. 3-1).

Chemical (alkaline) degradation

Hydrolysis is the only chemical process that can enable the degradation of organic polymers in the cementitious near-field of the L/ILW repository section. It however, only occurs to a very limited extent, depending on the polymers considered (Tab. 3-1).

IERs, bitumen, plastics (PE, PP), PMMA (Plexiglas®), and some SPs (SNF, PCE) are not susceptible to hydrolysis and should remain largely stable under strongly alkaline conditions. PVC is known to be a poorly degradable, alkali-resistant plastic and should therefore also be resistant to hydrolysis. However, there is some evidence that the material may be less stable in highly alkaline, saturated $Ca(OH)_2$ solutions. Further demonstration of the stability of PVC under these conditions would be required. Conversely, there is clear evidence that polyester and PC degrade under alkaline conditions. This is also true for cellulose.

As for radiolytic degradation of organic materials, no models allowing quantitative predictions of the degradation process based on chemical kinetic exist for the period under consideration of 100,000 years. The most advanced models have been developed for cellulose degradation. However, even in this case, the lack of understanding of the relevant long-term degradation reaction (mid-chain scission) introduces large uncertainties in the predictions. Therefore, current kinetic models predict the complete degradation of cellulose within a wide time span, i.e., ranging from a few hundred to a hundred thousand years. Furthermore, it is not even clear whether complete degradation of cellulose will occur or whether the process will be stopped due to the resistance of the crystalline part of the polymer to alkaline hydrolysis. As a result, quantitative predictions of the degradation of organic waste by alkaline hydrolysis are currently not available for safety analyses.

In the context of an L/ILW repository, it also appears that the degree of degradation by alkaline hydrolysis is critically affected when the polymers are exposed to oxidants (oxidative degradation), such as ·OH and peroxy radicals or hydrogen peroxide. Oxidative degradation could occur through exposure to air (O_2) during interim storage, waste emplacement and at the early post-closure stage of the L/ILW repository. In addition, radiolytic oxidative degradation could occur during these phases, and water radiolysis could produce oxidants. The change from oxic to anoxic conditions over the course of the waste emplacement history makes it even more difficult to develop accurate quantitative models of the long-term fate of organic materials in an L/ILW repository.

Thermal degradation

The thermal stability of a polymer chain depends on how easily the thermal cleavage of the main chain occurs. The thermal degradation reactions of all the polymers of interest are endothermic, related to their material properties and generally occur above ~ 200 °C under inert atmosphere. In an L/ILW repository, where temperatures at 900 m below ground level are expected to be < 50 °C after closure (Papafotiou & Senger 2016), purely thermal degradation is therefore not considered as relevant. At this temperature range, thermal degradation always occurs in combination with radiolytic or chemical (hydrolytic) degradation. More pertinently, a stronger radiolytic and hydrolytic degradation of organics by less than a factor of ~ 2 was indeed observed with increasing temperatures in the range between 25 and 60 °C (Tab. 3-1).

Tab. 3-1: Summary table of the abiotic degradation of the main organics present in L/ILW

n.a.: not available

Material	**Criteria**	**Radiolytic degradation**		**Chemical degradation**		**Thermal degradation ($T \leq 50$ °C)**	
	Environment	**Oxic**	**Anoxic**	**Oxic**	**Anoxic**	**Oxic**	**Anoxic**
IERs, PS, styrene	**Mechanisms**	scission	crosslinking	alkaline hydrolysis		heat treatment	
	Products	H_2, CH_4, CO_2, CO, SO_4^{2-}, amines, ammonia, oxalate, hydroxylic and carboxyphenolic compounds		n.a.		n.a.	
	Degree of degradation	degradation of IERs' surface groups, no degradation for PS		not susceptible to hydrolysis		n.a.	
	Parameters of influence	type of IERs (anionic vs cationic), total dose, IERs' water content and ionic load, hydrolysis, temperature		/		irradiation	
	Kinetics	only scission of the IERs' surface groups (first- and second-order kinetics)		/		n.a.	
	Impacts on the near-field	pH reduction (for cationic IERs) or pH increase (for anionic IERs), substrates for microbial activities		/		n.a.	
	Uncertainties	degradation of styrene, combination with hydrolysis, kinetics		lack of general data		lack of general data	
PVC	**Mechanisms**	scission	crosslinking	alkaline hydrolysis / Fenton process		heat treatment	
	Products	H_2, HCl, LMW water-soluble organics	CH_4, CO, CO_2, oxidised HCs, H_2, HCl, LMW water-soluble organics	plasticisers		HCl, H_2, CO_2, benzene, acetaldehyde, formic acid, propanal, acetic acid, succinic anhydride	
	Degree of degradation	degradable		limited		limited	
	Parameters of influence	dose rate, type of additives	total dose, type of additives	n.a.		total dose	
	Kinetics	n.a.		n.a.		n.a.	
	Impacts on the near-field	pH reduction (due to HCl release)		no pH reduction		pH reduction	pH reduction (lower in anoxic atmosphere)
	Uncertainties	type of degradation products (due to additives), degree of degradation, kinetics		type of degradation products (due to additives), degree of degradation, kinetics		degree of degradation, kinetics	

Tab. 3-1: Cont.

Material	Criteria	Radiolytic degradation		Chemical degradation		Thermal degradation (T ≤ 50 °C)	
	Environment	**Oxic**	**Anoxic**	**Oxic**	**Anoxic**	**Oxic**	**Anoxic**
Bitumen	**Mechanisms**	crosslinking		alkaline hydrolysis		heat treatment	
	Products	CO_2, oxalates, carboxylic acids, carbonates	H_2, NO, CO, C1-C3 HCs, CO_2, oxalate, carboxylic acids, carbonates	light gases (H_2, CH_4...), carboxylic acids, aliphatic alcohols aldehydes and ketones, glycols, aromatics, S- and N-containing compounds		n.a.	
	Degree of degradation	high stability at doses < 10 MGy	more stable than in oxic conditions	limited	limited (even below oxic conditions)	n.a.	
	Parameters of influence	chemical composition of the bitumen, O_2, total absorbed dose, type of radiation		chemical composition and structure of the bitumen, O_2, time exposure, pH, ionic strength of the solution, ratio of exposed surface area to volume solution		n.a.	
	Kinetics	n.a.		n.a.		n.a.	
	Impacts on the near-field	slight pH reduction		n.a.		n.a.	
	Uncertainties	comparison between studies due to the various chemical compositions, especially in terms of degradation products, impact on the near-field and kinetics		comparison between studies due to the various chemical composition, especially in term of degradation products, impact on the near field and kinetics		lack of general data	

Tab. 3-1: Cont.

Material	**Criteria**	**Radiolytic degradation**		**Chemical degradation**		**Thermal degradation (T ≤ 50 °C)**	
	Environment	**Oxic**	**Anoxic**	**Oxic**	**Anoxic**	**Oxic**	**Anoxic**
Plastics (PE, PP)	**Mechanisms**	scission	crosslinking	alkaline hydrolysis		heat treatment	
	Products	H_2, CO_2, CO, CH_4, alkanes, alkenes, alcohols, aldehydes, ketones, carboxylic acids		n.a.		n.a.	
	Degree of degradation	susceptible to radiation		not susceptible to hydrolysis		n.a.	
	Parameters of influence	crystallinity, absence of amorphous region, total absorbed dose, dose rate, temperature	crystallinity, absence of amorphous region, total absorbed dose, temperature	/		irradiation, O_2	
	Kinetics	n.a.		/		n.a.	
	Impacts on the near-field	carbonation of the cementitious near-field and substrates for microbial activities		/		n.a.	
	Uncertainties	type of degradation products (due to additives), especially water-soluble ones		lack of general data		lack of general data	
Plastics (poly-ester, PC)	**Mechanism**	scission		alkaline hydrolysis		heat treatment	
	Products	H_2, CO_2, CO		water-soluble monomer units		n.a.	
	Degree of degradation	moderate		complete degradation		limited	
	Parameters of influence	chemical structure and crystallinity of the polymer, dose rate, total absorbed dose		alkali concentration, temperature, time of exposure		hydrolysis (non-linear dependence)	
	Kinetics	n.a.		controversial data		n.a.	
	Impacts on the near-field	carbonation of the cementitious near-field		substrates for microbial activities		n.a.	
	Uncertainties	water-soluble degradation products, kinetics		extent and kinetics of the degradation		lack of general data	

Tab. 3-1: Cont.

Material	Criteria	Radiolytic degradation		Chemical degradation		Thermal degradation (T ≤ 50 °C)	
	Environment	**Oxic**	**Anoxic**	**Oxic**	**Anoxic**	**Oxic**	**Anoxic**
Cellulose	**Mechanisms**	scission		alkaline hydrolysis		heat treatment	
	Products	CO_2, CO, deoxysaccharides, carboxylic acids, aldehydes, ketones		ISA, carboxylic acids, alcohols		CO_2	
	Degree of degradation	degradable		degradable (but most likely partially)		limited	
	Parameters of influence	total absorbed dose, pH, temperature		mole fraction of reducing end groups, their accessibility, irradiation		irradiation	
	Kinetics	n.a.		two distinct rates (mid-chain scission followed by a decelerated reaction)		n.a.	
	Impacts on the near-field	substrates for microbial activities, carbonation of the near-field, generation of complexing agents		substrates for microbial activities, generation of complexing agents		carbonation of the cementitious near-field	
	Uncertainties	kinetics, synergy with alkaline and thermal types of degradation		degree of the degradation, kinetics		kinetics, synergy with radiolytic degradation	
LMW organics	**Mechanism**	fragmentation		alkaline hydrolysis		heat treatment	
	Products	CO_2, CH_4, carboxylic acids		CO_2, CH_4, carboxylic acids		n.a.	
	Degree of degradation	easily degradable		stable to degradation, except for esters		n.a.	
	Parameters of influence	total absorbed dose		temperature		hydrolysis	
	Kinetics	n.a.		n.a.		linear	
	Impacts on the near-field	carbonation of the cementitious near-field, substrates for microbial activities, degradation of complexing agents (ISA, EDTA, NTA)		pH reduction, carbonation of the cementitious near-field, substrates for microbial activities		n.a.	
	Uncertainties	degradation products, kinetics, impacts on the near-field (all due to the high variability of compounds)		degradation products, kinetics, impacts on the near-field (all due to the high variability of compounds)		lack of general data	

Tab. 3-1: Cont.

Material	Criteria	Radiolytic degradation		Chemical degradation		Thermal degradation (T ≤ 50 °C)	
	Environment	**Oxic**	**Anoxic**	**Oxic**	**Anoxic**	**Oxic**	**Anoxic**
Plexiglas®	**Mechanisms**	scission		alkaline hydrolysis		heat treatment	
	Products	CO_2, CH_4, H_2, CO, ester groups		n.a.		n.a.	n.a.
	Degree of degradation	limited		hardly degradable		n.a.	
	Parameters of influence	total absorbed dose		/		n.a.	
	Kinetics	n.a.		/		n.a.	
	Impacts on the near-field	carbonation of the near-field, substrates for microbial activities		/		n.a.	
	Uncertainties	general lack of knowledge under relevant conditions		lack of general data		lack of general data	
SPs	**Mechanism**	crosslinking (SMF), scission (others)		alkaline hydrolysis		heat treatment	
	Products	HCs, H_2, CO_2, SO_2, CH_4, alcohols, ketones, carboxylic acids	n.a.	n.a.		n.a.	
	Degree of degradation	limited stability		degradation only for SMF		n.a.	
	Parameters of influence	type of SPs, total absorbed dose, pH		chemical structure		n.a.	
	Kinetics	n.a.		n.a.		n.a.	
	Impacts on the near-field	limited		pH reduction during hydrolysis of PAE		n.a.	
	Uncertainties	lack of studies in anoxic conditions, kinetics		lack of general data		lack of general data	

4 Biotic degradation of organics

4.1 Life in selected "extreme environments"

4.1.1 Life in the deep biosphere

Until a few decades ago, life in the deep earth zones was mostly unexplored and thought to be biologically dead. In the 1970s, microbial activity was assumed to not be present after a few tens of meters (Jannasch et al. 1971). It is only since the 1990s that microbial life was expected to be much deeper and more important than previously thought. No absolute depth limit could be defined, but a steady decrease in cell numbers with depth was observed (Parkes et al. 1994). Some authors even referred to the deep biosphere as the "unseen majority" (e.g., Whitman et al. 1998). A decade later, Roussel et al. (2008) set a life boundary down to a depth of 1,626 metres below the seafloor, based on the identification of prokaryotes. A high phylogenetic diversity of these microorganisms was suggested based on DNA sequencing. However, the metabolism of these organisms were poorly constrained (Nealson et al. 2005, Parkes et al. 1994). Despite these recent discoveries, microbial activities in the deep earth remain relatively unexplored to date.

4.1.2 Microbial processes occurring under anaerobic conditions

Microbial metabolism under anaerobic conditions can be divided into several classes according to the energy conservation and carbon source for growth. If only H_2, H_2S, NH_4^+ or Fe^{2+} are used as inorganic electron donors to produce metabolic energy, the anaerobic microbial metabolism is described as being lithotrophic. Organotrophic metabolism uses organic substrates for energy production. Autotrophic organisms use CO_2 as a carbon source for growth, whereas heterotrophs use organic molecules. Mixotrophic organisms uses inorganic electron donors for energy production but organic molecules for growth. If NO_3^-, Fe^{3+}, SO_4^{2-} or CO_2 are available, certain microbes may use them as external electron acceptors as part of anaerobic respiration. In the near-field of a cementitious L/ILW repository, electron donors may be H_2 or reduced organic carbon. Here, the most relevant electron acceptor is likely SO_4^{2-}, which is present in the pore water of the OPA host rock (Wersin et al. 2022). In the absence of such electron acceptors, anaerobic degradation has to occur via different fermentation type reactions, producing dissolved organic intermediates and CH_4 and CO_2 as end products. This anaerobic degradation cascade yields less energy compared to anaerobic respiration and needs different specialised organisms for performing all the different metabolic steps. The complex anaerobic degradation cascade is sensitive to perturbations and can therefore be incomplete, forming acids and alcohols as end products instead of CH_4 and CO_2.

4.1.2.1 Anaerobic degradation cascade and CH_4 production

Anaerobic degradation cascade

Several types of microorganisms and degradation pathways are involved in the anaerobic degradation chain of complex organic polymers to CH_4 and CO_2 (Fig. 4-1). After enzymatic hydrolysis of the polymers, primary fermenters degrade the resulting oligomers and monomers to acetate, H_2, CO_2 and fermentation intermediates such as short chain fatty acids and alcohols. The organic fatty acids and alcohols formed may then be further degraded in a second fermentation to acetate, H_2 and CO_2 by so-called syntrophic bacteria. From these intermediate products, methanogens form CH_4. A distinction is made between hydrogenotrophic methanogenesis, generating CH_4 from H_2 and CO_2, and acetoclastic methanogenesis, which splits acetate into CH_4 and CO_2 (Rosenwinkel et al. 2015, Schink & Stams 2013). Homoacetogenic bacteria may also be involved in the anaerobic degradation of organics, producing acetate from H_2 and CO_2, which in turn can be used by the acetoclastic methanogens. The secondary fermentation of organic fatty acids and alcohols to acetate and H_2 is endergonic under standard conditions ($\Delta G^{0'} > 0$) and therefore represents an energetic problem (Tab. 4-1) (Rosenwinkel et al. 2015, Schink & Stams 2013). Nature solves this energetic bottleneck through so-called syntropy, which is the interaction of H_2-forming and H_2-consuming microorganisms, where the H_2-consuming methanogens depend on the release of H_2 by the syntrophs (Rosenwinkel et al. 2015, Schink & Stams 2013).

Tab. 4-1: Selected reactions within anaerobic degradation

e-donor / substrate	**Formula**	**$\Delta G^{0'}$ [kJ/mol]**
H_2-releasing reactions		
Ethanol	$CH_3CH_2OH + H_2O \rightarrow CH_3COO^- + H^+ + 2\ H_2$	+9.6
Butyric acid	$CH_3CH_2CH_2COO^- + 2\ H_2O \rightarrow 2\ CH_3COO^- + 2H^+ + 2\ H_2$	+48.2
Propanoic acid	$CH_3CH_2COO^- + 2\ H_2O \rightarrow CH_3COO^- + CO_2 + 3\ H_2$	+76.2
Acetic acid	$CH_3COO^- + H^+ + 2\ H_2O \rightarrow 2\ CO_2 + 4\ H_2$	+94.9
H_2-consuming reactions		
H_2 / CO_2	$4\ H_2 + CO_2 \rightarrow CH_4 + 2\ H_2O$	-131.0
H_2 / CO_2	$4\ H_2 + 2\ CO_2 \rightarrow CH_3COO^- + H^+ + 2\ H_2O$	-94.9
Further CH_4-forming reactions		
Formate	$4\ HCOOH \rightarrow CH_4 + 3\ CO_2 + 2\ H_2O$	-130.1
Acetate	$CH_3COOH \rightarrow CH_4 + CO_2$	-31.0

The H_2-releasing reactions are endergonic under standard conditions. The H_2-consuming, as well as the CH_4-forming reactions, are close to the thermodynamic limit.

The listed Gibbs energy values are based on standard biological conditions ($c° = 1$ mol/L, $H^+=10^{-7}$ mol/L, $p° = 1$ atm, $T = 298$ K) (Rosenwinkel et al. 2015, Schink & Stams 2013).

The calculations of Schink & Stams (2013) showed that the degradation of ethanol under standard biological conditions ($\Delta G^{0'}$) only occurs when methanogens keep the H_2 partial pressure below 10^{-3} bar. If the conditions vary (e.g., temperature, substrate and product concentrations, H^+ concentration), the thermodynamic equilibrium changes and the maximum H_2 partial pressure shifts. Furthermore, microorganisms require a certain minimum energy to gain energy from thermodynamically exergonic reactions. This minimum energy can be exploited by living cells and is called the minimum biological energy quantum and should be included in thermodynamic calculations. Schink (1997) studied the thermodynamics of anaerobic butyrate degradation under conditions prevailing in natural habitats (butyrate at 10 mM, CH_4 at 0.7×10^5 Pa, CO_2 0.3×10^5 Pa) and calculated a free energy change for each partial reaction of about -20 kJ/mol. A hydrogen partial pressure of 2 Pa (2×10^{-5} bar) at an acetate concentration of 50 µM was determined, comparable to real values in sediments or sludge. Hoehler et al. (2001) found evidence that methanogens are supported by energy yields as small as -10.6 kJ/mol CH_4. The exact value of the minimum biological energy quantum is discussed in detail by Müller & Hess (2017).

Due to the heterogeneity of the L/ILW, some parameters such as pH and substrate concentrations could vary at a small scale and cannot be defined at the scale of the repository. These parameters have a significant influence on the prevailing thermodynamics. In Warthmann et al. (2013), various thermodynamic considerations were made under various conditions. It can be clearly seen that the influence of the substrate concentration is considerable. When calculating the maximum H_2 pressures, the minimum energy quantum of about 20 kJ/mol was not included. If it is considered, the maximum H_2 partial pressures at which microbiological conversion could still take place are strongly reduced. While Warthmann et al. (2013) calculated maximum H_2 partial pressures of 2.2 bar and 217 bar to halt butyrate degradation present at concentrations of 10^{-2} to 10^{-6} M, respectively, H_2 partial pressures were reduced to 0.04 and 4.3 bar under the same conditions, taking into account the minimum energy quantum for microbial ATP synthesis of -20 kJ/mol proposed by Schink (1997). The development of a more in-depth thermodynamic modelling specifically adapted to a cementitious L/ILW repository including several syntrophic reactions should be undertaken to provide more insights into the limits of microbial activity in the context of an L/ILW repository.

CH_4 production

Methanogens are found in freshwater sediments, anaerobic digesters, bioreactors and various anoxic habitats and in the gastrointestinal tract of animals and humans (Madigan et al. 2020). The substrate spectrum of methanogens is limited to CO_2, which can be reduced to CH_4 with H_2, formate, CO as well as acetate and other "methyl substrates" (Fig. 4-1; Tab. 4-1) (Rosenwinkel et al. 2015). Methanogens can be divided into two subgroups: hydrogenotrophic methanogens that use H_2, CO_2 and formate and are phylogenetically diverse, and the acetoclastic ones, belonging to the *Methanosarcinaceae* family (Rosenwinkel et al. 2015). Acetate can only be used by the *Methanosarcinales* order, which includes the two genera, *Methanosarcina* and *Methanosaeta*. Species belonging to the genus *Methanosaeta* seem to only be able to split acetate to CH_4 and CO_2 to gain energy. The *Methanosarcinaceae* family contains another seven genera which can also convert other methyl compounds such as methanol, methylamines, methyl mercaptan and methyl sulphide to CH_4 (Rosenwinkel et al. 2015).

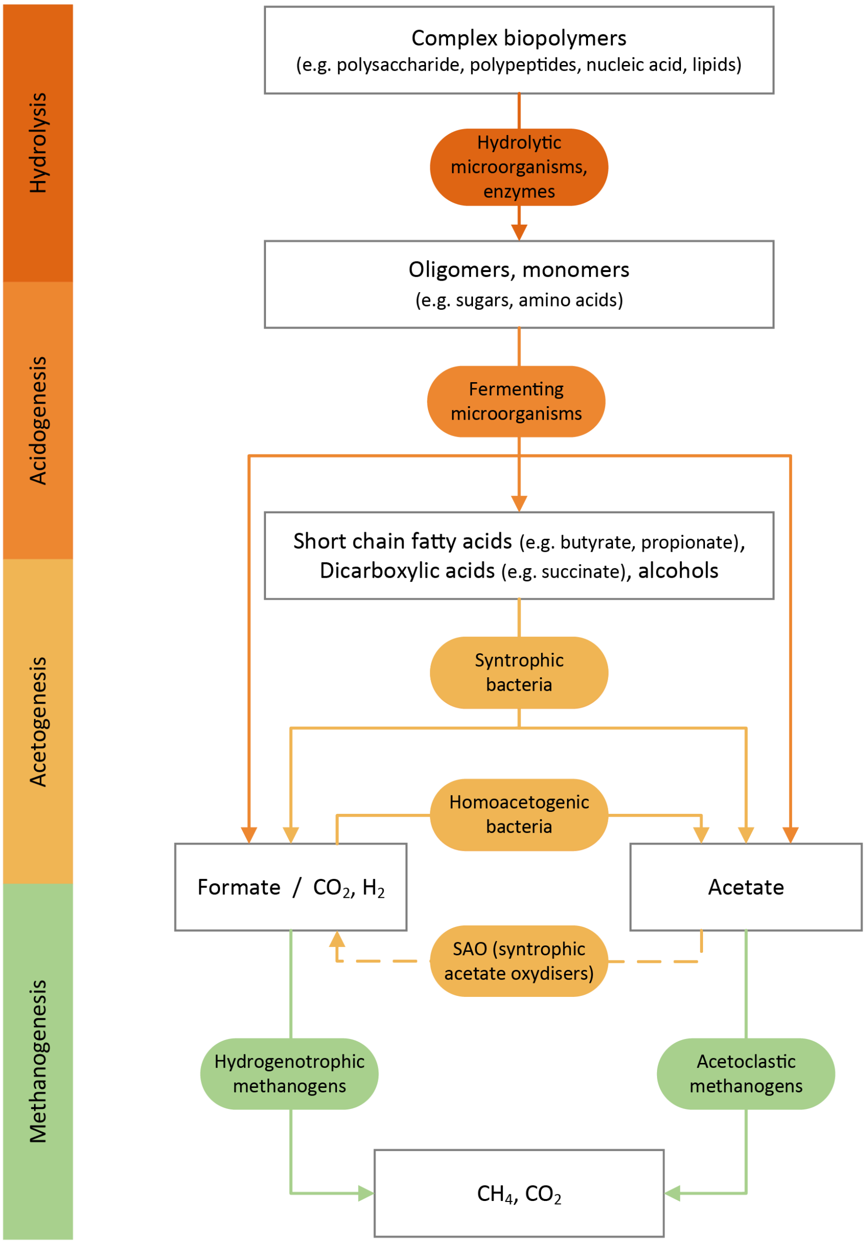

Fig. 4-1: Anaerobic degradation cascade

Complete anaerobic degradation of complex organic matter to CH_4 and CO_2 in the absence of electron acceptors such as SO_4^{2-} or NO_3^-. Degradation involves exoenzymes and several types of anaerobic microbes. Syntrophy is the key to connecting the metabolites from fermenting bacteria to the methanogens. If the process is disturbed at one point in the system, e.g., by environmental conditions, the entire degradation chain will be out of equilibrium and no, or much less, CH_4 will be produced. This figure was adapted from Leupin et al. (2016b), Wiborgh et al. (1986) and Madigan et al. (2015).

4.1.2.2 Anaerobic respiration

In the context of a cementitious L/ILW repository, not many electron acceptors for microbial respiration are available after the disappearance of O_2. SO_4^{2-} is one of them and present in the OPA porewater at around 16.6 mM (Wersin et al. 2022). It is, however, difficult to quantify whether the amount of SO_4^{2-} available after resaturation by the porewater is sufficient to allow the L/ILW organics to be oxidised significantly, particularly as H_2 may compete with the organic carbon for oxidation by sulphate.

Sulphate-reducing bacteria (SRB) gain energy by coupling the oxidation of H_2 or organic compounds (lactate, pyruvate, ethanol, propanol, butanol) with the reduction of SO_4^{2-} (Tab. 4-2). While H_2 is widely used by SRB, the use of organic electron donors is more limited. SRB are morphologically and biochemically diverse and are highly widespread in aquatic and terrestrial habitats containing SO_4^{2-}. A total of over 30 genera of SRB and archaea are known to date (Madigan et al. 2020). SRBs are known to have their optimal pH in the neutral range of 5.5 to 7.0, and many thermophilic species can grow at temperatures of up to 90 °C (Hamilton-Brehm et al. 2013). Various microbial studies in hyperalkaline environments affected by the process of serpentinisation found SRBs at a pH of up to 11.4 (Bath et al. 1987, Rempfert et al. 2017). Sulphate reducers also tolerate extreme salinities. In the Kyros Basin, sulphate-reducing activities were detected in almost saturated $MgCl_2$ brines, with a corresponding water activity of $a_w \approx 0.4$, representing a record for bacteria (Steinle et al. 2018).

In addition to SRB, some archaea are also capable of sulphate reduction. Mostly marine (1 – 3.6% NaCl), sulphate-reducing archaea grow in the temperature range of 60 – 95 °C with an optimum of 83 °C (e.g., *Archaeoglobus fulgidus* isolated from a hot marine spring in Italy). *Archaeoglobus* species oxidise a variety of organic compounds, as well as polymers such as xylan and even aromatics such as benzoate (Hafenbradl et al. 1996, Stetter 1988, Tor & Lovley 2001). In the near-field of an L/ILW repository, where temperatures are not expected to be above 60 °C (Papafotiou & Senger 2016), these hyperthermophilic archaea are most likely not relevant.

Tab. 4-2: SO_4^{2-} reduction

SRB can reduce SO_4^{2-} with H_2 or organic compounds (e.g., acetate) as electron donor. These reactions show a rather low Gibbs energy (Rosenwinkel et al. 2015).

Electron donor	**Formula**	**$\Delta G^{0\prime}$ [kJ/mol]**
H_2	$4\ H_2 + SO_4^{2-} + H^+ \rightarrow HS^- + 4\ H_2O$	-152.2
Acetate	$CH_3COOH + SO_4^{2-} + H^+ \rightarrow 2\ CO_2 + HS^- + 2\ H_2O$	-47.6

During sulphate reduction, SRB and archaea produced sulphide which may further react with metals, emphasising corrosion and associated H_2 production (Tab. 4-3).

Tab. 4-3: Reactions producing and consuming H_2S

H_2S can be produced by microbial sulphate reduction, which can be further consumed over corrosion (Mijnendonckx et al. 2019).

Reaction	**Formula**	**Located**
Microbial sulphate reduction	$4\ H_2 + SO_4^{2-} + 2\ H^+ \rightarrow H_2S + 4\ H_2O$	At different locations, H_2S might be transported
Copper corrosion	$2\ Cu + H_2S \rightarrow Cu_2S + H_2$	At the surface of the canister
Iron corrosion	$Fe + H_2S \rightarrow FeS + H_2$	At the surface of the canister

In addition to SO_4^{2-}, Fe(III) can also be used as an electron acceptor for microbial respiration. This is especially the case for iron-reducing bacteria (IRB), for which H_2 and a wide range of organic compounds (e.g., carboxylates, sugars, hydrocarbons, alcohols, phenols and amines) can serve as an electron donor, including in extreme environments (Nixon et al. 2022).

At near neutral to high pH, Fe(III) typically exists as crystalline or poorly-crystalline iron oxides (e.g., goethite, hematite and ferrihydrite). Despite the challenge of respiring a solid phase extracellular electron acceptor, many species have acquired the ability to reduce structural Fe(III) in (oxyhydr)oxides (Lovley et al. 2004). Likewise, structural Fe(III) in clay minerals may also serve as an electron acceptor by a variety of IRB. Indeed, such species have been identified in the OPA host rock (e.g., Mitzscherling et al. 2023) and in bentonite (Gilmour et al. 2021, Haynes et al. 2018, Perdrial et al. 2009).

Whilst the metabolic potential for microbial Fe(III) reduction may exist within the repository, its competition with sulphate as an electron acceptor is poorly constrained because the amount of bioavailable Fe(III) is not well defined. Three main sources of Fe(III) can be envisaged: structural Fe(III) in clay minerals within the OPA or bentonite; the oxidation of pyrite in OPA or bentonite by O_2 during the operational phase; and the aerobic corrosion of waste-associated steel (Leupin et al. 2016b). However, given the relatively high concentration of sulphate in the OPA porewater, the presence of gypsum in both bentonite and cement and the fact that oxidation of pyrite yields twice the number of moles of sulphate than Fe(III), sulphate reduction is expected to be the predominant electron accepting process. Indeed, both *in situ* experiments at Mont Terri underground rock laboratory and representative laboratory microcosm experiments indicate that microbial communities become dominated by SRB (Bagnoud 2015, Boylan et al. 2019).

4.1.2.3 H_2 – consumption-competition and thermodynamic consideration under L/ILW conditions

In a deep geological repository, H_2 can be generated by the anoxic corrosion of metals. As gas generation should be limited for the safety performance of the engineered barriers, microbial consumption of H_2 is generally viewed as beneficial (Bagnoud et al. 2016). Hydrogenotrophic methanogens, SRB and homoacetogenic bacteria compete for H_2 as an electron donor (Rosenwinkel et al. 2015). The reactions of the microorganisms competing for H_2 are listed in Tab. 4-4. Bagnoud et al. (2016) investigated the H_2 oxidation and SO_4^{2-} reduction rates of microorganisms native to OPA. The calculated rates are 1.13 – 1.93 µmol/cm^3 d^{-1} for H_2 and 0.14 – 0.20 µmol/cm^3 d^{-1} for SO_4^{2-}. The excess of H_2 consumed indicates that it serves as another electron donor to reduce electron acceptors other than SO_4^{2-} and/or that H_2 is lost by diffusion.

Tab. 4-4: H_2-consuming microorganisms

Different microorganisms compete for H_2 as electron donor (Müller 2003, Rosenwinkel et al. 2015).

H_2-consuming microorganisms	Formula	$\Delta G^{0'}$ [kJ/mol]
Sulphate-reducing bacteria	$4\ H_2 + SO_4^{2-} + H^+ \rightarrow HS^- + 4\ H_2O$	-152.2
Hydrogenotrophic methanogens	$4\ H_2 + CO_2 \rightarrow CH_4 + 2\ H_2O$	-135.6
Homoacetogenic bacteria	$2\ CO_2 + 4\ H_2 \rightarrow CH_3COOH + 2\ H_2O$	-95

In an anoxic environment, H_2 can be used exclusively for anaerobic respiration during microbial energy conservation. Extracellular electron acceptors available in nature include sulphur and nitrogen compounds, redox-active metal ions, and CO_2. The standard redox potential E^0 of each species determines how much energy under standard conditions (pH 0) the microorganisms can gain by reduction with H_2. The greater the difference, the higher the energy gain. In reality, however, the conditions are usually different from the standard conditions and depend on the pH.

According to the Nernst equation (Equation 4-1), the redox potential of hydrogen E_h is pH-dependent. Whereas E_h at pH 7 is -413 mV, it shifts to -649 mV at pH 11, thus influencing all H_2-dependent microbial reactions.

Equation 4-1: $E_h = E^0 + \frac{RT}{zF}\ ln\frac{C_{Ox}}{C_{Red}}$; at $T = 25\ °C$ simplifies to $E_h\ =\ -59.16\ mV * pH$

where R is the universal gas constant; T is the temperature (Kelvin); z is the number of electrons transferred in the cell reaction or half-reaction; F is the Faraday's constant; C_{Ox} concentration of oxidised hydrogen; C_{Red} concentration of reduced hydrogen.

In a competitive situation for H_2, the electron acceptors that give the highest energy yield will probably be consumed first, and the cells that perform this reaction will grow the fastest. A simple relationship between $\Delta E^{0'}$ and the change in Gibbs free energy $\Delta G^{0'}$ can be expressed as:

Equation 4-2: $\Delta G = -n * F * \Delta E^{0'}$

where n is the number of electrons transferred and F is Faraday's constant (96.5 kJ/mol V^{-1}).

In the near-field of an L/ILW repository, Equation 4-2 indicates that, according to the energy yield, Mn^{4+} may be reduced first after initial O_2 depletion, followed by NO_3^-, Fe^{3+}, SO_4^{2-} and sulphite reduction coupled to H_2 consumption. In the presence of H_2, all NO_3^-, porewater SO_4^{2-} and Fe^{3+} will most likely be completely consumed if the general physical and chemical conditions for life under extreme conditions are fulfilled. These are, among other things, the presence of water, nutrients and a suitable pH range (cf. Section 4.1.3).

To demonstrate the dependence of anaerobic respiration on pH, two examples of models for methanogenesis are illustrated below.

Example 1:

CO_2 serves as the electron acceptor for hydrogenotrophic CH_4 formation. Whether and under what conditions this occurs depends, among other things, on the availability of dissolved CO_2. Within the context of a cementitious environment, the questions are to what extent is dissolved CO_2 available at high pH and what are the thermodynamics for hydrogenotrophic CH_4 formation. Therefore, the Gibbs free energy of the CH_4 formation reaction was modelled for two different porewater compositions expected in the near-field of an L/ILW repository (Tab. 4-5) (Hummel et al. 2022), using the modelling software eQuilibrator 3.0 (Beber et al. 2022). Since the simulation with the eQuilibrator software is only possible up to a maximum of pH 10, results up to pH 13 (polynomial, 2nd degree) were extrapolated (Fig. 4-2).

Reaction 4-1: $4\ H_2\ (aq) + CO_2\ (total) \rightleftharpoons CH_4\ (aq) + 2\ H_2O\ (l)$

Tab. 4-5: Parameters for calculating the Gibbs energy

To estimate the Gibbs energy of the CH_4 formation reaction under L/ILW repository-like conditions, concentrations from two different porewater compositions were used: 1) DS-II-Z-mt, corresponding to cement porewater at degradation stage 2 using OPA porewater from the Zürich Nord Ost drilling number 22 (ZNO-22) in equilibrium with magnetite, i.e., at a suboxic redox state; and 2) DS-II-Z-py, corresponding to cement porewater at degradation stage 2 using OPA porewater from the ZNO-22 drilling in equilibrium with pyrite, i.e., at an anoxic redox state (Hummel et al. 2022).

Compounds	**Parameters for DS-II-Z-mt**	**Parameters for DS-II-Z-py**
Carbonate [mol/kg H_2O]	2.61×10^{-5}	2.21×10^{-5}
pH	6, 7, 8, 9, 10 calculated > 10 extrapolated	6, 7, 8, 9, 10 calculated > 10 extrapolated
Ionic strength [M]	0.34	0.34
H_2 (aq) [mM]	0.7	0.7
CH_4 (aq) [mM]	1	1

The result shows that the Gibbs energy decreases with higher pH values and is approximately -70 kJ/mol ± 24.0 kJ/mol at pH 12.5 for both cementitious porewaters, suggesting that the methanogenic archaea still have sufficient energy available under these conditions to provide ATP for metabolism and cell growth. As a comparison, Madigan et al. (2020) showed that some archaea can grow with only -31 kJ/mol, e.g., the acetoclastic methanogens (cf. Table 21.1 in Madigan et al. 2020). This calculation is a first approximation and requires further testing alongside a quantitative assessment of the availability of CO_2, particularly in a high pH cementitious environment.

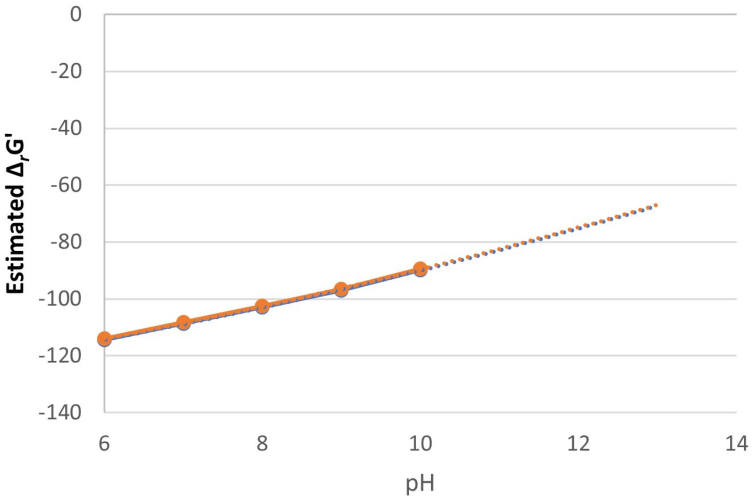

Fig. 4-2: Gibbs free energy simulation

The Gibbs energy of the hydrogenotrophic CH_4 formation was simulated for two cementitious porewaters DS-II-Z-mt (blue) and DS-II-Z-py (orange). The dotted line is an extrapolation to higher pH values such as 12.8, which yields a Gibbs energy $\Delta_r G'$ of about 70 ± 24.0 kJ/mol CH_4 formed.

Example 2:

A similar approach was described in Jin & Kirk (2018), who studied the thermodynamics of acetoclastic and hydrogenotrophic methanogenesis. They introduced the term "*thermodynamic drive*", which indicates how much energy is released (Gibbs free energy), including the ATP formation of the organisms. They modelled pH-dependent speciation of the metabolites involved in the reaction, whose concentration changes due to protonation, deprotonation and solubility. According to their calculations, the thermodynamic drive of acetoclastic methanogenesis increases with increasing pH. The opposite is true for hydrogenotrophic methanogenesis, where the thermodynamic drive decreases with increasing pH (Fig. 4-3). Above a pH of 11, hydrogenotrophic methanogenesis is thermodynamically unfavourable and becomes endergonic. Whilst this result confirms the impact of pH on reaction free energy as described by model 1 (Fig. 4-2), it also highlights the impact of differences in specific model parameters on the computed reaction free energy.

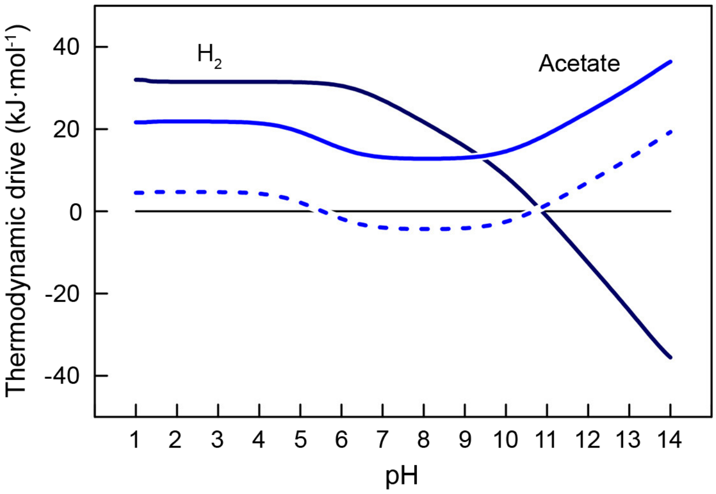

Fig. 4-3: Thermodynamic drive

Thermodynamic drive of acetoclastic (blue) and hydrogenotrophic methanogenesis (black) dependent on pH. The Y-axis is the thermodynamic drive in kJ/mol. Solid lines: hypothetical H_2 concentration in the modelled environment = 0.1 µM, and CH_4 = 1 µM; dashed line: CH_4 concentration = 1 mM (Jin & Kirk 2018).

4.1.3 Limits of life and extremophiles in conditions relevant for an L/ILW repository

Life in so-called "extreme environments" is exposed to extremely low (acidophilic) or high pH (alkaliphilic), extremely low (psychrophilic) or high (thermophile) temperatures, high hydrostatic pressure (barophile), high radiation (radiation-tolerant), low water activities (xerophilic) and high salt concentrations (halophile). Harrison et al. (2013) state that, apart from the premise of liquid water, there are no definitive limits of life, as microbial life can widely adapt to harsh environments. Certain limits of life, however, remain. A useful overview by Pikuta et al. (2007) attests that pH values at which microbial life is possible range from pH 0 – 12, temperatures from -5 to 120 °C (short-term up to 130 °C), salinity from 0 – 30% and pressures up to 700 MPa or more (Nogi & Kato 1999).

In conditions relevant for a cementitious L/ILW repository, these extreme boundaries are summarised and based on observations at natural extreme habitats or sites that have been contaminated by industrial activities (Butterworth et al. 2021).

4.1.3.1 Microbial activity at low water activities

The presence of water is central to the growth and activity of microorganisms. Harrison et al. (2013) state that liquid water is a requirement for terrestrial life and that the availability of liquid water is probably the most important constraint on extraterrestrial habitability. In a deep geological repository, water limitation actually represents one of the key factors affecting or inhibiting microbial life (Humphreys et al. 2010a, Leupin et al. 2017, Merino et al. 2019, Stroes-Gascoyne et al. 2010).

There are several types of free and bound water present in heterogeneous systems such as sediments. In microbiology, the term "water activity" (a_w) is used as a measure of the availability of free water and is significant for the activity of microorganisms. It should not be confused with soil wetness (g water/g substrate). The parameter a_w was developed to describe the vapour pressure of ideal liquid mixtures. In practice, it is used for the preservation of food. The great advantage is that the parameter can be measured very easily. The quotient a_w is the relative humidity in the equilibrium state and is described by the equilibrium vapour pressure of a material in comparison with the air humidity above pure water:

Reaction 4-2: $a_w = P/P_0$

where P is the vapour pressure of a solution and P_0 is the vapour pressure of pure water at the same temperature (Grant et al. 2004).

The air humidity is measured directly above a sample (water vapour partial differential pressure) after moisture equilibrium has been reached. The water activity ranges between 0 (absolute dryness) and 1 (pure water). The water activity a_w is decreased by dissolved substances such as NaCl or sugar and results in thermodynamically less water being available at lower a_w.

Because the parameter a_w is based on Raoult's Law for ideal solutions, it has limited applicability for describing microbial life under low-water conditions (Grant et al. 2004). However, there are other types of free and bound water. In soil science, four different forms of water are defined (Fig. 4-4) (e.g., Hartge & Horn 2016):

1) Gravitational water, i.e., free water moving through soil by the force of gravity. It is largely found in the macropores of soil. Very little gravitational water is available to plants as it drains rapidly down to the water table. It is, however, in principle available for microbial activity.
2) Capillary water held in the micropores of the soil by surface tension of the soil. It is the main water available to plants as it is trapped in the soil solution right next to the roots. It is most probably available for microbial activity.
3) Hygroscopic water forms as a very thin film (in the nanometer range) surrounding soil particles. It is generally not available to plants as it is too tightly bound to the soil by adhesion properties. As a result, very little can be taken up by roots. Since hygroscopic water is found in the soil particles and not in the pores, certain types of soils with few pores (e.g., clays) will contain a higher percentage of it. There are hardly any studies on the extent to which microorganisms can use this hygroscopic water on mineral surfaces. It depends strongly on the hygroscopic properties of the minerals whether microbes can survive under hygroscopic humidity conditions. Such effects are partially discussed in Stone et al. (2016a).
4) Water chemically combined in the structure of soil minerals is known as combined water. After the elimination of hygroscopic water by heating soil to about 150 °C, it is the only water that remains in the hydrated oxides of Al, Si, etc. This water is unavailable for organisms and can only be driven off from the soil minerals by heating the soil above 150 °C.

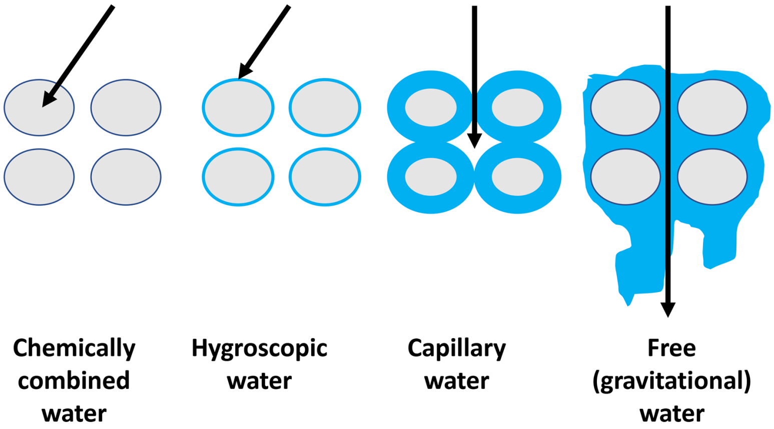

Fig. 4-4: Water in soil

There are four different types of water in soil: chemically combined water, hygroscopic water, capillary water and free (gravitational) water.

In the context of a combined deep geological repository, partially saturated conditions are expected to persist in the L/ILW repository section for several tens of thousands of years (Papafotiou & Senger 2016) (cf. Section 2.4). Capillary water could be available for microbial activity, initially at the bottom of the caverns, as water from the access tunnels and host rock will percolate into the caverns under gravity. It should be however noted that the waste packages present at the top of the caverns will saturate faster than their surrounding backfill due to suction from the waste packages located below (Nagra 2024a, in prep.). Hence, it is expected that free water will be available for microbial activity long after repository closure and only on limited areas.

In soil physics and plant physiology, the parameter water potential Ψ is used. It is expressed in units of Pascals and is composed of partial potentials describing different physical aspects, such as the osmotic, pressure, matrix, and gravitational effects (Taiz et al. 2014).

In a context of a deep geological repository, the water potential (Ψ) description used in soil science is probably more relevant than a_w for the characterisation of microbial activity, as neither high salt, nor high sugar concentrations are expected. Unfortunately, the Ψ parameter has received only little attention from microbiologists.

Experimental results on life under low water activities in soil and bentonite

In the presence of low water availability, microbes require a high energy expenditure for the synthesis of so-called "compatible solutes" to compensate for the high osmotic pressure prevailing across the cell membranes. As a result, they grow more slowly and exhibit lower metabolic activities (Yan et al. 2015). In general, data availability, as well as experimental methodologies, are still lacking, and there is no understanding of the exact relationships between water availability and microbial activity (Yan et al. 2015). In the study of Stone et al. (2016b), a multi-year microcosm experiment was performed with bentonite (compacted and non-compacted) incubated at two different relative humidities (30% and 75% RH), which correspond to a water activity a_w in the equilibrium state with the material. Survival rates and metabolic activity of the aerobic microbiota were measured using CO_2 production. At the bentonite-air interface, metabolic activity was in the ppm range at 75% RH, whereas at 30%, none of the inoculated samples showed any CO_2 production. Interestingly, the survival rate of the bacteria was higher at 30% RH, which was explained by the fact that the organisms quickly enter a dormant stage, thus managing to survive for a longer period of time. Whilst CO_2 production is a useful metric for aerobic metabolic activity in oxic systems, the activity of certain anaerobic metabolisms (e.g., fermentation and chemolithotrophy) remains uncharacterised where anoxia prevails. Hence, the relationship between water activity, survival and specific metabolisms and is not well defined.

4.1.3.2 Microbial activity at high salt concentration

Halophilic organisms

Halophilic (salt-loving) organisms are quite well studied and found among all domains of life on Earth, from Eucarya, Bacteria to Archaea. A high salt concentration corresponds to a low a_w. As an example, saturated solution with about 6.2 M NaCl (356 g/L at 0 °C) corresponds to an a_w of 0.755. Several obligate halophiles can live in such a habitat with a low a_w. This is especially the case for the green algae *Dunaliella salina* (Oren 2005), the hypersaline bacterium *Salinibacter ruber* (20% NaCl solution) (Antón et al. 2002) and the obligate halophile, phototrophic archaeon *Haloquadratum walsbyi* (a_w 0.709) (Grant et al. 2004, Stevenson et al. 2015) that live in the water column of hypersaline lagoons (Leong et al. 2011). The lowest limit for growth was determined for filamentous xerophilic fungi, e.g., *Xeromyces bisporus* with a minimum a_w of 0.66, which was however exposed to a concentrated glucose/fructose mixture as solute (Leong et al. 2011).

Relevance for the near-field of an L/ILW repository

While the porewater in the cementitious near-field of the L/ILW repository has a moderate salt concentration, the halophilic microorganisms are nevertheless interesting for the degradation of organics because they represent organisms that can cope with a low a_w and can be expected to prevail in the L/ILW caverns for around 70,000 years (Papafotiou & Senger 2016) (cf. Section 2.4.2). However, many of the known halophilic organisms are excluded as other requirements needed for survival are not met. Some of these organisms feed on sugars, such as the fungus *Xeromyces bisporus,* but no significant quantities of sugar will be available in an L/ILW repository. Due to the absence of light, the phototrophic organisms *D. salina* and *H. walsbyi* can also be excluded. This is not the case for halophilic methanogens, which could, in principle, live and produce CH_4 under the conditions relevant for an L/ILW repository.

Halophilic methanogens

Only strictly anaerobic methanogens could be present in an L/ILW repository. Anaerobiosis is not regarded as extremophilic, as life evolved from anaerobic thermophilic conditions towards oxygenic photosynthesis almost three billion years ago. Anaerobic degradation was first described by Pasteur in 1867 as the degradation of carbohydrates, called fermentation, and was directly linked to the presence and activity of living microorganisms. The highest salt concentration at which they could still be found is around 3.5 M, e.g., *Methanosalsum natronophilum*. They are hence not as extremely halophilic as the related Haloarchaea methanogens that live in a saturated NaCl solution (Sorokin et al. 2015). Most of these methanogens can only tolerate, rather than thrive, at higher salinities and are called halotolerant. They preferentially metabolise C1 compounds such as methanol and methylamine to form CH_4 and CO_2. Since all of these halotolerant methanogens have been found in hypersaline soda lakes where free water is present, it can be assumed that all methanogens require free water and a minimum a_w to operate their metabolism (Tab. 4-6) (Grant et al. 2004). It is important to mention that hydrogenotrophic methanogens produce larger amounts of water through their metabolism (reaction: $4\ H_2 + CO_2 \rightarrow CH_4 + 2\ H_2O$) and thus can greatly increase water availability locally.

Tab. 4-6: Halophile methanogens and their environments

Listed halophile methanogens were all found in salt or soda lakes, where free water is abundant (Grant et al. 2004).

Species	**Environment**	**Place of origin**
Methanocalculus halotolerans	oil well	France
Methanohalobrium evestigatum	saline lagoon	Crimea, Ukraine
Methanohalophilus mahii	salt lake	Great Salt Lake, USA
Methanohalophilus halophilus	salt lake	Australia
Methanohalophilus portucalensis	saltern	Portugal
Methanosalsum zhilinae	soda lake	Egypt
Methanococcus doii	saltern	California, USA

4.1.3.3 Microbial activity at high radiation doses

Radiation-tolerant microbes can grow continuously until 60 Gy (Pikuta et al. 2007). Interestingly, microorganisms are also able to tolerate or adapt to combinations of extreme environmental conditions, such as radiation tolerance / halophilic, low-pH / high temperatures (acido-thermophilic), high salt concentration / high-pH (halo-alkaliphilic) (Pikuta et al. 2007). Indeed, the extremely radioresistant *Deinococcus radiodurans* can survive 16 kGy (Cox & Battista 2005), though this is likely an incidental result of its adaptation to dessication, which also yields significant DNA damage (Mattimore & Battista 1996). This suggests that a range of organisms may be able to adapt to radiation doses expected within a L/ILW repository. However, the relationship between radiation tolerance and specific metabolic groups of bacteria is poorly described.

Moreover, most laboratory studies of radiation tolerance have been performed at relatively high dose rates, typically in the order of tens to hundreds of Gy/h. Here, oxidative stress responses and DNA repair mechanisms may be easily overwhelmed, leading such experimental data to suggest limited survival at the total absorbed doses anticipated in the early phase after repository closure. On the other hand, experiments employing chronic low dose rates have shown that microbial activity will likely not be precluded by dose rates expected within a repository, especially once significant decay of the main has occurred within the first few hundred years (main γ-/ β-emitters ^{60}Co, ^{137}Cs). For example, Brown et al. (2015) showed that at dose rates of 30 Gy/h and a total absorbed dose of 38.6 kGy, microbially mediated NO_3^-, Fe(III) and SO_4^{2-} reduction by sediment microbial communities were not restricted. Furthermore, in systems irradiated at 0.5 Gy/h, microbial Fe(III) reduction was even stimulated. Whilst changes in the relative abundances of different species were observed throughout the experiment, these appear to be related to the evolving geochemistry, rather than selection for radiation tolerance.

4.1.3.4 Microbial activity at high dissolved metal concentration

Another extreme condition expected in an L/ILW repository is high concentrations of dissolved metals, which can extend into the g/L range, especially at low (acidic) pH values. For example, the archaeon *Ferroplasma acidarmanus* can tolerate high dissolved concentrations of copper, arsenic, cadmium and zinc at pH 0, which would be lethal for other organisms (Gihring et al. 2003). However, the term "metallophilic" has not yet become accepted for such organisms. These grow at a very low pH and are unlikely to be present in a cementitious-based L/ILW repository. High concentrations of dissolved metallic ions are expected to inhibit microbial activities, thus confirming the conclusions of studies performed by Mijnendonckx et al. (2019).

4.1.3.5 Microbial activity in limited pore space

Microorganisms need pore space in the µm range for growth and mobility to seek out more suitable living conditions (i.e., availability of substrate, pH etc.). In the near-field of a cementitious L/ILW repository where the average pore space is ~ 0.1 µm in compact concrete (such as the type used for waste containers) and in a nm range for undisturbed OPA, respectively, microorganisms do not have enough space to be able to grow or move (Keller et al. 2011, Leupin et al. 2017). It should, however, be noted that microbes are often closely associated with clay minerals and are even involved in diagenetic transformations of clay minerals, such as smectite to kaolinite (Li et al. 2019). In undisturbed compact clay deposits, microorganisms can exhibit very low levels of activity over long periods of time. For example, Røy et al. (2012) demonstrated the activity of microorganisms in 83-million-year-old marine deep-sea clays, believed to be the original microorganisms arising from deposition of the sediments. Mijnendonckx et al. (2019) also demonstrated in their experiments that microbes could survive and grow in engineered compacted clays such as bentonite. This was explained by impurities in the clay with localised larger pore spaces that permitted colonisation by sulphide-producing bacteria. Hence, swelling pressure rather than pore size was identified as the important factor limiting microbial activity (Mijnendonckx et al. 2019). The cementitious materials present in the waste matrix, waste containers and excavated caverns have a pore space with a total volume ≥ 20% for gas storage. This porosity might also be favourable for microbial activities. It should be noted that the proportion of pore space in the total volume, the size distribution and connectivity of the pores present and the swelling pressure for clays are important parameters controlling the microbial activity but not the presence or survival of microbes. When space is created and substrates are present, microbial activity can increase rapidly (Mijnendonckx et al. 2019 and references therein).

4.1.3.6 Microbial activity at high pH and anaerobic conditions

Every microorganism grows and is active within a certain pH range. The fastest growth and the greatest activity occur at the pH optimum. Outside this optimum, growth and activity decrease. Studies have shown that microbial activity sharply decreases (up to 50%) when the pH value deviates from the optimum by one unit (Fernández-Calviño & Bååth 2010, Kotsyurbenko et al. 2004, O'Flaherty et al. 1998).

Microbial activity has been observed in a wide pH range from -0.06 to a maximum of 12 (Madigan et al. 2020). Species growing at an extremely high pH of up to 13 have even been reported in the literature. Sorokin (2015), however, points out that consistent buffering of solutions above pH 10.4 is challenging. Constant pH control during cultivation in highly alkaline conditions is therefore essential. Non-halophilic alkaliphilic organisms (such as microorganisms from freshwater cement sources) cannot grow at high osmotic pressures, making it difficult to properly buffer the growth medium. In addition, Sorokin (2015) indicates that if the external pH is above 12, the cytoplasmic pH would be around 10, which requires that all intracellular enzymes be adapted to highly alkaline conditions. This has so far never been observed in bacteria.

Microorganisms have different strategies to adapt to environmental stresses such as extreme pH values. As an example, biofilm formation is known to enhance survival during pH fluctuations (Davey & O'toole 2000, Flemming & Wingender 2010, Babauta et al. 2012, Flemming et al. 2023). In Charles et al. (2017), the adaptability of an aerobic microbial community (*Alishewannella* and *Dietzia* spp.) to hyperalkaline conditions through the formation of flocs was investigated. The experiments were conducted under hyperalkaline (pH 11 – 13), anaerobic and calcium-rich conditions, with unlimited access to water. The study shows the formation of flocs consisting of a complex mixture of extracellular polymeric substances that provides protection against hyperalkaline pH values by lowering the internal floc pH by about 0.4 – 0.8 units. By using this strategy, the microbial community studied was able to survive up to a pH of 12. At a higher pH (pH 13), the survival time was less than two weeks.

The extremophilic bacteria and archaea that could potentially survive under the highly alkaline conditions expected in the near-field of a cementitious L/ILW repository (pH 10.5 – 12) belong to the classes Clostridia, Betaproteobacteria, Gammaproteobacteria, Methanomicrobia, Methanobacteria and Thermococcus (Banciu et al. 2008, Bassil & Lloyd 2019, Blotevogel et al. 1985, Brazelton et al. 2017, Crespo-Medina et al. 2017, Keller et al. 1995, Yang et al. 2018). The only bacterium isolated and studied in a laboratory to date that can grow up to pH 12.5 is *Alkaliphilus transvaalensis*, part of the Clostridia. This organism was isolated from a gold mine at a depth of 3.2 km. It lives strictly anaerobically and grows at an optimum pH of 10.5, mesophilic temperatures (37 °C) and salinity levels of 5 g/L sea salts (0.1 of the ionic strength of seawater), suggesting that this organism could colonise an L/ILW repository (Takai et al. 2001). At a pH of 12.5, its growth was reduced by ~ 70%. Trutschel et al. (2022) isolated a *Rhodobacteraceae sp.* strain from Ney Springs, an extremely high-pH, marine-like terrestrial serpentinisation system, which can grow up to pH 12.4 under anaerobic conditions.

In hyperalkaline natural sites, various (groups of) microorganisms could be detected up to pH 13 with the help of molecular methods. Many of them belong to anaerobic microbial communities like methanogenic, nitrate-reducing (NRB) and SRB (Tab. 4-7). However, these microorganisms were not isolated and cultivated at hyperalkaline pH.

Tab. 4-7: Detected microorganisms, microorganism groups or metabolic processes at various hyperalkaline natural sites

Detected microorganisms / microorganism groups / metabolic processes	**Site**	**pH range (of tested sites)**	**Further parameters specified**	**Study**
Dominated by taxa affiliated with: • Thermodesulphovibrionaceae family • Candidate phylum OP1 class MSBL6 • *Meiothermus* genus Dominant metabolic processes: • Methanogenesis • Acetogenesis • Fermentation	Semail-Ophiolite Nappe, Oman	10.6 – 11.4 hyper-alkaline	T = 33.1 – 35.8 °C Eh = -32 – -546mV Conductivity = 354 – 3199 µS/cm SO_4^{2-} = 0.01 – 0.15 mM DIC = 0.19 – 0.22 mM	Rempfert et al. (2017)
Methanogenic genus: • *Methanobacterium*		11.05 / 11.28	T = 34.4 / 36.3 °C Eh = -415 / -253 mV SO_4^{2-} = 0.13 / 2×10^{-3} mM DIC = 0.05 – 0.13 mM	Kraus et al. (2021)
Dominant methanogenic archaea • Methanobacteriaceae family Dominant methanotrophic bacteria Methylococcaceae family	Voltari Massif, Italy	11.8 – 12.3	Eh = -75 – 202 mV DIC = 7.8 – 29 µM	Brazelton et al. (2017)

Tab. 4-7: Cont.

Detected microorganisms / microorganism groups / metabolic processes	**Site**	**pH range (of tested sites)**	**Further parameters specified**	**Study**
Methanotrophic archaea: - Different archaea from the anaerobic methanotroph group 1b (ANME-1b) Methanogens from the orders: - Methanosarcinales - Methanomicrobiales - Methanobacteriales	Santa Elena Ophiolite, Costa Rica	11.54 – 11.59	T = 26.1 – 29.2 °C Conductivity = 466 – 543 µS/cm ORP = -251 – -348mV DOC = 5.6 – 73.2 µM DIC = 126.3 – 254.3 µM	Crespo-Medina et al. (2017)
Dominant bacterial classes: - Clostridia - Proteobacteria Dominant Archaea - Euryarchaeota Key functional markers showed phylogenetic relationships with: - Sulphate-reducing bacteria - Chemolithoautotrophic sulphur-oxidising bacteria - Anaerobic methanotroph group 1 (ANME-1) - No methanogenic markers were found	Cabeço de Vide Aquifer, Portugal	11.4	No further information	Tiago and Veríssimo (2013)
Anaerobic microbial communities: - Nitrate-reducing bacteria - Fe(III)-reducing bacteria - Sulphate-reducing bacteria	Harpur Hill, Buxton, Derbyshire	10 – 12	Added electron donors and acceptors	Rizoulis et al. (2012)
Families detected at all investigated sites: - Comamonadaceae - Xanthomonadaceae *Gammaproteobacteria* are dominant at pH 13 from the families: - Pseudomonadaceae - Enterobacteriaceae		13	No further information	Smith et al. (2016)

Even though methanogens preferably live in neutral to slightly alkaline conditions, some can also survive and show metabolic activity at higher pH values. Indeed, although no methanogens growing above pH 10.2 have been isolated yet, evidence of methanogenic activity in hyperalkaline waters at pH values above 11 has been found (Tab. 4-7; Tab. 4-8) (Brazelton et al. 2017, Fones et al. 2019, Kraus et al. 2021).

Wormald et al. (2020) enriched methanogens from a very alkaline New Lime site (in-situ pH of 11.5 – 13.0). In the control experiment, they enriched the methanogens from a neutral sediment. The pH was increased in both cultures. The methanogen cultures from the New Lime enrichment showed a pH optimum at 9.0 and still registered some activity at pH 11, compared to the control culture where an optimum at pH 7 and activity up to pH 10 was measured. The hydrogenotrophic methanogenesis at pH > 9 was identified as being the predominant pathway.

Tab. 4-8: Methanogen species living at high pH

Different isolated methanogens are known to live and to be active at a higher pH range. However, the optimal pH, mentioned in brackets, never goes higher than 9.5 for the listed methanogens.

Methanogen strain	**Class**	**pH range (optimal pH)**	**Temp. (°C)**	**Study**
Methanocalculus natronophilus	*Methanomicrobia*	9 – 10.2	45	Sorokin et al. (2015)
Methanocalculus alkaliphilus	*Methanomicrobia*	8.0 – 10.2 (9.5)	≤ 41 (35)	Sorokin et al. (2015)
Methanosalsum zhilinae	*Methanomicrobia*	8.2 – 10.2	44 – 50	Sorokin et al. (2015)
Methanosalsum natronophilum	*Methanomicrobia*	8.2 – 10.2 (9.5)	37 – 43	Sorokin et al. (2015)
Methanosarcina soligelidi	*Methanomicrobia*	4.8 – 9.9 (7.8)	0 – 54 (28)	Wagner et al. (2013)
Methanosarcina spelaei	*Methanomicrobia*	4.9 – 10.0 (6.5)	0 – 54 (33)	Ganzert et al. (2014)
Methanobacterium alcaliphilum	*Methanobacteria*	7.0 – 9.9 (8.1 – 9.1)	25 – 45 (37)	Worakit et al. (1986)
Methanobacterium thermoalcaliphilum	*Methanobacteria*	6.5 – 10.0 (7.5 – 8.5)	40 – 69 (58 – 62)	Blotevogel et al. (1985)

4.1.4 Adaptation of microorganisms

By definition, life can adapt to environmental change. Almost every habitat on Earth is colonised by ubiquitous microorganisms. For instance, microbial studies in extreme sites usually attest to the presence of a particular biocoenosis that has adapted to the local environment using various strategies.

Adaptation is mediated by a spectrum of processes including gene regulation, natural selection, genetic recombination and horizontal gene transfer. It occurs at the cellular, genetic and molecular levels at the scale of the individual microorganism, species population and diverse microbial community. For instance, bacteria can change their membrane composition to adapt to changes in the environment such as pH, temperature, pressure, and salinity. These adaptations are passed on to subsequent generations, resulting in selection for the best adapted organisms. As an example, the so-called "compatible solutes" strategy allows the adaptation of the osmotic pressure in the cells to high-salinity conditions with LMW organics (Wani et al. 2022). Another adaptation mechanism called horizontal gene transfer relates to the transfer of gene(s) between micro-organisms, which can provide a selection advantage. This adaptation mechanism has been demonstrated in both bacteria and archaea (Goyal 2022, Wagner et al. 2017). Small microorganisms, typically growing in large populations and reproducing quickly, could rapidly adapt to environmental stressors compared to larger organisms. This is especially the case for free-living bacteria in water bodies that have enormous potential for rapid evolution over short timescales (months or years), due to their large population sizes and short generation times. Genetic evidence of the contemporary evolution of wild microbes and how fast the populations evolve is, however, scarce and not well understood (Brennan & Logares 2023). Adaptation by horizontal gene transfer in prokaryotes is usually very dynamic in places where cells aggregate, such as sediments or water surfaces. The basic requirement is physical contact between cells. In the near-field of an L/ILW repository and host rock (OPA), where mobility is limited to non-existent, it is expected that adaptations by horizontal gene transfer will be unlikely to occur. In rare cases, new proteins and associated genes can be generated *de novo*, i.e., from scratch, in order to adapt to environmental change. However, this is primarily limited to eukaryotes such as plants, fungi and yeasts and is very unlikely to be a significant processes during the degradation of organic waste inside a deep geological repository (Wang et al. 2020b). Furthermore, mutations in microorganisms leading to the degradation of previously non-degradable polymers are unlikely and, if so, will occur at very low rates. For example, hardly any organisms that can degrade persistent polymers such as PVC have yet emerged in the oceans, even though these polymers have been present in nature for fifty years. The anaerobic degradation of polymers depends on whether sufficient energy and carbon can be extracted from the reaction or, in other words, whether degradation is thermodynamically possible (Warthmann et al. 2013).

The adaptive strategies of microbial communities are diverse and occur at different levels. A clear prediction of these complex processes for specific extreme ecosystems such as an L/ILW repository is extremely difficult. Furthermore, natural limits of adaptation, such as thermodynamic limits, exist and determine whether such reactions are possible or not.

4.2 Possibility of microbial activities in the near-field of an L/ILW repository

Laboratory or in-situ studies can only give a limited picture of the potential microbial activity occurring in an L/ILW repository during the period under consideration of 100,000 years. Studies of natural analogues where conditions relevant to the cementitious near-field of an L/ILW repository have been established for long periods can provide additional information for the period under consideration (i.e., 100,000 years). Butterworth et al. (2021) have presented a compilation of microbial studies in natural analogues of a cement-based L/ILW repository.

The first subsection focuses on microbial life in natural analogues of the engineered barriers mainly made of cementitious materials, while the second one discusses potential microbial activity in clay rocks.

4.2.1 Microbial activity in cement

4.2.1.1 Semail-Ophiolite Nappe, Oman

The Semail-Ophiolite Nappe is the largest (~ 15,000 km^3) and best exposed ophiolite on Earth (Kraus et al. 2021). It is located in northern Oman and described as a good analogue for the cementitious engineered barriers of an L/ILW repository in an advanced degradation state, (pH < 12.5) (cf. Section 2.4) (Butterworth et al. 2021). Serpentinisation of olivine rocks resulted in strongly alkaline (pH 11.4) and reducing groundwaters (Eh = -363 mV; 35 °C) (Bath et al. 1987). The alkaline groundwaters of this region precipitated many unusual minerals, including brucite, magnesium hydroxide, and portlandite. In the study of Bath et al. (1987), a relatively low number of microbes was found by microscopy and culturing ($10^1 – 10^3$ cells/mL), including SRB. The authors attributed the low cell count to a lack of nutrients rather than to the high pH. Rempfert et al. (2017) investigated the microbial communities of fracture waters sampled from old boreholes in the Samail-Ophiolite, using 16S rRNA gene sequencing. The geochemical composition of the waters indicated the presence of several fluid types with different pH values. The results showed that the pH influenced the microbial diversity with communities present in hyperalkaline fracture waters (pH > 10), exhibiting lower diversity and different taxonomic composition compared to those found in alkaline or circumneutral (pH ~ 7 – 10) water. Taxa related to the Deinococcus-Thermus genus *Meiothermus* and the Thermodesulphovibrionaceae family are predominant in hyperalkaline fluids. The results further suggested that the metabolic processes supporting the dominant populations in the hyperalkaline waters include methanogenesis, acetogenesis, and fermentation. To better understand how microbial life survives under these hyperalkaline conditions in the Semail-Ophiolite fluids, Fones et al. (2019) performed geochemical measurements on water from different boreholes and exposed planktonic microbial cells to metagenomic and physiological analyses (Tab. 4-9). Water samples with a high pH (pH > 10.6) showed a negative oxidation-reduction potential and were generally enriched in compounds that microorganisms could theoretically use as reducing agents (H_2, CH_4). In contrast, these water samples were poor in compounds that could potentially be used by microorganisms as oxidising agents, such as SO_4^{2-}, NO_3^- and DIC. Planktonic cell abundances were lower in hyperalkaline than in alkaline or circumneutral water samples (Tab. 4-9), confirming the results of Rempfert et al. (2017). Various utilisation rates of the substrates were determined in microcosm-based activity assays. They showed that the utilisation rates of selected one-carbon compounds (formate, bicarbonate) were significantly lower in hyperalkaline than in alkaline water samples, while the assimilation rates for these compounds were comparable in hyperalkaline and alkaline water. This leads to a significantly higher assimilation-to-dissimilation ratio for hyperalkaline waters compared to the alkaline ones, which may represent an adaptation to minimising the energetic and physiological stress created by highly reducing, carbon-limited conditions. Furthermore, the estimated genome sizes were lower for hyperalkaline waters, which may suggest that microorganisms living under hyperalkaline conditions have physiological adaptations that allow them to survive under such polyextremophilic conditions. According to Fones et al. (2019), the lower average carbon oxidation levels in the derived proteomes for hyperalkaline waters supported this hypothesis.

Kraus et al. (2021) investigated the activity of the microbial CH_4 cycle in the subsurface waters in the Semail-Ophiolite, using molecular approaches based on both DNA and RNA extraction. Abundant 16S rRNA genes and transcripts associated with the methanogenic *Methanobacterium* genus were recovered from the most alkaline (pH > 10, up to pH 11.3) subsurface waters. The study was also able to demonstrate an enrichment of *Methanobacterium* in the DNA fraction relative to the DNA fraction of 16S rRNA in extracts from hyperalkaline waters, suggesting that these organisms were active. These studies reveal an important extension of the pH spectrum in which methanogenesis has been observed so far.

Tab. 4-9: Chemical, physical and microbiological parameters, measured in the Semail-Ophiolite

From Fones et al. (2019). Some selected parameters were compiled for hyperalkaline and circumneutral water samples.

Sampling point designation and parameters of the water samples	**Sampling points with pH 8.3 – 8.5**	**Sampling points with pH 10.6 – 11.3**
Oxidation-reduction potential (ORP) (mV)	178 – 214	-86 – -415
H_2 (µM)	below detection limit	0.51 – 164
CH_4 (mM)	0.02	12.6
Avg. cells (10^5 mL^{-1})	3.77 – 4.03	1.16 – 2.58
Avg. max. rate of $HCOO^-$ oxidation to CO_2 (pmol/mL d^{-1})	5,171 – 13,138	309 – 810
Avg. max. rate of HCO_3^- reduction to CH_4 (pmol/mL d^{-1})	1,057 – 2,267	18 – 26
Avg. max. rate of $HCOO^-$ assimilation to biomass (pmol/mL d^{-1})	79 – 143	220 – 230
Avg. max. rate of HCO_3^- assimilation to biomass (pmol/mL d^{-1})	28 – 69	56 – 70

4.2.1.2 Further serpentinite sites

Other environments have been affected by the process of serpentinisation and are the subject of numerous microbial studies, attesting to microbial activity related to the CH_4 cycle at pH values up to 12.3 (Tiago & Veríssimo 2013, Brazelton et al. 2017, Crespo-Medina et al. 2017, Zwicker et al. 2018).

In their metagenomic study, Brazelton et al. (2017) provide evidence of active methanogenesis and methanotrophy by microbial communities in serpentinite springs of the Voltri Massif, Italy. The ultrabasic springs (pH 12) transported various archaeal and bacterial communities from subsurface habitats, including methanogenic archaea (dominated by the Methanobacteriaceae family) and methanotrophic bacteria (dominated by the Methylococcaceae family).

Tiago & Veríssimo (2013) examined the microbial and functional diversity of a subterrestrial alkaline groundwater (pH 11.4) associated with serpentinisation at the Cabeço de Vide Aquifer in Portugal. Molecular analyses showed a diverse bacterial composition dominated by the Clostridia class, followed by Proteobacteria. Among the Archaea, the diversity was lower, with the majority of sequences belonging to the Euryarchaeota. Examination of key functional markers showed phylogenetic relationships with SRB, chemolithoautotrophic sulphur-oxidising bacteria and archaeans of anaerobic methanotroph group 1 (ANME-1). However, no methanogenic markers were found in this study.

Crespo-Medina et al. (2017) studied CH_4 dynamics in the Santa Elena Ophiolite, Costa Rica. The hyperalkaline springs had pH values of 11.2 – 11.6, strongly reducing oxidation-reduction potentials between -380 and -251 mV, and temperatures of 26.1 – 29.2 °C. The DOC and DIC concentrations were in the range of 5.6 – 73.2 µM and 126 – 254.3 µM, respectively. The CH_4 concentration ranged from 145 to 900 µM and had an elevated $\delta^{13}C\text{-}CH_4$ signature of -0.9 to -44.0‰. An enriched $\delta^{13}C\text{-}CH_4$ signature generally indicates a primarily abiotic CH_4 production.

However, the biological processes could simply be masked by the abiotic ones. Likewise, the enriched δ^{13}C-CH_4 signature of the samples could also be explained by the hydrology of the system. Alternatively, this isotopic signature may represent a combination of hydrogenotrophic methanogenesis and subsequent CH_4 oxidation, leading to its relatively "heavy" isotopic signature. Molecular data indicate methanogenic as well as anaerobic methanotrophic activities, which are likely facilitated by nutrients, including DIC from the surface water and their infiltration into the serpentinisation-influenced groundwater. The molecular data show sequences related to methanotrophic ANME-1b archaea and methanogens from the Methanosarcinales, Methanomicrobiales and Methanobacteriales orders. These sequences account for between 40 and 90% of the total archaeal sequences.

4.2.1.3 Harpur Hill, Buxton

Another natural analogue of the cementitious engineered barriers present in an L/ILW repository is the old limestone quarry at Harpur Hill, Buxton (Derbyshire, UK). This sediment shows a wide pH range from 6.5 to 13. Various microbial studies have been conducted in this environment or with microorganisms and microorganism communities derived from it. Rizoulis et al. (2012) found evidence of active NO_3^--, Fe(III)- and SO_4^{2-}-reducing bacterial communities. They also conducted laboratory studies, adding various electron donors and acceptors to the lime under anaerobic and alkaline conditions in order to investigate bioreduction. A clear sequence of electron acceptor use was found (NO_3^- > Fe(III) citrate > Fe(III) oxyhydroxide > SO_4^{2-}), with the rate of bioreduction decreasing with increasing pH (pH range studied 10 – 12). Smith et al. (2016) investigated the microbial composition at different sampling sites in Harpur Hill with pH values ranging from 7.5 to 13 and clearly showed a decrease of the total cell count with increasing pH (from about 2.5×10^6 cells mL^{-1} at pH 7.5 to about 3.0×10^5 cells mL^{-1} at pH 13). While members of the *Comamonadaceae* and *Xanthomonadaceae* families were detected at all investigated sites based on the analysis of 16S rRNA genes, *Gammaproteobacteria* of the *Pseudomonadaceae* and *Enterobacteriaceae* families dominated at pH 13. In anaerobic microcosm experiments, the microbial community of this site reduced Fe(III) to a pH of 11.5. Furthermore, studies on the microbial utilisation of the cellulose degradation product ISA have been conducted with microbial communities derived from Harpur Hill (Bassil et al. 2015). Bassil & Lloyd 2019 successfully isolated the new strain *Anaerobacillus isosaccharinicus* sp. nov. from these microbial communities that can degrade ISA under high pH conditions. Butterworth et al. (2021) concluded that from a microbiological perspective, Harpur Hill is a prime example of the ability of microorganisms to adapt to an environment altered by anthropogenic activity.

4.2.2 Microbial activity in clay

4.2.2.1 Microbial activity in OPA

OPA has a very low porosity, with the majority of the pores having radii of 0.001 – 0.05 µm (Keller et al. 2011, Senger et al. 2013). The smallest bacteria have a diameter of 0.15 – 0.2 µm, and the Archaea an average diameter > 1 µm (Lovley 2000). OPA also has a relatively low a_w of 0.931 – 0.962 (Leupin et al. 2017, Stroes-Gascoyne et al. 2011) and a TOC of around 0.9% w/w (Courdouan et al. 2007a). Only a small fraction of this is present as DOC in the porewater and defined as easily microbially degradable (Courdouan et al. 2007a, Courdouan et al. 2007b). For these reasons, microbial activity is suppressed in OPA but not completely inhibited (Leupin et al. 2017). Various studies in OPA and water-filled boreholes were able to show with culture-based and molecular investigations that various microorganisms are present, but with a majority metabolically almost inactive or dormant (Leupin et al. 2017 and reference therein). Most of the microorganisms detected or isolated belong to the gram-negative SRB. IRB, anaerobic lithotrophic bacteria and methanogens were also found. In Bagnoud et al. (2015), the microbial community in OPA borehole water was studied with sedimentary organic carbon as the only C-source. The analyses indicate a microbial community that has a surprisingly low diversity and is dominated by two most likely indigenous organisms. One of the dominating organisms identified was *Pseudomonas sp.*, a fermenting bacterium which can degrade organic macromolecules from OPA or dead microbial biomass to organic acids and H_2. The other dominating organism identified was a sulphate-reducing *Peptococcaceae* which can oxidise organic molecules (e.g., acetate present in OPA porewater up to 200 μM) to CO_2. Bagnoud et al. (2015) state that such a microbial system probably establishes itself in OPA where the pore space allows it. Whether the microorganisms are native to the OPA or introduced by drilling was discussed in many studies but could not be definitively determined (Bagnoud et al. 2015, Mauclaire et al. 2007, Stroes-Gascoyne et al. 2007, Wersin et al. 2011).

4.2.2.2 Microbial activity in bentonite

Many studies on microbial activities have also been performed in bentonite, used as a backfill material only in the HLW emplacement drifts of the repository (Nagra 2021a) (cf. Section 2.3). Fukunaga et al. (2005) investigated the microbial activity of bentonite deposits in Japan that had been undisturbed for several years. Both aerobic and anaerobic heterotrophic bacteria could be isolated (10^5 – 10^7 CFU and 10^3 – 10^5 CFU/g DW, respectively). The number of culturable cells decreased with depth and was below the detection limit (< 10^2 CFU/g DW) for one site at 90 cm depth. However, this could be due to the filtration effect of the bentonite. It was also shown that increasing dry density (decreasing water content) tended to correlate with decreasing bacterial numbers. Laboratory studies with high density bentonite confirmed this result and also show a negative effect of the bentonite density on microorganisms (Bengtsson & Pedersen 2016, Pedersen et al. 2000, Stroes-Gascoyne et al. 2010).

Povedano-Priego et al. (2021) studied the microbial diversity in compacted bentonite from Almeria, Spain, under anaerobic conditions. The ground bentonite was dried in the laboratory, ground into small particles (< 2 mm) and sprayed with acetate in an attempt to stimulate microbial activity. The ground and acetate-amended bentonite were compacted into cylindrical blocks (30.3 × 12.3 mm) with densities of 1.5 and 1.7 g/cm^3, respectively and incubated under anoxic conditions at room temperature up to 24 months. Microscopic characterisation showed that the compacted bentonite samples at both dry densities had pores and cracks that may harbor small bacteria and allow microbial activity. Molecular analysis based on 16S rRNA gene sequences revealed several genera involved in the biogeochemical sulphur cycle such as sulphur-oxidising bacteria (SOB) (e.g., *Delftia, Paracoccus, Mesorhizobium* and *Sulphurifustis*) and SRB (e.g., *Pseudomonas, Desulphuromonas, Desulphovibrio* and *Desulphosporosinus*). In addition, IRB (*Geobacillus, Stenotrophomonas, Thermicanus* and *Ralstonia*) were identified. A slight enrichment of typically acetate-utilising taxa (including *Delftia, Paracoccus, Stenotrophomonas, Thermicanus, Desulphuromonas* and *Pseudomonas*) was detected in the acetate-treated samples. However, these samples showed no difference in their microbial composition compared to the control samples not treated with acetate, which the authors attributed to an insufficient incubation period. Molecular analysis did not show significant differences in bacterial community structures with dry densities of 1.5 and 1.7 g/cm^3, respectively, suggesting that both densities had the same effect on native bacterial diversity. Povedano-Priego et al. (2021) concluded that the compacted bentonite only inhibits bacterial activity rather than killing bacteria It should also be noted that the entire study of Povedano-Priego et al. (2021) is based on DNA extractions, which indicate microbial diversity. However, the conclusions that can be drawn regarding microbial activity are limited because the DNA can also come from dead cells trapped within the bentonite.

Within the MIND project, microbial activity in bentonite was investigated in detail. This project showed that culturable sulphide-producing bacteria were present in all clays studied, regardless of their density and swelling pressure. The high bacterial and fungal diversity in bentonites was detected using 16S rDNA sequencing and fungal markers of the internal transcribed spacer gene, respectively. A high bacterial diversity with representatives of the genera *Nocardia, Pseudomonas, Pseudonocardia, Saccharopolyspora*, *Streptomyces* and the spore-forming sulphide-producing bacteria *Desulphosporosinus* were identified. The swelling pressure was also defined as a relevant limiting factor for microbial activity, but not for their presence and survival.

In northern Saskatchewan, Canada, a high-grade uranium deposit called Cigar Lake is enclosed by a clay-rich halo. Although this uranium deposit is embedded in a porous sandy rock, no radiological evidence of this ore deposit can be found at the surface, indicating that the deposit has been very well sealed over a long period of time (Brown & Sherrief 1999, Cramer & Smellie 1994). Microbial analyses of water samples from different areas of this deposit showed a microorganism density of about $10^3 - 10^7$ cells mL^{-1}, with the number of anaerobic microorganisms about the same or up to an order of magnitude higher than the aerobic ones (Stroes-Gascoyne et al. 1994). The anaerobic microorganisms tended to be distributed as follows: SRB in the ore zone, methanogens below the ore zone, iron reducers everywhere.

Another example cited by Butterworth et al. (2021) for the preservative effect of bentonite is the so-called fossil forest at Dunarobba in Italy. Around 2.5 Ma ago, a microbial organic degradation process, preserved by rapid sedimentation of clays and sands, was suppressed but not killed by the properties of the dense clay until today.

4.3 Anaerobic microbial degradation of selected organics

4.3.1 IERs, PS and styrene

Microbial degradation of PS

Pure PS has been assessed as being nonbiodegradable for several reasons. Firstly, the HC backbone chain is entirely composed of C-C bonds that are extremely stable and cannot readily be enzymatically cleaved (Albertsson et al. 2020). Further, enzymatic attack is difficult to impossible due to the hydrophobicity of the polymer surface, which affects how easily microorganisms can attach to the surface and makes most thermoplastics like PS resistant to hydrolysis. If microorganisms manage to attach the surface of the polymer, biological processes start outside the microbial cell by the secretion of extracellular enzymes (exo-enzymes). However, these enzymes are too large to penetrate deep into the polymer and are only able to cleave the polymer chain at the surface via hydrolytic mechanisms (Ho et al. 2018). Finally, the thermodynamics of depolymerisation of the polymer are endergonic, making biodegradation unlikely. During polymer condensation, more than -70 kJ/mol of heat is usually released (Berufsgenossenschaft Rohstoffe und chemische Industrie 2015, Lechner et al. 2010). This energy must be used to break down the polymers, through redox reactions with O_2, which could be conceivable under an aerobic environment.

In recent studies, PS has been shown to be aerobically attacked by oxidases from microorganisms colonising the gut of insect larvae (waxworm *Galleria mellonella* and mealworm *Tenebrio molitor* larvae) and feeding on some large polyolefins (Brandon et al. 2021, Yang et al. 2015). Based on the change in chemical composition of the PS, especially the reduction in molecular weight and its isotopic signature after its passage through the intestinal tract, it has been estimated that up to 50% of ingested Styrofoam can be degraded over 24 h by *T. molitor* mealworm larvae (Yang et al. 2015). *Zophobas atratus* larvae were also fed on Styrofoam as sole diet. A depolymerisation of PS and a partial mineralisation to CO_2 were observed (Yang et al. 2020). For further information, the degradation of PS by soil bacteria and mealworm's gut bacteria is summarised by Ru et al. (2020).

Conditions in an insect gut are very different from those expected in an L/ILW repository. The absence of O_2 in particular prevents the enzymatic attack of the polymer structure by oxidase or peroxidase enzymes. Moreover, how the polymer could be hydrolysed under anoxic conditions still remains unknown, especially because no chemical energy source is available from a thermodynamic point of view. Based on these arguments, it was assumed that PS was very unlikely to be biotically degraded in the cementitious near-field of an L/ILW repository, especially where anaerobic, highly alkaline and low-water availability conditions prevailed, supporting the conclusions of Warthmann et al. (2013).

Microbial degradation of styrene

The monomer of PS, styrene, can be degraded microbiologically under aerobic conditions via phenylacetic acid (Fig. 4-5). The initial degradation of styrene involves monooxygenase, an enzyme that requires free O_2. The complete degradation pathway and the required enzymes were described in detail in Ho et al. (2018).

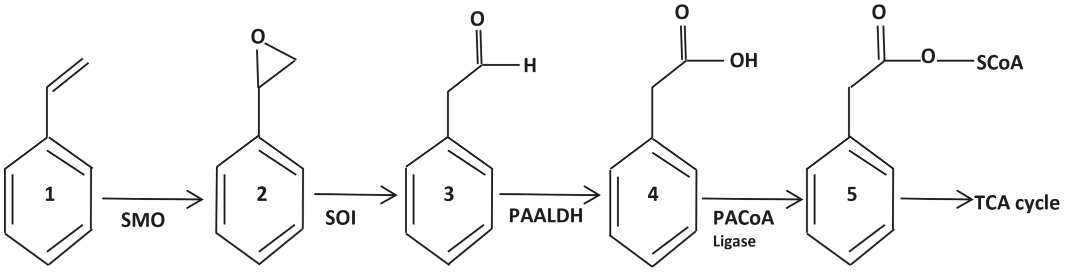

Fig. 4-5: Degradation pathway for styrene

1-styrene, 2-styrene oxide, 3-phenyl acetaldehyde, 4-phenylacetic acid, 5-phenylacetyl coenzyme A

SMO: styrene monooxygenase; SOI: styrene oxide isomerase; PAALDH: phenylacetaldehyde dehydrogenase; PACoA ligase: phenylacetyl coenzyme A ligase

Figure from Ho et al. (2018)

Similarly to PS, the biotic degradation process of styrene under anoxic conditions is unknown and thought to be limited in the context of a cement-based L/ILW repository.

Degradation of IERs

As IERs have a styrene-based structure, similarities with the biodegradation of PS are expected. Warthmann et al. (2013) described that IERs could be partially degraded by microbial activity, especially the surface-functional groups that can be cleaved radiolytically from the backbone (Filby et al. 2016, Small 2019) (cf. Sections 3.1.2 and 3.2.2) and metabolised by anaerobic organisms if the basic conditions for microbial activity are given. Concerning the PS backbone, it is most probably not anaerobically degradable, as previously discussed.

Cationic IERs

Radiolysis mainly releases SO_4^{2-} from the cationic IERs (cf. Section 3.1.2), that result in the splitting off of the sulphonic acid groups, followed by the oxidation of SO_3. Under anaerobic conditions, SO_3^- will not be oxidised to SO_4^{2-} but directly used by anaerobic assimilatory microbes as an electron acceptor for dissimilatory SO_4^{2-} reducers such as *Desulphovibrio desulphuricans*

(Simon & Kroneck 2013, Steuber & Kroneck 1998). The product of sulphite reduction will be sulphide (S^{2-}), which combines with metal ions to nearly insoluble metal sulphides (Blais et al. 2008).

Anionic IERs

Radiolysis of anionic IERs releases organic N-compounds, such as trimethylamine, dimethylamine, acetate nitrile, acetone and 2-butanone (cf. Section 3.1.2). These organic compounds can fuel microbial activity by aerobic methylotrophic bacteria such as *Methylotenera* and *Methyloversatilis,* metabolising CH_4 and methylamine, or *Sphingobium* and *Novosphingobium* capable of metabolising various aromatic organic compounds. (Small 2019)

In anaerobic environments, the amines can serve as precursors for CH_4 formation by methylotrophic methanogens, especially from the Methanosarcinales order (Tab. 4-10). Methylamines (i.e., monomethylamine, dimethylamine and trimethylamine) are converted to CH_4, ammonia and CO_2, from which the energy gain for the microbes is rather low ($\Delta G'^{\circ} = - 31$ kJ/mol CH_4 from trimethylamine) (Kurth et al. 2020, Watkins et al. 2012). Because of this low energy gain, it can be assumed that this process takes place very slowly.

Tab. 4-10: Methanogens of the order *Methanosarcinales* using methylamines as a substrate for CH_4 formation under strictly anaerobic conditions

Table derived from Madigan et al. (2020)

Genus	Substrates
Methanosarcina	$H_2 + CO_2$, methanol, methylamines, acetate, CO
Methanolobus	methanol, methylamines
Methanohalobium	methanol, methylamines
Methanococcoides	methanol, methylamines
Methanohalophilus	methanol, methylamines, methylsulphids
Methanosaeta	acetate
Methanosalsum	methanol, methylamines, dimethylsulphide
Methanimicrococcus	methanol, methylamines (H_2 is required with any methanogenic substrate)

4.3.2 PVC

PVC usually appears to be largely resistant to biodegradation (Danso et al. 2019, Mohanan et al. 2020), which seems plausible considering the high polymerisation heat of -1,534 kJ/kg (Fischer et al. 2014).

Many publications have been found concerning the biotic degradation of PVC by soil fungi (Ali et al. 2014, Khatoon et al. 2019, Pardo-Rodríguez & Zorro-Mateus 2021), bacteria (Anwar et al. 2016, Giacomucci et al. 2019, Khandare et al. 2021, Zhang et al. 2022) or even microorganisms colonising the gut of insect larvae such as mealworms (Peng et al. 2020, Wu et al. 2019, Zhang et al. 2022) in aerobic conditions. Despite the fact that many of these studies attest to the biotic degradation of PVC, only a few have determined the degree or rates of degradation, such as Khandare et al. (2021), who registered a maximum weight loss of PVC films of 1.76% after 60 days, and Peng et al. (2020), who measured a chloride loss of 2.9% from the PVC ingested by larvae.

Only the study of Giacomucci et al. (2020) attested to possible anaerobic degradation of PVC. In their recent work, the biodegradation of PVC films was studied by consortia enriched from marine samples in anaerobic microcosms with four different culture media. After 7 months, significant gas production was measured in 10 out of 16 microcosms. While CO_2 was detected in all microcosms, CH_4 was produced only in the ones with a methanogenic medium (the exact media composition was not provided). Further analysis after 7 and 24 months of incubation showed that 6 out of the 16 enriched consortia were able to degrade the PVC films. Dense biofilms were detected on the plastic surfaces with measured gravimetric weight losses up to 11.7 ± 0.6% and significant decreases in thermal stability and average molecular weight. According to Giacomucci et al. (2020), the microorganisms apparently degraded both the additives and the polymer chains. Molecular analyses of the microbial community show a close relationship with degraders of halogenated organic compounds.

The only study found that investigated the biotic degradation of PVC under alkaline conditions was published by Nixon et al. (2018). Irradiated / non-irradiated pure PVC powder as well as plasticised PVC films were used, pretreated with hydrolysis (at pH 12.4). Similarly, the biotic degradation of the often-used PVC additives triphenyl phosphate and phthalate were studied in non-irradiated and irradiated form at pH 10. No NO_3^- reduction was observed with non-irradiated pure PVC powder, while a small amount of NO_3^- reduction was measured with irradiated PVC powder. In contrast, significant NO_3^- reduction was measured with plasticised PVC films after 90 days of incubation (i.e., 90% and 63% for non-irradiated and irradiated plasticised PVC films, respectively). The additive triphenyl phosphate led to a slight but still significant increase in nitrite, while phthalate as an electron donor did not support NO_3^- reduction at all. Analysis of the microbial community composition showed that bacteria dominated the enrichments, while Archaea accounted for less than 1% of the community. Based on these results, Small (2019) assumed that pure PVC is most likely not degraded by microbial activity under conditions relevant to a cement-based L/ILW repository and thus will not contribute to the gas generation rate, confirming the conclusions of Filby et al. (2016). Conversely, plasticisers are relatively easily biodegradable.

In general, the biodegradability of PVC is rather difficult to tackle because it contains large amounts of various additives, which can account for up to 50 – 75% of the total weight (Kotova et al. 2021) and many of the studies available used mixed-species microbial communities. Studies on pure PVC powder (Wu et al. 2019) or pure PVC sheets are therefore needed to avoid an overestimation of the degradation taking place (Ali et al. 2014, Khatoon et al. 2019). Furthermore, no defined enzymes or degradation pathways were identified for the degradation of PVC (Danso et al. 2019).

Biodegradation of PVC additives

The abiotic degradation of plasticised PVC released additives that, together with their degradation products, could stimulate the growth of a wide range of microorganisms (Mijnendonckx et al. 2021).

Liang et al. (2008) reviewed many studies about the aerobic and anaerobic biodegradation of phthalates and listed a variety of bacteria and fungi-degrading phthalates. In general, degradation of phthalates under anaerobic conditions is much slower than in aerobic conditions. The complete degradation of phthalates was shown for both aerobic and anaerobic mixed cultures, requiring different metabolic genes and enzymes.

The biodegradation of typical plasticisers in a landfill environment was later assessed by Smith et al. (2013) and can be summarised as: "Typical plasticisers have thus been shown to be biodegradable by microbes present in landfills. High concentrations of phthalic acid were found in landfill leachates, indicating that the phthalic diesters and monoester intermediates are hydrolysed to phthalic acid but that conversion from phthalic acid to final degradation products

(CH_4 and CO_2) by microbes occurs much less readily" (Filby et al. 2016). Under these conditions, the microflora might be capable of a complete biodegradation of phthalates into biogas, according to their exposure time and concentrations. Wang et al. (2020a) investigated the removal of di(2-ethylhexyl)phthalate from the leachate of an aged landfill and attested that biodegradation played a minor role because the di(2-ethylhexyl)phthalate was mainly adsorbed on activated sludge. Sun et al. (2022) also measured the removal of di(2-ethylhexyl)phthalate from aged landfill leachate in a reactor, reaching 42.8%, 17.6% and 15.3% in the anaerobic, anoxic and oxic parts, respectively. The authors concluded that only a small fraction of di(2-ethylhexyl)phthalate was degraded by the microorganisms and that adsorption to activated sludge was the main mechanism for di(2-ethylhexyl)phthalate removal from leachate, confirming the previous assumption of Wang et al. (2020a).

The only study dealing with the degradation of PVC additives under conditions relevant to a cement-based L/ILW repository was performed by Nixon et al. (2018) (cf. section above). Their results indicate that some additives in flexible PVC can be used as electron donors for NO_3^- reduction, while phthalate does not promote reduction of NO_3^- and of triphenyl phosphate only to a minor extent. Based on this study, Small (2019) states that some additives can readily leach from plasticised materials and be oxidised by NO_3^- under conditions relevant for a cement-based L/ILW repository. Small (2019) further added that an important next step is to evaluate which specific additives or combinations of additives ultimately promote NO_3^- and SO_4^{2-} reduction and gas generation, and what impact these additives have on radionuclide mobility, as leached phthalates are able to form complexes with radionuclides (Mijnendonckx et al. 2019).

The biotic degradation pathway of phthalates was published in the review of Boll et al. (2020). The microbial strategies for the degradation of phthalates in aerobic conditions differ from those in anaerobic conditions. The anaerobic degradation of phthalates is illustrated for SRB and NRB with the involved genes, enzymes and metabolites in Fig. 4-6. In the anaerobic degradation, phthalates are converted to the central intermediate benzoyl-CoA (Fig. 4-6), which is further dearomatised to cyclohesa-1,-5-diene-1-carboxyl-CoA and then degraded to acetyl-CoA units and CO_2 by the so-called benzoyl-CoA degradation pathway. The degradation of phthalates to benzoyl-CoA is very similar for SRB and NRB. Phthalates is taken up by a tripartite ATP-independent periplasmic transporter combined with a periplasmic binding protein and a permease subunit. Aside from the tripartite ATP-independent periplasmic-uptake approach in some NRB, an additional three-component ABC transporter system was identified. However, it is not clear whether both transporter types can take up phthalate. In denitrifying bacteria, phthalate is initially degraded by a class III CoA transferase to Phthaloyl-CoA. CoA transferase uses succinyl-CoA as CoA donor and phthalates as the CoA acceptor. In SRB, no gene encoding for a CoA transferase was detected (Geiger et al. 2019). Instead, Geiger et al. (2019) identified a gene encoding for a putative ATP-dependent CoA ligase, which also seems to be able to transform phthalate to phthaloyl-CoA. Phthaloyl-CoA decarboxylase further catalyses the decarboxylation of phthaloyl-CoA to benzoyl. Phthaloyl-CoA decarboxylase belongs to the UbiD enzyme family and contains a modified prenylated flavin adenosine mononucleotide cofactor. This cofactor is formed by a second component, called UbiX, that uses dimethylallyl-monophosphate for the conversion of flavin adenosine mononucleotide to prenylated flavin adenosine mononucleotide. An explanation for why SRB use a phthalate CoA ligase instead of a less energy-consuming succinyl-CoA-dependent CoA transferase, could be that they oxidise fatty acids via the Wood-Ljungdahl pathway rather than via the citric cycle (Boll et al. 2020, Geiger et al. 2019). Boll et al. (2020) classify PCD as a key enzyme of anaerobic phthalate degradation and conclude at the end of their review that the current anaerobic solution may indeed represent an early stage of the ongoing evolution of a degradation pathway for an essentially xenobiotic compound. While denitrifying and SRB both show a phthalate catabolic gene, none was found in the genomes of obligately anaerobic F(III)-respiring or fermenting bacteria with sequenced genomes (e.g., *Geobacter* or syntrophic fermenting species) (Geiger et al. 2019).

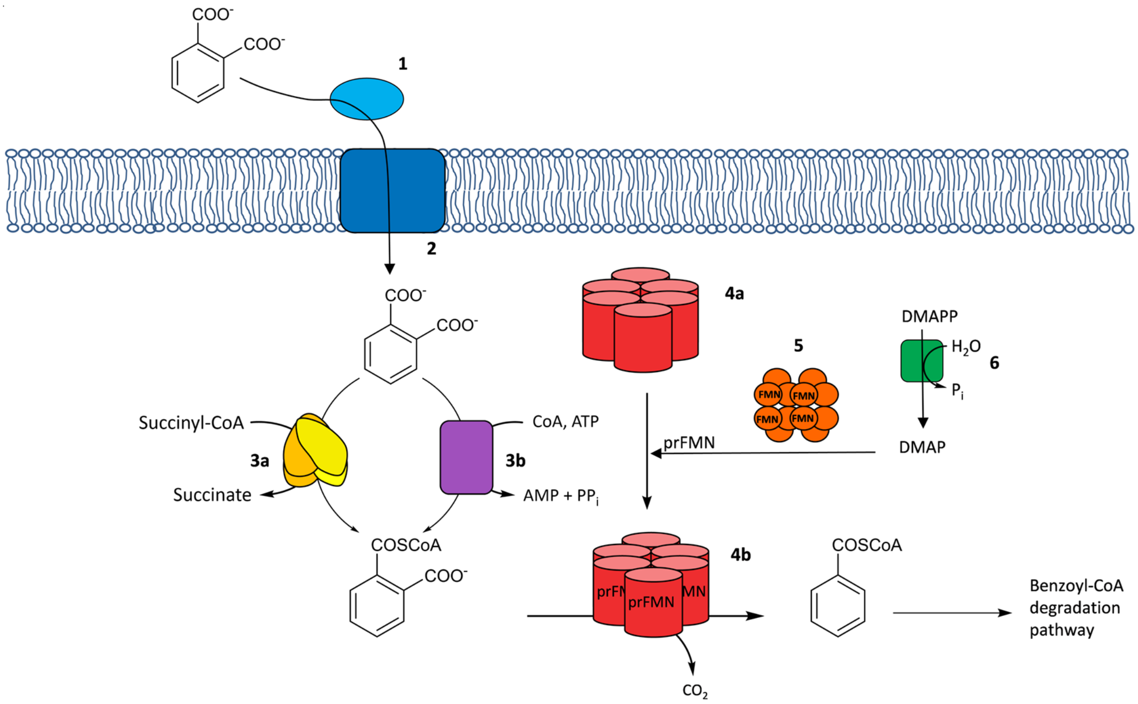

Fig. 4-6: Anaerobic degradation pathway of phthalate

Phthalate is taken up by anaerobic microbes, converted to instable PA-CoA and further to central intermediate benzoyl-CoA. 1) Periplasmic binding protein; 2) TRAP transporter; 3a) Heterodimeric SptAB subunits of succinyl-CoA:phthalate CoA transferase (nitrate-reducing bacteria); 3b) Phthalate-CoA ligase of unknown multimerisation state (sulphate-reducing bacteria); 4) Hexameric UbiD-like PCB; 4a) Inactive PCD apo-form; 4b) Active PCD with prFMN cofactor; 5) Dodecameric UbiX-like subunit of prFMN forming prenyl-transferase; 6) Nudix-like hydrolase putatively involved in synthesis of DMAP from DMAPP (nitrate-reducing bacteria). Adopted from Boll et al. (2020).

4.3.3 Bitumen

Microbial degradation of bitumen is important for gas generation (Mijnendonckx et al. 2021). Various studies have been conducted under both aerobic and anaerobic conditions, and the measured biotic degradation rates are summarised in Tab. 4-11.

Wolf & Bachofen (1991a) and Wolf & Bachofen (1991b) mechanically powdered bitumen to obtain a highly increased surface area. Under anaerobic conditions, the calculated degradation rate of 0.2 – 0.6 g bitumen/m^2 a^{-1} was about a factor of 100 lower than under aerobic conditions (Tab. 4-11). Bitumen-degrading organisms hence seem to be ubiquitous. By extrapolating this degradation rate, a degradation of 0.3 – 0.8% of bitumen would occur over a period of 1 ka under anaerobic conditions. It should be noted, however, that these experiments were conducted in a solution that optimally supplied the degrading organisms with water and nutrients at a neutral pH value, which is not expected to happen in the near-field of a cement-based L/ILW repository.

Roffey & Norqvist (1991) measured an anaerobic bitumen degradation rate of 1.1 – 1.5 µmol CO_2 month/mg bitumen or 13 – 18 mmol CO_2 /a m^{-2} bitumen over one year in laboratory vessels under anaerobic and various pH conditions (up to pH 10 – 10.5) (Tab. 4-11).

More recently, Pannekens et al. (2021) studied the microbial degradation of natural bitumen from Pitch Lake (Trinidad and Tobago) using a new technique of reverse stable isotope labelling which allows the measurement of deep mineralisation rates in the ng range. The experiments were carried out in mesocosms in artificially prepared anaerobic brackish water at a pH of 8. Approximately 100 g of fresh bitumen containing 140 mL of brackish water was added to each microcosm and incubated for 945 days. Depending on the assumed bitumen-water surface area, the calculated degradation rate ranged from 9.4 mmol to 38.6 mmol CO_2/L bitumen a^{-1}, which corresponded to a biodegradation of 0.11 – 0.46 g carbon/L bitumen a^{-1} (Tab. 4-11). One liter of bitumen was therefore assumed to need between 0.9 to 2.2 ka to degrade. Pannekens et al. (2021) assumed that the degradation rates calculated in experimental microcosms might also overestimate the real degradation rates due to the relatively large volume of the overlaying water added to the microcosms, which might have affected the microbial activity and the cohesive oil–water transition zone and the available sulphate concentration (9.7 mM $NaHSO_4$) that could artificially increase the degradation rates. By comparison, the SO_4^{2-} concentration in the cementitious porewater of the L/ILW repository will be around 0.35 and 1.16 mM during stage II degradation (Hummel et al. 2022).

Instead of measuring the bitumen degradation rate directly, Rezende et al. (2020) studied methanogenesis in heavily depleted oil reservoirs. Oil sand bitumen as the only organic substrate was used to which nutrients and electron acceptors (i.e., NO_3^-, SO_4^{2-}, bicarbonate, and a mixture of these) were added. CH_4 was detected in all microcosms except those containing NO_3. Methanogenesis was measured over 3,000 days, with the highest measured CH_4 production rate in the bicarbonate-amended microcosms reaching 0.15 µmol CH_4/g oil d^{-1}, which corresponds to a production rate of around 55 mmol CH_4/L bitumen a^{-1} (considering a bitumen density of 1 g/cm^3) (Tab. 4-11). The degradation rates are comparable with the study of Pannekens et al. (2021) but much lower than the ones reported by Roffey & Norqvist (1991), Wolf & Bachofen (1991a) and Wolf & Bachofen (1991b). In the microcosms amended with SO_4^{2-} where bitumen was the only carbon substrate, methanogenesis was detected in the presence of SO_4^{2-} and putative SRB. Since SO_4^{2-} reduction is normally energetically more favourable than methanogenesis, the observed methanogenesis in the presence of higher SO_4^{2-} concentrations (> 20 mM SO_4^{2-}) is surprising. The authors assumed that the syntrophic metabolism by these bacteria may have supported methanogenesis. Closer examination of the bitumen showed no significant molecular changes, suggesting that the very slow methanogenesis induced the biodegradation of the bitumen in a non-specific way. After the 3,000-day incubation, benzoate was added, which led to a 110-fold increase in methanogenesis. Based on this results, Rezende et al. (2020) concluded that the very low CH_4 production was due to the recalcitrant nature of the oil sand bitumen and not to the microbial community in the heavy oil reservoir.

Tab. 4-11: Bitumen degradation rates

The microbial degradations rate of bitumen are given in different units in the various publications, which makes comparison difficult. The degradation rates on grey background were taken from the corresponding studies. Values on white background were converted under certain assumptions.

Units	**Wolf and Bachofen (1991a, 1991b)**	**Roffey and Norqvist (1991)**	**Pannekens et al. (2021)**	**De Rezende et al. (2020)**
Degradation rates based on mass				
g bitumen/m^2 a^{-1}	**0.2 – 0.6**	0.45 – 0.62*		
g C/L$_{\text{bitumen}}$ a^{-1}**		453 – 617	0.32 – 1.32	1.01
Degradation rates based on produced gas (CO_2 + CH_4) ***				
mmoles gas/m^2 a^{-1}		37.1 – 51.4		
mmol gas/L$_{\text{bitumen}}$ a^{-1}		37,714 – 51,429	26.9 – 110	84.2
Degradation rates based on CO_2 ***				
mmoles CO_2/m^2 a^{-1}		**13 – 18**		
µmol CO_2/mg$^{-1}_{\text{bitumen}}$ month^{-1}		**1.1 – 1.5**	0.001 – 0.003	0.0025
mmol CO_2/L$_{\text{bitumen}}$ a^{-1}		13,200 – 18,000 4)	**9.4 – 38.6**	29.5
Degradation rates based on CH_4 ***				
mmoles CH_4/m^2 a^{-1}		24.1 – 33.4		
µmol CH_4/g$_{\text{bitumen}}$ d^{-1}		67.2 – 91.6	0.05 – 0.2	**0.15**
mmol CH_4/L$_{\text{bitumen}}$ a^{-1}		24,514 – 33,428	17.5 – 71.7	54.8****

* Assumption: the mass loss of bitumen is due to carbon loss - the rather small mass fraction of H_2 is neglected.

** The amount of produced gas (CO_2 and CH_4) was converted into the corresponding mass of carbon (g).

*** Assumption: elemental analysis indicates that most bitumens contain primarily HCs with an average mass composition of C = 79 – 88%, H = 7 – 13%, O = 2 – 8%, S = traces to 8%, N = 3% (IARC 2013). From this mass composition, theoretical empiric formulas were calculated and used to calculate the potential CH_4/CO_2 ratio with the Buswell model (Symons & Buswell 1933). An average CH_4/CO_2 ratio 65%/35% was calculated.

**** Assumption: Density of bitumen is equal to 1 kg/L.

The microbial diversity present in natural asphalts was studied by Kim & Crowley (2007). Molecular analyses revealed a wide range of phylogenetic groups within both bacteria and archaea present in the asphalts from the Rancho La Brea Tar Pits in Los Angeles. Many of the detected microorganisms belong to new genera and families. Among these, three methanogenic species were found in the phylogenetic analysis of the archaea. Schulze-Makuch et al. (2011) also studied microbial life in natural asphalt. They found a unique microbial diversity in a liquid asphalt desert, which differs from the one identified in the La Brea Tar Pits (Kim & Crowley 2007). The detection of the gene marker mcrA, as well as the sequencing of the archaeal small subunit ribosomal RNA demonstrated an active methanogenic metabolism. Schulze-Makuch et al. (2011) also attested to a microbial fractionation effect by registering lower $\delta^{13}C$ values for CH_4 and C_2H_6 (-49.0‰ and -34.1‰, respectively) in comparison to carbon in natural asphalt (-28.1‰) (microorganisms generally preferring lighter isotopes).

In their study with natural bitumen from Pitch Lake (Trinidad and Tobago), Pannekens et al. (2021) identified fermenting and SRB in the biofilm developed on the bitumen after incubation with brackish water at pH 8. Rezende et al. (2020) detected several methanogenic archaea and potential syntrophic bacteria by molecular analysis after incubation of oil sand bitumen to which nutrients and electron acceptors were added.

During the degradation of bitumen, not all fractions were degraded to the same extent (Nzila & Musa 2021). For instance, saturates and aromatics preferentially degraded in comparison to asphaltenes and resins. Nzila & Musa (2021) highlighted in their review that our understanding of the biodegradation is not complete and that there is so far no evidence for a complete degradation of asphaltenes and resins.

4.3.4 Plastics (PP, PET)

Various studies have investigated the microbial degradation of plastics. Among these, the review publication of Kotova et al. (2021) provides a well-structured compilation of studies on the microbial degradation of plastics. Although the results of extensive research show that the reliably documented processes of plastic degradation are very slow, the diversity of fungi and bacteria capable of degrading different types of plastics is impressive. Kotova et al. (2021) conclude that only a limited number of ecological niches have been studied so far, suggesting that the actual diversity of plastic-degrading microorganisms might be even greater. Very few studies have investigated anaerobic degradation of plastics.

PP

No clear evidence for anaerobic degradation of PP could be found in the literature. Skariyachan et al. (2018) described the anaerobic degradation of PP and PE under landfill conditions by *Bacillus cereus* at pH 7.2 and 50 °C as optimum conditions, but strictly anaerobic degradation could not be demonstrated.

PET

Many studies inventoried PET-degrading organisms and enzymes. Some examples were summarised in Tab. 4-12. PET particles used are often very small, presumably to provide a larger surface area to the microorganisms for facilitating their fixation on the hydrophobic surface of the polymer and their degradation through exo-enzymes.

Webb (2012) describes several PET-degrading bacteria, including *Celeribacter neptunius*, a facultative anaerobic halophilic member of the Rhodobacteraceae, which can degrade PET in the temperature range of 5 – 35 °C (optimally 25 °C) and pH range of 4.0 – 10.0, requiring an NaCl content of 1 – 8%. Similarly, *Oceanicola marinus* was identified as a facultatively anaerobic member of the Rhodobacteraceae and could degrade PET at the temperature range of 4 – 42 °C, a pH range of 6 – 9, and an NaCl concentration of 2 – 8% (optimal: 28 – 35 °C, pH 7, 3 – 5% NaCl). In general, PET was identified as being highly resistant to microbial degradation presumably due to the high proportion of crystalline domains.

Some microorganisms were also genetically modified to be able to degrade PET (Yan et al. 2021, Qi et al. 2021). Yan et al. (2021) especially showed that a modified strain of the thermophilic anaerobic bacterium *Clostridium thermocellum* that did not possess the intrinsic ability to degrade PET was able to act as a biocatalyst under anaerobic conditions at 60 °C. In this process, the enzyme LC-cutinase, which degrades the waxy layer of leaves in nature, cleaves PET into its monomeric form. Qi et al. (2021) also used genetically modified *B. subtilus* to secrete PETase enzymes and measured up to 31% wt. PET that degraded within three days.

So far, PET has not yet been observed to degrade in natural aerobic environments such as soils and thermophilic composting (Gómez & Michel 2013). It should also be noted that with the exception of genetically modified microorganisms, the organisms identified as being able to degrade PET are all aerobes, and that PET has also not been observed to degrade under anoxic environmental conditions.

To better characterise the degradation process of PET, bacterial enzymes were also isolated during experiments (Tab. 4-12) (Papadopoulou et al. 2019). Most of the investigated enzymes perform a classical hydrolysis reaction and are able to degrade PET to its monomer, the mono(2-hydroxyethyl) terephthalic acid. As O_2 is not involved in this reaction (except for cutinases), it can be assumed that depolymerisation of PET could take place under anaerobic conditions. A sustainable plastic waste management by application of these so-called PETases is discussed in more details in Papadopoulou et al. (2019).

Tab. 4-12: PET degrading enzymes

From Papadopoulou et al. (2019)

Enzyme (if specified)	Source	Substrate
TfH	*Thermobifida fusca*	Melt-pressed PET from beverage bottle (10% crystallinity)
HiC	*Thermomyces insolens*	*lc*PET (7% crystallinity), *bo*PET (35% crystallinity)
Thh_Est	*Thermobifida halotolerans*	PET film (properties not reported)
LC-Cutinase	Metagenome from leaf branch compost	Amorphous PET film
	Nocardia species	PET transparency sheets
Tcur1278 **Tcur0390**	*Thermomonospora curvata*	Nanoparticles of *lc*PET film
Cut190 (S226P/R228S)	*Saccharomonospora viridis*	*lc*PET (6 – 7% crystallinity) PET film for packaging (PET-S) (8.3% crystallinity)
	Comamonas testosterone F6.	Micro-size PET particles (23% crystallinity)
	Uncultured bacterium	Amorphous PET foil
	Streptomyces species	Powdered PET from beverage bottle
PETase	*Ideonella sakaiensis* 201-F6	*lc*PET (1.9% crystallinity) and high crystallinity *hc*PET (commercial bottle)

4.3.5 Cellulose, ISA and LMW organics

The biotic degradation of cellulose and its main degradation product ISA, including their degradation pathways, have been studied extensively since the 1970s (cf. Leschine 1995). Relevant studies realised in conditions expected in a cement-based L/ILW repository are summarised below.

In Bassil et al. (2015), microcosm experiments were performed on cellulose and ISA inoculated by a sample from a hyperalkaline site contaminated with lime-kiln waste. Within 30 months, the initial pH of 12 was reduced to circumneutral pH due to the production of organic acids (mainly acetic acid). The pH decrease seems to have started in some niches located in the non-shaken N_2-gassed bottles. Beaton et al. (2019) also measured the formation of organic acids such as acetic acid during the degradation of cellulose. The main bacterium identified in the microcosm experiments was *Clostridia*, a typical anaerobic bacterium producing spores able to survive extreme conditions and already characterised as a cellulose-degrader (Leschine 1995).

Degradation of cellulose generates a range of organic compounds, including α- and β-ISA as the main products. Under aerobic or denitrifying conditions (i.e., using NO_3^- as electron acceptor), microbial degradation of ISA even up to 0.5 mM/d was measured by Bassil et al. (2015). Rout et al. (2014) showed that ISA-degrading bacteria were ubiquitous in soils and able to degrade cellulose under relatively high pH values of 11 in microcosm studies. The end product of ISA by microbial degradation was ultimately CH_4. Under fermentative anaerobic conditions, experimental data are scarce. Only Bassil & Lloyd (2019) identified the alkaliphilic (pH 8.5 – 11) and moderately halophilic (0 – 6% NaCl) bacterium *Anaerobacillus isosaccharinicus*, which is able to degrade ISA under anaerobic NO_3^--reducing conditions. Dependent on the substrate, the strain produces acetate and formic acid, which can drive the pH into the neutral range, as observed in Bassil et al. (2015) and Beaton et al. (2019). The observed products of ISA and cellulose degradation could serve as substrates for hydrogenotrophic and acetoclastic methanogens. However, CH_4 production was never observed, not even after a 30-month incubation experiment (Bassil et al. 2020). Based on the results of these studies, microbial degradation cannot be excluded in conditions relevant for a cement-based L/ILW repository. ISA could be microbially degraded in the cementitious porewater. This might locally lower the pH, thereby limiting the abiotic production of ISA by alkaline hydrolysis and preventing an enhanced mobilisation of radionuclides that preferably form complexes with ISA (Humphreys et al. 2010b). Additionally, decreased pH will likely favour microbial activities through the development of new or larger niches (Bassil & Lloyd 2019).

Concerning the biotic degradation of complexing agents such as NTA and EDTA, Means et al. (1980) determined and compared the rates of degradation in soil under optimal laboratory conditions. Even though NTA seemed to be more degradable than EDTA, their biodegradation was rather limited under optimum laboratory conditions (i.e., presence of nutrients, light and O_2). The study of Bolton et al. (1993) also showed a higher biodegradability of NTA than EDTA under soil conditions with a maximum degradation rate of 43% for NTA and 15% for EDTA, over 115 days. The relative rates, however, varied between soil strata, suggesting that different microbial assemblages could be involved for the degradation of these two complexing agents. More recently, Maset et al. (2006) measured the biotic degradation of ISA, NTA and EDTA in sealed soil microcosm experiments stored in the dark. They calculated that < 4% of the ISA were respired over 70 days, which was comparable with NTA, while the respiration of EDTA was negligible, putting the relative order of biodegradation at ISA~NTA > EDTA and confirming the previous results of Means et al. (1980) and Bolton et al. (1993). The biotic degradation of NTA and EDTA also depends on the metals present as they can form a variety of metal complexes. For example, in the context of a cement-based L/ILW repository, their complexation with calcium allows them to be transported into bacteria cells (VanBriesen et al. 2000, Egi 2001). In the review of

Bucheli-Witschel & Egi (2001), the NTA-monooxygenase enzyme was specifically used to identify obligate aerobes and facultatively denitrifying bacteria as NTA degraders. In the near-field of a cementitious L/ILW repository, these communities are not expected to predominate (cf. Section 4.1), confirming the statement of Keith-Roach (2008) who highlighted that the biotic degradation rates of EDTA and NTA could be expected to be low under conditions relevant to the deep subsurface in the absence of light, under anaerobic conditions and with a limited availability of nutrients, as they were already limited under optimum laboratory conditions.

It is generally assumed that amines can be degraded anaerobically under nitrate-reducing conditions (Wanner et al. 1990). Using nitrate as electron acceptor, the biotic degradation of diethanolamine was especially attested under anaerobic conditions and in near-neutral solution (Knapp et al. 1996). Acetaldehyde, ethanol, acetic acid, glycoladehyde and glycolic acid were the main degradation products measured and facultative anaerobes, gram-negative bacteria were identified. In the absence of nitrate, diethanolamine did not degrade. According to Knapp et al. (1996), it is assumed that the process of degradation involves the cleavage of alkyl-N bonds by a dehydrogenase enzyme of the type reported by Jenal-Wanner & Egli (1993).

4.3.6 Plexiglas®

Very few studies of the biodegradation of PMMA have been published and none have examined degradation under anoxic and highly alkaline conditions.

Kaplan et al. (1979) studied the biodegradation of ^{14}C-PMMA in axenic cultures with 17 species of fungi, five groups of soil invertebrates (i.e., isopods, millipedes, snails, slugs and earthworms) and a variety of mixed microbial communities present in soils, manure, decaying plastics, garbage and activated sludges, under aerobic and neutral (pH 7) conditions, with and without cellulose. After 35 days, only between 0 and 0.29% of the polymer was converted to $^{14}CO_2$ by the fungi. Neither the soil invertebrates nor the microbes egested by them in their fecal pellets were able to degrade PMMA. After five weeks in anaerobic sludge, manure, garbage, and soils, PMMA was highly recalcitrant to biological decay and registered a total decomposition rate of between 0 and 0.15%. The addition of cellulose failed to increase any decomposition rates.

In more recent literature, the biodegradability of PMMA was studied for environmental purposes (Bhat & Kumar 2006, Sudhakar et al. 2022). Due to their resistance towards microbial degradation, attempts have been made to make PMMA more biodegradable by blending it with biodegradable materials such as cellulose acetate (by the formation of a hydrogen bond between the carboxyl group of PMMA and the free hydroxyl group of cellulose acetate). The blending of these two materials exhibits novel physical properties of interest for biomedical applications (e.g., higher optical transparency, thermal stability, hygro-mechanical properties). Such materials are not present within the L/ILW inventory, and their application in the NPP industry and research facilities is not foreseen. In Sudhakar et al. (2022), the biotic degradation of PMMA blending with cellulose acetate was studied with a mixture of *Pseudomonas*, *E.-coli*, *Bacillus*, and *Klebsiella* under aerobic conditions at pH 7. Soil tests detected a degradation fraction of between 0.3 and 2.95%. In activated sludge, degradation of about 1.1 to 5.21% was measured after 15 days. This range was the highest measured in this study and was probably the combined result of microbial degradation and hydrolysis. According to Fourier-transform infrared spectrometry results, the breakage of the long-chain polymer and hydrolytic degradation of esters into CO_2 and H_2O have been observed but the degradation was localised only in the blended film. Bhat & Kumar (2006) and Sudhakar et al. (2022) also noted that a higher cellulose acetate content in the polymer increases biodegradability but can unfortunately decrease the useful properties of PMMA.

4.3.7 SPs

LS-based SPs

In wastewater treatment, LS can be completely degraded to CO_2 and H_2O by a combined chemical ozone and aerobic biological treatment (Nakamura et al. 2004). Hernandez-Perez et al. (1998) identified an aerobic bacterium called *Streptomyces viridosporus* that is able to degrade LS partially, partly forming non-biodegradable acid-precipitable polymeric lignin. Anaerobic degradation of LS is hardly mentioned in the literature. Only Yin et al. (2000) report a complete inhibitory effect of the LS on the strictly anaerobic acetate-metabolising methanogens at a concentration of 2.6% (w/w).

SMF-based SPs

The study of Tian et al. (2012) reported on the degradation of SMF resin from paint sludge by thermophilic bacteria under aerobic and optimum conditions (i.e., humid, pH-buffered at 7.3, 30 – 55 °C, presence of nutrients). Melamine, ammeline, ammelide and cyanuric acid were identified as degradation products. The melamine monomers accumulated first and were almost completely degraded within 147 days by a mixed population of melamine-degrading microorganisms when the temperature was lowered to 30 °C. No data on the anaerobic biodegradation of SMF-based SPs under anaerobic and/or alkaline conditions is available.

In the BASF safety data sheet for an SMF polycondensate (Melment L 10/40%), the product is qualified as "not easily biodegradable", according to OECD regulations. However, by considering the chemical structure of this SP, it is likely that melamine-based compounds are microbially degraded in anaerobic conditions and may even be used as an N-source.

SNF-based SPs

SNF have been studied in connection with their environmental impact on groundwater quality (Ruckstuhl et al. 2002, Ruckstuhl et al. 2003), but never in conditions relevant for an L/ILW repository. Monomers of SNF (mono-naphthalene) and short oligomers (up to four units) were found in the aquifer about 60 m below a construction site, meaning that they were partially leached from concrete construction, while long-chain polymers appear to be firmly bound in the concrete. From calculations of concentration declines, it was concluded that about 80% of the substances had been biodegraded, and about 20% remained in the aquifer. The degradation pathway of SNF was found to be a desulphonation followed by a ring cleavage. Larger molecules such as naphthalene-1,5-disulphonate were neither degraded in the aquifer nor in laboratory tests (Ruckstuhl et al. 2003, Ruckstuhl et al. 2002).

PCE-based SPs

The biotic degradation and associated gas generation of PCE-based SPs in microcosm laboratory tests was reported by Stroes-Gascoyne & Hamon (2013). A very low amount of CH_4 was measured during these experiments. Unfortunately, the degradation of PCE-based SPs could not be confirmed with certainty, as such a low concentration of CH_4 could possibly also have been generated by other reactions with other organics or the gas phase (i.e., H_2 and CO_2).

In principle, ether bonds, relatively common in biology, e.g., in ether lipids, are enzymatically cleavable. The study of Schink & Stieb (1983) showed that polyether compounds such as polyethylene glycol are enzymatically degradable by certain strictly anaerobic bacteria. The product of polyethylene glycol degradation was acetaldehyde, which can be directly introduced into the metabolism. In co-culture with a methanogen, CH_4 and acetate were additionally formed.

Similarly to SMF-based SPs, the manufacturer BASF does not disclose much information on the degradation of PCE-based SP and only states in their safety data sheet (CASTAMENT FS 10) that "the polymer component of the product is poorly biodegradable". In the safety data sheet (SDS) for the product Melflux (Melflux 1641 F and Melflux 1643 F), the polycarboxylate PCE-based SP is also "not expected to substantially degrade, decompose or depolymerise under normal environmental conditions". What these "normal conditions" were was not clarified.

PAE-based SPs

To the best of the authors' knowledge, no data are available about the microbial degradation of these compounds.

4.4 Overview

This literature study has shown that microorganisms have different strategies to adapt to conditions relevant for the L/ILW repository.

Under anoxic conditions, the degradation of complex organic matter is a multistage process involving various anaerobic organisms. The complete degradation to CO_2 and CH_4 is based on a complex interaction of these syntrophic communities and can therefore easily be disturbed if conditions are not optimal or if inhibition occurs. If one step fails, the whole process of CH_4 formation comes to a halt.

Under highly alkaline conditions (pH values of up to 12.5), microbial life is possible but will be limited. In such conditions, hydrogenotrophic methanogenesis has been identified as the predominant methanogenesis pathway. Regarding hydrogenotrophic methanogenesis, thermodynamic calculations estimated a rather low $\Delta_r G'$ at -70 kJ/mol ± 24.0 kJ/mol in highly alkaline cementitious porewater at pH 12.5. As slow-growing methanogens can live with even a lower energy yield, an important implication is that CH_4 formation could most probably still take place from a thermodynamic point of view in the near-field of a cementitious L/ILW repository even at the early stage following repository closure, when the pH is highest (i.e., 12.5; during stage II of cement degradation; cf. Section 2.4.2). On the contrary, other thermodynamic calculations have suggested that hydrogenotrophic methanogenesis will stop at pH 10.9 under conditions relevant to a cementitious L/ILW repository. Hence, more specific thermodynamic modelling including various parameters describing the near-field evolution (e.g., pH, substrates) would provide additional insights concerning the limits of microbial activity, and more specifically, methanogenesis. Existing microbial experimental studies showed that microorganisms can develop different strategies to protect themselves from extreme environmental conditions, such as floc- or biofilm formation and can only survive up to a pH of 12 if water availability is unlimited and using easily available C-sources. However, these conditions are not expected to be present in the near-field of an L/ILW repository. In the literature, doubts exist about the potential for microbial activity above pH 12, as it becomes difficult to develop biocompatible buffer systems for such high pH values. Whether the entire microbial biochemistry (enzymes, proteins) in the cell can adapt to such pH values remains relatively unknown.

Serpentinite sites where hyperalkaline and anoxic conditions prevail were examined as a potential natural analogue. Various microbial species, metabolic pathways and functions could be detected with a pH of 12.5. This represents a clear limit above which microbial activity is strongly inhibited. The ratio of assimilation to dissimilation (for selected one-carbon substrates such as formate and bicarbonate) was much higher in hyperalkaline samples than in alkaline ones, which may represent an adaptation to minimise the energetic and physiological stress caused by highly reducing, carbon-limited conditions. All these studies of natural analogues clearly indicate that microbial life can take place under highly alkaline and anoxic conditions. The environmental conditions specific to these natural analogues and laboratory studies cannot however be compared to those in an L/ILW repository, especially in terms of the a_w.

No evidence was found in the literature that microorganisms are active and could grow without free water. The minimum thickness of a water film needed for microbial activity remains unknown. In the near-field of an L/ILW repository, other water-consuming chemical reactions such as the anoxic corrosion of metals suppress water availability. It is therefore conceivable that

no significant microbial community development may occur until the L/ILW repository is saturated enough to allow the presence of capillary water, low water availability not killing microbial life but simply inhibiting it, as shown in clay-rich rocks.

As a general statement, it can be assumed that at more extreme conditions (i.e., pH, low water availability), microbial activity is less likely to occur even though some exceptions cannot be excluded (such as the haloalkaliphilic bacteria from soda lakes that can withstand extreme pH and salinity). The importance of microbial activity in the near-field of a cementitious L/ILW repository when exposed to anoxic, highly alkaline conditions, limited nutrient availability and low water availability cannot be definitively determined. Due to the heterogeneity of the waste and conditioning processes, there may be small-scaled niches in the L/ILW repository where relatively favourable living conditions for microbial activity exist in terms of the pH, availability of nutrients, water and physical space (e.g., at the bottom of the caverns or in the EDZ). A slow spread of microbes from these niches into other parts of the repository is also conceivable. In the long term, the development of a significant microbial community, once conditions have become more favourable, cannot be excluded.

A summary of the biotic degradation of the main organic substances present in L/ILW has been compiled in Tab. 4-13. Since a combination of extreme parameters is expected in the near-field of an L/ILW repository in terms of water and substrate availability, highly alkaline pH and limited pore space (anaerobic conditions not being defined as extreme), most of the organic polymers are assumed to be only partially degradable by microorganisms over the period of consideration. This will especially be the case for IERs, PS, PVC, bitumen and thermoplastics in general. In contrast cellulose, ISA and LMW organics such as polymer additives are assumed to be fully biodegradable over 100,000 years (cf. Tab. 4-13). Only a limited number of experimental studies (and even sometimes none) in conditions relevant for a cementitious L/ILW repository are available as studies that do not show clear degradation are usually not published. This creates a bias in the information available in the literature. From a thermodynamic point of view, various studies have investigated the extent to which degradation processes in an L/ILW repository occur and have shown that the degradation of some polymers is often at the energetic limit. More in-depth thermodynamic modelling, including the evolution of specific parameters such as pH and water saturation, would potentially provide important insights into the limits of microbial activity under L/ILW repository conditions.

Tab. 4-13: Microbial degradation of organics

For the most abundant organic substances, information about whether or not microbial degradation can take place aerobically or anaerobically was indicated. If reliable degradation rates exist in the literature, these are also noted. An expert assessment was also given about the complete degradation of the organics over the period under consideration of 100,000 years.

n.r.d.: non-reliable data.

n.d.: non-determined.

Material	**Biodegradation**		**Rates (under anaerobic and favourable conditions)**	**Expert assessment**
	Aerobic	**Anaerobic**		
IERs	Partly	Partly	n.d.	The PS backbone of IERs is most probably not degraded under anaerobic conditions. However, their surface functional groups (i.e., SO_4^{2-} and amines), released after radiolytic degradation, can be used as substrates for anaerobic microorganisms as long as the general conditions for microbial activity (i.e., water availability, pH) are met. The degradation products released after the biotic degradation of the surface functional groups are CH_4 and sulphides.
PS	Partly	n.r.d.	n.d.	PS could be aerobically degradable in the digestive tracts of mealworms and waxworms with the help of bacteria using oxygenases. However, the process of depolymerisation under anaerobic conditions remains unknown and is quite unlikely from a thermodynamic point of view in the context of an L/ILW repository as unsufficient chemical energy source is available. However, degradation of styrene monomers could occur in principle.
PVC	Partly	n.r.d.	n.d.	To date, no enzymes or metabolic pathways of possible PVC degradation are known. The depolymerisation of PVC is endergonic and therefore unlikely to happen without specific energy input. Hence, as long as there is no physical, chemical or radiolytic degradation of PVC to vinyl chloride, no significant degradation is likely to take place in conditions relevant for an L/ILW repository, specifically with regard to pH and water activity. This view is also held by different experts (cf., Wartmann et al. 2013 and references therein).

Tab. 4-13: Cont.

Material	Biodegradation		Rates (under anaerobic and favourable conditions)	Expert assessment
	Aerobic	Anaerobic		
PVC-additives (phthalate)	Yes	Yes	n.d.	Various thermoplastic additives, such as phthalate, are biodegradable under anaerobic and alkaline conditions. Hence, PVC degradation could be misled by the degradation of these chemical additives. It is not clear to what extend fermenting bacteria and methanogenic co-cultures are capable of degrading phthalate, especially under conditions expected in the near-field of a cementitious L/ILW repository in terms of water availability and a pH above 12.5. It has, however, been shown that PVC additives can act as electron donors for NO_3^- reduction at high pH. The extent to which this also applies to SRB needs to be further investigated.
Bitumen	Yes	Yes	10 – 40 mmol $CO_2/L_{bitumen}$ a^{-1} (Pannekens et al., 2021) ~ 55 mmol $CH_4/L_{crude\ oil}$ a^{-1} (de Rezende et al., 2020)	Partial degradation of bitumen has been attested in both aerobic and anaerobic conditions up to pH 10.5. Many studies measured the degradation rates, which were much lower under anaerobic conditions, noting that a comparison between the rates was not always possible. The rates obtained from recent studies were clearly lower than those from previous studies, probably due to better analytical techniques and longer experiment duration. Due to the different chemical compositions of the bitumen used, rates range over several orders of magnitude, and it is very difficult to define a fixed rate, especially for the period under consideration of 100,000 years. Interestingly, CH_4 production was increased from bitumen when SO_4^{2-} and bicarbonate were added as electron acceptors, but not when NO_3^- was supplemented. However, the experiments were always performed under optimal conditions (in terms of water availability, micronutrients, pH and surface access). Despite optimal conditions, there is no evidence of the complete biodegradation of bitumen. Bitumen is therefore assumed to partly degrade in the near-field of an L/ILW repository.

Tab. 4-13: Cont.

Material	**Biodegradation**		**Rates (under anaerobic and favourable conditions)**	**Expert assessment**
	Aerobic	**Anaerobic**		
Plastics: PP	Unclear	n.r.d.	n.d.	Biotic degradation does not readily occur in plastics composed of conventional synthetic polymers containing only C-C bonds in their backbones. Only one publication describing the aerobic microbial degradation of PP is available. In an anaerobic environment, oxidases and peroxidases (able to break C-C bonds in natural bio-macromolecules) may not work due to the absence of O_2 and H_2O_2. It can be assumed that PP is hardly degradable under anaerobic conditions, except in the presence of SO_4^{2-} or NO_3^- as electron acceptors.
Plastics: polyester; PET	Yes	n.r.d.	n.d.	Aerobic microbial degradation of PET is feasible as it involves mostly esterases which could work without the presence of O_2 (except for cutinase). The organisms discovered so far able to degrade PET are all aerobes, and degradation has not yet been observed in natural environments or under anaerobic conditions. Similarly, as is the case for PVC and other thermoplastics, the degradation by exo-enzymes is also probably hindered by the hydrophobic surfaces of the polymer.
Cellulose	Yes	Yes	Complete degradation of 4 g/L within 5 days under optimum conditions (i.e., pH 7.2 and T = 37 °C). Under alkaline conditions, the chemical degradation of cellulose to ISA is faster than the microbial one (Humphreys et al., 2010).	The biodegradation of cellulose can take place under anaerobic conditions and has been well studied. It produces organic metabolites such as acids and alcohols by the enzymatic hydrolysis of cellulose to glucose which is kinetically and thermodynamically favoured. Glucose is one of the most readily metabolised substrates for microorganisms. No study showed the microbial degradation of cellulose in both anaerobic and highly alkaline conditions (pH 12.5), but cellulose is expected to fully degrade in an L/ILW repository within 100,000 years.

Tab. 4-13: Cont.

Material	**Biodegradation**		**Rates (under anaerobic and favourable conditions)**	**Expert assessment**
	Aerobic	**Anaerobic**		
ISA	Yes	Yes	Degradation of 0.5 mM/d under aerobic conditions and equivalent with NO_3^- (Bassil et al., 2015b). Degradation rates of 0.2 to 5.6 mol ISA/a g^{-1} according to (Rout et al. 2014)	ISA, a glucose-derived organic acid is expected to be fully degradable by microbes under both aerobic and anaerobic conditions (with only NO_3^- as electrons acceptors). It seems quite certain that biodegradation can take place up to pH 11. At higher pH values (pH 12.5), the potential pathways for microbial degradation of ISA are not yet fully understood. Hence, it is conceivable that microbial activity may proceed in more favourable niches and degrade ISA into organic acids, locally pulling the pH into the neutral range and propagating niches over larger areas. The production of organic acids might however stop methanogenesis, potentially explaining why CH_4 formation has not been yet experimentally confirmed.
Plexiglas®	Yes	n.r.d.	n.d.	Very few studies on the biotic degradation of PMMA are available in the literature, and none have been performed at conditions relevant for a cement-based L/ILW repository. PMMA is a highly stable polymer and barely degradable under optimal conditions for microbial activities. The aliphatic HC backbone of PMMA is therefore expected to remain stable in the near-field of an L/ILW repository during the period under consideration of 100,000 years. Only the ester groups, prone to cleavage during irradiation can be used as substrate for microbial degradation, such as the potential additives probably used to improve the material properties.
SPs	Yes	n.d.	n.d.	The data available on the biotic degradation of SPs are very limited. LS-based SPs are presumed to not be degraded like the related lignin. SNF-based SPs may be partially biodegraded under neutral and aerobic conditions and with sufficient water availability, if they are leached out of concrete as mono- or oligomers. Such conditions are, however, not expected in the near-field of an L/ILW repository. It is believed that PCE-based SPs are biodegradable, as is the case for polyethylene glycol. However, conclusive proof is still lacking, as data availability is limited and uncertain. Unfortunately, no information on the biotic degradation of PAE-based SPs could be found, not even under aerobic conditions.

5 Gas generation rates

5.1 International approach to research on gas generation by organic degradation

In this section, the way in which WMOs determined and modelled the degradation of organic waste and associated gas generation rates is discussed. Relatively few reports are publicly available. It represents the state of knowledge available in the literature at the time of writing.

Finland

The large-scale Gas Generation Experiment (GGE) conducted in the context of the Finnish research programme for geological waste disposal since 1997 has provided extensive geochemical and microbiological data on gas generation from L/ILW (Small et al. 2006, Small et al. 2008, Small et al. 2017, Vikman et al. 2019). The materials used for these experiments are a representative mixture of L/ILW generated at the Olkiluoto NPPs and include cellulosic materials (paper, cardboard, cotton, gloves), as well as other organic materials degrading more slowly (PVC, plastics, rubber) and metals (mostly stainless steel). The proportion of each substance was deliberately varied within the drums. Each drum contained a built-in sampling tube, allowing the composition of the gas and water phases to be monitored over time. Solid samples consisting of small steel plates made from the waste drums, together with organics, were also used in the experiment in order to characterise the microbial population present (Small et al. 2006, Small et al. 2008, Small et al. 2017, Vikman et al. 2019). The waste drums were emplaced in a concrete box filled with local, untreated river water. A cooling system maintained the water temperatures at 8 °C and 11 °C at the base of the box and drum lid, respectively. The concrete box containing the drums was surrounded by a gas-tight tank. Small & Dutton (2009) asserted that the GGE was not representative of a cement-based repository because of the high-water content, low cement:water ratio and limited pH buffering to alkaline pH (pH 9 – 11). The water present in the drums was neutral to moderately acidic, highlighting that microbial activity preferably grew in the waste matrix at lower pH, reducing the pH further and enabling small-scale niches to be established. The long-term experiment was modelled by the Generalised Repository Model reactive transport code, from which rate constants for the hydrolysis of cellulose in the pH range 5 – 11 were derived (Small et al. 2006, Small et al. 2008, Small et al. 2017). For the configuration of the model, the biodegradable materials were divided into two categories "reactive cellulose" including paper, cardboard, cotton and gloves, and "less reactive cellulose" for materials such as PVC, plastics and rubber.

United Kingdom

Over the last 20 years, the largest programme that combines experiments and model development and examines the degradation of organics and the associated gas generation rates was conducted in the context of the UK's research programme for the disposal of L/ILW.

In the large-scale experiment reported by Macdonald et al. (1997), gas generation rates were monitored from twelve drums containing 80 kg of simulated waste (mainly cellulose with small amounts of plastics and metals), exposed to various pH and moisture contents. Out of the twelve drums, only three drums had an initial pH of 12.5 and only one was backfilled with cement. The drums were buried in a shallow pit for a period of 1,239 days, and gas samples were withdrawn periodically for analysis. In general, lower rates of gas generation were measured in the drums with very high alkalinity. At the end of the experiment, the drums were removed from the pit, opened and their content was analysed. No visible change in the waste had occurred over the experimental period. All final pH values were either neutral or slightly acidic with the exception of the pH in the drum backfilled with cement, which was kept alkaline by a large excess of concrete. There was little moisture left in almost half of the drums. The vertical distribution of moisture content in the drums varied, suggesting that the degradation of organics did not occur at a uniform rate. The conclusion from this large-scale experiment is that the degradation of organics in a neutral or slightly acidic environment leads mainly to the production of carboxylic acid intermediates rather than their consumption to generate CH_4 and CO_2. According to the experimental observations in the drum backfilled with cement, alkaline hydrolysis of the cellulose proceeds relatively rapidly, so that the growth of microbial populations in the highly alkaline environment relevant to an L/ILW repository probably determines the limiting step of cellulose degradation. The data obtained from this large-scale experiment was used to assist in the testing of GAs generation by Microbial degradation and Metal corrosionON (GAMMON), the first model to be developed within the Nirex safety assessment research programme and to provide reliable estimates of the cumulative amounts and time-varying generation rates of gas within a potential repository. The GAMMON model took into account, among other processes, the microbial degradation of the organic components (mainly cellulose) (Metcalfe et al. 2008), by mimicking a complex scheme of microbial reactions with microbial hydrolysis rates and parameters simulating microbial growth and death (Small & Dutton 2009) (Tab. 5-1).

A successor model for gas generation assessments, SMOGG (Simplified Model Of Gas Generation) was developed as a replacement for the GAMMON model (Swift 2016, NDA 2010, NDA 2016) (Tab. 5-1). Concerning microbial degradation of organic waste, SMOGG is simpler and more empirical than GAMMON. Data sets for the parameterisation and validation of SMOGG were provided by both experimental data from the UK LLW repository and the large-scale gas generation experiment from Finland (cf. paragraph above). SMOGG is based on the idea that cellulose is first hydrolysed chemically to produce water-soluble organic molecules (glucose-like monomers under acid and near-neutral conditions or ISA under alkaline conditions), rather than by microbial mediation (NDA 2010, NDA 2016). Kinetic rate constants for mid-chain scission, chemical stopping and hydrolysis of cellulose to monomers are integrated into SMOGG. The hydrolysis of organic substrates is considered as the principal rate-limiting reactive process. The monomers are then considered as substrates for microbial processes (e.g., methanogenesis) to produce CO_2 and CH_4. The mechanisms of gas production from glucose and ISA are considered to be identical.

The GRM (Generalised Repository Model) was the latest reactive transport code developed for gas generation assessments in the UK programme (Tab. 5-1). It includes kinetic processes such as microbial degradation (Small et al. 2008). Results from small-scale experiments were included in the GRM in order to parameterise the biogeochemical reactions (Small & Dutton 2009). These experiments were carried out under acidic and near-neutral conditions with reactive cellulose (Small et al. 2004). When modelling gas production during the degradation of reactive cellulose, Small et al. (2006) used a first-order rate constant of 4.27×10^{-11} s^{-1} (1.35×10^{-3} a^{-1}), assumed to correspond to the hydrolysis of reactive cellulose, which is the first and rate-determining step in degradation. For the slowly degrading, less reactive cellulose (e.g., plastic materials), Small et al. (2006) assumed a rate of 4.27×10^{-12} s^{-1} (1.35×10^{-4} a^{-1}), which is a factor ten lower that for reactive cellulose. These rates, based on experiments and expert assumptions, were used to accurately determine the cellulose hydrolysis rates for the production of glucose monomers under acid and near-neutral conditions (Small & Dutton 2009). As for the previous models, the GRM model could not be validated and parameterised for cellulose degradation under alkaline conditions as the available experimental data did not cover the alkaline conditions expected in the near-field of a cementitious L/ILW repository (Small & Dutton 2009). The GRM code has also been used to model the results of the Finnish large-scale gas generation experiments (cf. section above). By fitting the degradation rate to experimental data from the Finnish large-scale experiment, a rate of 1.5×10^{-11} s^{-1} (4.73×10^{-4} a^{-1}) for reactive cellulose was determined (Small et al. 2006, Small et al. 2008, Small et al. 2017, Vikman et al. 2019).

Tab. 5-1: Modelling approaches for gas generation assessment used in the UK waste programme including the degradation of organics

Models	Data inputs	Processes considered	Output models	Comments
GAMMON	large-scale experiment (MacDonald et al. 1997)	microbial hydrolysis rates; microbial growth and death rates	total gas generation assessments	mainly cellulose taken into account
SMOGG	large-scale experiment (MacDonald et al. 1997); large-scale gas generation experiment (Small et al. 2008)	microbial hydrolysis rates; microbial growth and death rates	total gas generation assessments	successor model of GAMMON (simpler and more empirical)
GRM	large-scale experiment (MacDonald et al. 1997); large-scale gas generation experiment (Small et al. 2008); small-scale experiments (Small &Dutton 2009)	microbial hydrolysis rates; microbial growth and death rates; hydrolysis as first and principal rate-limiting reactive process	total gas generation assessments and rate constants for hydrolysis of reactive and less reactive cellulose at pH 5-11	latest reactive transport code from UK programme

USA

Experimental studies on gas generation from representative transuranic waste containing cellulose material subject to microbial degradation have been conducted under conditions relevant to the Waste Isolation Pilot Plant (WIPP) repository, USA. The WIPP porewater is characteristic for salt deposits (i.e., highly saline brines with neutral pH) (Gillow & Francis 2006). The experiments conducted at WIPP are therefore not representative of the conditions expected in the Swiss L/ILW repository. Additional information can be found in Small et al. (2006).

Hungary

A Hungarian research project examined quantitative estimates of gas generation rates from L/ILW packages (Molnár et al. 2006, Molnár et al. 2010). However, the inventory of the materials present in the drums was not accurately documented, so that no model development based on these results was possible.

5.2 Nagra's approach

5.2.1 Historical background

The following section provides a chronological description of how Nagra dealt with degradation of organics and associated gas generation.

The first measurements of gas released during degradation of organics predominantly present in radioactive waste were done by Molecke (1979), who quantified the CO_2 release from the degradation of transuranic composite organic waste exposed to an anoxic atmosphere, at temperatures ranging from 25 °C to 70 °C, partially/fully saturated conditions and neutral pH. Many experiments were conducted using different types of cellulosic materials whereas for HMW organics, only one experiment on asphalt (mix of aggregate, sand and bitumen) was conducted.

Gas generation rates derived from these experiments were later calculated by Wiborgh et al. (1986) (Tab. 5-2). As no experimental data was available for bitumen and IERs, predominant at that time in the Swiss waste inventory, reference gas generation rates for these organics were determined based on expert judgement (e.g., Brandberg & Wiborgh 1982 for bitumen). In Nagra's first performance assessments on gas generation and transport, the maximum gas generation rates were taken as reference rates (0.7 mol/kg a^{-1} for cellulose and 0.05 mol/kg a^{-1} for bitumen; Tab. 5-2) for the sake of conservatism (Grogan et al. 1992; Nagra 2004).

Tab. 5-2: Gas generation rates produced during the anoxic degradation of organic wastes used as the basis for Nagra's performance assessment on gas generation

Gas generation rates are based on the experimental data of Molecke (1979) and calculated by Wiborgh et al. (1986).

Substance	**Degradation rate moles total gas/kg. year**		
	Minimum	**Average**	**Maximum**
Cellulose			
Organic comp. (35% cellulose)	0.05	(0.1 – 0.4)	0.7
Plywood box (mainly cellulose)	0.02	(0.04 – 0.2)	0.3
LASL comp.	0.01		0.4
Sawdust plywood (mainly cellulose)	0.03		0.2
CM-cellulose	0.0003		0.2
Bitumen			
Asphalt	0	(0.004 – 0.04)	0.05
Asphalt	0.002		0.04
Bitumen		(0.002 – 0.008)	
Bitumen		(0.001)	
Ion exchange resins		(0 – 0.01)	

Wiborgh et al. (1986) assumed that the degradation of organics in an L/ILW repository will most likely take place through a combination of hydrolysis and microbial degradation. Hydrolysis reduces the molecular size of complex polymers before microorganisms can degrade them into even smaller molecules. Due to a combined general lack of knowledge and for the sake of conservatism, methanogenesis was assumed to play a major role, producing equimolar amounts of CH_4 and CO_2 as final products. CO_2 (or its aqueous species HCO_3^- and CO_3^{2-}) and CH_4 being the thermodynamically stable carbon species in anoxic alkaline conditions at complete thermodynamic equilibrium.

The degradation model for cellulosic organics could therefore be represented by the reaction:

Reaction 5-1: $[C_6H_{10}O_5]_x + xH_2O \rightarrow xC_6H_{12}O_6 \rightarrow 3xCH_4 + 3xCO_2$

Which was simplified by Stumm & Morgan (1996) as:

Reaction 5-2: $2\{CH_2O\} \rightarrow CH_4 + CO_2$, where $\{CH_2O\}$ represents an average composition of organic materials.

Wiborgh et al. (1986) however pointed out that the CH_4/CO_2 ratio was never equimolar in degradation experiments previously conducted (Khan 1977, Winter & Cooney 1980), suggesting that the degradation mechanisms were not fully understood and that reactions other than methanogenesis might take place. In the first of Nagra's performance assessments on gas generation and transport in an L/ILW repository, Grogan et al. (1992) indicated that gas formation rates are likely to be at least one order of magnitude smaller than those calculated by Wiborgh et al. (1986). A similar observation was reported by Kannen & Müller (1999), in which gas generation rates of mixed wastes in both brine and cementitious water indicated rates more than one order of magnitude lower. Based on these statements, Hooker (2007) was commissioned to review the decomposition of organics and gas generation rates previously used in Nagra's performance assessments (Grogan et al. 1992, Nagra 2004). Hooker (2007) used several literature sources from a range of relevant performance assessment programmes to compare and evaluate gas generation rates with focus on cellulose as insufficient information on the degradation of HMW organics (i.e., IERs, bitumen) was available. Hooker (2007) confirmed that the CH_4/CO_2 generation rates calculated by Wiborgh et al. (1986) and used in Nagra (2004) appear to be highly conservative. Several reasons were highlighted. First, the gas generation rates measured by Molecke (1979) were based on the CO_2 production during the degradation of transuranic composite organic waste under neutral conditions, which is not relevant for the near-field of a cement-based L/ILW repository. Moreover, the rates proposed by Wiborgh et al. (1986) were based on the assumption that methanogenesis is the main anaerobic reaction responsible for the degradation of organic waste in an L/ILW repository. In reality, several microbial degradation reactions may take place depending on the redox potential of the environment and the presence of electron acceptors (Reactions 5-3-5-6). For example, if NO_3^- and SO_4^{2-} are present in the repository system, other degradation reactions, i.e., denitrification and SO_4^{2-} reduction, would occur in place of methanogenesis, reducing the amount of CH_4 and CO_2 produced (Hooker 2007, Vugrin et al. 2015, Wang & Brush 1996).

Reaction 5-3: $C_6H_{12}O_6 + 4.8\ NO_3^- \rightarrow 6\ CO_3^{2-} + 2.4\ N_2 + 2.4\ H_2O + 7.2\ H^+$
(using the glucose molecule as a substrate)

Reaction 5-4: $C_6H_{12}O_6 + 12\ MnO_2 \rightarrow 6\ MnCO_3 + 6\ Mn(OH)_2$
(using the glucose molecule as a substrate)

Reaction 5-5: $C_6H_{12}O_6 + 24\ FeO(OH) \rightarrow 6\ FeCO_3 + 18\ Fe(OH)_2 + 24\ H_2O$
(using the glucose molecule as a substrate)

Reaction 5-6: $C_6H_{12}O_6 + 3\ SO_4^{2-} \rightarrow 6\ CO_3^{2-} + 3\ HS^- + 6\ H^+$
(using the glucose molecule as a substrate)

Another aspect, not considered by Wiborgh et al. (1986) which explains the overly conservative gas generation rates used in Grogan et al. (1992) and Nagra (2004), concerns the biotic degradation rate. Some references cited by Hooker (2007) suggest a decrease in the rate of microbial degradation with time, leading to a decrease in the long-term CO_2 generation rate by several orders of magnitude. Such a process is common and generally attributed to the sequential use of different electron acceptors, different substrates and the build-up of microbial metabolites (Monod 1949). The last point not considered by Wiborgh et al. (1986) which could also be responsible for a reduction of the gas generation rates is the chemical structure of the organic polymers. For instance, cellulose consists of a reactive amorphous and a recalcitrant crystalline part, both of which degrade at distinct rates (Hooker 2007 and references therein).

On the basis of the review by Hooker (2007), the reference gas generation rates used in Nagra's first gas generation assessments (Grogan et al. 1992, Nagra 2004) were re-defined and used in the gas generation assessments for Stage 2 of the Sectoral Plan for Deep Geological Repositories (SGT) (Diomidis et al. 2016, Leupin et al. 2016b, Poller et al. 2016, Papafotiou & Senger 2016)

(Tab. 5-3). The upper bounds, based on the maximum gas generation rates measured and calculated by Molecke (1979) and Wiborgh et al. (1986), respectively, were considered as worst-case scenarios (Johnson & Schwyn 2007). For the reference case, the rates of cellulose and bitumen degradation were lowered by a factor of 10, i.e., at 0.07 mol gas/kg a^{-1} and 0.005 mol gas/kg a^{-1}, respectively. A reduction by a factor of 10 was chosen, as Molecke (1979) observed gas generation rates about one order of magnitude lower under partially saturated conditions versus fully saturated conditions and it was assumed that such conditions would prevail for a long time in the deep geological repository. The newly proposed reference rates were still described as "clearly pessimistic" by Johnson & Schwyn (2007). However, they could not be further lowered due to the large remaining uncertainties concerning the various processes of organic waste degradation.

Two categories of organic materials were also implemented in SGT Stage 2 based on their chemical structure and associated degradation rates (Cloet et al. 2014). O1 organics represent easily degradable organic compounds such as non-polymeric and short-chained molecules with a gas generation rate of 0.07 mol gas/kg a^{-1} (i.e., cellulose, ISA). In contrast, O2 organics are less degradable substances such as long HC-chained and aromatic polymers with a gas generation rate of 0.005 mol gas/kg a^{-1} (i.e., IERs, PS, PVC, bitumen, plastics and Plexiglas®) (Tab. 5-3). This classification represents a simplification of the complexity of the degradation processes that organic waste undergoes in an L/ILW repository. In the more recent Swiss L/ILW waste inventory, O2 corresponded to ~ 93% of the total mass of organics present (Nagra 2023b).

Tab. 5-3: Amounts and gas generation rates for O1 and O2 organics

Unit: mol gas/kg a^{-1}

Class	**Amount** [% of total mass]	**Reference**	**Lower bound**	**Upper bound**
O1	9	0.07	0	0.7
O2	91	0.005	0	0.05

During SGT Stage 2, estimates of the total amounts of NO_3^-, Fe(III), SO_4^{2-} and Mn(IV) in waste materials and cement paste showed that they were lower than the ones required for the microbially mediated oxidation of the organic materials (Kosakowski et al. 2014). Hence, only a small portion of the organic matter is expected to decompose by microbial degradation using NO_3^-, Fe(III), SO_4^{2-} and Mn(IV) as terminal electron acceptors. Consequently, the decomposition of organic matter is expected to occur (if all conditions are met) predominately via methanogenesis in the long term, as initially proposed by Wiborgh et al. (1986) (Reactions 5-7; 5-8).

Reaction 5-7: $C_6H_{12}O_6 + 3\ H_2O \rightarrow 3\ HCO_3^- + 3\ CH_4 + 3\ H^+$ $(6 < pH < 10)$
(using the glucose molecule as a substrate)

Reaction 5-8: $C_6H_{12}O_6 + 3\ H_2O \rightarrow 3\ CO_3^{2-} + 3\ CH_4 + 6\ H^+$ $(pH > 10)$
(using the glucose molecule as a substrate)

As methanogenesis needs water, such as for hydrolysis (cf. Section 3.2), the amount of water available in the different waste forms is considered as the crucial parameter for estimating the kinetics of organic matter degradation and the rate of gas production (Wieland et al. 2018, Wieland & Kosakowski 2020). It should be noted that under high pH conditions, if biotic degradation processes such as NO_3^--, SO_4^{2-}-reductions and methanogenesis occurred, these would locally reduce the pH by the release of H^+, promoting the spreading of microbiological niches (Reactions 5-3; 5-6; 5-8).

To estimate the amount of gas produced during the degradation of organics, the disproportionation of organic matter into CO_2 and CH_4 was assumed to depend on the carbon content and the average oxidation state of carbon in the organics, while no dependence on pH was considered (Cloet et al. 2014). The same stoichiometric approach for disproportionation was subsequently used to develop a simplified kinetic model of the degradation of O1 and O2 organics, based on their gas generation rates (Tab. 5-3) (Wieland et al. 2018). In this way, the gas generation rates could be converted into degradation rates of the organics. More pertinently, the simplified kinetic model of the degradation of organics allowed CO_2 and CH_4 to be fed as source terms into thermodynamic modelling codes, such as the GEM-Selektor (GEMS) code for chemical equilibrium calculations.

Fig. 5-1 illustrates the degradation of a representative endmember of the readily degradable organic material, cellulose, and an endmember representing only the slowly degrading one, the PS, as a function of time (Wieland et al. 2018). The rate constant, derived from the gas generation rates, is equal to 1.89×10^{-3} a^{-1} in the case of the decomposition of cellulose, while the one for PS decomposition corresponds to 6.51×10^{-5} a^{-1}. The first-order kinetic model predicts that cellulose will be almost completely degraded (1% residual inventory) within ~ 2.5 ka, while the degradation of PS is much slower, i.e., a 1% residual is reached after ~ 70 ka (Fig. 5-1) (Wieland et al. 2018). It should be noted that the currently available degradation rates of cellulose derived from experimental data predict that cellulose will be degraded within a few hundred years (Pavasars et al. 2003) to several tens of thousands of years (van Loon & Glaus 1998, van Loon et al. 1999). The model thus accounts for cellulose degradation in a pessimistic (conservative) way, as the modelled lifetime is closer to that predicted by Pavasars et al. (2003).

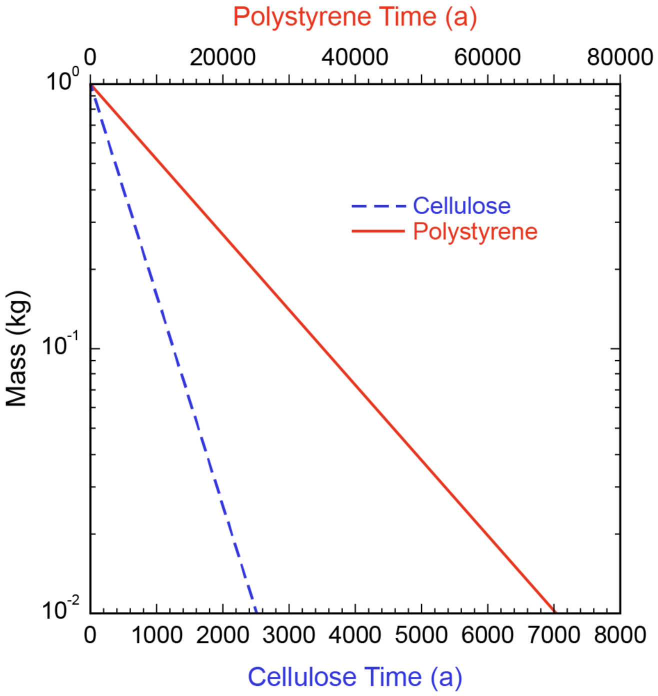

Fig. 5-1: Kinetics of the degradation of cellulose and PS

Bottom: time scale for cellulose; top: time scale for PS

From Wieland et al. (2018)

The kinetic model involves simplifications for some organic compounds as it considers the stoichiometry of the carbon source term (including H_2 and O_2), while other heteroatoms (e.g., N, S, P) are not considered. For example, the splitting off of sulphonated and tertiary amine groups during the degradation of IERs is currently not taken into account, meaning that the degradation of IERs is comparable to PS. Even though both thermodynamic and kinetic approaches have recently been published (Bagaria et al. 2021), further improvement of the models is needed for all organic materials with specific C, N, S stoichiometries (e.g., IERs, bitumen, SPs).

5.2.2 Approach selected for the general license application

After the large literature review summarised in Chapters 3 and 4, whether gas generation rates and associated modelled lifetime can be qualitatively assessed with regard to the expected near-field evolution of a cementitious L/ILW repository over the period of consideration of 100,000 years:

i) Early L/ILW repository post-closure phase (i.e., up to 1,000 years after closure)

During the post-closure phase, degradation of the organic materials is mainly radiolytic due to the presence of remaining O_2 and radiolysis of the remaining water within the waste matrix. Radiolytic degradation of organics by scission may be favoured, producing mainly oxidised gaseous species (CO, CO_2) and water-soluble organic compounds. It should be noted, however, that the influence of radiolytic degradation might be strongly limited by O_2 supply (through diffusion) at the initially high dose rate. This indicates that radiolytic degradation of polymers probably occurs both via crosslinking and scission mechanisms that generate radiolytic gases (H_2, CO, CO_2, CH_4). Within several hundreds of years after repository closure, anoxic conditions are expected to prevail, favouring the process of crosslinking. The consequence of radiolytic degradation by scission is the production of LMW molecules available as substrates for microbial activities, while crosslinking improves the stability of the polymers against chemical (alkaline hydrolysis) and microbial degradation. Only organic compounds such as cellulose, polyester, and PC can slowly degrade by alkaline hydrolysis. Microbial degradation is expected to be limited due to the highly alkaline conditions present in the cemented waste forms ($pH \sim 12.5$) and the surrounding cementitious backfill, the low water and substrate availability expected in the waste matrices and the initial strong radiation field. The radiation tolerance of microbes may be overcome, although it can be re-established by adaptation. In waste packages solidified by bitumen or styrene (i.e., IERs), near-neutral to slightly alkaline conditions (due to the equilibration with cement porewater) could prevail, which are more favourable towards microbial activity. On the L/ILW repository scale, it can be assumed that microbial activity is strongly limited during this stage.

ii) In the long-term (i.e., after 1,000 years after closure and over the period under consideration of 100,000 years)

With time, the dose rates to which the organic waste are exposed will strongly decrease due to the short half-life of ^{60}Co and ^{137}Cs, the main γ-/β-emitters to which more than 99% of the total organic materials are exposed. After the period under consideration of 100,000 years, the total absorbed dose is expected to reach an average of 1 MGy. Only < 1% of the total organic waste will be exposed to internal irradiation by α-radiation, due to their presence in ATW. This small portion of organics will, however, be exposed to much stronger doses, reaching an average of 100 MGy after 100,000 years. In the absence of O_2, the chemical stability of the carbon backbones of PVC, IERs, bitumen, PE and PP may have improved over time due to the radiolytic, crosslinking mechanism (three-dimensional network of polymer chains). Hence, a non-negligeable proportion of the organic waste is probably not susceptible to subsequent degradation processes. Concerning the hydrolysis, it only impacts the chemical stability of cellulose, polyester, and PC. Generally, microbial activity may be enhanced over time due to: (i) the presence of LMW molecules as degradation products that can be used as substrates; (ii) the weakened radiation field; (iii) the slow resaturation of the caverns from the bottom and (iv) the presence of niches with lower pH due to the ongoing internal degradation and carbonation of the solidifying cementitious matrix. Microbially-mediated degradation of organic compounds via methanogenesis especially contribute to both to gas production (i.e., CH_4) and carbonation of the cementitious materials (due to CO_2 production). It should be noted, however, that all the degradation processes (i.e., abiotic and biotic) are strongly limited by water availability, which is also consumed by the anoxic corrosion of metals and the ongoing pozzolanic reactions within the cement matrix (Kosakowski et al. 2023). Once the initial water content of the waste forms has been consumed, ingress of porewater from the backfill is needed to pursue degradation processes.

Based on this phenomenological evolution, gas generation and associated degradation rates for IERs, PS, bitumen and Plexiglas® used in SGT Stage 2 are expected to be significantly lower and considered as highly conservative (Tab. 5-4). Complete degradation within the period under consideration of 100,000 years is unlikely to occur in view of recent process understanding and expert judgement. Concerning PVC, PE, PP, cellulose and SPs (except SMF), gas generation rates determined for SGT Stage 2 are considered to be conservative (Tab. 5-4). In the case of LMW organics and SMF-based SPs, the rates are considered to be realistic (Tab. 5-4). For polyesters and PC, the literature review regarding the chemical degradation of organics suggests that, on the contrary to the other polymers included in the plastic category, they are susceptible to hydrolysis and may be easily degraded under the highly alkaline conditions of the L/ILW repository near-field (cf. Section 3.2.5). For this reason, the respective gas generation and associated degradation rates are assumed to be too low (Tab. 5-4). For conservativity, these rates require revision.

Tab. 5-4: Summary of the degradation processes of organic L/ILW, associated gas generation and degradation rates used in SGT Stage 2 and expert judgement considering recent process understanding

Waste	**Type of organics**	**Radiolytic degradation**	**Chemical degradation**	**Microbial degradation**	**Gas generation rate (SGT Stage 2)**	**Degradation rate (SGT Stage 2)**	**Modelled lifetime (SGT Stage 2*)**	**Expert judgement****	
		Mechanism	**Hydrolysis**	**(confirmed in optimal anaerobic conditions)**	**(mol gas/kg a^{-1})**	**(a^{-1})**	**(ka)**	**Opinion regarding SGT Stage 2 rates**	**Complete degradation in 100,000 years**
IERs***, PS***	O2	CL	no	very unlikely	0.005	6.51×10^{-5}	~ 70	highly conservative	very unlikely
PVC***	O2	CL	no	very unlikely	0.005	3.91×10^{-5}	> 100	conservative	very unlikely
Bitumen	O2	CL	no	likely	0.005	6.93×10^{-5}	~ 70	highly conservative	very unlikely
PE, PP***	O2	CL	no	unlikely	0.005	3.51×10^{-5}	> 100	conservative	unlikely
Polyester, PC	O2	CL	yes	n.d.	0.005	3.51×10^{-5}	> 100	unrealistic (too low)	very likely
Cellulose	O1	SC	yes	very likely	0.07	1.89×10^{-3}	< 5	conservative	very likely
LMW organics***	O1	F	no, except esters	very likely	0.07	2.10×10^{-3}	< 5	realistic	very likely
Plexiglas®***	O2	SC	no	very unlikely	0.005	1.00×10^{-4}	~ 50	highly conservative	unlikely
SPs (SMF)	O1	SC	yes	likely	0.07	n.d.	n.d.	/	likely
SPs (SNF/PCE/PAE)	O2	CL	no	unlikely	0.005	n.d.	n.d.	/	unlikely

* Lifetime was estimated based on first order-kinetics, assuming 1% residual inventory (Fig. 5-1) (Wieland et al. 2018).

** Expert judgement: Is the gas generation rate adequate (realistic), too optimistic (not conservative), too pessimistic (conservative) or overly pessimistic (highly conservative)? In the case of an L/ILW repository, can complete degradation occur over the period under consideration (i.e., 100,000 years)?

*** Pure PVC, PE and PP: additives (plasticisers, stabilisers, etc.) are grouped with small LMW organics. The degradation of IERs does not include the cleavage of sulphonated and amine functional groups of cationic and anionic IERs, respectively, but only the degradation of the PS backbone. The surface functional groups of IERs are included in the group LMW organics.

n.d.	not determined
CL	Crosslinking
SC	Scission
F	Fragmentation

Definition of the degradation and gas generation rates for the RBG

The experimental studies available in the literature, reporting gas generation rates of the organic materials predominantly present in the Swiss L/ILW inventory, are summarised in Tab. 5-5. In the experiments of Molecke (1979), the gas generation rates reported for cellulose ranged over several orders of magnitude, from 0.7 to 0.0003 mol gas/kg a^{-1}. The two experiments conducted with asphalt led to rates between 0 (no CO_2 measured) and 0.05 mol gas/kg a^{-1}. In their small-scale laboratory experiments, Small et al. (2004) measured the gas generation from the degradation of cellulose under near-neutral conditions. By modelling the gas generation rates, Small et al. (2006) defined a first-order degradation rate for cellulose of 4.27×10^{-11} s^{-1} (1.35×10^{-3} a^{-1}), which corresponds to a gas generation rate of 0.05 mol gas/kg a^{-1} according to the model proposed by Wieland et al. (2018). From the Finnish large-scale gas generation experiment reported by Small et al. (2017), where near-neutral conditions prevail in the waste matrix, a degradation rate for cellulose of 1.5×10^{-11} s^{-1} (4.73×10^{-4} a^{-1}) was determined. This value corresponds to a gas generation rate of 0.02 mol gas/kg a^{-1} according to the model calculations of Wieland et al. (2018). In the study of Pannekens et al. (2021), anaerobic degradation of bitumen was studied in near-neutral conditions in the presence of brackish water. Averaged mineralisation rates ranged between 9.4 and 38.6 mmol $CO_2/L_{bitumen}$ a^{-1}, corresponding to gas generation rates which ranged between 0.04 and 0.009 mol gas/kg a^{-1}. In the Gas Monitoring Experiment (GME) launched by Nagra in 2015 and still currently running, the gas generation rates (i.e., CH_4, no CO_2 has been detected) from IERs and PVC in near-neutral OPA porewater were found to be extremely low, i.e., in the range of 10^{-7} mol gas/kg a^{-1}. More detailed information on the experimental set-up and the results can be found in Appendix B.

In the light of the newest experimental data available in the literature, the simplified classification into easily degradable (O1) and slowly degradable (O2) organics has to be retained when assessing the gas generation rates for the RBG as individual rates could not be attested for each of the organics inventoried in MIRAM-RBG. The only difference in the O1/O2 classification concerns polyester and PC, which are prone to hydrolysis in contrast to the other plastics and O2 organics in general. It was therefore decided to assign them to the easily degradable O1 organics (Tab. 5-5).

When assessing the degradation of organics for SGT Stage 2, Warthmann et al. (2013) questioned whether polymers (especially O2) can be degraded at all over the period under consideration of 100,000 years. Therefore, the lower bounds of the degradation rates of the O1 and O2 organics were set to zero for SGT Stage 2 (Diomidis et al. 2016). The current review suggests that degradation can occur for all considered organics in the near-field of a cementitious L/ILW repository over the period under consideration of 100,000 years. For this reason, the lower bounds of gas generation rates assigned to the two group of organics, previously set to 0, were revised. It was assumed that the lower bound is equal to the smallest value measured for the group considered. In the case of the O2 organics, the lower bound corresponds to the rounded value determined in the GME (i.e., 1×10^{-6} mol gas/kg a^{-1}). In the case of the O1 organics, the lower bound was set at 0.0003 mol gas/kg a^{-1} and has been calculated by Wiborgh et al. (1986) from the experiments of Molecke (1979) for cellulosic materials (Tab. 5-5).

The upper bounds were set to the highest value measured for the group of organics considered, equal to 0.05 mol gas/kg a^{-1} for O2 (asphalt) and 0.7 mol gas/kg a^{-1} for O1 (cellulose), both based on the degradation experiments of Molecke (1979) (Tab. 5-5).

The reference rate for the gas production from cellulose degradation can be revised due to the newly available data from the Finnish Gas Generation Experiment reported by Small et al. (2017). The excellent quality of the experimental data and modelling allowed us to revise the reference rate of gas production from cellulose to 0.02 mol gas/kg a^{-1} (Tab. 5-5). This value was further assigned to gas production by polyester and PC, while the higher rate for gas production by the degradation of LMW organics was retained (0.07 mol gas/kg a^{-1}) in order to account for the expected difference in the reactivity of monomeric and polymeric organic materials under near-field conditions. Hence, the O1 group could be divided into two subclasses: O1a for cellulose, polyester and PC, and O1b for LMW organics.

Tab. 5-5: Recommended gas generation rates from the degradation of organics assigned based on experimental evidence

	Gas generation rates based on experimental data					Nagra's gas generation rates for the RBG			Type of organics
Waste	**Molecke (1979)**	**Small et al. (2004; 2006)**	**Small et al. (2017)**	**Pannekens et al. (2021)**	**GME (Nagra)**	**Upper bound**	**Reference**	**Lower bound**	**RBG**
	(mol gas/kg a^{-1})					**(mol gas/kg a^{-1})**			
IERs, PS					$4.38 – 6.57 \times 10^{-7}$	0.05	0.005	1×10^{-6}	O2
PVC					3.58×10^{-7}	0.05	0.005	1×10^{-6}	O2
Bitumen	0 – 0.05			0.04 – 0.009		0.05	0.005	1×10^{-6}	O2
PE, PP						0.05	0.005	1×10^{-6}	O2
Plexiglas®						0.05	0.005	1×10^{-6}	O2
SPs (SNF/PCE/PAE)						0.05	0.005	1×10^{-6}	O2
Polyester, PC						0.7	0.02	0.0003	O1a
Cellulose	0.7 – 0.0003	0.05	0.02			0.7	0.02	0.0003	O1a
LMW organics						0.7	0.07	0.0003	O1b
SPs (SMF)						0.7	0.02	0.0003	O1a

In the literature, appraisals of gas generation rates from the degradation of organics are sometimes available and summarised in Tab. 5-6. They include the report of Brandberg & Wiborgh (1982) who made an assessment on the gas generation rate of bitumen. Additionally, the studies of Small et al. (2006) and Small et al. (2017) employing small-scale laboratory and large-scale gas generation experiments, assumed lower degradation rates for less reactive organics (i.e., plastic materials and rubber) by a factor of 10 in comparison to the rate for cellulose (Tab. 5-5). The rates suggested by expects actually cover the ranges defined for O2 and O1 organics (i.e., between upper and lower bounds) (Tab. 5-6).

Tab. 5-6: Comparison of gas generation rates defined for the RBG with expert appraisals

Waste	Gas reference rates estimated by experts			Nagra's gas generation rates for the RBG		
	Brandberg and Wiborgh (1982)	Small et al. (2004; 2006)	Small et al. (2017)	Upper bound	Reference	Lower bound
	(mol gas/kg a^{-1})			(mol gas/kg a^{-1})		
IERs, PS				0.05	0.005	1×10^{-6}
PVC		0.02	0.006	0.05	0.005	1×10^{-6}
Bitumen	0.008 – 0.002			0.05	0.005	1×10^{-6}
PE, PP		0.02	0.007	0.05	0.005	1×10^{-6}
SPs (SNF/PCE/PAE)				0.05	0.005	1×10^{-6}
Plexiglas®				0.05	0.005	1×10^{-6}
Polyester, PC				0.7	0.02	0.0003
Cellulose				0.7	0.02	0.0003
LMW organics				0.7	0.07	0.0003
SPs (SMF)				0.7	0.02	0.0003

The decrease of the gas reference rate for cellulose also corresponds to a decrease of the degradation rates and an increase of associated lifetimes, i.e., from < 5 ka to ~ 10 ka (Tab. 5-7). In contrast, the lifetime of polyester and PC (grouped with O2 organics in SGT Stage 2) is reduced by a factor of 10, i.e., from > 100,000 years to ~ 10,000 years (Tab. 5-7). As a consequence, these new rates could be defined as conservative and no longer as unrealistic (Tab. 5-4; Tab. 5-7).

Tab. 5-7: New degradation rates and associated modelled lifetimes of organic L/ILW for the RBG

Waste	Gas generation rates for SGT Stage 2		Gas generation rates for RBG		Expert judgement*
	Degradation rate (a^{-1})	Modelled lifetime (ka)	Degradation rate (a^{-1})	Modelled lifetime (ka)	Opinion about RBG rates
IERs, PS	6.51×10^{-5}	~ 70	6.51×10^{-5}	~ 70	highly conservative
PVC	3.91×10^{-5}	> 100	3.91×10^{-5}	> 100	conservative
Bitumen	6.93×10^{-5}	~ 70	6.93×10^{-5}	~ 70	highly conservative
PE, PP	3.51×10^{-5}	> 100	3.51×10^{-5}	> 100	conservative
SPs (PCE/ SNF/PAE)	n.d.	n.d	1.00×10^{-4}	~ 50**	realistic
Plexiglas®	1.00×10^{-4}	~ 50	1.00×10^{-4}	~ 50	highly conservative
Polyester, PC	3.51×10^{-5}	> 100	4.73×10^{-4}	~ 10***	realistic
Cellulose	1.89×10^{-3}	< 5	4.73×10^{-4}	~ 10	realistic
LMW organics	2.10×10^{-3}	< 5	2.10×10^{-3}	< 5	realistic
SPs (SMF)	n.d.	n.d.	4.73×10^{-4}	~ 10***	realistic

* Expert judgement: Is the gas generation rate adequate (realistic), too optimistic (not conservative), too pessimistic (conservative) or overly pessimistic (highly conservative)?

** Based on the degradation rates of Plexiglas®, as PCE-based SPs (the most abundant ones in the Swiss L/ILW inventory) are expected to have a similar reactivity to PMMA under the highly alkaline conditions of an L/ILW repository.

*** Based on the degradation rates of cellulose, as polyesters, PC and SMF-based SPs are expected to have a similar reactivity under the highly alkaline conditions of an L/ILW repository.

n.d. Non determined

6 Conclusion

A comprehensive literature review on the abiotic and biotic degradation of the main organics present in the Swiss L/ILW under conditions relevant to a cementitious deep geological L/ILW repository was conducted in order to improve process understanding and to define reference gas generation rates to be used in performance and safety assessments.

During interim storage and the first thousand of years after closure phase of the repository, degradation of the organic materials is expected to be mainly radiolytic due to the initial dose rate in the waste matrix, which also contains residual O_2 and water. The resistance of the different types of polymers to radiation is largely determined by their chemical structure. In general, polymers with aromatic groups in their molecular structure have a significantly higher radiation resistance than aliphatic polymers, regardless of the position of the aromatic groups in the chain. In the case of the less degradable O2 organics (which are also the main abundant ones), the consequence of radiolytic degradation is expected to be mainly crosslinking. This further improves their chemical stability by forming a three-dimensional network of polymer chains. In the case of the easily degradable O1 organics, scission or fragmentation of the polymers into LMW compounds is likely more important. Hydrolysis is one of the degradation processes in operation since interim storage, especially in the waste packages backfilled with cementitious materials, where highly alkaline conditions prevail. However, only few organic compounds such as cellulose, polyester, and PC are susceptible to degradation by alkaline hydrolysis, and these are not the most abundant in the inventory. Concerning the thermal degradation of the organic wastes in the context of the Swiss deep geological repository, it should be noted that the temperature at 900 m below ground level is expected to be < 50 °C after closure (Papafotiou and Senger 2016). Therefore, "pure" thermal degradation processes like pyrolysis that occur at strongly enhanced temperatures (above ~ 200 °C, depending on the polymer) are almost of no importance. In the temperature range expected for the L/ILW repository section (i.e., between 25 and 60 °C), the radiolytic and alkaline degradation rates are expected to increase by less than a factor of ~ 2. The biotic degradation of organics by microbial activities might be initially limited after L/ILW repository closure due to: (i) the highly alkaline conditions present in the cemented waste forms and surrounding cementitious backfill (pH ~ 12.5); (ii) the low water availability (only in the waste matrix); (iii) the limited nutrient accessibility; and (iv) the strong radiation field. Because of spatial and temporal heterogeneities in the L/ILW repository in term of pH, water and substrat availability, the importance of microbial activity cannot be precisely assessed for the period under consideration of 100,000 years. In general, it can be assumed that as more extreme conditions come together, the likelihood of microbial activity decreases. However, it should be noted that methanogenesis is possible from a thermodynamic point of view up to pH 12.5, and low water availability per se does not completely inhibit microbial life. There may still be small-scaled niches where relatively good living conditions for microbial activity exist, especially at the bottom of the caverns that resaturate more quickly, or in waste packages solidified by bitumen or styrene, where near-neutral to slightly alkaline conditions prevail. Due to limited water availability and pore space, a slow spread of microbes from these niches is to be expected.

Once conditions are anoxic (i.e., after several hundreds of years), radiolytic degradation is expected to have only a limited impact on organics due to the absence of O_2. Moreover, the dose rate in the L/ILW matrices will strongly decrease over time as the external radiation field by γ-/β-emission is strongly weakened due to the short half-life of ^{60}Co and ^{137}Cs, the two main γ-/β-emitters inventoried. The total absorbed dose after 100,000 years is expected to reach less than 1 MGy. In the ATW, the total absorbed dose will be much higher (around 100 MGy in average) but the inventory of organics exposed to such doses is extremely small (< 1 %) and

α-radiation has a low penetration and can thus only affect organics that are in direct contact with α-emitters. The chemical stability of the carbon backbone of the main O2 organics may have improved over time due to a predominance of the radiolytic crosslinking mechanism. Therefore, a relatively negligeable proportion of the organic waste is expected to be susceptible to further degradation. For cellulose, polyester and PC, alkaline hydrolysis is, however, continuously in action. Over time, microbial activity may increase and contribute both to gas production (i.e., CH_4, CO_2) and carbonation of the cementitious materials due to: (i) the presence of LMW molecules that could be used as substrates and are produced by hydrolysis and through radiolytic scission and fragmentation processes; (ii) the weakened radiation field; (iii) the slow resaturation of the caverns from the bottom increasing water availability; and (iv) the increase in the number of small-scale environments with lower pH due to ongoing internal degradation and carbonation of the solidifying cementitious matrix. In general, it should be noted that water availability is considered to be the most important limiting factor for all abiotic and biotic degradation processes described above as well as for the anoxic corrosion of metals and pozzolanic reaction within the cement matrix.

This literature review provides a comprehensive review of the current state-of-the-art process understanding of the degradation of organic materials predominantly present in L/ILW. It also inventories all published degradation/gas generation rates from the abiotic and biotic degradation of organics, based on the latest experimental data available. The simplified classification into slowly degradable O2 and easily degradable O1 organics has been retained for the RBG, as no individual rates could be attested for each of the organics inventoried in L/ILW. The only changes made in this classification concerns the two types of plastics polyesters and PC. They are now assigned to the O1 group of organics, as they are susceptible to hydrolysis (in contrast to other organics of the O2 group) and their associated gas generation rates could be now considered as realistic. For all organic materials, new lower bounds were set as it was assumed that degradation of organic materials might be possible in the near-field of an L/ILW repository during the period under consideration of 100,000 years. The reference rate of gas production associated with cellulose degradation was re-assessed based on new experimental data reported in the literature. Based on a simple kinetic model, the gas formation rates can be related to the degradation rates of organics. This tentatively allows an estimate of the lifetime of the organics in the L/ILW repository. It is expected that only a minor amount of organics, such as LMW organics, polyester, PC and cellulose, will be completely degraded at the early stage of the repository closure (i.e., in the first ten of thousand years). For the remaining organics, complete degradation is expected to occur after 50,000 years. The main abundant ones such as IERs, PVC and bitumen actually have lifetimes estimated to be close to or even beyond the period under consideration of 100,000 years.

7 References

Abbas-Abadi, M.S. (2021): The effect of process and structural parameters on the stability, thermo-mechanical and thermal degradation of polymers with hydrocarbon skeleton containing PE, PP, PS, PVC, NR, PBR and SBR. Journal of thermal analysis and calorimetry 143/4, 2867-2882. DOI: 10.1007/s10973-020-09344-0.

Abrahamsen, L., Arnold, T., Brinkmann, H., Leys, N., Merroun, M., Mijnendonckx, K., Moll, H., Polvika, P., Sevcu, A., Small, J.S., Vikman, M. & Wouters, K. (2015): A review of anthropegenic organic wastes and their degradation behaviour. MIND D1.1. European Comission, Microbiology in Nuclear Waste Disposal.

Acierno, D., La Mantia, F.P., Titomanlio, G., Calderaro, E. & Castiglia, F. (1980): γ-radiation effects on a polycarbonate. Radiation Physics and Chemistry 16/2, 95-99. DOI: 10.1016/0146-5724(80)90213-7.

Ahmed, M.T., Clay, P.G. & Hall, G.R. (1966): Radiation-induced decomposition of ion-exchange resins. Part II. The mechanism of the deamination of anion-exchange resins. Journal of the Chemical Society, 1155-1157. DOI: 10.1039/J29660001155.

Albertsson, A.-C., Bødtker, G., Boldizar, A., Filatova, T., Jiménez, M., Loss, K., Poortinga, W., Sander, M., Seppälä, J., Thompson, R. & Weber, M. (2020): Biodegradability of Plastics in the Open Environment.

Alexander, P. & Charlesby, A. (1954): Energy transfer in macromolecules exposed to ionizing radiations. Nature 173/4404, 578-579. DOI: 10.1038/173578a0.

Ali, M.I., Ahmed, S., Robson, G., Javed, I., Ali, N., Atiq, N. & Hameed, A. (2014): Isolation and molecular characterization of polyvinyl chloride (PVC) plastic degrading fungal isolates: Fungal degradation of PVC plastics. Journal of Basic Microbiology 54/1, 18-27. DOI: 10.1002/jobm.201200496.

Aliev, R., Navarro-González, R. & Medina, R. (2006): A comparative radiation degradation of some aromatic polyesters. Polymer Bulletin 57/4, 499-504. DOI: 10.1007/s00289-006-0571-x.

Allard, S. & Ekberg, C. (2006): Complexing properties of α-isosaccharinate: thorium. Radiochimica Acta 94/9-11, 537-540. DOI: 10.1524/ract.2006.94.9-11.537.

Allayarov, S.R., Confer, M.P., Bogdanova, S.A., Rudneva, T.N., Allayarova, U.Y., Shaimukhametova, I.F., Demidov, S.V., Mishchenko, D.V., Klimanova, E.N., Sashenkova, T.E., Chekalina, S.D., Aldoshin, S.M. & Dixon, D.A. (2022): Characteristics and radiolysis behavior of polyvinylchloride under accelerated proton and γ-irradiation. Radiation Physics and Chemistry 201. DOI: 10.1016/j.radphyschem.2022.110436.

Allen, G. & Bevington, J.C. (ed.) (1989): Comprehensive polymer science: the synthesis, characterization, reactions & applications of polymers. 6th ed. Pergamon Press, Oxford, UK.

Altmaier, M., Blin, V., Garcia, D., Henocq, P., Missana, T., Ricard, D. & Vanderborre, J. (2021): SOTA on cement-organic-radionuclide interactions. Final version as of 19.05.2021 of deliverable D3.1 of the HORIZON 2020 project EURAD. (D3.1). EURAD CORI.

Andersson, M., Ervanne, H., Glaus, M.A., Holgersson, S., Karttunen, P., Laine, H., Lothenbach, B., Puigdomenech, I., Schwyn, B., Snellmann, M., Ueda, H., Vuorio, M., Wieland, E. & Yamamoto, T. (2008): Development of methodology for evaluation of long-term safety aspects of organic cement paste components. Posiva working report 2008-28. Posiva Oy, Eurajoki, Finland.

Antón, J., Oren, A., Benlloch, S., Rodríguez-Valera, F., Amann, R. & Rosselló-Mora, R. (2002): Salinibacter ruber gen. nov., sp. nov., a novel, extremely halophilic member of the Bacteria from saltern crystallizer ponds. International Journal of Systematic and Evolutionary Microbiology 52/2, 485-491. DOI: 10.1099/00207713-52-2-485.

Anwar, M.S., Kapri, A., Chaudhry, V., Mishra, A., Ansari, M.W., Souche, Y., Nautiyal, C.S., Zaidi, M.G.H. & Goel, R. (2016): Response of indigenously developed bacterial consortia in progressive degradation of polyvinyl chloride. Protoplasma 253/4, 1023-1032. DOI: 10.1007/s00709-015-0855-9.

Arakawa, K., Seguchi, T., Watanabe, Y. & Hayakawa, N. (1982): Radiation-induced oxidation of polyethylene, ethylene–butene copolymer, and ethylene–propylene copolymer. Journal of Polymer Science 20/9, 2681-2692. DOI: 10.1002/pol.1982.170200926.

Araújo, E.S., Khoury, H.J. & Silveira, S.V. (1998): Effects of gamma-irradiation on some properties of durolon polycarbonate. Radiation Physics and Chemistry 53/1, 79-84. DOI: 10.1016/S0969-806X(97)00300-9.

Askarieh, M.M., Chambers, A.V., Daniel, F.B.D., FitzGerald, P.L., Holtom, G.J., Pilkington, N.J. & Rees, J.H. (2000): The chemical and microbial degradation of cellulose in the near field of a repository for radioactive wastes. Waste Management 20/1, 93-106. DOI: 10.1016/S0956-053X(99)00275-5.

Ayscough, P.B., Mach, K., Oversby, J.P. & Roy, A.K. (1971): Electron spin resonance studies of fundamental processes in radiation- and photo-chemistry. Part 6.—The radiolysis of acetic acid. Transactions of the Faraday Society 67/0, 360-374. DOI: 10.1039/TF9716700360.

Ayscough, P.B. & Oversby, J.P. (1971): Electron spin resonance studies of fundamental processes in radiation- and photo-chemistry. Part 7 - The γ-radiolysis of carboxylic acids at cryogenic temperatures. Transactions of the Faraday Society 67/0, 1365-1375. DOI: 10.1039/TF9716701365.

Ayscough, P.B. & Oversby, J.P. (1972): Electron spin resonance studies of elementary processes in radiation- and photo-chemistry. Part 9 - Carboxylic esters at cryogenic temperatures. Transactions of the Faraday Society 68/0, 1153-1163. DOI: 10.1039/F19726801153.

Babauta, J.T., Nguyen, H.D., Harrington, T.D., Renslow, R. & Beyenal, H. (2012): pH, redox potential and local biofilm potential microenvironments within Geobacter sulfurreducens biofilms and their roles in electron transfer. Biotechnology and Bioengineering 109/10, 2651-2662. DOI: 10.1002/bit.24538.

Bacaloglu, R. & Fisch, M. (1994a): Degradation and stabilization of poly(vinyl chloride). I. Kinetics of the thermal degradation of poly(vinyl chloride). Polymer Degradation and Stability 45/3, 301-313. DOI: 10.1016/0141-3910(94)90200-3.

Bacaloglu, R. & Fisch, M. (1994b): Degradation and stabilization of poly(vinyl chloride). II. Simulation of the poly(vinyl chloride) degradation processes initiated in the polymer backbone. Polymer Degradation and Stability 45/3, 315-324. DOI: 10.1016/0141-3910(94)90201-1.

Bacaloglu, R. & Fisch, M. (1995): Degradation and stabilization of poly (vinyl chloride). V. Reaction mechanism of poly(vinyl chloride) degradation. Polymer Degradation and Stability 47/1, 33-57. DOI: 10.1016/0141-3910(94)00086-N.

Bagaria, F., Riba, O., Albrecht, A., Robinet, J.-C., Madé, B. & Román-Ross, G. (2021): Predicting degradation of organic molecules in cementitious media. Progress in Nuclear Energy 140/103888. DOI: 10.1016/j.pnucene.2021.103888.

Bagnoud, A. (2015): Microbial metabolism in the deep subsurface; case study of Opalinus Clay PhD. Thesis, Lausanne.

Bagnoud, A., Bruijn, I., Andersson, A.F., Diomidis, N., Leupin, O.X., Schwyn, B. & Bernier-Latmani, R. (2015): A minimalistic microbial food web in an excavated deep subsurface clay rock. FEMS Microbiology Ecology 92/1, fiv138. DOI: 10.1093/femsec/fiv138.

Bagnoud, A., Leupin, O., Schwyn, B. & Bernier-Latmani, R. (2016): Rates of microbial hydrogen oxidation and sulfate reduction in Opalinus Clay rock. Applied Geochemistry 72, 42-50. DOI: 10.1016/j.apgeochem.2016.06.011.

Baidak, A. & LaVerne, J.A. (2010): Radiation-induced decomposition of anion exchange resins. Journal of Nuclear Materials 407/3, 211-219. DOI: 10.1016/j.jnucmat.2010.10.025.

Banciu, H., Sorokin, D., Tourova, T., Galinski, E., Muntyan, M., Kuenen, J.G. & Muyzer, G. (2008): Influence of salts and pH on growth and activity of a novel facultatively alkaliphilic, extremely salt-tolerant, obligately chemolithoautotrophic sufur-oxidizing Gammaproteobacterium Thioalkalibacter halophilus gen. nov., sp. nov. from South-Western Siberian soda lakes. Extremophiles : life under extreme conditions 12, 391-404. DOI: 10.1007/s00792-008-0142-1.

Bassil, N.M., Bryan, N. & Lloyd, J.R. (2015): Microbial degradation of isosaccharinic acid at high pH. The ISME Journal 9/2, 310-320. DOI: 10.1038/ismej.2014.125.

Bassil, N.M. & Lloyd, J.R. (2019): Anaerobacillus isosaccharinicus sp. nov., an alkaliphilic bacterium which degrades isosaccharinic acid. International Journal of Systematic and Evolutionary Microbiology 69/12, 3666-3671. DOI: 10.1099/ijsem.0.002721.

Bassil, N.M., Small, J.S. & Lloyd, J.R. (2020): Enhanced microbial degradation of irradiated cellulose under hyperalkaline conditions. FEMS Microbiology Ecology 96/7, fiaa102. DOI: 10.1093/femsec/fiaa102.

Baston, G., Cowper, M.M., Davies, P., Dawson, J., Farahani, B., Heath, T.G., Schofield, J., Smith, V., Watson S. P. & Wilson, J. (2017): The impacts of PVC additives and their degradation products on radionuclide behaviour. (RWM005769).

Baston, G. & Dawson, J. (2014): NAPL generation from PVC and the fate of plasticiser additives when aged in aqueous solutions. (AMEC/PPE/002834/003). Edited by AMEC. RWMD.

Baston, G., Dawson, J., Farahani, B., Saunders, R., Schofield, J. & Smith, V. (2019): Further studies to underpin the use of PCE superplasticisers in the packaging of low-heat-generating wastes. Update on the effects of radiolysis products on sorption and solubility. (RWM007901). RWM.

Baston, G.M., Berry, J.A., Bond, K.A., Boult, K.A., Brownsword, M. & Linklater, C.M. (1994): Effects of cellulosic degradation products on uranium sorption in the geosphere. Journal of Alloys and Compounds 213-214, 475-480. DOI: 10.1016/0925-8388(94)90965-2.

Baston, G.M.N., Brownsword, M., Cowper, M.M., Manning, M.C., Pilkington, N.J. & Williams, S.J. (2002): The influence of gamma irratiation on alkaline degradation of cellulose and the effect on plutonium solubility. (SC2882/20). Nirex.

Baston, G.M.N., Cowper, M.M., Heath, T.G., Marshall, T.A. & Swanton, S.W. (2012): The effect of cellulose degradation products on thorium sorption onto hematite: studies of a model ternary system. The Mineralogical Magazine 76/8. DOI: 10.1180/minmag.2012.076.8.51.

Baston, G.M.N., Berry, J.A., Bond, K.A., Brownsword, M. & Linklater, C.M. (1992): Effects of organic degradation products on the sorption of actinides. Radiochimica Acta 58-59/2, 349-356. DOI: 10.1524/ract.1992.5859.2.349.

Bath, A.H., Christofi, N., Neal, C., Philp, J.C., Cave, M.R., McKinley, I.G. & Berner, U. (1987): Trace element and microbiological studies of alkaline groundwaters in Oman, Arabian Gulf: A natural analogue for cement pore-waters. Nagra Technical Report NTB 87-16.

Beaton, D., Pelletier, P. & Goulet, R.R. (2019): Microbial degradation of cellulosic material and gas generation: Implications for the management of low- and intermediate-level radioactive waste. Frontiers in Microbiology Sec. Microbiotechnology 10.
DOI: 10.3389/fmicb.2019.00204.

Beber, M.E., Gollub, M.G., Mozaffari, D., Shebek, K.M., Flamholz, A.I., Milo, R. & Noor, E. (2022): eQuilibrator 3.0: a database solution for thermodynamic constant estimation. Nucleic Acids Res 50/D1, D603-D609. DOI: 10.1093/nar/gkab1106.

Bélan, F., Bellenger, V., Mortaigne, B. & Verdu, J. (1997): Relationship between the structure and hydrolysis rate of unsaturated polyester prepolymers. Polymer Degradation and Stability 56/3, 301-309. DOI: 10.1016/S0141-3910(96)00203-0.

Bellenger, V., Ganem, M., Mortaigne, B. & Verdu, J. (1995): Lifetime prediction in the hydrolytic ageing of polyesters. Polymer Degradation and Stability 49/1, 91-97. DOI: 10.1016/0141-3910(95)00049-R.

Bengtsson, A. & Pedersen, K. (2016): Microbial sulphate-reducing activity over load pressure and density in water saturated Boom Clay. Applied Clay Science 132-133, 542-551. DOI: 10.1016/j.clay.2016.08.002.

Berufsgenossenschaft Rohstoffe und chemische Industrie (2015): Polyreaktionen und polymerisationsfähige Systeme. (R 008). BG RCI Berufsgenossenschaft Rohstoffe und chemische Industrie, Heidelberg, available online at
https://downloadcenter.bgrci.de/resource/downloadcenter/downloads/R008_Gesamtdokument.pdf, status as of 01.07.2020.

Bhat, D.K. & Kumar, M.S. (2006): Biodegradability of PMMA blends with some cellulose derivatives. Journal of Polymers and the Environment 14, 385-392. DOI: 10.1007/s10924-006-0032-5.

Blais, J.-F., Djedidi, Z., Cheikh, R., Tyagi, R. & Mercier, G. (2008): Metal precipitation from effluents: Review. Practice Periodical of Hazardous, Toxic, and Radioactive Waste Management 12/3. DOI: 10.1061/(ASCE)1090-025X(2008)12:3(135).

Blotevogel, K.-H., Fischer, U., Mocha, M. & Jannsen, S. (1985): Methanobacterium thermoalcaliphilum spec. nov., a new moderately alkaliphilic and thermophilic autotrophic methanogen. Archives of Microbiology 142, 211-217. DOI: 10.1007/BF00693392.

Bluďovský, R., Procházka, M. & Kopoldová, J. (1984): The influence of oxygen on the radiolytical products of cellulose. Journal of Radioanalytical and Nuclear Chemistry 87, 69-79. DOI: 10.1007/BF02167672.

Boll, M., Geiger, R., Junghare, M. & Schink, B. (2020): Microbial degradation of phthalates: biochemistry and environmental implications. Environmental Microbiology Reports 12/1, 3-15. DOI: 10.1111/1758-2229.12787.

Bolton, H., Li, S.W., Workman, D.J. & Girvin, D.C. (1993): Biodegradation of synthetic chelates in subsurface sediments from the southeast coastal-plain. Journal of environmental quality 22/1, 125-132.

Boughattas, I., Pellizzi, E., Ferry, M., Dauvois, V., Lamouroux, C., Dannoux-Papin, A., Leoni, E., Balanzat, E. & Esnouf, S. (2016): Thermal degradation of γ-irradiated PVC: II-Isothermal experiments. Polymer Degradation and Stability 126, 209-218. DOI: 10.1016/j.polymdegradstab.2015.05.010.

Bourbon, X. & Toulhoat, P. (1996): Influence of organic degradation products on the solubilisation of radionuclides in intermediate and low level radioactive wastes. Radiochimica Acta 74/s1, 315-320. DOI: 10.1524/ract.1996.74.special-issue.315.

Bowmer, T.N. (1979): Determination of scission and crosslinking yields in irradiated polymers: molecular weight distribution effects for soluble polymers. Polymer Preprints of the American Chemical Society 20/1, 376-378.

Bowmer, T.N., O'Donnell, J.H. & Winzor, D.J. (1981): Irradiation of aromatic polymers: the effect of irradiation temperature on crosslinking and scission in polystyrene. Journal of Polymer Science 19/5, 1167-1174.

Boylan, A.A., Perez-Mon, C., Guillard, L., Burzan, N., Loreggian, L., Maisch, M., Kappler, A., Byrne, J.M. & Bernier-Latmani, R. (2019): H_2-fuelled microbial metabolism in Opalinus Clay. Applied Clay Science 174, 69-76.

Brandberg, S. & Wiborgh, M. (1982): Langtidsförändringar i SFR. SFR Progress Report SFR 81-10. Rennerfelt, J., in Appendix; Roffey, R. (1982): Microbial decomposition of bitumen and asphalt (in Swedish). AR-82-49. SKBF/KBS/SKB, Stockholm, Sweden.

Brandon, A.M., Garcia, A.M., Khlystov, N.A., Wu, W.-M. & Criddle, C.S. (2021): Enhanced bioavailability and microbial biodegradation of polystyrene in an enrichment derived from the gut microbiome of Tenebrio molitor (Mealworm Larvae). Environmental Science & Technology 55/3, 2027-2036. DOI: 10.1021/acs.est.0c04952.

Braun, D. (1971): Thermal degradation of polyvinyl chloride. Pure and Applied Chemistry 26/2, 173-192. DOI: 10.1351/pac197126020173.

Brazelton, W.J., Thornton, C.N., Hyer, A., Twing, K.I., Longino, A.A., Lang, S.Q., Lilley, M.D., Früh-Green, G.L. & Schrenk, M.O. (2017): Metagenomic identification of active methanogens and methanotrophs in serpentinite springs of the Voltri Massif, Italy. PeerJ 5/e2945. DOI: 10.7717/peerj.2945.

Brennan, G.L. & Logares, R. (2023): Tracking contemporary microbial evolution in a changing ocean. Trends in Microbiology 31/4, 336-345. DOI: 10.1016/j.tim.2022.09.001.

Brown, A.R., Boothman, C., Pimblott, S.M. & Lloyd, J.R. (2015): The impact of gamma radiation on sediment microbial processes. Applied and Environmental Microbiology 81/12, 4014-4025.

Brown, D.A. & Sherrief, B.L. (1999): Evaluation of the effect of microbial subsurface ecosystems on spent nuclear fuel repositories. Environmental Technology 20/5, 469-477. DOI: 10.1080/09593332008616842.

Brueckner, T., Eberl, A., Heumann, S., Rabe, M. & Guebitz, G.M. (2008): Enzymatic and chemical hydrolysis of poly(ethylene terephthalate) fabrics. Journal of Polymer Science 46/19, 6435-6443. DOI: 10.1002/pola.22952.

Bucheli-Witschel, M. & Egi, T. (2001): Environmental fate and microbial degradation of aminopolycarboxylic acids. FEMS microbiology reviews 25/1, 69-106. DOI: 10.1016/S0168-6445(00)00055-3.

Butterworth, S.J., Stroes-Gascoyne, S. & Lloyd, J.R. (2021): Chapter 2 - The microbiology of natural analogue sites. *In:* Lloyd, J. R. & Cherkouk, A.(eds.): The Microbiology of Nuclear Waste Disposal. 1st Edition: Elsevier, 21-39, status as of 2023-25-05.

Buxbaum, L.H. (1968): The degradation of Poly(ethylene terephthalate). Review. Angewandte Chemie International Edition in English 7/3, 182-190. DOI: 10.1002/anie.196801821.

Castañeda-Facio, A., Benavides, R. & Martínez-Pardo, M.E. (2014): Thermal stability of PVC formulations gamma irradiated at different dose rates. Radiation Physics and Chemistry 97, 75-80. DOI: 10.1016/j.radphyschem.2013.11.004.

Chang, Z. & LaVerne, J.A. (2000a): Hydrogen production in the heavy ion radiolysis of polymers. 1. Polyethylene, polypropylene, poly(methyl methacrylate), and polystyrene. The Journal of Physical Chemistry B 104/45, 10557-10562. DOI: 10.1021/jp002518v.

Chang, Z. & LaVerne, J.A. (2000b): Hydrogen production in γ-ray and helium-ion radiolysis of polyethylene, polypropylene, poly(methyl-methacrylate), and polystyrene. Journal of Polymer Science 38/9, 1656-1661.
DOI: 10.1002/(SICI)1099-0518(20000501)38:9<1656::AID-POLA31>3.0.CO;2-S.

Chang, Z. & LaVerne, J.A. (2001): The gases produced in gamma and heavy-ion radiolysis of poly(methyl methacrylate). Radiation Physics and Chemistry 62/1, 19-24. DOI: 10.1016/S0969-806X(01)00417-0.

Chantreux, M., Ricard, D., Asia, L., Rossignol, S. & Wong-Wah-Chung, P. (2021): Additives as a major source of radiolytic organic byproducts of polyvinyl chloride (PVC). Radiation Physics and Chemistry 188. DOI: 10.1016/j.radphyschem.2021.109671.

Chapiro, A. (1962): Radiation chemistry of polymeric systems. Volume XV. Interscience Publishers.

Chapiro, A. (1995): General consideration of the radiation chemistry of polymers. Nuclear Instruments and Methods in Physics Research Section B: Beam Interactions with Materials and Atoms 105/1-4, 5-7. DOI: 10.1016/0168-583X(95)00861-6.

Charles, C.J., Rout, S.P., Patel, K.A., Akbar, S., Laws, A.P., Jackson, B.R., Boxall, S.A., Humphreys, P.N. & Voordouw, G. (2017): Floc formation reduces the pH stress experienced by microorganisms living in alkaline environments. Applied and Environmental Microbiology 83/6. DOI: 10.1128/AEM.02985-16.

Chernyshev, A.N., Jonsson, M. & Forsberg, K. (2018): Characterization and degradation of a polyaryl ether based superplasticizer for use in concrete barriers in deep geological repositories. Applied Geochemistry 95, 172-181. DOI: 10.1016/j.apgeochem.2018.05.014.

Chytiri, S., Goulas, A.E., Badeka, A., Riganakos, K.A. & Kontominas, M.G. (2005): Volatile and non-volatile radiolysis products in irradiated multilayer coextruded food-packaging films containing a buried layer of recycled low-density polyethylene. Food Additives and Contaminants. 22/12, 1264-1273. DOI: 10.1080/02652030500241645.

Cloet, V., Schwyn, B. & Wieland, E. (2014): Geochemische Nahfeld-Daten zu den SMA und ATA für die provisorischen Sicherheitsanalysen in SGT Etappe 2. Nagra Arbeitsbericht NAB 14-52 Rev. 1.

Clough, R.L. (2001): High-energy radiation and polymers: A review of commercial processes and emerging applications. Nuclear Instruments and Methods in Physics Research Section B: Beam Interactions with Materials and Atoms 185/1-4, 8-33. DOI: 10.1016/S0168-583X(01)00966-1.

Clough, R.L. & Gillen, K.T. (1981): Radiation-thermal degradation of PE and PVC: Mechanism of synergism and dose rate effects. Radiation Physics and Chemistry 18/3-4, 661-669. DOI: 10.1016/0146-5724(81)90189-8.

Collard, F.-X. & Blin, J. (2014): A review on pyrolysis of biomass constituents: Mechanisms and composition of the products obtained from the conversion of cellulose, hemicelluloses and lignin. Renewable and Sustainable Energy Reviews 38, 594-608. DOI: 10.1016/j.rser.2014.06.013.

Colombani, J., Herbette, G., Rossi, C., Joussot-Dubien, C., Labed, V. & Gilardi, T. (2009): Leaching of plasticized PVC: Effect of irradiation. Journal of Applied Polymer Science 112/3, 1372-1377. DOI: 10.1002/app.29612.

Colombani, J., Labed, V., Joussot-Dubien, C., Périchaud, A., Raffi, J., Kister, J. & Rossi, C. (2007): High doses gamma radiolysis of PVC: Mechanisms of degradation. Nuclear Instruments and Methods in Physics Research Section B: Beam Interactions with Materials and Atoms 265/1, 238-244. DOI: 10.1016/j.nimb.2007.08.053.

CORI (2021): Task 2 Hydrolytic/radiolytic degradation of organics. Description of first results on hydrolytic and radiolytic organic degradation and identification of released species. CORI Technical Report Milestone DMS97. European Comission, Euratom Horizon2020.

Courdouan, A., Christl, I., Meylan, S., Wersin, P. & Kretzschmar, R. (2007a): Characterization of dissolved organic matter in anoxic rock extracts and in situ pore water of the Opalinus Clay. Applied Geochemistry 22/12, 2926-2939. DOI: 10.1016/j.apgeochem.2007.09.001.

Courdouan, A., Christl, I., Meylan, S., Wersin, P. & Kretzschmar, R. (2007b): Isolation and characterization of dissolved organic matter from the Callovo–Oxfordian formation. Applied Geochemistry 22/7, 1537-1548. DOI: 10.1016/j.apgeochem.2007.04.001.

Cox, M.M. & Battista, J.R. (2005): Deinococcus radiodurans - the consummate survivor. Nature Reviews Microbiology/3, 882-892.

Cramer, J.J. & Smellie, J. (1994): Final Report of the AECL/SKB Cigar Lake Analog Study. In: Atomic Energy of Canada Limited Report AECL-10851, also COG-93-147 and SKB TR-94-04. Swedish Nuclear Fuel and Waste Management Co., Stockholm, Sweden., 401.

Crespo-Medina, M., Twing, K.I., Sánchez-Murillo, R., Brazelton, W.J., McCollom, T.M. & Schrenk, M.O. (2017): Methane dynamics in a tropical serpentinizing environment: The Santa Elena Ophiolite, Costa Rica. Frontiers in Microbiology Sec. Microbiotechnology 8. DOI: 10.3389/fmicb.2017.00916.

Da Silva, am Betioli, Gleize, P.J., Roman, H.R., La Gómez & Ribeiro, J.L. (2005): Degradation of recycled PET fibers in Portland cement-based materials. Cement and Concrete Research 35/9, 1741-1746. DOI: 10.1016/j.cemconres.2004.10.040.

Danso, D., Chow, J., Streit, W.R. & Drake, H.L. (2019): Plastics: Environmental and biotechnological perspectives on microbial degradation. Applied and Environmental Microbiology 85/19. DOI: 10.1128/AEM.01095-19.

Dave, J., Kumar, R. & Srivastava, H.C. (1987): Studies on modification of polyester fabrics I: Alkaline hydrolysis. Journal of Applied Polymer Science 33/2, 455-477. DOI: 10.1002/app.1987.070330215.

Davey, M.E. & O'toole, G.A. (2000): Microbial biofilms: from ecology to molecular genetics. Microbiology and Molecular Biology Reviews 64/4, 847-867. DOI: 10.1128/MMBR.64.4.847-867.2000.

Davis, A. & Golden, J.H. (1968): Thermal degradation of polycarbonate. Journal of the Chemical Society/0, 45-47. DOI: 10.1039/J29680000045.

Davis, A. & Golden, J.H. (1969): Stability of polycarbonate. Journal of Macromolecular Science, Part C 3/1, 49-68. DOI: 10.1080/15583726908545896.

Dawson, J. (2013a): NAPL generation from the radiolysis of polyethylene and chlorosulphonated polyethylene elastomer (Hypalon). (NPO003431). NDA-RWMD.

Dawson, J. (2013b): The potential for non-aqueous phase liquid production from irradiated neoprene and ion-exchange resin. (NPO1186). NDA-RWMD, Oxford.

Dawson, J. (2013c): The potential for non-aqueous phase liquid production from irradiated PVC and vinylesterstyrene (VES). (NPO1042 (Nirex#513770)). NDA-RWMD, Oxford.

Dawson, J. & Magalhaes, S. (2012): The potential for non-aqueous phase liquid production in irradiated polymers. (NPO1042 (Nirex#513770)). NDA-RWMD.

Decker, C. (1976): Oxidative degradation of poly(vinyl chloride). Journal of Applied Polymer Science 20/12, 3321-3336. DOI: 10.1002/app.1976.070201213.

Demertzis, P.G., Franz, R. & Welle, F. (1999): The effects of γ-irradiation on compositional changes in plastic packaging films. Packaging Technology & Science 12/3, 119-130. DOI: 10.1002/(SICI)1099-1522(199905/06)12:3<119::AID-PTS460>3.0.CO;2-G.

Diesen, V., Forsberg, K. & Jonsson, M. (2017): Effects of cellulose degradation products on the mobility of Eu(III) in repositories for low and intermediate level radioactive waste. Journal of Hazardous Materials 340, 384-389. DOI: 10.1016/j.jhazmat.2017.07.008.

Diomidis, N., Cloet, V., Leupin, O.X., Marschall, P., Poller, A. & Stein, M. (2016): Production, consumption and transport of gases in deep geological repositories according to the Swiss disposal concept. Nagra Technical Report NTB 16-03.

Doi, S., Takumi, N., Kakihana, Y. & Higa, M. (2020): Alkali attack on cation-exchange membranes with polyvinyl chloride backing and binder: Comparison with anion-exchange membranes. Membranes. 10/9. DOI: 10.3390/membranes10090228.

Dole, M. (1973): The radiation chemistry of macromolecules. Volume II. Academic Press.

Dunn, J.B., Burns, M.L., Hunter, S.E. & Savage, P.E. (2003): Hydrothermal stability of aromatic carboxylic acids. The Journal of Supercritical Fluids 27/3, 263-274. DOI: 10.1016/S0896-8446(02)00241-3.

Egi, T. (2001): Biodegradation of metal complexing aminopolycarboxylic acids. Journal of Bioscience and Bioengineering 92/2, 89-97.

Enomoto, K., LaVerne, J.A., Tandon, L., Enriquez, A.E. & Matonic, J.H. (2008): The radiolysis of poly(4-vinylpyridine) quaternary salt ion exchange resins. Journal of Nuclear Materials 373/1-3, 103-111. DOI: 10.1016/j.jnucmat.2007.05.032.

Ershov, B.G. (1998): Radiation-chemical degradation of cellulose and other polysaccharides. Russian Chemical Reviews 67/4. DOI: 10.1070/RC1998v067n04ABEH000379.

Ershov, B.G. & Klimentov, A.S. (1984): The radiation chemistry of cellulose. Russian Chemical Reviews 53/12. DOI: 10.1070/RC1984v053n12ABEH003148.

Eschrich, H. (1980): Properties and long-term behaviour of bitumen and radioactive waste-bitumen mixtures. (SKB Technical Report 80-14). SKB.

Evans, N., Warwick, P., Felipe-Sotelo, M. & Vines, S. (2012): Prediction and measurement of complexation of radionuclide mixtures by α-isosaccharinic, gluconic and picolinic acids. Journal of Radioanalytical and Nuclear Chemistry 293, 725-730. DOI: 10.1007/s10967-012-1828-5.

Faravelli, T., Pinciroli, M., Pisano, F., Bozzano, G., Dente, M. & Ranzi, E. (2001): Thermal degradation of polystyrene. Journal of Analytical and Applied Pyrolysis 60/1, 103-121. DOI: 10.1016/S0165-2370(00)00159-5.

Feng, Y., Wang, B., Wang, F., Zhao, Y., Liu, C., Chen, J. & Shen, C. (2014): Thermal degradation mechanism and kinetics of polycarbonate/silica nanocomposites. Polymer Degradation and Stability 107, 129-138. DOI: 10.1016/j.polymdegradstab.2014.05.012.

Fernández-Calviño, D. & Bååth, E. (2010): Growth response of the bacterial community to pH in soils differing in pH: Growth response of the bacterial community to pH. FEMS Microbiology Ecology 73/1, 149-156. DOI: 10.1111/j.1574-6941.2010.00873.x.

Fernandez-Prini, R. & Schulman, P. (1984): The effect of temperature on the stability of ion-exchange resins in aqueous medium. Journal of Applied Polymer Science 29/1, 341-352. DOI: 10.1002/app.1984.070290132.

Ferriol, M., Gentilhomme, A., Cochez, M., Oget, N. & Mieloszynski, J.L. (2003): Thermal degradation of poly(methyl methacrylate) (PMMA): modelling of DTG and TG curves. Polymer Degradation and Stability 79/2, 271-281. DOI: 10.1016/S0141-3910(02)00291-4.

Ferry, M., Dannoux-Papin, A., Dély, N., Legand, S., Durand, D., Roujou, J.L., Lamouroux, C., Dauvois, V., Coignet, P., Cochin, F. & Esnouf, S. (2014): Chemical composition effects of methylene containing polymers on gas emission under γ-irradiation. Nuclear Instruments and Methods in Physics Research Section B: Beam Interactions with Materials and Atoms 334, 69-76. DOI: 10.1016/j.nimb.2014.05.007.

Ferry, M., Pellizzi, E., Boughattas, I., Fromentin, E., Dauvois, V., Combarieu, G., Coignet, P., Cochin, F., Ngono-Ravache, Y., Balanzat, E. & Esnouf, S. (2016): Effect of cumulated dose on hydrogen emission from polyethylene irradiated under oxidative atmosphere using gamma rays and ion beams. Radiation Physics and Chemistry 118, 124-127. DOI: 10.1016/j.radphyschem.2015.06.006.

Filby, A., Deissmann, G. & Wiegers, R. (2016): LILW degradation processes and products. (OPERA-PU-IBR512). OPERA.

Fisch, M.H. & Bacaloglu, R. (1995): Kinetics and mechanism of the thermal degradation of poly(vinyl chloride). Journal of Vinyl & Additive Technology 1/4, 233-240. DOI: 10.1002/vnl.730010409.

Fischer, I., Schmitt, W.F., Porth, H.-C., Allsopp, M.W. & Vianello, G. (2014): Poly(Vinyl Chloride). *In:* Ullmann's Encyclopedia of Industrial Chemistry: Wiley-VCH Verlag GmbH & Co. KGaA. Weinheim, Germany, 1-30.

Flemming, H.-C., van Hullebusch, E.D., Neu, T.R., Nielsen, P.H., Seviour, T., Stoodley, P., Wingender, J. & Wuertz, S. (2023): The biofilm matrix: multitasking in a shared space. Nature Reviews Microbiology 21, 70-86. DOI: 10.1038/s41579-022-00791-0.

Flemming, H.-C. & Wingender, J. (2010): The biofilm matrix. Nature Reviews Microbiology 8, 623-633. DOI: 10.1038/nrmicro2415.

Földváry, C., Takács, E. & Wojnárovits, L. (2003): Effect of high-energy radiation and alkali treatment on the properties of cellulose. Radiation Physics and Chemistry 67/3-4, 505-508. DOI: 10.1016/S0969-806X(03)00094-X.

Fones, E.M., Colman, D.R., Kraus, E.A., Nothaft, D.B., Poudel, S., Rempfert, K.R., Spear, J.R., Templeton, A.S. & Boyd, E.S. (2019): Physiological adaptations to serpentinization in the Samail Ophiolite, Oman. The ISME Journal 13, 1750-1762. DOI: 10.1038/s41396-019-0391-2.

Fujita, H., Haga, K., Shibata, M. & Mihara, M. (2008): Concentration and molecular weight of superplasticizer contained in pore solution extracted from hardened cement pastes. Journal of Advanced Concrete Technology 6/3, 389-395. DOI: 10.3151/jact.6.389.

Fukunaga, S., Jintoku, T., Iwata, Y., Nakayama, M., Tsuji, T., Sakaya, N., Mogi, K. & Ito, M. (2005): Investigation of microorganisms in bentonite deposits. Geomicrobiology Journal 22/7-8, 361-370. DOI: 10.1080/01490450500248788.

Gałko, G. & Sajdak, M. (2022): Trends for the thermal degradation of polymeric materials: Analysis of available techniques, issues, and opportunities. Applied sciences 12/18. DOI: 10.3390/app12189138.

Gaona, X., Montoya, V., Colàs, E., Grivé, M. & Duro, L. (2008): Review of the complexation of tetravalent actinides by ISA and gluconate under alkaline to hyperalkaline conditions. Journal of Contaminant Hydrology 102/3-4, 217-227.
DOI: 10.1016/j.jconhyd.2008.09.017.

García, D., Grivé, M., Duro, L., Brassinnes, S. & Pablo, J. de (2018): The potential role of the degradation products of cement superplasticizers on the mobility of radionuclides. Applied Geochemistry 98, 1-9. DOI: 10.1016/j.apgeochem.2018.09.004.

García, D., Henocq, P., Riba, O., Lopez-Garcia, M., Madé, B. & Robinet, J.-C. (2020): Adsorption behaviour of isosaccharinic acide onto cementitious materials. Applied Geochemistry 118/104625. DOI: 10.1016/j.apgeochem.2020.104625.

Geetha, R., Torikai, A., Yoshida, S., Nagaya, S., Shirakawa, H. & Fueki, K. (1989): Radiation-induced degradation of polyethylene: Effect of processing and density on the chemical changes and mechanical properties. Polymer Degradation and Stability 23/1, 91-98. DOI: 10.1016/0141-3910(89)90071-2.

Geiger, R.A., Junghare, M., Mergelsberg, M., Ebenau-Jehle, C., Jesenofsky, V.J., Jehmlich, N., Bergen, M. von, Schink, B. & Boll, M. (2019): Enzymes involved in phthalate degradation in sulphate-reducing bacteria. Environmental Microbiology 21/10, 3601-3612. DOI: 10.1111/1462-2920.14681.

Giacomucci, L., Raddadi, N., Soccio, M., Lotti, N. & Fava, F. (2019): Polyvinyl chloride biodegradation by Pseudomonas citronellolis and Bacillus flexus. New Biotechnology 52, 35-41. DOI: 10.1016/j.nbt.2019.04.005.

Giacomucci, L., Raddadi, N., Soccio, M., Lotti, N. & Fava, F. (2020): Biodegradation of polyvinyl chloride plastic films by enriched anaerobic marine consortia. Marine Environmental Research 158/104949. DOI: 10.1016/j.marenvres.2020.104949.

Gihring, T.M., Bond, P.L., Peters, S.C. & Banfield, J.F. (2003): Arsenic resistance in the archaeon "Ferroplasma acidarmanus": new insights into the structure and evolution of the ars genes. Extremophiles 7, 123-130. DOI: 10.1007/s00792-002-0303-6.

Gillow, J.B. & Francis, A.J. (2006): Microbial gas generation under expected waste isolation pilot plant repository conditions: Final report. (BNL-96148-2011-IR). Brookhaven National Laboratory, Upton, NY.

Gilmour, K.A., Davie, C.T. & Gray, N. (2021): An indigenous iron-reducing microbial community from MX80 bentonite - A study in the framework of nuclear waste disposal. Applied Clay Science 205, 106039.

Glaus, M., van Loon, L., Achatz, S., Chodura, A. & Fischer, K. (1999a): Degradation of cellulosic materials under the alkaline conditions of a cementitious repository for low and intermediate level radioactive waste: Part I: Identification of degradation products. Analytica Chimica Acta 398/1, 111-122. DOI: 10.1016/S0003-2670(99)00371-2.

Glaus, M.A. & van Loon, L.R. (2004a): A generic procedure for the assessment of the effect of concrete admixtures on the retention behaviour of cement for radionuclides: Concept and case studies. (Nagra Technical Report NTB 03-09). Nagra, Wettigen, Switzerland.

Glaus, M.A. & van Loon, L.R. (2004b): Cellulose degradation at alkaline conditions: Long-term experiments at elevated temperatures. Nagra Technical Report NTB 03-08.

Glaus, M.A. & van Loon, L.R. (2008): Degradation of cellulose under alkaline conditions: New insights from a 12 years degradation study. Environmental Science & Technology 42/8, 2906-2911. DOI: 10.1021/es7025517.

Glaus, M.A., van Loon, L.R., Achatz, S., Chodura, A. & Fischer, K. (1999b): Degradation of cellulosic materials under the alkaline conditions of a cementitious repository for low and intermediate level radioactive waste. Analytica Chimica Acta 398/1. DOI: 10.1016/S0003-2670(99)00371-2.

Glaus, M.A., van Loon, L.R., Schwyn, B., Vines, S., Steve, W., Larsson, P. & Puigdomenech, I. (2008a): Long-term predictions of the concentration of α-isosaccharinic acid in cement pore water. Materials Research Society symposium proceedings 1107. DOI: 10.1557/PROC-1107-605.

Glaus, M.A., van Loon, L.R., Schwyn, B., Vines, S., Steve, W., Larsson, P. & Puigdomenech, I. (2008b): Long-term predictions of the concentration of α-isosaccharinic acid in cement pore water. Materials Research Society symposium proceedings/1107, 605-612.

Gómez, E.F. & Michel, F.C. (2013): Biodegradability of conventional and bio-based plastics and natural fiber composites during composting, anaerobic digestion and long-term soil incubation. Polymer Degradation and Stability 98/12, 2583-2591. DOI: 10.1016/j.polymdegradstab.2013.09.018.

González-López, L., Kearney, L., Janke, C.J., Wishart, J., Kanbargi, N. & Al-Sheikhly, M. (2022): On the mechanism of the steady-state gamma radiolysis-induced scissions of the phenyl-vinyl polyester-based resins. Frontiers in Chemistry 9. DOI: 10.3389/fchem.2021.803347.

González-Siso, M.R., Gaona, X., Duro, L., Altmaier, M. & Bruno, J. (2018): Thermodynamic model of Ni(II) solubility, hydrolysis and complex formation with ISA. Radiochimica Acta 106/1, 31-45. DOI: 10.1515/ract-2017-2762.

Goyal, A. (2022): Horizontal gene transfer drives the evolution of dependencies in bacteria. iScience 25/5. DOI: 10.1016/j.isci.2022.104312.

Grant, W.D., Daniel, R.M., Finney, J.L. & Stoneham, M. (2004): Life at low water activity. Philosophical Transactions of the Royal Society of London. Series B: Biological Sciences 359/1448, 1249-1267. DOI: 10.1098/rstb.2004.1502.

Greenfield, B.F., Holtom, G.J., Hurdus, M.H., O'Kelly, N., Pilkington, N.J., Rosevear, A., Spindler, M.W. & Williams, S.J. (1994): Identification and degradation of isosaccharinic acid, a cellulose degradation product. Materials Research Society symposium proceedings 353, 1151-1158. DOI: 10.1557/PROC-353-1151.

Greenfield, B.F., Ito, M., Spindler, M.W., Williams, S.J. & Yui, M. (1996): The effects of the chemical and radiolytic degradation of asphalt on plutonium solubility. Materials Research Society symposium proceedings 465, 721-728. DOI: 10.1557/PROC-465-721.

Grogan, H., Worgan, K.J., Smith, G.M. & Hodkinson, D.P. (1992): Post-disposal implications of gas generated from a repository for low and intermediate level wastes. Nagra Technical Report NTB 92-07.

Hacıoğlu, F., Özdemir, T., Çavdar, S. & Usanmaz, A. (2013): Possible use of EPDM in radioactive waste disposal: Long term low dose rate and short term high dose rate irradiation in aquatic and atmospheric environment. Radiation Physics and Chemistry 83, 122-130. DOI: 10.1016/j.radphyschem.2012.10.011.

Hafenbradl, D., Keller, M., Dirmeier, R., Rachel, R., Roßnagel, P., Burggraf, S., Huber, H. & Stetter, K.O. (1996): Ferroglobus placidus gen. nov., sp. nov., a novel hyperthermophilic archaeum that oxidizes Fe^{2+} at neutral pH under anoxic conditions. Archives of Microbiology 166/5, 308-314. DOI: 10.1007/s002030050388.

Hakkarainen, M. & Albertsson, A.-C. (2004): Environmental degradation of polyethylene. Advances in polymer science 169.

Hall, G.R. (1963): Radiation-induced decomposition of ion-exchange resins. part I. Anion-exchange resins. Journal of the Chemical Society.

Hamilton-Brehm, S.D., Gibson, R.A., Green, S.J., Hopmans, E.C., Schouten, S., van der Meer, M.T.J., Shields, J.P., Damsté, J.S.S. & Elkins, J.G. (2013): *Thermodesulfobacterium geofontis* sp. nov., a hyperthermophilic, sulfate-reducing bacterium isolated from Obsidian Pool, Yellowstone National Park. Extremophiles 17, 251-263. DOI: 10.1007/s00792-013-0512-1.

Harrison, J.P., Gheeraert, N., Tsigelnitskiy, D. & Cockell, C.S. (2013): The limits for life under multiple extremes. Review. Trends in Microbiology 21/4, 204-212. DOI: 10.1016/j.tim.2013.01.006.

Hartge, K.H. & Horn, R. (2016): Essential Soil Physics - An introduction to soil processes, functions, structure and mechanics. 1st edition, based on the 4th, completely revised and extended German edition. 1st ed. Schweizerbart Science Publisher, Stuttgart.

Haynes, H.M., Pearce, C.I. & Boothman, C. (2018): Response of bentonite microbial communities to stresses relevant to geodisposal of radioactive waste. Chemical Geology 501, 58-67.

Hegazy, E.-S.A., Seguchi, T., Arakawa, K. & Machi, S. (1981): Radiation-induced oxidative degradation of isotactic polypropylene. Journal of Applied Polymer Science 26/4, 1361-1372. DOI: 10.1002/app.1981.070260427.

Heggs, T.G. (2014): Polypropylene. *In:* Ullmann's Encyclopedia of Industrial Chemistry: Wiley-VCH Verlag GmbH & Co. KGaA. Weinheim, Germany.

Hernandez-Perez, G., Goma, G. & Rols, J.L. (1998): Enhanced degradation of lignosulfonated compounds by Streptomyces viridosporus. Water Science and Technology 38/4-5, 289-297. DOI: 10.1016/S0273-1223(98)00511-3.

Hill, D.J., O'Donnell, J.H., Pomery, P.J. & Winzor, C.L. (1992): Gamma radiolysis of poly(acrylic acid) and poly(methacrylic acid). International Journal of Radiation Applications and Instrumentation. Part C. Radiation Physics and Chemistry 39/3, 237-241. DOI: 10.1016/1359-0197(92)90147-8.

Hill, D.J., O'Donnell, J.H., Winzor, C.L. & Winzor, D.J. (1990): Evaluation of scission and crosslinking yields in γ-irradiated poly(acrylic acid) and poly(methacrylic acid) from weight- and Z-average molecular weights determined by sedimentation equilibrium. Polymer 31/3, 538-542. DOI: 10.1016/0032-3861(90)90399-J.

Hiraoka, H. (1977): Radiation chemistry of poly(methacrylates). IBM Journal of Research and Development 21/2, 121-130. DOI: 10.1147/rd.212.0121.

Ho, B.T., Roberts, T.K. & Lucas, S. (2018): An overview on biodegradation of polystyrene and modified polystyrene: the microbial approach. Critical Reviews in Biotechnology 38/2, 308-320. DOI: 10.1080/07388551.2017.1355293.

Hoehler, T.M., Alperin, M.J., Albert, D.B. & Martens, C.S. (2001): Apparent minimum free energy requirements for methanogenic Archaea and sulfate-reducing bacteria in an anoxic marine sediment. FEMS Microbiology Ecology 38/1, 33-41. DOI: 10.1111/j.1574-6941.2001.tb00879.x.

Hoff, A., Jacobsson, S., Pfäffli, P., Zitting, A. & Frostling, H. (1982): Degradation products of plastics. Polyethylene and styrene-containing thermoplastics - analytical, occupational and toxicologic aspects. Scandinavian Journal of Work, Environment & Health 8/Suppl. 2, 1-60.

Hooker, P. (2007): A review of the decomposition of organics and gas generation rates. Unpublished. Nagra internal documentation. Nagra, Wettigen, Switzerland.

Huang, J., Meng, H., Luo, X., Mu, X., Xu, W., Jin, L. & Lai, B. (2022): Insights into the thermal degradation mechanisms of polyethylene terephthalate dimer using DFT method. Chemosphere 291/2. DOI: 10.1016/j.chemosphere.2021.133112.

Hummel, W., Kulik, D.A. & Miron, G.D. (2022): Solubility of radionuclides and influence of EDTA for use in the development of the cement sorption database (SDB 2022). Nagra Arbeitsbericht NAB 22-38.

Humphreys, P., West, J. & Metcalfe, R. (2010a): Microbial effects on repository performance. Technical Report QRS-1378Q-1 Version 3. UK NDA, UK, available online at http://eprints.hud.ac.uk/7613/, status as of 2023-23-05.

Humphreys, P.N., Laws, A. & Dawson, J. (2010b): A review of cellulose degradation and the fate of degradation products under repository conditions. WT 15 05 15. Edited by Serco Assurance. NDA & RWMD, Oxfordshire, UK.

IARC (2013): Bitumens and bitumen emissions. World Health Organization, available online at https://www.ncbi.nlm.nih.gov/books/NBK294237/, status as of 01.11.2022.

Ichikawa, T. & Hagiwara, Z. (1973): Effect of gamma-irradiation on cation exchange resin. Journal of Nuclear Science and Technology 10/12, 746-752. DOI: 10.1080/18811248.1973.9735486.

Ivanov, V.S. (1992): New concepts in polymer science. Radiation chemistry of polymers. VSP, Utrecht, the Netherlands.

Jabarin, S.A. & Lofgren, E.A. (1984): Thermal stability of polyethylene terephthalate. Polymer Engineering and Science 24/13, 1056-1063. DOI: 10.1002/pen.760241311.

Jannasch, H.W., Eimhjell, K., Wirsen, C.O. & Farmanfa, A. (1971): Microbial degradation of organic matter in deep sea. SCIENCE 171/3972, 672-&. DOI: 10.1126/science.171.3972.672.

Jenal-Wanner, U. & Egli, T. (1993): Anaerobic degradation of nitrilotriacetate (NTA) in a denitrifying bacterium: purifiction and characterisation of the NTA dehydroenase-nitrate reductase enzyme complex. Applied and Environmental Microbiology 59, 3350-3359. DOI: 10.1128/aem.59.10.3350-3359.1993.

Jin, Q. & Kirk, M.F. (2018): pH as a primary control in environmental microbiology: 1. Thermodynamic perspective. Frontiers in Environmental Science 6. DOI: 10.3389/fenvs.2018.00021.

Johnsen, R.H. (1959): Some aspects of the radiation chemistry of liquid aliphatic carboxylic acids. The Journal of Physical Chemistry B 63/12, 2041-2043. DOI: 10.1021/j150582a015.

Johnson, D.R., Wen, W.Y. & Dole, M. (1973): Radiation chemistry of polyethylene. XII. Alkyl radical decay and amorphous content. The Journal of Physical Chemistry B 77/18, 2174-2179. DOI: 10.1021/j100637a003.

Johnson, L. & Schwyn, B. (2007): Recommended gas generation rates for the decomposition of organic materials and corrosion of metals in an SMA repository. Unpublished. Nagra internal documentation. Nagra, Wettigen, Switzerland.

Jones, A.R. (1971a): The radiolysis of aliphatic carboxylic acids. On the decarboxylation of normal acids in the liquid state. Radiation Research 48/3, 447-453. DOI: 10.2307/3573332.

Jones, A.R. (1971b): The radiolysis of aliphatic carboxylic acids: The decarboxylation of normal acids at 38 degrees. Radiation Research 47/1, 35-40. DOI: 10.2307/3573286.

Jones, A.R. (1972): The radiolysis of aliphatic carboxylic acids: On the decarboxylation of normal acids at 77 degrees K. Radiation Research 50/1, 41-47. DOI: 10.2307/3573465.

Jusner, P., Schwaiger, E., Potthast, A. & Rosenau, T. (2021): Thermal stability of cellulose insulation in electrical power transformers – A review. Carbohydrate Polymers 252. DOI: 10.1016/j.carbpol.2020.117196.

Kagawa, A., Fukumoto, M. & Kawamura, K. (2000): Influence of chemical and radiolytic degradation of bitumen on its performance for disposal. Journal of Nuclear Science and Technology 37/10, 934-937. DOI: 10.1080/18811248.2000.9714975.

Kagiya, T., Nishimoto, S., Watanabe, Y. & Kato, M. (1985): Importance of the amorphous fraction of polypropylene in the resistance to radiation-induced oxidative degradation. Polymer Degradation and Stability 12/3, 261-275. DOI: 10.1016/0141-3910(85)90094-1.

Kani, Y., Noshita, K., Kawasaki, T., Nasu, Y., Nishimura, T., Sakuragi, T. & Asano, H. (2008): Decomposition of 14C containing organic molecules released from radioactive waste by gamma-radiolysis under repository conditions. Radiation Physics and Chemistry 77/4, 434-438. DOI: 10.1016/j.radphyschem.2007.06.009.

Kani, Y., Noshita, K., Kawasaki, T., Nishimura, T., Sakuragi, T. & Asano, H. (2009): Radiolytic decomposition of organic C-14 released from TRU Waste. Proceedings of the 11th International Conference on Environmental Remediation and Radioactive Waste Management 2007/Part A, 275-280. DOI: 10.1115/ICEM2007-7147.

Kannen, H. & Müller, W. (1999): Gas generation of radioactive wastes - Comparison between laboratory experiments and measurements on real waste. Proceedings of the 7th International Conference on Radioactive Waste Management and Environmental Remediation.

Kaplan, D.L., Hartensen, R. & Sutter, J. (1979): Biodegradation of polystyrene, poly(methyl methacrylate) and phenol formaldehyde. Applied and Environmental Microbiology 38/3, 551-553. DOI: 10.1128/aem.38.3.551-553.1979.

Kashiwagi, T., Inabi, A. & Hamins, A. (1989): Behavior of primary radicals during thermal degradation of poly(methyl methacrylate). Polymer Degradation and Stability 26/2, 161-184. DOI: 10.1016/0141-3910(89)90007-4.

Keith-Roach, M.J. (2008): The speciation, stability, solubility and biodegradation of organic co-contaminant radionuclide complexes: A review. Science of the Total Environment 396/1, 1-11. DOI: 10.1016/j.scitotenv.2008.02.030.

Keller, L.M., Holzer, L., Wepf, R. & Gasser, P. (2011): 3D geometry and topology of pore pathways in Opalinus clay: Implications for mass transport. Applied Clay Science 52/1-2, 85-95. DOI: 10.1016/j.clay.2011.02.003.

Keller, M., Braun, F.-J., Dirmeier, R., Hafenbradl, D., Burggraf, S., Rachel, R. & Stetter, K.O. (1995): *Thermococcus alcaliphilus* sp. nov., a new hyperthermophilic archaeum growing on polysulfide at alkaline pH. Archives of Microbiology 164/6, 390-395. DOI: 10.1007/s002030050280.

Kennedy, J.F., Phillips, G.O., Wedlock, D.J. & Williams, P.A. (ed.) (1985): Cellulose and its derivatives - Chemistry, biochemistry and applications. Ellis Horwood Limited Publishers, Chichester, UK.

Kerry Thomas, J. (2007): Fundamental aspects of the radiolysis of solid polymers, crosslinking and degradation. Nuclear Instruments and Methods in Physics Research Section B: Beam Interactions with Materials and Atoms 265/1, 1-7. DOI: 10.1016/j.nimb.2007.08.021.

Khan, A.W. (1977): Anaerobic degradation of cellulose by mixed culture. Canadian Journal of Microbiology 23/12, 1700-1705. DOI: 10.1139/m77-245.

Khandare, S.D., Chaudhary, D.R. & Jha, B. (2021): Bioremediation of polyvinyl chloride (PVC) films by marine bacteria. Marine Pollution Bulletin 169. DOI: 10.1016/j.marpolbul.2021.112566.

Khatoon, N., Jamal, A. & Ali, M.I. (2019): Lignin peroxidase isoenzyme: a novel approach to biodegrade the toxic synthetic polymer waste. Environmental Technology 40/11, 1366-1375. DOI: 10.1080/09593330.2017.1422550.

Kim, J.-S. & Crowley, D.E. (2007): Microbial diversity in natural asphalts of the Rancho La Brea Tar Pits. Applied and Environmental Microbiology 73/14, 4579-4591. DOI: 10.1128/AEM.01372-06.

Kint, D. & Muñoz-Guerra, S. (1999): A review on the potential biodegradability of poly(ethylene terephthalate). Polymer International 48/5, 346-352. DOI: 10.1002/(SICI)1097-0126(199905)48:5<346::AID-PI156>3.0.CO;2-N.

Knapp, J.S., Jenkey, N.D. & Townsley, C.C. (1996): The anaerobic biodegradation of diethanolamine by a nitrate reducing bacterium. Biodegradation 7, 183-189.

Knill, C.J. & Kennedy, J.F. (2003): Degradation of cellulose under alkaline conditions. Carbohydrate Polymers 51/3, 281-300. DOI: 10.1016/S0144-8617(02)00183-2.

Kobayashi, T., Sasaki, T. & Kitamura, A. (2019): Thermodynamic interpretation of uranium(IV/VI) solubility in the presence of α-isosaccharinic acid. The Journal of Chemical Thermodynamics 138, 151-158. DOI: 10.1016/j.jct.2019.06.006.

Kobayashi, T., Teshima, T., Sasaki, T. & Kitamura, A. (2017): Thermodynamic model for Zr solubility in the presence of gluconic acid and isosaccharinic acid. Journal of Nuclear Science and Technology 54/2, 233-241. DOI: 10.1080/00223131.2016.1255573.

Kosakowski, G., Churakov, S., Glaus, M., Guillemot, T., Kulik, D., Ma, B., Martin, L., Miron, D. & Prasianakis, N. (2023, in prep.): Geochemical evolution of the L/ILW near field. Nagra Technical Report NTB 23-03.

Kotova, I.B., Taktarova, Y.V., Tsavkelova, E.A., Egorova, M.A., Bubnov, I.A., Malakhova, D.V., Shirinkina, L.I., Sokolova, T.G. & Bonch-Osmolovskaya, E.A. (2021): Microbial degradation of plastics and approaches to make it more efficient. Microbiology 90, 671-701. DOI: 10.1134/S0026261721060084.

Kotsyurbenko, O.R., Chin, K.-J., Glagolev, M.V., Stubner, S., Simankova, M.V., Nozhevnikova, A.N. & Conrad, R. (2004): Acetoclastic and hydrogenotrophic methane production and methanogenic populations in an acidic West-Siberian peat bog. Environmental Microbiology 6/11, 1159-1173. DOI: 10.1111/j.1462-2920.2004.00634.x.

Kovalev, G.V. & Bugaenko, L.T. (2003): On the crosslinking of cellulose under exposure to radiation. High Energy Chemistry 37, 209-215. DOI: 10.1023/A:1024790415083.

Kraus, E.A., Nothaft, D., Stamps, B.W., Rempfert, K.R., Ellison, E.T., Matter, J.M., Templeton, A.S., Boyd, E.S., Spear, J.R. & Atomi, H. (2021): Molecular evidence for an active microbial methane cycle in subsurface serpentinite-hosted groundwaters in the Samail Ophiolite, Oman. Applied and Environmental Microbiology 87/2. DOI: 10.1128/AEM.02068-20.

Kudoh, H., Kasai, N., Sasuga, T. & Seguchi, T. (1996): Low temperature gamma-ray irradiation effects on polymer materials—3. Gas evolution and change of molecular weight. Radiation Physics and Chemistry 48/1, 95-100. DOI: 10.1016/0969-806X(95)00433-X.

Kumar, M., Rao, M.H. & Rao, K.N. (1986): Gamma radiolysis of polycyclohexyl methacrylate. Radiation Physics and Chemistry 27/3, 219-223.

Kurth, J.M., Op den Camp, Huub J. M. & Welte, C.U. (2020): Several ways one goal—methanogenesis from unconventional substrates. Applied Microbiology and Biotechnology 104, 6839-6854. DOI: 10.1007/s00253-020-10724-7.

Labed, V., Obeid, H. & Ressayre, K. (2013): Effect of relative humidity and temperature on PVC degradation under gamma irradiation: Evolution of HCl production Yields. Radiation Physics and Chemistry 84, 26-29. DOI: 10.1016/j.radphyschem.2012.06.052.

Lanyon, G.W. & Herbert, A.W. (2021): GAST: GPT1 interpretation report. Nagra Arbeitsbericht NAB 19-28.

Launay, A., Thominette, F. & Verdu, J. (1994): Hydrolysis of poly(ethylene terephthalate): a kinetic study. Polymer Degradation and Stability 46/3, 319-324. DOI: 10.1016/0141-3910(94)90148-1.

Le Caër, S. (2011): Water radiolysis: Influence of oxide surfaces on H_2 production under ionizing radiation. Water 3/1, 235-253. DOI: 10.3390/w3010235.

Lechner, M.D., Nordmeier, E.H. & Gehrke, K. (2010): Synthese von Makromolekülen, Polyreaktionen. *In:* Lechner, M. D., Nordmeier, E. H. & Gehrke, K. (ed.): Makromolekulare Chemie: Ein Lehrbuch für Chemiker, Physiker, Materialwissenschaftler und Verfahrenstechniker: Birkhäuser Basel. Basel, 48-170.

Leong, S.L., Pettersson, O.V., Rice, T., Hocking, A.D. & Schnürer, J. (2011): The extreme xerophilic mould *Xeromyces bisporus* -- Growth and competition at various water activities. International Journal of Food Microbiology 145/1, 57-63. DOI: 10.1016/j.ijfoodmicro.2010.11.025.

Lerke, I. & Szymański, W. (1983): Stabilization of gamma-irradiated poly(vinyl chloride) by epoxy compounds. II. Production of hydroperoxides in gamma-irradiated PVC–stabilizer mixtures. Journal of Applied Polymer Science 28/2, 513-518. DOI: 10.1002/app.1983.070280207.

Leschine, S.B. (1995): Cellulose degradation in anaerobic environments. Annual review of Microbiology 49/1, 399-426.

Leupin, O.X., Bernier-Latmani, R., Bagnoud, A., Moors, H., Leys, N., Wouters, K. & Stroes-Gascoyne, S. (2017): Fifteen years of microbiological investigation in Opalinus Clay at the Mont Terri rock laboratory (Switzerland). Swiss Journal of Geosciences, Special Issue: Mont Terri rock laboratory, 20 years of research 110, 343-354.

Leupin, O.X., Smith, P.A., Marschall, P., Johnson, L., Savage, D., Cloet, V., Schneider, J. & Senger, R.K. (2016a): Low- and intermediate-level waste repository-induced effects. Nagra Technical Report NTB 14-14.

Leupin, O.X., Zeyer, J., Cloet, V., Smith, P., Bernier-Latmani, R., Marschall, P., Papafotiou, A., Schwyn, B. & Stroes-Gascoyne, S. (2016b): An assessment of the possible fate of gas generated in a repository for low- and intermediate-level waste. Nagra Technical Report NTB 16-05.

Li, G.L., Zhou, C.H., Fiore, S. & Yu, W.H. (2019): Interactions between microorganisms and clay minerals: New insights and broader applications. Applied Clay Science 177, 91-113. DOI: 10.1016/j.clay.2019.04.025.

Liang, D.-W., Zhang, T., Fang, H.H.P. & He, J. (2008): Phthalates biodegradation in the environment. Applied Microbiology and Biotechnology 80, 183-198. DOI: 10.1007/s00253-008-1548-5.

Lloyd, J.R. & Cherkouk, A. (ed.) (2021): The Microbiology of Nuclear Waste Disposal. 1st Edition. Elsevier.

Lodge, T.E. & Hiemenz, P.C. (2020): Polymer Chemistry. 3rd Edition. CRC Press.

Lőrinc, I. (1966): Acceleration of the thermal decomposition of bitumen. Nature 212/5069. DOI: 10.1038/2121459a0.

Lovley, D.R. (2000): Anaerobic benzene degradation. Biodegradation/11, 107-116.

Lovley, D.R., Holmes, D.E. & Nevin, K.P. (2004): Dissimilatory Fe(III) and Mn(IV) reduction. Advances in microbial physiology 49, 219-286.

Macdonald, C., Ambrose, D., Brewer, A.J., Campbell, D.J.V., James, L. & Sopp, C. (1997): Investigations into the potential rate, composition and cumulative amount of gas generated from the biodegradation of simulated low-level waste. (NSS/R322). AEA Technology, Harwell, UK.

Madigan, M., Martinko, J., Bender, K., Buckley, D. & Stahl, D. (2015): Brock biology of microorganisms. 14th edition. Pearson, London.

Madigan, M.T., Bender, K.S., Buckley, D.H., Sattley, W.M. & Stahl, D.A. (2020): Brock Mikrobiologie. 15., aktualisierte Aufglage. Pearson Education Deutschland GmbH, Hallbergmoos, Germany.

Madorsky, S.L. (1964): Thermal degradation of organic polymers. Interscience Publishers.

Malavasi, I., Consolati, G., Quasso, F., Soccio, M., Gigli, M., Negrin, M., Macerata, E., Giacobbo, F., Lotti, N., Munari, A. & Mariani, M. (2016): Effect of gamma irradiation on poly(butylene naphthalate) based polyesters. Radiation Physics and Chemistry 124, 58-61. DOI: 10.1016/j.radphyschem.2015.11.034.

Mariani, M., Consolati, G., Quasso, F., Lotti, N., Munari, A., Galletta, M. & Macerata, E. (2010): Effects of gamma irradiation on poly(ethylene isophthalate). Journal of Radioanalytical and Nuclear Chemistry 286, 625-629. DOI: 10.1007/s10967-010-0778-z.

Mariani, M., Ravasio, U., Consolati, G., Buttafava, A., Giola, M. & Faucitano, A. (2007): Gamma irradiation of polyethyleneterephthalate and polyethylenenaphthalate. Nuclear Instruments and Methods in Physics Research Section B: Beam Interactions with Materials and Atoms 265/1, 245-250. DOI: 10.1016/j.nimb.2007.08.054.

Marshall, P., Lanyon, B., Gaus, I. & Rüedi, J. (2013): Gas transport processes at Mont Terri Test Site (EDZ and host rock) - Field results and conceptual understanding of self-sealing processes. FORGE Report D4.16 - Final. European Commission, Euroatom 7th Framework Programme.

Martin, J.W., Dickens, B., Waksman, D., Bentz, D.P., Byrd, W.E., Embree, E. & Roberts, W.E. (1987): Thermal degradation of poly(methyl methacrylate) at 50°C to 125°C. Journal of Applied Polymer Science 34/1, 377-393. DOI: 10.1002/app.1987.070340130.

Maset, E.R., Sidhu, S.H., Fisher, A., Heydon, A., Worsfold, P.J., cartwright, A.J. & Keith-Roach, M.J. (2006): Effect of organic co-contaminants on technetium and rhenium speciation and solubility under reducing conditions. Environmental Science & Technology 40/17, 5472-5477.

Matsui, T., Takano, T., Takayama, S., Ito, M. & Narisawa, I. (2002): Degradation of crosslinked polyethylene in water by gamma-irradiation. Radiation Physics and Chemistry 63/2, 193-200. DOI: 10.1016/S0969-806X(01)00229-8.

Mattimore, V. & Battista, J.R. (1996): Radioresistance of Deinococcus radiodurans: functions necessary to survive ionizing radiation are also necessary to survive prolonged dessication. Journal of Bacteriology 178/3, 633-637.

Mauclaire, L., McKenzie, J.A., Schwyn, B. & Bossart, P. (2007): Detection and cultivation of indigenous microorganisms in Mesozoic claystone core samples from the Opalinus Clay Formation (Mont Terri Rock Laboratory). Physics and Chemistry of the Earth, Parts A/B/C 32/1-7, 232-240. DOI: 10.1016/j.pce.2005.12.010.

Maul, J., Frushour, B.G., Kontoff, J.R., Eichenauer, H., Ott, K.-H. & Schade, C. (2014): Polystyrene and styrene copolymers. *In:* Ullmann's Encyclopedia of Industrial Chemistry: Wiley-VCH Verlag GmbH & Co. KGaA. Weinheim, Germany.

McNeill, I.C. (1997): Thermal degradation of polystyrene in different environments. Die Angewandte Makromolekulare Chemie 247/1, 179-195. DOI: 10.1002/apmc.1997.052470112.

Means, J.L., Kucak, T. & Crerar, D.A. (1980): Relative degradation rates of NTA, EDTA and DTPA and environmental implications. Environmental Pollution Serie B, Chemical and Physical 1/1, 45-60.

Merino, N., Aronson, H.S., Bojanova, D.P., Feyhl-Buska, J., Wong, M.L., Zhang, S. & Giovannelli, D. (2019): Living at the extremes: Extremophiles and the limits of life in a planetary context 10. DOI: 10.3389/fmicb.2019.00780.

Metcalfe, R., Watson S. P., Rees, J.H., Humphreys, P.N. & King, F. (2008): Gas generation and migration from a deep geological repository for radioactive waste. A review of Nirex/NDA's work. NWAT/NDA/RWMD/2008/002. (QSR-1223A-4 version 2, GEHO1108BOZN-E-E). Edited by Environment Agency, Bristol, UK.

Mijnendonckx, K., Bassil, N.M., Nixon, S., Boylan, A. & Leys, N. (2021): Chapter 10 - Organic materials and their microbial fate in radioactive waste. *In:* Lloyd, J. R. & Cherkouk, A. (ed.): The Microbiology of Nuclear Waste Disposal. 1st Edition: Elsevier, 213-244, status as of 2023-25-05.

Mijnendonckx, K., Small, J.S., Abrahamsen-Mills, L., Pedersen, K. & Leys, N. (2019): MIND project: Final integration and evaluation report. (D3.7).

Miller, A.A., Lawton, E.J. & Balwit, J.S. (1956): The radiation chemistry of hydrocarbon polymers: I. Polyethylene, polymethylene and octacosane. The Journal of Physical Chemistry B 60/5. DOI: 10.1021/j150539a021.

Mincher, B.J. & Mezyk, S.P. (2009): Radiation chemical effects on radiochemistry: A review of examples important to nuclear power. Radiochimica Acta 97/9, 519-534. DOI: 10.1524/ract.2009.1646.

Missana, T., García-Gutiérrez, M., Alonso, U. & Fernández, A.M. (2022): Effects of the presence of isosaccharinate on nickel adsorption by calcium silicate hydrate (CSH) gels: Experimental analysis and surface complexation modelling. Journal of Environmental Chemical Engineering 10/5. DOI: 10.1016/j.jece.2022.108500.

Mitzscherling, J., Genderjahn, S., Schleicher, A.M., bartholomäus, A., Kallmeyer, J. & Wagner, D. (2023): Clay-associated microbial communities and their relevance for a nuclear waste repository in the Opalinus Clay rock formation. MicrobiologyOpen 12/4, 1-23.

Mohanan, N., Montazer, Z., Sharma, P.K. & Levin, D.B. (2020): Microbial and enzymatic degradation of synthetic plastics 11. DOI: 10.3389/fmicb.2020.580709.

Mohanty, A.D., Tignor, S.E., Krause, J.A., Choe, Y.-K. & Bae, C. (2016): Systematic alkaline stability study of polymer backbones for anion exchange membrane applications. Macromolecules. 49/9. DOI: 10.1021/acs.macromol.5b02550.

Molecke, M. (1979): Gas generation from transuranic waste degradation, data summary and interpretation. Sand report 79-1245. Sandia National Laboratories, Alburquerque, NM, USA.

Molnár, M., Palcsu, L., Futó, I., Svingor, É., Major, Z., Veres, M., Ormai, P. & Barnabás, I. (2010): Study of gas generation in real L/ILW containers. Journal of Radioanalytical and Nuclear Chemistry 286, 745–750. DOI: 10.1007/s10967-010-0795-y.

Molnár, M., Palcsu, L., Svingor, É., Futó, I., Major, Z., Rinyu, L. & Veres, M. (2006): Isotope-analytical results of a study of gas generation in L/ILW. Czechoslovak Journal of Physics 56/Suppl. 4, D637-D644. DOI: 10.1007/s10582-006-0559-7.

Monod, J. (1949): The growth of bacterial cultures. Annual review of Microbiology 3, 371-394.

Montaudo, G., Puglisi, C. & Samperi, F. (1993): Primary thermal degradation mechanisms of PET and PBT. Polymer Degradation and Stability 42/1, 13-28. DOI: 10.1016/0141-3910(93)90021-A.

Moreno, L., Skagius, K., Södergren, S. & Wiborgh, M. (2001): Project SAFE: Gas related processes in SRF. R-01-11. SKB, Stockholm, Sweden.

Müller, V. (2003): Energy Conservation in Acetogenic Bacteria. Applied Environmental Microbiology 69, 9.

Müller, V. & Hess, V. (2017): The minimum biological energy quantum. Frontiers in Microbiology 8. DOI: 10.3389/fmicb.2017.02019.

Murthy, N., Wilson, S. & Sy, J.C. (2012): Biodegradation of polymers. Polymer science 9. DOI: 10.1016/B978-0-444-53349-4.00240-5.

Nagra (2004): Effects of post-disposal gas generation for spent fuel, high level waste and long lived Intermediate level waste sited in Opalinus Clay. Nagra Technical Report NTB 04-06.

Nagra (2016): Entsorgungsprogramm 2016 der Entsorgungspflichtigen. Nagra Technischer Bericht NTB 16-01 D.

Nagra (2021a): Entsorgungsprogramm 2021 der Entsorgungspflichtigen. Nagra Technischer Bericht NTB 21-01.

Nagra (2021b): The Nagra Research, Development and Demonstration (RD&D) Plan for the Disposal of Radioactive Waste in Switzerland. Nagra Technical Report NTB 21-02.

Nagra (2022a): Grundlagen des schweizerischen Lagerkonzepts für die geologische Tiefenlagerung aus Sicht Langzeitsicherheit. Nagra Arbeitsbericht NAB 21-29.

Nagra (2023a): Chemical criteria for waste group classification: A model approach. Nagra Arbeitsbericht NAB 23-28.

Nagra (2023b): Modellhaftes Inventar radioaktiver Materialien MIRAM-RBG. Nagra Technischer Bericht NTB 22-05.

Nagra (2024a, in prep.): Gas synthesis report. Nagra Technical Report NTB 24-023.

Nagra (2024b, in prep.): Phenomenological description of the evolution of a combined geological repository for radioactive waste at Nördlich Lägern in Opalinus Clay. Nagra Work Report NAB 24-20.

Nagra (2024c, in prep.): Rahmenbewilligungsgesuch geologisches Tiefenlager für radioaktive Abfälle der Schweiz: Argumentenbericht. Nagra Technischer Bericht NTB 24-02.

Nagy, T.T., Iván, B., Kelen, T., Turcsányi, B. & Tüdös, F. (1980a): Crosslinking and scission in thermooxidative degradation of PVC. Polymer Bulletin 2, 83-88. DOI: 10.1007/BF00275558.

Nagy, T.T., Iván, B., Turcsányi, B., Kelen, T. & Tüdös, F. (1980b): Crosslinking, scission and benzene formation during PVC degradation under various conditions. Polymer Bulletin 3, 613-620. DOI: 10.1007/BF01135332.

Nakamura, Y., Daidai, M. & Kobayashi, F. (2004): Ozonolysis mechanism of lignin model compounds and microbial treatment of organic acids produced. Water Science and Technology 50/3, 167-172. DOI: 10.2166/wst.2004.0188.

Nassoy, P., Scanlan, F.P., Muller, J.-F. & Kister, J. (1989): An analytical investigation of the thermal degradation of a cation-exchange resin — part 1. Journal of Analytical and Applied Pyrolysis 16/3, 255-268. DOI: 10.1016/0165-2370(89)80029-4.

NDA (2010): Geological disposal. Gast Status Report. NDA/RWMD/037. NDA, Oxford, UK.

NDA (2012): Geological disposal. Summary of NAPL studies March 2010. Technical Note no. 17779488. NDA, Oxford, UK.

NDA (2016): Geological disposal. Gas Status Report. DSSC/455/01. RWM, Oxford, UK.

Nealson, K.H., Inagaki, F. & Takai, K. (2005): Hydrogen-driven subsurface lithoautotrophic microbial ecosystems (SLiMEs): do they exist and why should we care? Trends in Microbiology 13/9, 405-410. DOI: 10.1016/j.tim.2005.07.010.

Negrin, M., Macerata, E., Consolati, G., Di Landro, L. & Mariani, M. (2018): Ionizing radiation effects on polymer biodegradation. Radiation Effects and Defects in Solids 173/9-10. DOI: 10.1080/10420150.2018.1528610.

Niemelä, K. (1990): The formation of hydroxy monocarboxylic acids and dicarboxylic acids by alkaline thermochemical degradation of cellulose. Journal of Chemical Technology & Biotechnology 48/1, 27-28. DOI: 10.1002/jctb.280480103.

Niemelä, K. & Sjöström, E. (1986): The conversion of cellulose into carboxylic acids by a drastic alkali treatment. Biomass 11/3, 215-221. DOI: 10.1016/0144-4565(86)90068-5.

Nixon, S.L., Bonsall, E. & Cockell, C.S. (2022): Limitations of microbial iron reduction under extreme conditions. FEMS microbiology reviews 46/6, 1-17.

Nixon, S.L., van Dongen, B.E., Boothman, C., Small, J.S. & Lloyd, J.R. (2018): Additives in plasticised polyvinyl chloride fuel microbial nitrate reduction at high pH: Implications for nuclear waste disposal. Frontiers in Environmental Science 6.
DOI: 10.3389/fenvs.2018.00097.

Nogi, Y. & Kato, C. (1999): Taxonomic studies of extremely barophilic bacteria isolated from the Mariana Trench and description of Moritella yayanosii sp. nov., a new barophilic bacterial isolate. Extremophiles 3/1, 71-77. DOI: 10.1007/s007920050101.

Norris, S., Lemy, F., Del Honeux, C.-A., Volckaert, G., Weetjens, E., Wouters, K., Wendling, J., Dymitrowski, M., Pellegrini, D., Sellin, P., Johnson, L., Sentis, M. & Harrington, J. (2013): Synthesis report: Updated treatment of gas generation and migration in the safety case. FORGE Report D31.5R. European Commission, Euroatom 7th Framework Programme.

Nzila, A. & Musa, M.M. (2021): Current knowledge and future challenges on bacterial degradation of the highly complex petroleum products asphaltenes and resins. Frontiers in Environmental Science 9. DOI: 10.3389/fenvs.2021.779644.

O'Flaherty, V., Mahony, T., O'Kennedy, R. & Colleran, E. (1998): Effect of pH on growth kinetics and sulphide toxicity thresholds of a range of methanogenic, syntrophic and sulphate-reducing bacteria. Process Biochemistry 33/5, 555-569. DOI: 10.1016/S0032-9592(98)00018-1.

O'Donnell, J.H. (1989): The effects of radiation on hig-technology polymers. Chapter 1: Radiation chemistry of polymers. American Chemical Society.

O'Donnell, J.H., Rahman, N.P., Smith, C.A. & Winzor, D.J. (1979): Crosslinking and scission yields for polystyrene subjected to gamma irradiation in vacuo. Journal of Polymer Science 17/12, 4081-4088. DOI: 10.1002/POL.1979.170171227.

Okamura, K. (1991): Structure of cellulose. In: Hon, D.N.-S. and Shiraishi, S. (eds.): Wood and Cellulosic Chemistry. pp. 89-112. Marcel Dekker Inc., New York and Basel, New York and Basel.

Onuaguluchi, O. & Banthia, N. (2017): Durability performance of polymeric scrap tire fibers and its reinforced cement mortar. Materials and Structures 50. DOI: 10.1617/s11527-017-1025-7.

Oren, A. (2005): A hundred years of Dunaliella research: 1905–2005. Saline Systems 1. DOI: 10.1186/1746-1448-1-2.

Pannekens, M., Voskuhl, L., Mohammadian, S., Köster, D., Meier, A., Köhne, J.M., Kulbatzki, M., Akbari, A., Haque, S. & Meckenstock, R.U. (2021): Microbial degradation rates of natural bitumen. Environmental Science & Technology 55/13, 8700-8708. DOI: 10.1021/acs.est.1c00596.

Papadopoulou, A., Hecht, K. & Buller, R. (2019): Enzymatic PET degradation. Chimia International Journal for Chemistry 73/9, 743-749. DOI: 10.2533/chimia.2019.743.

Papafotiou, A. & Senger, R.K. (2016): Sensitivity analyses of gas release from a L/ILW repository in the Opalinus Clay including the microbial consumption of hydrogen. Nagra Arbeitsbericht NAB 16-07.

Pardo-Rodríguez, M.L. & Zorro-Mateus, P.J.P. (2021): Biodegradation of polyvinyl chloride by Mucor s.p. and Penicillium s.p. isolated from soil. Revista de Investigación, Desarrollo e Innovación 11/2, 387-400. DOI: 10.19053/20278306.v11.n2.2021.12763.

Parkes, R.J., Cragg, B.A., Bale, S.J., Getlifff, J.M., Goodman, K., Rochelle, P.A., Fry, J.C., Weightman, A.J. & Harvey, S.M. (1994): Deep bacterial biosphere in Pacific Ocean sediments. Nature 371/6496, 410-413. DOI: 10.1038/371410a0.

Pavasars, I., Hagberg, J., Borén, H. & Allard, B. (2003): Alkaline degradation of cellulose: Mechanisms and kinetics. Journal of Polymers and the Environment 11, 39-47. DOI: 10.1023/A:1024267704794.

Pedersen, K., Motamedi, M., Karnland, O. & Sandén, T. (2000): Mixing and sulphate-reducing activity of bacteria in swelling, compacted bentonite clay under high-level radioactive waste repository conditions. Journal of Applied Microbiology 89/6, 1038-1047. DOI: 10.1046/j.1365-2672.2000.01212.x.

Peng, B.-Y., Chen, Z., Chen, J., Yu, H., Zhou, X., Criddle, C.S., Wu, W.-M. & Zhang, Y. (2020): Biodegradation of polyvinyl chloride (PVC) in Tenebrio molitor (Coleoptera: Tenebrionidae) larvae. Environment International 145.
DOI: 10.1016/j.envint.2020.106106.

Perdrial, J.N., Warr, L.N., Perdiral, N., Lett, M.-C. & Elsass, F. (2009): Interaction between smectite and bacteria: Implications fro bentonite as backfill material in the disposal of nuclear waste. Chemical Geology 264/1-4, 281-294.

Peterson, J.D., Vyazovkin, S. & Wight, C.A. (1999): Kinetic study of stabilizing effect of oxygen on thermal degradation of poly(methyl methacrylate). The Journal of Physical Chemistry B 103/38. DOI: 10.1021/jp991582d.

Peterson, J.D., Vyazovkin, S. & Wight, C.A. (2001): Kinetics of the thermal and thermo-oxidative degradation of polystyrene, polyethylene and poly(propylene). Macromolecular Chemistry and Physics 202/6, 775-784. DOI: 10.1002/1521-3935(20010301)202:6<775::AID-MACP775>3.0.CO;2-G.

Pikuta, E.V., Hoover, R.B. & Tang, J. (2007): Microbial extremophiles at the limits of life. Critical Reviews in Microbiology 33/3, 183-209. DOI: 10.1080/10408410701451948.

Pillay, K.K.S. (1986): The effects of ionizing radiations on synthetic organic ion exchangers. Journal of Radioanalytical and Nuclear Chemistry 97/1. DOI: 10.1007/BF02060420.

Plota, A. & Masek, A. (2020): Lifetime prediction methods for degradable polymeric materials—A short review. Materials. 13/20. DOI: 10.3390/ma13204507.

Poller, A., Mayer, G., Darcis, M. & Smith, P. (2016): Modelling of gas generation in deep geological repositories after closure. Nagra Technical Report NTB 16-04.

Ponomarev, A.V. & Ershov, B.G. (2018): Radiation-induced degradation of cellulose: From partial depolymerization to complete self-disassembly. Radiation Physics and Chemistry 152, 63-68. DOI: 10.1016/j.radphyschem.2018.07.004.

Povedano-Priego, C., Jroundi, F., Lopez-Fernandez, M., Shrestha, R., Spanek, R., Martin-Sanchez, I., Villar, M.V., Sevcu, A., Dopson, M. & Merroun, M.L. (2021): Deciphering indigenous bacteria in compacted bentonite through a novel and efficient DNA extraction method: Insights into biogeochemical processes within the Deep Geological Disposal of nuclear waste concept. Journal of Hazardous Materials 408.
DOI: 10.1016/j.jhazmat.2020.124600.

Qi, X., Ma, Y., Chang, H., Li, B., Ding, M. & Yuan, Y. (2021): Evaluation of PET degradation using artificial microbial consortia. Frontiers in Microbiology Sec. Microbiotechnology 12.

Rabie, S.M., Moharram, M.A. & Daghistani, A.Y. (1985): Infrared study of combined effect of γ-radiation and elevated temperature on poly(vinyl chloride). Journal of Applied Polymer Science 30/1, 279-287. DOI: 10.1002/app.1985.070300122.

Ranzi, E., Dente, M., Faravelli, T., Bozzano, G., Fabini, S., Nava, R., Cozzani, V. & Tognotti, L. (1997): Kinetic modeling of polyethylene and polypropylene thermal degradation. Journal of Analytical and Applied Pyrolysis 40-41, 305-319. DOI: 10.1016/S0165-2370(97)00032-6.

Rao, V. (2009): Radiation processing of polymers. Advances in polymer processing. DOI: 10.1533/9781845696429.3.402.

Read, J. & Witheoak, D. (2006): The shell bitumen handbook. H. RN. Vol. Fifth edition. Thomas Telford Publishing, London.

Rébufa, C., Traboulsi, A., Labed, V., Dupuy, N. & Sergent, M. (2015): Experimental design approach for identification of the factors influencing the γ-radiolysis of ion exchange resins. Radiation Physics and Chemistry 106, 223-234.
DOI: 10.1016/j.radphyschem.2014.07.020.

Reed, D.T. & Molecke, M.A. (1994): Generation of volatile organic compounds by alpha particle degradation of WIPP plastic and rubber material. Materials Research Society symposium proceedings 333, 233-240.

Rempfert, K.R., Miller, H.M., Bompard, N., Nothaft, D., Matter, J.M., Kelemen, P., Fierer, N. & Templeton, A.S. (2017): Geological and geochemical controls on subsurface microbial life in the Samail Ophiolite, Oman. Frontiers in Microbiology 8.
DOI: 10.3389/fmicb.2017.00056.

Rezende, J.R. de, Oldenburg, T.B.P., Korin, T., Richardson, W.D.L., Fustic, M., Aitken, C.M., Bowler, B.F.J., Sherry, A., Grigoryan, A., Voordouw, G., Larter, S.R., Head, I.M. & Hubert, C.R.J. (2020): Anaerobic microbial communities and their potential for bioenergy production in heavily biodegraded petroleum reservoirs. Environmental Microbiology 22/8, 3049-3065. DOI: 10.1111/1462-2920.14995.

Rizoulis, A., Steele, H.M., Morris, K. & Lloyd, J.R. (2012): The potential impact of anaerobic microbial metabolism during the geological disposal of intermediate-level waste. 76/8, 3261-3270.

Rizzato, C., Shcherbina, N. & Reiller, P.E. (2017): CAST: Compilation and comparaison of data on C14 from spent ion-exchange resins. (D4.8).

Rizzo, A., Bruni, S., Gessi, A., Marghella, G., Moretti, L., Telloli, C., Rizzato, C. & Luce, A. (2018): Morphological study of ionic exchange resins to support the C14 release investigation from radioactive wastes-EURATOM CAST project. Radiocarbon 60/6, 1809-1817.

Roffey, R. & Norqvist, A. (1991): Biodegradation of bitumen used for nuclear waste disposal. Experientia 47/6, 539-542. DOI: 10.1007/BF01949874.

Rosenwinkel, K.-H., Kroiss, H., Weiland, P., Seyfried, C.-F. & Dichtl, N. (2015): Anaerobtechnik: Abwasser-, Schlamm- und Reststoffbehandlung, Biogasgewinnung. 3., neu bearb. Aufl. 2015. Springer Berlin Heidelberg, Berlin, Heidelberg.

Rostami, R., Zarrebini, M., Mandegari, M., Mostofinejad, D. & Abtahi, S.M. (2020): A review on performance of polyester fibers in alkaline and cementitious composites environments. Construction and building materials 241. DOI: 10.1016/j.conbuildmat.2020.117998.

Rotif, F., Valcke, E., Boven, P., Ooms, H., Peeters, J. & Smets, S. (2006): Ageing of Eurobitumen bituminised radioactive waste under gamma irradiation. Materials Research Society symposium proceedings 932/471.

Roussel, E., Cambon-Bonavita, M.-A., Querellou, J., Cragg, B., Webster, G., Prieur, D. & Parkes, R. (2008): Extending the sub-sea-floor biosphere. SCIENCE 320, 1046. DOI: 10.1126/science.1154545.

Rout, S.P., Radford, J., Laws, A.P., Sweeney, F., Elmekawy, A., Gillie, L.J., Humphreys, P.N. & Janssen, P.J. (2014): Biodegradation of the alkaline cellulose degradation products generated during radioactive waste disposal. PLoS ONE 9/9, e107433. DOI: 10.1371/journal.pone.0107433.

Røy, H., Kallmeyer, J., Adhikari, R.R., Pockalny, R., Jørgensen, B.B. & D'Hondt, S. (2012): Aerobic microbial respiration in 86-Million-year-old deep-sea red clay. SCIENCE 336/6083, 922-925. DOI: 10.1126/science.1219424.

Ru, J., Huo, Y. & Yang, Y. (2020): Microbial degradation and valorization of plastic wastes. Frontiers in Microbiology Sec. Microbiotechnology 11. DOI: 10.3389/fmicb.2020.00442.

Ruckstuhl, S., Suter, M.J. & Giger, W. (2003): Sorption and mass fluxes of sulfonated naphthalene formaldehyde condensates in aquifers. Journal of Contaminant Hydrology 67/1-4, 1-12. DOI: 10.1016/S0169-7722(03)00090-1.

Ruckstuhl, S., Suter, M.J., Kohler, H.P. & Giger, W. (2002): Leaching and primary biodegradation of sulfonated naphthalenes and their formaldehyde condensates from concrete superplasticizers in groundwater affected by tunnel construction. Environmental Science & Technology 36/15, 3284-3289. DOI: 10.1021/es010297g.

Rydz, J., Sikorska, W., Kyulavska, M. & Christova, D. (2015): Polyester-based (bio)degradable polymers as environmentally friendly materials for sustainable development. International Journal of Molecular Sciences 16/1, 564-596. DOI: 10.3390/ijms16010564.

Salovey, R., Luongo, J.P. & Yager, W.A. (1969): On the irradiation of poly(vinyl chloride). macromolecules. 2/2, 198-200. DOI: 10.1021/ma60008a018.

Scanlan, F.P., Muller, J.-F., Ziegler, J.-M. & Fiquet, J.-M. (1989): An analytical investigation of the thermal degradation of a cation-exchange resin — part 2. Journal of Analytical and Applied Pyrolysis 16/3, 269-289. DOI: 10.1016/0165-2370(89)80030-0.

Scheirs, J., Camino, G. & Tumiatti, W. (2001): Overview of water evolution during the thermal degradation of cellulose. European polymer journal 37/5, 933-942. DOI: 10.1016/S0014-3057(00)00211-1.

Schink, B. (1997): Energetics of syntrophic cooperation in methanogenic degradation. Microbiology and Molecular Biology Reviews 61/2, 262-280. DOI: 10.1128/mmbr.61.2.262-280.1997.

Schink, B. & Stams, A.J.M. (2013): Syntrophism among prokaryotes. *In:* Rosenberg, E., DeLong, E. F., Lory, S., Stackebrandt, E. & Thompson, F. (ed.): The Prokaryotes: Prokaryotic Communities and Ecophysiology: Springer. Berlin, Heidelberg, Germany, 471-493.

Schink, B. & Stieb, M. (1983): Fermentative degradation of polyethylene glycol by a strictly anaerobic, gram-negative, nonsporeforming bacterium, Pelobacter venetianus sp. nov. Applied and Environmental Microbiology 45/6, 1905-1913. DOI: 10.1128/aem.45.6.1905-1913.1983.

Schulze-Makuch, D., Haque, S., Resendes de Sousa Antonio, M., Ali, D., Hosein, R., Song, Y.C., Yang, J., Zaikova, E., Beckles, D.N., Guinan, E., Lehto, H.J. & Hallam, S.J. (2011): Microbial life in a liquid asphalt desert. Astrobiology 11/3. DOI: 10.1089/ast.2010.0488.

Seguchi, T., Arakawa, K., Hayakawa, N. & Machi, S. (1981a): Radiation induced oxidative degradation of polymers—IV. Dose rate effects on chemical and mechanical properties. Radiation Physics and Chemistry 18/3-4, 671-678. DOI: 10.1016/0146-5724(81)90190-4.

Seguchi, T., Hashimoto, S., Arakawa, K., Hayakawa, N., Kawakami, W. & Kuriyama, I. (1981b): Radiation induced oxidative degradation of polymers—I: Oxidation region in polymer films irradiated in oxygen under pressure. Radiation Physics and Chemistry 17/4, 195-201. DOI: 10.1016/0146-5724(81)90331-9.

Semenenko (1973): Investigation of gaseous products of gamma radiolysis of polymers in irradiation with small doses. Soviet plastics/5.

Senger, R., Papafotiou, A. & Marschall, P. (2013): Gas related property distributions in the proposed host rock formations of the candidate siting regions in Northern Switzerland and in the Helvetic Zone. Nagra Arbeitsbericht, NAB 13-083, Nagra, Wettingen, Switzerland.

Shah, A.A., Hasan, F., Hameed, A. & Ahmed, S. (2008): Biological degradation of plastics: A comprehensive review. Biotechnology advances 26/3. DOI: 10.1016/j.biotechadv.2007.12.005.

Simon, J. & Kroneck, P.M.H. (2013): Microbial sulfite respiration. Advances in microbial physiology 62, 45-117. DOI: 10.1016/B978-0-12-410515-7.00002-0.

Šimon, P. & Valko, L. (1990): Kinetics of polymer degradation involving the splitting off of small molecules: Part 2—Thermal dehydrochlorination of PVC in an inert atmosphere. Polymer Degradation and Stability 29/3, 253-261. DOI: 10.1016/0141-3910(90)90037-8.

Skariyachan, S., Patil, A., Shankar, A., Manjunath, M., Bachappanavar, N. & S Vasist, K. (2018): Enhanced polymer degradation of polyethylene and polypropylene by novel thermophilic consortia of *Brevibacillus* sps. and *Aneurinibacillus* sp. screened from waste management landfills and sewage treatment plants. Polymer Degradation and Stability 149, 52-68. DOI: 10.1016/j.polymdegradstab.2018.01.018.

Small, J.S. (2019): Final synthesis report for MIND WP1. Microbiology In Nuclear waste Disposal (MIND). MIND D1.9. European Comission, Microbiology in Nuclear Waste Disposal.

Small, J.S., Abraitis, P.K., Beadle, I.R., Johnstone, K.P., Pettit, C.L. & Stevens, G.A. (2004): Scientific basis for nuclear waste management XXVII. Materials Research Society symposium proceedings 807, 905-910, available online at http://toc.proceedings.com/08002webtoc.pdf.

Small, J.S. & Dutton, M. (2009): Review of research on cellulose degradation and input data for the Simplified Model of Gas Generation (SMOGG). (Issue 3, NLL (09) 8870). National Nuclear Laboratory.

Small, J.S., Nykyri, M., Helin, M., Hovi, U., Sarlin, T. & Itävaara, M. (2008): Experimental and modelling investigations of the biochemistry of gas production from low and intermediate level radioactive waste. Applied Geochemistry 23, 1383-1418. DOI: 10.1016/j.apgeochem.2007.11.020.

Small, J.S., Nykyri, M., Paaso, N., Hovi, U., Itävaara, M. & Sarlin, T. (2006): Testing of a near-field biogeochemical model against data from a large-scale gas generation experiment. Materials Research Society symposium proceedings 932. DOI: 10.1557/PROC-932-116.1.

Small, J.S., Nykyri, M., Vikman, M., Itävaara, M. & Heikinheimo, L. (2017): The biogeochemistry of gas generation from low-level nuclear waste: Modelling after 18 years study under in situ conditions. Applied Geochemistry 84, 360-372. DOI: 10.1016/j.apgeochem.2017.07.012.

Smith, S.L., Rizoulis, A., West, J.M. & Lloyd, J.R. (2016): The microbial ecology of a hyper-alkaline spring, and impacts of an alkali-tolerant community during sandstone batch and column experiments representative of a geological disposal facility for intermediate-level radioactive waste. Geomicrobiology Journal 33/6, 455-467. DOI: 10.1080/01490451.2015.1049677.

Smith, V., Magalhaes, S. & Schneider, S. (2013): The role of PVC additives in the potential formation of NAPLs. Report to NDA RWMD. (AMEC/PPE-2834/001).

Sohma, J. (1983): Radical migration as an elementary process in degradation. Pure and Applied Chemistry 55/10, 1595-1601. DOI: 10.1351/pac198355101595.

Song, J., Fischer, C.-H. & Schnabel, W. (1992): Thermal oxidative degradation of poly(methyl methacrylate). Polymer Degradation and Stability 36/3, 261-266. DOI: 10.1016/0141-3910(92)90065-D.

Sorokin, D.Y. (2015): Is there a limit for high-pH life? International Journal of Systematic and Evolutionary Microbiology 55, 1405-1406. DOI: 10.1099/ijs.0.63737-0.

Sorokin, D.Y., Abbas, B., Merkel, A.Y., Rijpstra, W.I.C., Damsté, J.S.S., Sukhacheva, M.V. & van Loosdrecht, M.C.M. (2015): *Methanosalsum natronophilum* sp. nov., and *Methanocalculus alkaliphilus* sp. nov., haloalkaliphilic methanogens from hypersaline soda lakes. International Journal of Systematic and Evolutionary Microbiology 65/Pt_10, 3739-3745. DOI: 10.1099/ijsem.0.000488.

Speight, J.G. (2018): Chapter 6 - Hydrolysis. *In:* Speight, J. G. (ed.): Reaction Mechanisms in Environmental Engineering: Butterworth-Heinemann, 203-229, available online at https://www.sciencedirect.com/science/article/pii/B9780128044223000067.

Spinks, J.W.T. & Woods, R.J. (1990): An introduction to radiation chemistry. Third Edition. Wiley, University of Saskatchewan, Canada.

Starnes, W.H. (2002): Structural and mechanistic aspects of the thermal degradation of poly(vinyl chloride). Progress in Polymer Science 27/10, 2133-2170. DOI: 10.1016/S0079-6700(02)00063-1.

Steinle, L., Knittel, K., Felber, N., Casalino, C., Lange, G. de, Tessarolo, C., Stadnitskaia, A., Sinninghe Damsté, J.S., Zopfi, J., Lehmann, M.F., Treude, T. & Niemann, H. (2018): Life on the edge: active microbial communities in the Kryos $MgCl_{(2)}$-brine basin at very low water activity. The ISME Journal 12/6, 1414-1426. DOI: 10.1038/s41396-018-0107-z.

Stetter, K.O. (1988): *Archaeoglobus fulgidus* gen. nov., sp. nov.: A new taxon of extremely thermophilic Archaebacteria. Systematic and Applied Microbiology 10/2, 172-173. DOI: 10.1016/S0723-2020(88)80032-8.

Steuber, J. & Kroneck, P.M. (1998): Desulfoviridin, the dissimilatory sulfite reductase from Desulfovibrio desulfuricans (Essex): new structural and functional aspects of the membranous enzyme. Inorganica Chimica Acta 275-276, 52-57. DOI: 10.1016/S0020-1693(97)06143-4.

Stevenson, A., Cray, J.A., Williams, J.P., Santos, R., Sahay, R., Neuenkirchen, N., McClure, C.D., Grant, I.R., Houghton, J., Quinn, J.P., Timson, D.J., Patil, S.V., Singhal, R.S., Antón, J., Dijksterhuis, J., Hocking, A.D., Lievens, B., Rangel, D.E.N., Voytek, M.A., Gunde-Cimerman, N., Oren, A., Timmis, K.N., McGenity, T.J. & Hallsworth, J.E. (2015): Is there a common water-activity limit for the three domains of life? The ISME Journal 9/6, 1333-1351. DOI: 10.1038/ismej.2014.219.

Stone, W., Kroukamp, O., Korber, D.R., McKelvie, J. & Wolfaardt, G.M. (2016a): Microbes at surface-air interfaces: The metabolic harnessing of relative humidity, surface hygroscopicity, and oligotrophy for resilience. Frontiers in Microbiology 7. DOI: 10.3389/fmicb.2016.01563.

Stone, W., Kroukamp, O., McKelvie, J., Korber, D.R. & Wolfaardt, G.M. (2016b): Microbial metabolism in bentonite clay: Saturation, desiccation and relative humidity. Applied Clay Science 129, 54-64. DOI: 10.1016/j.clay.2016.04.022.

Stroes-Gascoyne, S., Francis, A.J. & Vilks, P. (1994): Microbial research. In: Cramer, J., Smelle, J.A.T. (Eds.), Final Report of the AECL/SKB Cigar Lake Analog Study. Atomic Energy of Canada Limited Report AECL-10851, also COG-93-147 and SKB TR-94-04, Swedish Nuclear Fuel and Waste Management Co, Stockholm, Sweden, pp. 261–265., 261-265.

Stroes-Gascoyne, S. & Hamon, C. (2013): Microbial gas production from superplasticizers in shotcrete. Nagra Work Report NAB 13-85.

Stroes-Gascoyne, S., Hamon, C.J., Maak, P. & Russell, S. (2010): The effects of the physical properties of highly compacted smectitic clay (bentonite) on the culturability of indigenous microorganisms. Applied Clay Science 47/1-2, 155-162. DOI: 10.1016/j.clay.2008.06.010.

Stroes-Gascoyne, S., Schippers, A., Schwyn, B., Poulain, S., Sergeant, C., Simonoff, M., Le Marrec, C., Altmann, S., Nagaoka, T., Mauclaire, L., McKenzie, J., Daumas, S., Vinsot, A., Beaucaire, C. & Matray, J.-M. (2007): Microbial community analysis of Opalinus Clay drill core samples from the Mont Terri Underground Research Laboratory, Switzerland. Geomicrobiology Journal 24/1, 1-17. DOI: 10.1080/01490450601134275.

Stroes-Gascoyne, S., Sergeant, S., Schippers, A., Hamon, C.J., Nèble, S., Vesvres, M.-H., Barsotti, V., Poulain, S. & Le Marrec, C. (2011): Biogeochemical processes in a clay formation in situ experiment: Part D - Microbial analyses - Synthesis of results. Applied Geochemistry 26/6, 980-989. DOI: 10.1016/j.apgeochem.2011.03.007.

Stumm, W. & Morgan, J.J. (1996): Aquatic Chemistry. Chemical Equilibria and Rates in Natural Waters. 3rd ed. John Wiley & Sons, New York, NY.

Sudhakar, Y.N., Selvakumar, M. & Bhat, D.K. (2022): Enhancement and investigation of biodegradability of poly(methyl methacrylate) and poly(vinyl chloride) by blending with cellulose derivatives. Polymer Bulletin 563, 1-19. DOI: 10.1007/s00289-022-04319-7.

Sultanov, K. & Turaev, A.S. (1996): Mechanism of the radiolytic transformation of cellulose. II. Cleavage of the glycosidic bonds. Chemistry of Natural Compounds 32, 728-733. DOI: 10.1007/BF01375125.

Sun, P., Mao, H., Fang, C. & Long, Y. (2022): Effect of hydraulic parameters of leachate treatment process on di(2-ethylhexyl) phthalate removal from aged leachate. Environmental Technology. DOI: 10.1080/09593330.2022.2029951.

Sunny, A.T., Thomas, S. & Yang, W. (2009): 1 - Recent advances in polymer processing: the state of the art, new challenges and opportunities. *In:* Thomas, S. & Yang, W. (ed.): Advances in Polymer Processing. From Macro- to Nano- Scales: Woodhead Publishing, 3-12.

Swift, B.T. (2016): Specification for SMOGG Version 7.0. A simplified model of gas generation from radioactive wastes. (RWM007409). Radioactive Waste Management.

Swyler, K.J., Dodge, C.J. & Dayal, R. (1983): Irradiation effects on the storage and disposal of radwaste containing organic ion-exchange media. 3 functional forms of resin - sulfonic acid cation exchanger, quarternary ammonium anion exchanger and mixed bed combination of the two NUREG/CR--3383. Brookhaven National Laboratory, Upton, NY, USA.

Szymański, W. & Śmietańska, G. (1979): Synergistic effect in gamma-irradiated poly(vinyl chloride) hard foils stabilized by plasticizer–stabilizer systems. Journal of Applied Polymer Science 23/3, 791-795. DOI: 10.1002/app.1979.070230314.

Tabata, Y., Oshima, A., Kazunobu, T. & Tadao, S. (1996): Temperature effects on radiation induced phenomena in polymers. Radiation Physics and Chemistry 48/5, 563-568.

Taiz, L., Zeiger, E., Moller, I.M. & Murphy, A. (ed.) (2014): Plant Physiology and Development. 6th ed. Sinauer Associates, Sunderland, Massachusetts, USA.

Takács, E., Wojnárovits, L., Földváry, C., Hargittai, P., Borsa, J. & Sajó, I. (2000): Effect of combined gamma-irradiation and alkali treatment on cotton–cellulose. Radiation Physics and Chemistry 57/3-6, 399-403. DOI: 10.1016/S0969-806X(99)00409-0.

Takai, K., Moser, D., Onstott, T., Spoelstra, N., Pfiffner, S., Dohnalkova, A. & Fredrickson, J. (2001): Alkaliphilus transvaalensis gen. nov., sp. nov., an extremely alkaliphilic bacterium isolated from a deep South African gold mine. International Journal of Systematic and Evolutionary Microbiology 51/4. DOI: 10.1099/00207713-51-4-1245.

Talandier, J. (2005): La production et le transfert de gaz dans un stockage et dans la couche du Callovo-Oxfordien - Lien avec le transitoire hydraulique - Site de Meuse/Haute-Marne. Rapport Andra n°C NT ASCCM 03-0042. Andra, Paris, France.

Tasi, A., Gaona, X., Fellhauer, D., Böttle, M., Rothe, J., Dardenne, K., Polly, R., Grivé, M., Colàs, E., Bruno, J., Källström, K., Altmaier, M. & Geckeis, H. (2018a): Thermodynamic description of the plutonium – α-d-isosaccharinic acid system I: Solubility, complexation and redox behavior. Applied Geochemistry 98, 247-264.
DOI: 10.1016/j.apgeochem.2018.04.014.

Tasi, A., Gaona, X., Fellhauer, D., Böttle, M., Rothe, J., Dardenne, K., Polly, R., Grivé, M., Colàs, E., Bruno, J., Källstrom, K., Altmaier, M. & Geckeis, H. (2018b): Thermodynamic description of the plutonium – α–d–isosaccharinic acid system ii: Formation of quaternary Ca(II)–Pu(IV)–OH–ISA complexes. Applied Geochemistry 98, 351-366. DOI: 10.1016/j.apgeochem.2018.06.014.

Tiago, I. & Veríssimo, A. (2013): Microbial and functional diversity of a subterrestrial high pH groundwater associated to serpentinization: Microbial and functional diversity of subsurface aquifer. Environmental Microbiology 15/6, 1687-1706. DOI: 10.1111/1462-2920.12034.

Tian, Y.Q., Chen, L.M., Gao, L.H., Michel, F.C., Wan, C.X., Li, Y.B. & Dick, W.A. (2012): Composting of waste paint sludge containing melamine resin as affected by nutrients and gypsum addition and microbial inoculation. Environmental Pollution 162, 129-137. DOI: 10.1016/j.envpol.2011.10.001.

Tissot, C., Grdanovska, S., Barkatt, A., Silverman, J. & Al-Sheikhly, M. (2013): On the mechanisms of the radiation-induced degradation of cellulosic substances. Radiation Physics and Chemistry 84, 185-190. DOI: 10.1016/j.radphyschem.2012.06.020.

Tits, J. & Kunz, D. (2020): The Nagra Gas Monitoring Experiment (GME) at Zwilag: Status Report 2020. (TM-44-21-03). PSI, Nuclear energy and safety research department, Laboratory for Waste Management, Villigen.

Tor, J.M. & Lovley, D.R. (2001): Anaerobic degradation of aromatic compounds coupled to Fe(III) reduction by *Ferroglobus placidus*. Environmental Microbiology 3/4, 281-287. DOI: 10.1046/j.1462-2920.2001.00192.x.

Torikai, A. (1994): Photo- and radiation-induced degradation of synthetic polymers: Polymer structure and stability. Die Angewandte Makromolekulare Chemie 216/1, 225-241. DOI: 10.1002/apmc.1994.052160115.

Torikai, A. & Fueki, K. (1985): Elementary processes in the radiation-induced degradation of poly(ethylene terephthalate)—A note. Polymer Degradation and Stability 13/2, 183-189. DOI: 10.1016/0141-3910(85)90067-9.

Torikai, A., Geetha, R., Nagaya, S. & Fueki, K. (1986): Radiation-induced degradation of polyethylene: Role of amorphous region in the formation of oxygenated products and the mechanical properties. Polymer Degradation and Stability 16/2, 199-212. DOI: 10.1016/0141-3910(86)90064-9.

Torikai, A., Murata, T. & Fueki, K. (1984): Radiation-induced degradation of polycarbonate: Electron spin resonance and molecular weight measurements. Polymer Degradation and Stability 7/1, 55-64. DOI: 10.1016/0141-3910(84)90030-2.

Toste, A.P. (1999): Detailed study of the γ-radiolysis of nitrilotriacetic acid in a simulated, mixed nuclear waste. Journal of Radioanalytical and Nuclear Chemistry 239, 433-439. DOI: 10.1007/BF02349046.

Toste, A.P., Polach, K.J. & White, T.W. (1994): Degradation of citric acid in a simulated, mixed nuclear waste: Radiolytic versus chemical forces. Waste Management 14/1, 27-34. DOI: 10.1016/0956-053X(94)90018-3.

Traboulsi, A., Dupuy, N., Rebufa, C., Sergent, M. & Labed, V. (2012): Investigation of gamma radiation effect on the anion exchange resin Amberlite IRA-400 in hydroxide form by Fourier transformed infrared and ^{13}C nuclear magnetic resonance spectroscopies. Analytica Chimica Acta 717, 110-121. DOI: 10.1016/j.aca.2011.12.046.

Traboulsi, A., Labed, V., Dauvois, V., Dupuy, N. & Rebufa, C. (2013): Gamma radiation effect on gas production in anion exchange resins. Nuclear Instruments and Methods in Physics Research Section B: Beam Interactions with Materials and Atoms 312, 7-14. DOI: 10.1016/j.nimb.2013.06.021.

Trutschel, L.R., Chadwick, G.L., Kruger, B., Blank, J.G., Brazelton, W.J., Dart, E.R. & Rowe, A.R. (2022): Investigation of microbial metabolisms in an extremely high pH marine-like terrestrial serpentinizing system: Ney Springs. Science of the Total Environment 836. DOI: 10.1016/j.scitotenv.2022.155492.

Tulupov, P.E. & Polyanskii, N.G. (1973): Thermal stability of anion-exchange resins. Russian Chemical Reviews 42/9. DOI: 10.1070/RC1973v042n09ABEH002730.

Valcke, E., Bleyen, N. & Mariën, A. (2022): The long-term behaviour of Eurobitum bituminised radioative waste in geological disposal conditions. Integration report - Status December 2014 SCK CEN/41023459. SCK-CEN, Mol, Belgium.

Valcke, E., Bleyen, N. & Smets, S. (2017): Ageing and radiolytic gas generation in Eurobitum bituminised radioactive waste. Topical report - status 2014 SCK CEN/26529773. SCK-CEN, Mol, Belgium.

Valcke, E., Rorif, F. & Smets, S. (2009): Ageing of EUROBITUM bituminised radioactive waste: An ATR-FTIR spectroscopy study. Journal of Nuclear Materials 393/1, 175-185. DOI: 10.1016/j.jnucmat.2009.06.001.

Valcke, E., Sneyers, A. & van Iseghem, P. (2001): The effect of radiolytic degradation products of Eurobitum on the solubility and sorption of Pu and Am in Boom Clay. Materials Research Society symposium proceedings 663. DOI: 10.1557/PROC-663-141.

van Loon, L.R. & Glaus, M. (1998): Experimental and theroritical studies on alkaline degradation of cellulose and its impact on the sorption of radionuclides. Nagra Technical Report NTB 97-04.

van Loon, L.R. & Glaus, M.A. (1997): Review of the kinetics of alkaline degradation of cellulose in view of its relevance for safety assessment of radioactive waste repositories. Journal of Environmental Polymer Degradation 5, 97-109. DOI: 10.1007/bf02763593.

van Loon, L.R., Glaus, M.A., Laube, A. & Stallone, S. (1999): Degradation of cellulosic materials under the alkaline conditions of a cementitious repository for low- and intermediate-level radioactive waste. II. Degradation kinetics. Journal of Environmental Polymer Degradation 7, 41-51. DOI: 10.1023/A:1021894102937.

van Loon, L.R. & Hummel, W. (1995): The radiolytic and chemical degradation of organic ion exchange resins under alkaline conditions: Effect on radionuclide speciation. PSI Bericht Nr. 95-13. Paul Scherrer Institute, Villigen, Switzerland.

van Loon, L.R. & Hummel, W. (1999a): Radiolytic and chemical degradation of strong acidic ion-exchange resins: Study of the ligands formed. Nuclear Technology 128/3, 359-371. DOI: 10.13182/nt99-a3037.

van Loon, L.R. & Hummel, W. (1999b): The degradation of strong basic anion exchange resins and mixed-bed ion-exchange resins: Effect of degradation products on radionuclide speciation. Nuclear Technology 128/3, 388-401. DOI: 10.13182/nt99-a3039.

van Loon, L.R. & Kopajtic, Z. (1991): Complexation of Cu^{2+}, Ni^{2+} and UO_2^{2+} by radiolytic degradation products of bitumen. Radiochimica Acta 54/4, 193-200. DOI: 10.1524/ract.1991.54.4.193.

van Speybroeck, V., Martelé, Y., Waroquier, M. & Schacht, E. (2001): Ab initio and experimental study on thermally degradable polycarbonates: The effect of substituents on the reaction rates. Journal of the American Chemical Society 123/43, 10650-10657. DOI: 10.1021/ja004075e.

VanBriesen, J.M., Rittmann, B.E., Xun, L., Girvin, D.C. & Bolton, H. (2000): The rate-controlling substrate of nitrilotriacetate for biodegradation by Chelatobacter heintzii. Environmental Science & Technology 34/16, 3346-3353.

Vercammen, K., Glaus, M.A. & van Loon, L.R. (2001): Complexation of Th(IV) and Eu(III) by α-isosaccharinic acid under alkaline conditions. Radiochimica Acta 89/6, 393-401. DOI: 10.1524/ract.2001.89.6.393.

Vikman, M., Marjamaa, K., Nykyri, M., Small, J.S., Miettinen, H., Heikinheimo, L., Haavisto, T. & Itävaara, M. (2019): The biogeochemistry of gas generation from low-level nuclear waste: Microbiological characterization during 18 years study under in situ conditions. Applied Geochemistry 105, 55-67. DOI: 10.1016/j.apgeochem.2019.04.002.

Vinhas, G.M., Souto Maior, R.M. & Almeida, Y.M.B. (2004a): Radiolytic degradation and stabilization of poly(vinyl chloride). Polymer Degradation and Stability 83/3, 429-433. DOI: 10.1016/j.polymdegradstab.2003.08.005.

Vinhas, G.M., Souto-Maior, R.M., Almeida, Y.M. de & Neto, B.B. (2004b): Radiolytic degradation of poly(vinyl chloride) systems. Polymer Degradation and Stability 86/3, 431-436. DOI: 10.1016/j.polymdegradstab.2004.05.013.

Vinhas, G.M., Souto-Maior, R.M., Lapa, C.M. & Almeida, Y.M.B. (2003a): Degradation studies on plasticized PVC films submited to gamma radiation. Materials Research 6/4, 497-500. DOI: 10.1590/S1516-14392003000400012.

Vinhas, G.M., Souto-Maior, R.M., Lapa, C.M. & Almeida, Y.M.B. de (2003b): Degradation studies on plasticized PVC films submited to gamma radiation. Materials Research 6/4, 497-500.

Vugrin, E., Nemer, M.B. & Wagner, S. (2015): Uncertainties affecting MgO effectiveness and calculation of the MgO effectiveness excess factor. (WIPP:1.4.1.2:PA:QA-L:543261). Sandia National Laboratories Waste Isolation Pilot Plant.

Wagner, A., Whitaker, R.J., Krause, D.J., Heilers, J.-H., van Wolferen, M., van der Does, C. & Albers, S.-V. (2017): Mechanisms of gene flow in archaea. Nature Reviews Microbiology 15/8, 492-501. DOI: 10.1038/nrmicro.2017.41.

Walczak, I., Libert, M.-F., Camaro, S. & Blanchard, J.-M. (2001): Quantitative and qualitative analysis of hydrosoluble organic matter in bitumen leachates. Agronomie 21/3, 247-257. DOI: 10.1051/agro:2001121.

Wang, J. & Wan, W. (2015): Treatment and disposal of spent radioactive ion-exchange resins produced in the nuclear industry. Progress in Nuclear Energy 78, 47-55. DOI: 10.1016/j.pnucene.2014.08.003.

Wang, Q., Jiang, L., Fang, C., Mao, H. & Zhuang, H. (2020a): Transformation of phthalic acid diesters in an anaerobic/anoxic/oxic leachate treatment process. Chinese Journal of Chemical Engineering 28/1, 249-253. DOI: 10.1016/j.cjche.2019.07.005.

Wang, Y. & Brush, L. (ed.) (1996): Estimates of gas-generation parameters for the long-term WIPP performance assessment. ERMS 231943. Memorandum to Martin S. Tierney. Albuquerque, NM, January 26. Sandia National Laboratories.

Wang, Y.-W., Hess, J., Slot, J.C. & Pringle, A. (2020b): De novo gene birth, horizontal gene transfer, and gene duplication as sources of new gene families associated with the origin of symbiosis in Amanita. Genome Biology and Evolution 12/11, 2168-2182. DOI: 10.1093/gbe/evaa193.

Wani, A.K., Akhtar, N., Sher, F., Navarrete, A.A. & Américo-Pinheiro, J.H.P. (2022): Microbial adaptation to different environmental conditions: molecular perspective of evolved genetic and cellular systems. Archives of Microbiology 204. DOI: 10.1007/s00203-022-02757-5.

Wanner, U., Kemmler, J., Weilenmann, H.-U., Egli, T., El-Banna, T. & Auling, G. (1990): Isolation and growth of a bacterium able to degrade nitriloacetic acid under denitrifying conditions. Biodegradation 1, 31-41.

Warthmann, R., Mosberger, L. & Baier, U. (2013): Langzeit-Degradation von organischen Polymeren unetr SMA-Tiefenlagerbedingungen. Nagra Technischer Bericht NTB 13-04.

Watkins, A.J., Roussel, E.G., Webster, G., Parkes, R.J. & Sass, H. (2012): Choline and n,n-dimethylethanolamine as direct substrates for methanogens. Applied and Environmental Microbiology 78/23, 8298-8303. DOI: 10.1128/AEM.01941-12.

Webb, H. (2012): Biodegradation of poly (ethylene terephthalate) by marine bacteria, and strategies for its enhancement. PhD thesis. Swinburne University of Technology, Melbourne, Australia. Environmental and Biotechnology Centre, Faculty of Life and Social Sciences.

Wersin, P., Johnson, L., Schwyn, B., Berner, U. & Curti, E. (2003): Redox conditions in the near field of repository for SF/HLW and ILW in Opalinus Clay. Nagra Technischer Bericht NTB 02-13.

Wersin, P., Mazurek, M. & Gimmi, T. (2022): Porewater chemistry of Opalinus Clay revisited: Findings from 25 years of data collection at the Mont Terri Laboratory. Applied Geochemistry 138, 105234.

Wersin, P., Stroes-Gascoyne, S., Pearson, F.J., Tournassat, C., Leupin, O.X. & Schwyn, B. (2011): Biogeochemical processes in a clay formation in situ experiment: Part G – Key interpretations and conclusions. Implications for repository safety. Applied Geochemistry 26/6, 1023-1034. DOI: 10.1016/j.apgeochem.2011.03.010.

Whitman, W.B., Coleman, D.C. & Wiebe, W.J. (1998): Prokaryotes: the unseen majority. Proceedings of the National Academy of Sciences of the United States of America 95/12, 6578-6583. DOI: 10.1073/pnas.95.12.6578.

Wiborgh, M., Höglund, L.O. & Pers, K. (1986): Gas formation in a L/ILW repository and gas transport in the host rock. Nagra Technical Report NTB 85-17.

Wieland, E. & Hummel, W. (2015): Formation and stability of ^{14}C-containing organic compounds in alkaline iron-water systems: preliminary assessment based on a literature survey and thermodynamic modelling. The Mineralogical Magazine 79/6, 1275-1286. DOI: 10.1180/minmag.2015.079.6.03.

Wieland, E. & Kosakowski, G. (2020): Review of the compositions of hydrated cements and cement-type pore water at different stages of the cement degradation. Nagra Wrok Report NAB 20-12.

Wieland, E., Kosakowski, G., Lothenbach, B., Kulik, D.A. & Cloet, V. (2018): Preliminary assessment of the temporal evolution of waste packages in the near field of a L/ILW repository. Nagra Work Report NAB 18-05.

Winter, I.U. & Cooney, C.L. (1980): Fermentation of cellulose and fatty acids with enrichments from sewage sludge. European Journal of Microbiology and Biotechnology 11, 60-66.

Wolf, M. & Bachofen, R. (1991a): Microbial degradation of bitumen matrix used in nuclear waste repositories. The Science of Nature 78/9, 414-417. DOI: 10.1007/BF01133415.

Wolf, M. & Bachofen, R. (1991b): Microbial degradation of bitumen. Experientia 47, 542-548. DOI: 10.1007/BF01949875.

Wormald, R.M., Rout, S.P., Mayes, W., Gomes, H. & Humphreys, P.N. (2020): Hydrogenotrophic methanogenesis under alkaline conditions. Frontiers in Microbiology Sec. Microbiotechnology 11, 1-9. DOI: 10.3389/fmicb.2020.614227.

Wu, Q., Tao, H. & Wong, M.H. (2019): Feeding and metabolism effects of three common microplastics on Tenebrio molitor L. Environmental Geochemistry and Health 41, 17-26. DOI: 10.1007/s10653-018-0161-5.

Yan, F., Wei, R., Cui, Q., Bornscheuer, U.T. & Liu, Y.-J. (2021): Thermophilic whole-cell degradation of polyethylene terephthalate using engineered *Clostridium thermocellum*. Microbial Biotechnology Special Issue on Advances in Microbial Biotechnology in China 14/2, 374-385. DOI: 10.1111/1751-7915.13580.

Yan, N., Marschner, P., Cao, W., Zuo, C. & Qin, W. (2015): Influence of salinity and water content on soil microorganisms. International Soil and Water Conservation Research 3/4, 316-323. DOI: 10.1016/j.iswcr.2015.11.003.

Yang, H., Yan, R., Chen, H., Lee, D.H. & Zheng, C. (2007): Characteristics of hemicellulose, cellulose and lignin pyrolysis. Fuel 86/12-13, 1781-1788. DOI: 10.1016/j.fuel.2006.12.013.

Yang, L., Muhadesi, J.-B., Wang, M.-M., Wang, B.-J., Liu, S.-J. & Jiang, C.-Y. (2018): Thauera hydrothermalis sp. nov., a thermophilic bacterium isolated from hot spring. International Journal of Systematic and Evolutionary Microbiology 68/10, 3163-3168. DOI: 10.1099/ijsem.0.002960.

Yang, Y., Wang, J. & Xia, M. (2020): Biodegradation and mineralization of polystyrene by plastic-eating superworms Zophobas atratus. Science of the Total Environment 708. DOI: 10.1016/j.scitotenv.2019.135233.

Yang, Y., Yang, J., Wu, W.-M., Zhao, J., Song, Y., Gao, L., Yang, R. & Jiang, L. (2015): Biodegradation and mineralization of polystyrene by plastic-eating mealworms: Part 1. Chemical and physical characterization and isotopic tests. Environmental Science & Technology 49/20, 12080-12086.

Yilmaz, V.T., Odabaoğlu, M., İçbudak, H. & Ölmez, H. (1993): The degradation of cement superplasticizers in a high alkaline solution. Cement and Concrete Research 23/1, 152-156. DOI: 10.1016/0008-8846(93)90146-Z.

Yin, C.R., Di Seo, Kim, M.K. & Lee, S.T. (2000): Inhibitory effect of hardwood lignin on acetate-utilizing methanogens in anaerobic digester sludge. Biotechnology Letters 22, 1531-1535. DOI: 10.1023/A:1005620726731.

Yu, J., Sun, L., Ma, C., Qiao, Y. & Yao, H. (2016): Thermal degradation of PVC: A review. Waste Management 48, 300-314. DOI: 10.1016/j.wasman.2015.11.041.

Zaikov, G.E. & Livshits, V.S. (1984): The mechanism of chemical degradation of polymers: Part I—Quantitative prediction of hydrolytic stability of polyesters. Polymer Degradation and Stability 9/1, 41-50. DOI: 10.1016/0141-3910(84)90083-1.

Zhang, H., Lin, X., Chin, S. & Grinstaff, M.W. (2015): Synthesis and characterization of poly(glyceric acid carbonate): A degradable analogue of poly(acrylic acid). Journal of the American Chemical Society 137/39, 12660-12666. DOI: 10.1021/jacs.5b07911.

Zhang, Z., Peng, H., Yang, D., Zhang, G., Zhang, J. & Ju, F. (2022): Polyvinyl chloride degradation by a bacterium isolated from the gut of insect larvae. Nature Communications 13. DOI: 10.1038/s41467-022-32903-y.

Zwicker, J., Birgel, D., Bach, W., Richoz, S., Smrzka, D., Grasemann, B., Gier, S., Schleper, C., Rittmann, S.-M., Koşun, E. & Peckmann, J. (2018): Evidence for archaeal methanogenesis within veins at the onshore serpentinite-hosted Chimaera seeps, Turkey. Chemical Geology 483, 567-580. DOI: 10.1016/j.chemgeo.2018.03.027.

App. A L/ILW organics, associated chemical formulae, group and mass

Adapted from Nagra (2023b). Based on the waste package inventory.

Materials	Chemical formulae	Group	Total mass (kg)
Cationic IERs (polystyrene / sulphonate groups)	$C_8H_7SO_3Na$	O2	6.2E+05
PVC	C_2H_3Cl	O2	5.9E+05
Anionic IERs (polystyrene / quaternary amino groups)	$C_{11}H_{16}NCl$	O2	4.0E+05
Bitumen	$C_{160}H_{200}ONS_2$	O2	3.5E+05
Polystyrene (including styrene and polystyrene/divinylbenzol)	$(C_8H_8)_n$	O2	1.1E+05
Plastic	C_2H_4	O2	9.1E+04
Cellulose (including cotton)	$C_6H_{10}O_5$	O1a	6.8E+04
Plexiglas	$C_5H_8O_2$	O2	3.4E+04
Polyethylene	$(C_2H_4)n$	O2	3.0E+04
Polyester	$C_{15}H_{16}O_2$	O1a	2.8E+04
Diethanol amine	$C_4H_{11}NO_2$	O1b	2.7E+04
Polycarboxylate	$C_3H_3O_2Na$	O2	2.4E+04
Rubber	C_4H_4	O2	2.3E+04
Urea	CH_4N_2O	O1b	1.8E+04
Ethylenediaminetetraacetic acid	$C_{10}H_{14}N_2O_8Na_2$	O1b	1.4E+04
Polypropylene	$(C_3H_6)n$	O2	1.4E+04
Gluconic acid	$C_6H_{12}O_7$	O1b	1.3E+04
Epoxyphenollac	$C_{18}H_{20}O_3$	O2	8.4E+03
Formaldehyde	CH_2O	O1b	8.3E+03
Polyacrylamid	C_3H_5NO	O2	8.1E+03
Tartaric acid	$C_4H_6O_6$	O1b	6.3E+03
Na-dimethyldithiocarbamat	$C_3H_6NS_2Na$	O1b	5.9E+03
Laurylamine PE Glycolether	$C_{22}H_{49}O_6N$	O1b	5.5E+03
Surfactants	n.a.	O1b	3.1E+03
Methanol	CH_3OH	O1b	2.9E+03
Naphtalinsulphonate	$C_{10}H_7SO_3Na$	O2	2.7E+03
Ethylen glycol	$C_2H_6O_2$	O1b	2.3E+03
Melamine resin	$C_3H_6N_6$	O2	1.4E+03
Tributylphosphate	$C_{12}H_{27}O_4P$	O1b	1.2E+03
Palmitin acid	$C_{16}H_{32}O_2$	O1b	1.1E+03
Butyl diglycol	$C_8H_{18}O_3$	O1b	6.4E+02
Benzyl alcohol	C_7H_8O	O1b	6.4E+02
Distearyl dimethyl ammonium Cl	$C_{38}H_{80}ClN$	O1b	4.0E+02
Nylon	$C_{12}H_{22}N_2O_2$	O2	3.7E+02
Diethylenglycol	$C_4H_{10}O_3$	O1b	3.1E+02
Sodium citrate	$C_6H_5O_7Na_3$	O1b	3.0E+02

Materials	Chemical formulae	Group	Total mass (kg)
Melamine / Formaldehyde sulphonate	$C_9H_{17}O_8N_6SNa$	O1a	3.0E+02
Lignin sulphonate	$C_{11}H_{14}O_7SNa$	O2	1.8E+02
Oil	C_8H_{16}	O1b	9.5E+01
Isopropanol	C_3H_8O	O1b	8.6E+01
Hexamethylentetramine	$C_6H_{12}N_4$	O1b	5.6E+01
Detergents	$C_{23}H_{39}O_3SNa$	O1b	2.9E+01
Nitrilotriacetic acid	$C_6H_6NO_6Na_3$	O1b	2.2E+00
Total mass (kg)			2.5E+06

App. B Gas Monitoring Experiment

In 2015, Nagra started the Gas Monitoring Experiment (GME) at Zwilag (Swiss interim storage facility in Würenlingen). It is a long-term monitoring experiment investigating gas generation from the degradation of organic materials under conditions relevant for deep geological disposal.

The GME is a large-scale experiment consisting of four 200 L steel drums filled with OPA porewater and organic materials expected to be predominantly present in the Swiss L/ILW inventory and an empty reference drum. The five drums were stored without a lid and placed in gas-tight, heatable outer containers. Pressure and temperature in all outer containers are constantly monitored with digital sensors. At regular time intervals (i.e., four times a year), 50 mL of gas are sampled and analysed for quantifying N_2, O_2, CO_2, H_2, CH_4, C_2H_6 and HCs (i.e., C_2H_4, C_3H_6, C_3H_8, C_4H_{10}, C_5H_{12}).

B.1 Gas evolution in Drum #1

Drum #1 contains powder IERs as organic material. The gas evolution with time showed a relatively stable N_2 concentration over the first 1200 days, followed by a slow decrease. The O_2 initially present in the gas phase sharply dropped to zero after between ~ 300 and 400 days of reaction time (Fig. B-1). After 400 days, the conditions remained anoxic. CO_2 showed an increase during the first ~ 350 days and has stayed constant throughout the further course of the experiment. It should be noted that the CO_2 concentration seemed to increase as long as O_2 was present (Fig. B-1). Once all the O_2 was consumed, the CO_2 concentration remained constant, suggesting that the CO_2 was produced by aerobic respiration. In comparison with the other gases, the concentration of CH_4 is pretty low (Fig. B-1). CH_4 increased with time, following a two-step process with a faster gas formation rate followed by a slower one. The transition from the fast to the slower step seemed to occur after approximately 400 days, coinciding with the depletion of the O_2 in the gas phase (Fig. B-1).

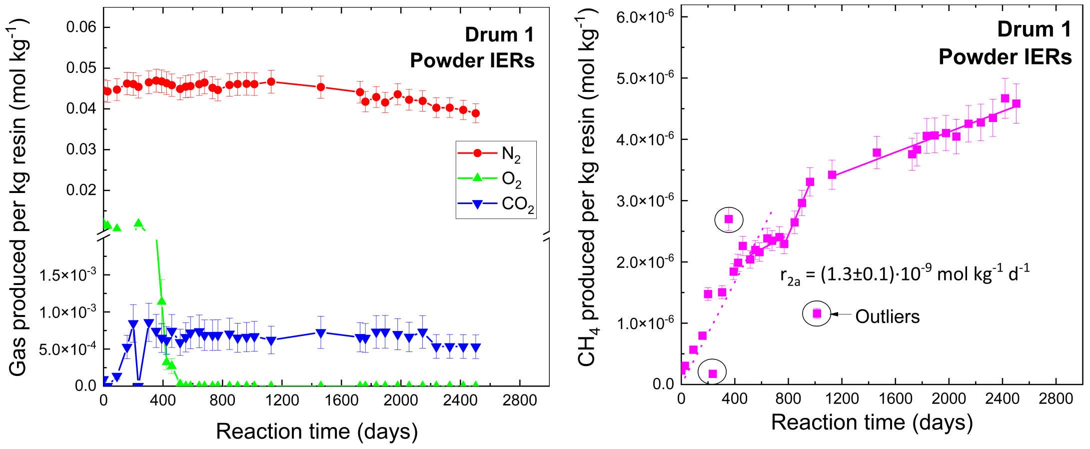

Fig. B-1: Gas evolution in Drum #1 filled with powder IERs

Left: N_2, O_2, CO_2 evolution per unit mass of organic material (mol kg^{-1}). Right: CH_4 evolution per unit mass of organic material (mol kg^{-1}). r_2 is the CH_4 production rate measured during the anoxic period of the experiment and expressed in mol kg^{-1} d^{-1}.

B.2 Gas evolution in Drum #2

Drum #2 contained organic materials in the form of bead IERs wetted with styrene. Over the long-term monitoring experiment, a leakage unfortunately occurred in February 2021, causing an instantaneous increase in the N_2 concentration. Aside from this, N_2 slowly decreased with time (Fig. B-2). CO_2 gradually decreased with time and did not increase significantly after the February 2021 leak. The O_2 concentration dropped to zero almost immediately after the start of the experiment, indicating a process (either abiotic or biotic) acting as a strong sink. It fluctuated for ~ 400 days and remained stable afterwards (Fig. B-2). Similarly to Drum #1, the concentration of CH_4 was relatively low compared to the other gas species and showed a two-step process. The second, slower rate of CH_4 production was comparatively similar in both Drums #1 and #2 (Fig. B-1; Fig. B-2).

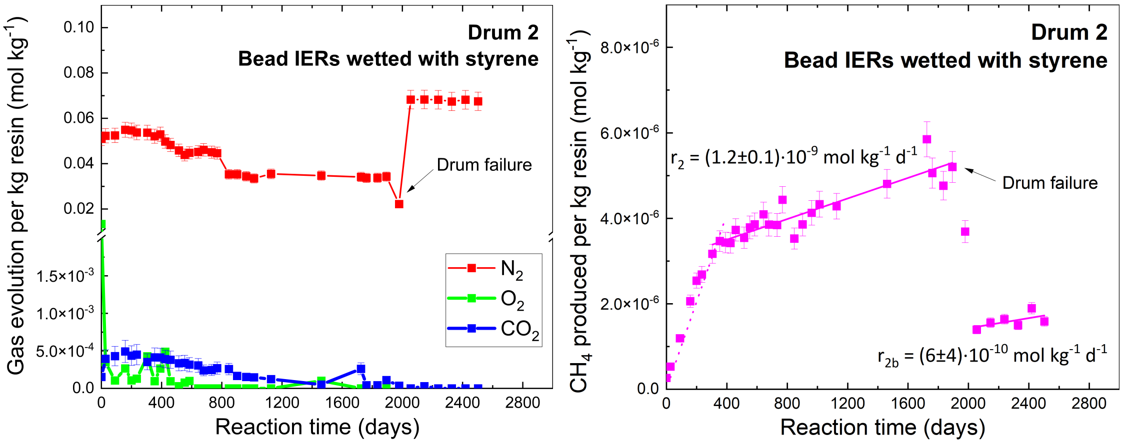

Fig. B-2: Gas evolution in Drum #2 filled with bead IERs wetted with styrene

Left: N_2, O_2, CO_2 evolution per unit mass of organic material (mol kg^{-1}). Right: CH_4, evolution per unit mass of organic material (mol kg^{-1}). r_2 is the gas generation rates measured during the anoxic period of the experiment and expressed in mol kg^{-1} d^{-1}. r_{2b} is the equivalent of the r_2 rate but measured once Drum #2 was fixed after its failure.

B.3 Gas evolution in Drum #3

Drum #3 was filled with bead IERs only. The N_2 content was approximately stable over the entire duration of the experiment, and the CO_2 content in the gas phase increased as long as O_2 was available (Fig. B-3). In this drum, the CH_4 concentration suggests a three-step behaviour. After a fast generation during the first ~ 400 days, the formation rate significantly decreased during a second stage and eventually appeared to stabilise after ~ 700 days of the experiment (Fig. B-3). The transition from the fast generation stage to the slower one after ~ 400 days seems again to correlate with the disappearance of O_2 from the system. Furthermore, a constant CH_4 concentration after ~ 1,800 days suggests that the process responsible for its production terminated (Fig. B-3).

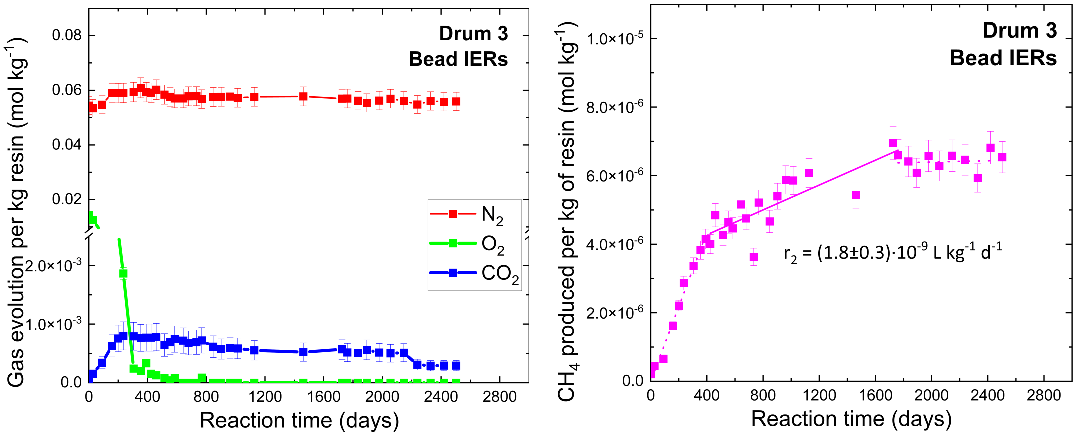

Fig. B-3: Gas evolution in Drum #3 filled with bead IERs

Left: N_2, O_2, CO_2 evolution per unit mass of organic material (mol kg^{-1}). Right: CH_4, evolution per unit mass of organic material (mol kg^{-1}). r_2 is the gas generation rates measured during the anoxic period of the experiment and expressed in mol kg^{-1} d^{-1}.

B.4 Gas evolution in Drum #4

Drum #4 contained PVC and plasticisers. The overall evolution of the various measured gases is very similar to the ones measured in Drums #1 and #3. The N_2 concentration was relatively stable over the first ~ 1,800 days, but seemed to slowly decline afterwards. O_2 was consumed over a period of ~ 800 days but did not show as sharp a decrease as the drums containing IERs (Fig. B-4). The CO_2 concentration in the gas phase increased as long as O_2 was available and remained constant over the course of the experiment. After a slow increase during the first ~ 1600 days, the CH_4 concentration seemed to stabilise or even decrease afterwards, indicating that the production rate during the slow step agrees well within a factor of 2 with the ones measured in the other drums (Fig. B-1; Fig. B-2; Fig. B-3; Fig. B-4).

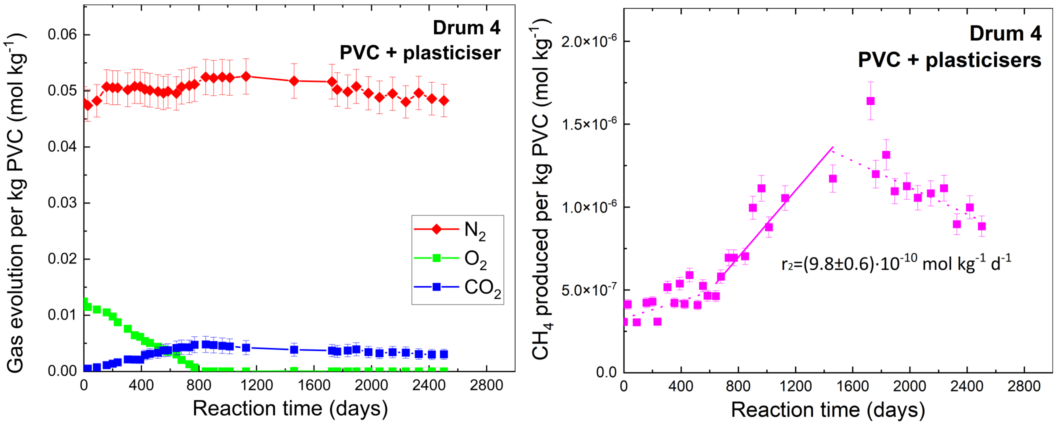

Fig. B-4: Gas evolution in Drum #4 filled with PVC and plasticisers

a) N_2, O_2, CO_2 evolution per unit mass of organic material (mol kg^{-1}). b) CH_4 evolution per unit mass of organic material (mol kg^{-1}). r_2 is the gas generation rates measured during the anoxic period of the experiment and expressed in mol kg^{-1} d^{-1}.

B.5 Gas evolution in Drum #5

The gas composition in the empty drum did not change with time (Fig. B-5).

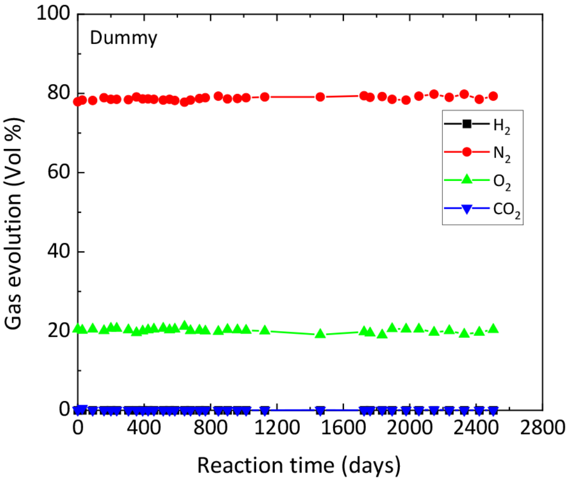

Fig. B-5: Evolution of the gas phase composition in empty Drum #5

B.6 Discussion

The degradation of organics in a cement-based L/ILW repository is expected to take place through a combination of hydrolysis and microbial degradation. Nagra's concept conservatively assumed the end products to be CH_4 and CO_2 and to be thermodynamically stable in anoxic alkaline conditions. Hence, the gas generation rates of these two compounds were of particular interest in the GME. In Tab. B-1, only CH_4 formation rates were calculated as the CO_2 formation was only measured while O_2 was still present in the drums and therefore not associated to the degradation of organics in anoxic conditions. Two distinct gas generation rates of CH_4 were derived from the concentrations measured: r_1 in the presence of O_2 during the first ~ 400 days and r_2 when O_2 could no longer be detected in the drum. The generation rates of CH_4 were always significantly faster during the oxic phase than during the following anoxic phase (difference ~ factor of 3 – 8) (Tab. B-1). The slow production of CH_4 during the anoxic phase of the experiment was surprisingly similar in all four drums, i.e., ranging between 0.98 – 1.8 × 10^{-10} mol kg^{-1} d^{-1}.

In Drums #1, # 2 and #3 containing IERs, O_2 was depleted within ~ 400 days and the conditions remained anoxic afterwards (Fig. B-1; Fig B-2; Fig. B-3). In Drum #2, a faster decrease of O_2 was registered than in the other two drums (#1 and #3) (Fig. B-2), most probably because this drum was the only one containing styrene, an IER degradation product that degrades more easily than the PS backbone. The fluctuations of O_2 observed until ~ 400 days could not be explained so far. In Drum #4 containing PVC and superplasticisers, O_2 depletion was slower and it took twice longer to disappear from the gas phase (i.e., only after ~ 800 days) (Fig. B-4). Furthermore, CH_4 production rates are slightly lower than those registered in the other drums containing IERs. This suggests that different processes occurred presumably due to the different types of organics and/or environmental conditions. In all drums except Drum #2, the production of CO_2 was observed over ~ 400 days as long as O_2 was present (Fig. B-1; Fig. B-2; Fig. B-3; Fig. B-4). As soon as anoxic conditions prevailed, maximum CO_2 concentrations were reached and decreased very slowly with time. In the case of Drum #2, the maximum CO_2 concentration was already reached during the initial phase of the experiments, i.e., within ~ 30 days, remained almost constant for up to ~ 200 days and then slowly decreased with time as in the other drums (Fig. B-2). Thus, the main difference between the evolution of the gas phase composition in Drum #2 compared to the other ones is the early, fast drop in O_2 leading to the early maximum in CO_2. This suggests that a large amount of readily degradable organics acting as carbon source was already available at the onset of microbial activity. A notable observation is that CH_4 production was found to be faster as long as O_2 was present, while it strongly declined afterwards, suggesting that the different environmental conditions (oxic/anoxic) directly influenced gas production.

Similar to the rates derived from the experiments of Molecke (1979), the derived gas generation rates have to be taken with caution when extrapolating these to the strongly alkaline conditions expected in a the near-field of a cement-based L/ILW repository, as the organic materials have not been embedded in a cementitious environment and have not been exposed to an alkaline-buffered solution. The experiments have been performed in a near-neutral pH (OPA porewater) with the aim of accelerating the degradation of the organics to be able to measure gas fluxes, as previous experiments with more readily degradable polymers reported rather low rates under near-neutral pH conditions (i.e., Molecke, 1979, Small et al. 2017) and the degradation under highly alkaline conditions is expected to be even more reduced due to the inhibition of microbial activities.

In the GME, chemical parameters such as pH and Eh have unfortunately not been monitored, strongly limiting a more detailed interpretation of the processes. The decommissioning of the experiment foreseen for 2024 should be able to provide a deeper understanding of the processes that occurred in the four drums.

Tab. B-1: CH_4 production rates obtained during the anoxic period of the GME experiment

		Drum 1	**Drum 2**	**Drum 3**	**Drum 4**
Rates (mol kg^{-1} d^{-1})	**r_{2a}**	$(1.3 \pm 0.1) \times 10^{-9}$	$(1.2 \pm 0.1) \times 10^{-9}$	$(1.8 \pm 0.3) \times 10^{-9}$	$(9.8 \pm 0.6) \times 10^{-10}$
	r_{2b}		$(6 \pm 4) \times 10^{-10}$		